INSPIRe

D3.1 – Technical Report of Developments and Test of DFMC M(G)RAIM

Prepared for:

Prepared by:	GMV INSPIRe TEAM
Contributions by:	GRAD INSPIRe TEAM
Approved by:	M Pattinson (GMV)
Authorized by:	T Richardson (GMV)
Code:	INSPIRe-GMV-D3.1-v1.2
Version:	1.2
Date:	January - 2024

Change Record

Issue / Rev	Date	Change Record	Authors
v1.0	05/05/2023	The first version of the deliverable submitted ESA	GMV INSPIRe Team
V1.1	20/10/2023	Updated the document to include results on the evaluation of the GNSS data with DFMC SBAS and Monte- Carlos simulation executed (Section 5.2)	GMV INSPIRe Team
V1.2	18/01/2024	Updated the results presented in Section 5.2: • Replaced GNSS-only Monte-Carlo simulation results with new ones (for MGRAIM and MRAIM) using same noise/multipath assumptions as EGNOS case • Added some further comment to Monte-Carlo simulation conclusions to explain apparent inconsistency between red/green flag % for GPS only and EGNOS scenarios • Added safety index cumulative distribution to Monte Carlo analysis • Added Monte Carlo results for modified MRAIM algorithm with Rayleigh distribution assumption for HPL Other grammatical and formatting details updated	GMV INSPIRe Team

TABLE OF CONTENTS

List of Tables and Figures

1 INTRODUCTION

1.1 Purpose

This document is deliverable D3.1 of the INSPIRe project, titled 'Technical report of developments and test of DFMC M(G)RAIM and MRAIM. This deliverable document is one of the main outputs of WP3. WP3 extends the work performed in WP2 to explore, develop and evaluate algorithms for dual frequency multi-constellation GNSS integrity. This document reports on the activities that have been completed within WP3, including:

- Overall description of the chosen M(G) RAIM and MRAIM algorithms
- Outcomes of testing of DFMC M(G)RAIM and MRAIM algorithms
- Description of the suitability and shortcomings of the algorithms for use in the maritime environment, highlighting any areas that need improvement
- Assessment of the need for a maritime-specific EGNOS message to support MRAIM
- Preliminary definition of system-level integrity data requirements for a maritime-specific message

In this iteration of the assessment results presented, the focus was on evaluating the functionality of the DFMC M(G)RAIM and MRAIM algorithms developed and comparing the output of both algorithms against each other. Further comparisons will be done against the integrity algorithm developed with EGNOS V3 enabled and presented in the final iteration of the deliverable. Also, further evaluation will be done to comprehensively compare MRAIM and MGRAIM detection capabilities. Firstly, this will be done using the INSPIRe M(G)RAIM Performance Prediction Prototype Tool developed within WP6 [RD.53], which will provide service volume simulation to examine service availability (considering HDOP and horizontal accuracy). Preliminary comparisons results were documented with the Spec 3.1 Test Report [RD.54]. Additionally, Monte Carlo Simulations will be done to investigate the algorithm's performance and highlight advantages and disadvantages of the algorithm.

1.2 Scope

Following the introduction to the document presented in Section 1, the layout of the remainder of the document is as follows:

- **Section 2** contains a list of applicable and reference documents
- **Section 3** describes the high-level algorithm design
- **Section 4** presents the description of testing
- **Section 5**summarises the suitability of the algorithm and highlights any further areas for investigation
- **Section 6** contains an assessment of the need for a maritime specific EGNOS message and a discussion on the preliminary definition of requirements for a maritime specific message

1.3 Definitions and Acronyms

1.3.1 Definitions

Concepts and terms used in this document and need defining are included in the following table:

Table 1-1 Definitions

Concept / Term	Definition
M(G)RAIM	Maritime General-RAIM: is a chi-squared fault-detection process with simple geometric screening rules to ensure safety
MRAIM	Maritime RAIM: is a maritime-specific implementation of the aviation ARAIM concept and performs a multiple-hypothesis solution-separation process, then computes a protection level and iteratively optimises this PL through re-allocation of integrity risk

1.3.2 Acronyms

Acronyms used in this document and need defining are included in the following table:

Table 1-2 Acronyms

Acronym	Definition
AL	Alert Limits
ARAIM	Advanced Receiver Autonomous Integrity Monitoring
CDF	Cumulative distribution function
DFMC	Dual Frequency Multiconstellation
DGNSS	Differential GNSS
DGPS	Differential GPS
DOP	Dilution of Precision
ECAC	European Civil Aviation Conference
EGNOS	European Geostationary Navigation Overlay Service
ESA	European Space Agency
FD	Fault Detection
FDE	Fault Detection and Exclusion
GBAS	Ground-Based Augmentation System
GEAS	GNSS Evolutionary Architecture Study
GLONASS	GLObal NAvigation Satellite System
GNSS	Global Navigation Satellite System
GPS	Global Positioning System
GRAD	GLA Research and Development
GSA	European GNSS Agency
HAL	Horizontal alarm Limit
HDOP	Horizontal Dilution of Precision
HMI	Hazardous Misleading Information
HPE	Horizontal Position Error
HPL	Horizontal Protection Level
IALA	International Association of Marine Aids to Navigation and Lighthouse Authorities
ICAO	International Civil Aviation Organisation
IEC	International Electrotechnical Commission
INSPIRe	Integrated Navigation System-of-Systems PNT Integrity for Resilience
IMO	International Maritime Organisation
IR	Integrity Risk
ISM	Integrity Support Message
LPV	Localizer Performance with Vertical guidance
MHSS	Multiple Hypothesis Solution Separation
MOPS	Minimum Operational Performance Standards
MGRAIM	Maritime General RAIM
MRAIM	Maritime RAIM
MSC	Maritime Safety Committee
MSI	Maritime Safety Information
MSR	Multi-system shipborne receiver
N/A	Not Applicable
NLOS	Non-Line of sight
NPA	Non-Precision Approach
PFA	Probability of False Alarm
PL	Protection Level
PHMI	Probability of Hazardously Misleading Information
PMD	Probability of Miss detection
PNT	Positioning Navigation and Timing
PVT	Position, Velocity and Time
RAIM	Receiver Autonomous Integrity Monitoring
RTCA	Radio Technical Commission for Aeronautics
RTK	Real-time kinematic positioning
SARPS	Standards and Recommended Practices
SBAS	Satellite Based Augmentation System
SIS	Signal in Space

SOLAS	Safety at Life at Sea
TBC	To Be Confirmed
TTA	Time to Arrival
VAL	Vertical alarm Limit
VHF	Very High Frequency

2 REFERENCES

2.1 Applicable Documents

The following documents, of the exact issue shown, form part of this document to the extent specified herein. Applicable documents are those referenced in the Contract or approved by the Approval Authority. They are referenced in this document in the form [AD.x]:

Table 2-1 Applicable Documents

Ref.	Title	Code	Version	Date
[AD.1]	INSPIRe Technical Proposal, Taylor Airey	T-062-001-02 Part 1	-	June 2022
[AD.2]	INSPIRe Management Proposal, Taylor Airey	T-062-001-02 Part 2	-	June 2022
[AD.3]	INSPIRe Proposal GMV	GMV 10842/21	V2/21	

2.2 Reference Documents

Although not part of this document, the following documents amplify or clarify its contents. Reference documents are those not applicable and referenced within this document. They are referenced in this document in the form [RD.x]:

Table 2-2 Reference Documents

Ref.	Title	Code	Version	Date
[RD.1]	ICAO, Annex 10, Aeronautical Telecommunications, Volume 1 (Radio Navigation Aids), Amendment 86, effective 17 November 2011. GNSS standards and recommended practices (SARPs) are contained in Section 3.7 and subsections, Appendix B, and Attachment D.	-	6th	07/2006
[RD.2]	"High integrity for GNSS applications" Marco Caparole. SOGEI Workshop GNSS technology advances in a multi-constellation framework	-	-	26/09/2014
[RD.3]	GNSS Measurements Modelling from Navipedia website. http://www.navipedia.net/index.php/GNSS_Measurements_Modelling	-	-	01/2017
[RD.4]	Minimum Operational Performance Standards (MOPS) for Global Positioning System/Satellite-Based Augmentation System Airborne Equipment	RTCA DO-229E		11/06/2020
[RD.5]	EGNOS SoL Service Definition Document	EGNOS-SoL-SDD	3.4	2021
[RD.6]	"Beyond accuracy – the integrity era" Allison Kealy. SBAS 2015 workshop sponsored by Thales Australia	-	-	2015
[RD.7]	"Integrity" from Navipedia website http://www.navipedia.net/index.php/Integrity	-	-	-
[RD.8]	SBAS Fundamentals https://gssc.esa.int/navipedia/index.php/SBAS_Fundamentals	-	-	Accessed 3/10/2022
[RD.9]	GBAS Fundamentals https://gssc.esa.int/navipedia/index.php/GBAS_Fundamentals	-	-	Accessed 3/10/2022

Ref.	Title	Code	Version	Date
[RD.10]	EUSPA EGNOS APV-I and LPV-200 Availability Map (https://egnos-user-support.essp-sas.eu/new_egnos_ops/maps_apv1 / https://egnos-user-support.essp-sas.eu/new_egnos_ops/lpv200_maps)	-	-	Accessed 3/10/2022
[RD.11]	GNSS Evolutionary Architecture Study. Phase I – Panel Report. February 2008	-	-	2008
[RD.12]	Channel Characterisation for Spread Spectrum Satellite Communication, Jahn, A., Bischil, H and Heib, G.	IEEE 4th International Symposium		09/1996
[RD.13]	Combined Performance for Open GPS/Galileo Receivers EU-US Cooperation on Satellite Navigation Working Group C		Final	19/07/2010
[RD.14]	Minimum Operational Performance Standards (MOPS) for Global Positioning System/Aircraft Based Augmentation System Airborne Equipment	RTCA DO-316		14/04/2009
[RD.15]	Advanced RAIM Reference Airborne Algorithm Description Document	ARAIM ADD	V4.0	02/2022
[RD.16]	GNSS Evolutionary Architecture Study. Phase II – Panel Report. February 2010	-	-	2010
[RD.17]	Interim Report. EU-U.S. Cooperation on Satellite Navigation Working Group C, ARAIM Technical Subgroup. Date: December 1th, 2012, available at the following address: https://www.gps.gov/policy/cooperation/europe/2013/working-group-c/ARAIM-report-1.0.pdf	-	-	2012
[RD.18]	Milestone 2 Report. EU-U.S. Cooperation on Satellite Navigation Working Group C, ARAIM Technical Subgroup. Date: February 11th, 2015, available at the following address: https://ec.europa.eu/docsroom/documents/9567/attachments/1/translations/en/renditions/pdf	-	-	2015
[RD.19]	Milestone 3 Report. EU-U.S. Cooperation on Satellite Navigation Working Group C, ARAIM Technical Subgroup. Date: February 25th, 2016, available at the following address: https://ec.europa.eu/newsroom/growth/redirection/item/48690	-	-	2016
[RD.20]	S. Paternostro, T. Moore, C. Hill, J. Atkin, G. De Maere and H. P. Morvan, "Examples of user algorithms implementing ARAIM techniques for integrity performance prediction, procedures development and pre-flight operations," 2016 8th ESA Workshop on Satellite Navigation Technologies and European Workshop on GNSS Signals and Signal Processing (NAVITEC) , 2016, pp. 1-15, doi: 10.1109/NAVITEC.2016.7849330.	-	-	2016
[RD.21]	J. Blanch, T. Walter, P. Enge, Y. Lee, B. Pervan and A. Spletter. Advanced RAIM User Algorithm Description: Integrity Support Message Processing Fault Detection Exclusion and Protection Level Calculation", Proceedings of ION GNSS, 2012, pp. 2828-2849	-	-	09/2012
[RD.22]	Zabalegui, Paul & De Miguel, Gorka & Perez, Alejandro & Mendizabal, Jaizki & Goya, Jon & Adin, Inigo. (2020). A Review of the Evolution of	-	-	03/2020

Ref.	Title	Code	Version	Date
	the Integrity Methods Applied in GNSS. IEEE Access. PP. 1-1.			
[RD.23]	GPS Integrity and Potential Impact on Aviation Safety. Civil Aviation Authority 2004	CAA PAPER 2003/9	-	April 2004
[RD.24]	A.915(22) Revised Maritime Policy and Requirements for a Future Global Navigation Satellite System (GNSS)	IMO/A.915 (22)	-	29/11/2001
[RD.25]	A.1046(27) Service Requirements for Worldwide Radio Navigation Systems	IMO/A.1046(27)	-	30/11/2011
[RD.26]	MSC.401(95) Performance Standards for Multi-System Shipborne Radionavigation Receivers	IMO/MSC.401(95)	-	8/06/2015
[RD.27]	MSC.1/Circular.1575 - Guidelines for Shipborne Position, Navigation and Timing (PNT) Data Processing – (16 June 2017)	MSC.1/Circular.1575	-	06/2017
[RD.28]	Resolution MSC.112(73) - Adoption of the Revised Performance Standards for Shipborne Global Positioning System (GPS) Receiver Equipment	MSC.112(73)	-	12/2000
[RD.29]	Resolution MSC.53(66) - Performance Standards for Shipborne GLONASS Receiver Equipment - (Adopted on 30 May 1996)	MSC.53(66)	-	05/1996
[RD.30]	Resolution MSC.233(82) Adoption of The Performance Standards for Shipborne Galileo Receiver Equipment - (Adopted On 5 December 2006)	MSC.233(82)	-	12/2006
[RD.31]	RESOLUTION MSC.114(73)) Adoption of The Revised Performance Standards for Shipborne DGPS And DGLONASS Maritime Radio Beacon Receiver Equipment. (Adopted on 1 December 2000	MSC 73/21/Add.3	-	12/2000
[RD.32]	SEASOLAS D030 - Final Report	SEASOLAS-GMV-D030	1.2	05/10/2018
[RD.33]	MaRrinav D1 Maritime Context and Requirement v2.0	-	-	
[RD.34]	Greves, P. D., et al, A portfolio Approach to NLOS and Multipath in Dense Urban Areas Proceedings of ION GNSS	-	-	2013
[RD.35]	Satellite derived Time and Position: A study of Critical Dependence, Government Office for Science	-	-	2018
[RD.36]	P.Y Montgomery, T.E. Humphreys, B.M. Ledvina Receiver Autonomous Spoofing Detection: Experimental Results of a Multi-antenna Receiver Defence Against a portable Civil GPS spoofer	-	-	2009
[RD.37]	MarRINav D3b GNSS Integrity: Maritime Integrity at User Level with EGNOS V3 & MRAIM v2.0	-	2.0	28/02/22
[RD.38]	Hargreaves, Chris. (2019). ENC 2019 - Maritime Receiver Autonomous Integrity Monitoring (MRAIM).	-	-	2019
[RD.39]	Pervan, B., Pullen, S. and Christine, J. “A Multiple Hypothesis Approach to Satellite Navigation Integrity”. Navigation, v.45, no. 1, 1998.	-	-	1998
[RD.40]	IEC, ‘Maritime navigation equipment - GNSS, part 1: GPS’.	IEC 61108-1	-	2003
[RD.41]	INSPIRe State of the Art	1.0	-	10/2022
[RD.42]	Blázquez, F, et al, Revision of RAIM implementations for Maritime, Proceedings of ION GNSS	-		2020
[RD.43]	IALA Worldwide Radio Navigation Plan.	-	1.0	December 2009
[RD.44]	Service development status in the maritime	-	-	December 2021

Ref.	Title	Code	Version	Date
	Domain, EGNOS workshop 2021, Manuel Lopez Martinez, Silvia Porfili			
[RD.45]	IALA guideline G1152 SBAS maritime service	-	1.1	December 2019
[RD.46]	IALA guideline G1129 the retransmission of SBAS corrections using MF-radio beacon and AIS	-	2.0	June 2022
[RD.47]	Minimum Operational Performance Standard for dual-frequency multi-constellation satellite-based augmentation system airborne equipment	ED-259A	Draft	August 2022
[RD.48]	EGNOS Message Server (EMS) User Interface Document http://www.egnos-pro.esa.int/ems/EMS_UID_2_0.pdf	E-RD-SYS-E31-011-ESA	Issue 2 Revision 0	26/11/2004.
[RD.49]	INSPIRe D2.1 Technical Report of Developments and Test of GPS M(G)RAIM	INSPIRe-GMVNSL-D2.1	1.1	February 2023
[RD.50]	INSPIRe Alg3.1 Algorithm documentation DFMC M(G)RAIM	INSPIRe-GMVNSL-Alg3.1-v1.0	1.0	May 2023
[RD.51]	IMO Resolution A.915(22). Revised maritime policy and requirements for a future Global Navigation Satellite System (GNSS)	IMO A.915(22)		29/11/2001
[RD.52]	INSPIRe Data3.1 - Test and Validation Data Description	INSPIRe-GMVNSL-Data3.1-v1.0	1.0	05/05/2023
[RD.53]	INSPIRe D6.1 RAIM Prototype Report	INSPIRe-GMV-D6.1-v1.0	1.0	05/2023
[RD.54]	INSPIRe Spec3.1 - Functional and software design and Test Specifications (TEST REPORT)– DFMC M(G)RAIM	INSPIRe-GMVNSL-Spec3.1-v1.0		05/2023

3 HIGH LEVEL ALGORITHM DESIGN

The algorithm design functional and software architecture is described in [RD.1]. A high-level description is presented here for completeness for both M(G) RAIM and MRAIM.

3.1 M(G)RAIM General Description

The maritime integrity algorithm proposed for M(G) RAIM is based on a Classical RAIM algorithm, used for decades in maritime receivers, that is applied to the overall solution and to measurement subsets to ensure the fault detection (and exclusion if needed) capabilities.

The algorithm is based on two sequential steps once the position is calculated with all the available satellites.

- Availability check: A set of simple checks are applied to determine whether the derived all-in-view solution is suitable for navigation as defined by the maritime receiver specifications [RD.2]. If any of these tests fail, then an integrity alarm is raised.
- Fault detection: If all the previous test meets the defined conditions, a Chi-Squared test is performed to identify a fault in the positioning estimation.
- Geometry screening: For each potentially faulty element of the navigation solution, a subset navigation solution is formed by eliminating the faulty element from the all-in-view solution. Then, availability checks are performed to check if the remaining solution would pass, to determine if the detection capability of the solution is sufficient.

Figure 3-1 and Figure 3-2 provides a high-level view of the rationale, inputs outputs and relationships of each of the functions detailed.

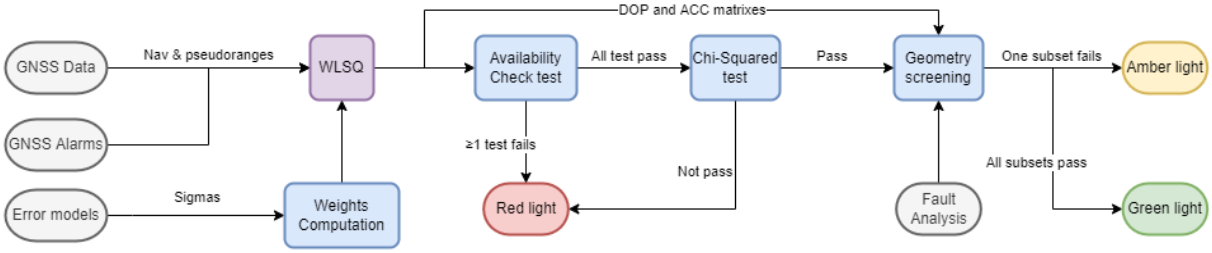

Figure 3-1. MGRAIM conceptual flowchart without augmentation

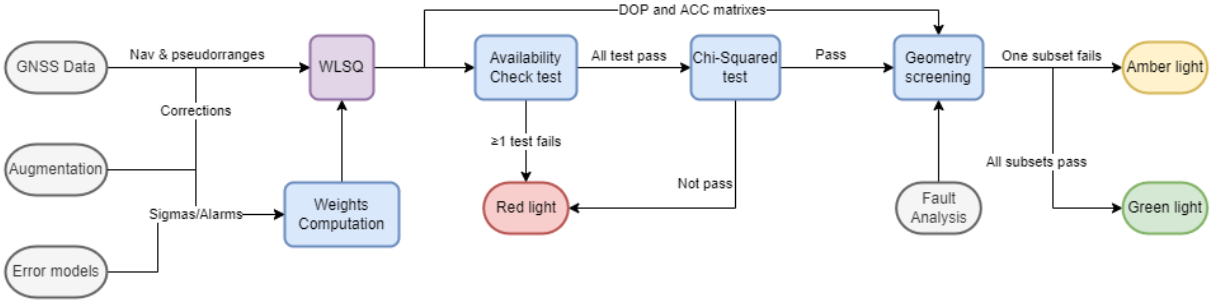

Figure 3-2. MGRAIM conceptual flowchart with augmentation

Where:

- Grey bubbles are the required inputs
- Purple box is the PVT engine which computes the user estimated state vector
- Blue boxes are the functions involved in the integrity algorithm
  - Weights computation: computes satellite error models considered as nominal for the maritime environment.

- Availability Check Test: the function that checks if the current solution is suitable for maritime in terms of expected accuracy.
- Fault Detection, Chi-Squared test: function that detects if solution complies with the nominal error models.
- Geometry screening: function that identifies the potential failure and performs additional tests to measurements subsets.

- Red, amber and green light bubbles are integrity warning output information provided to mariners;
  - Red light: provided to the mariner when at least one of the availability check or the fault detection test do not pass.
  - Amber light: provided to the mariner when geometry screening raises an alarm for at least one subset
  - Green light: provided to the mariner when all the tests are performed successfully, and the solution is therefore suitable for navigation.

3.2 MRAIM General Description

The maritime integrity algorithm proposed, is a maritime-specific implementation of the aviation ARAIM concept and performs a multiple-hypothesis solution-separation process, then computes a protection level and iteratively optimises this PL through re-allocation of integrity risk. Solution separation methods are characterised using the distance (separation) between position estimates obtained with subsets of the available satellites.

ARAIM is an evolution of the RAIM techniques and has been developed considering DFMC environment with the goal to protect multi-constellation users by means of a robust user integrity algorithm. Being Civil Aviation applications the driver for the development of ARAIM concept, ARAIM intends to provide a service for stringent aviation operations: LPV-200.

The algorithm is based on the following main principles.

- Ground monitoring system: Different ARAIM concepts might have different levels of ground monitoring and hence would imply different levels of fault detection by the ground segment. This would have a significant impact on the user ARAIM architectures in terms of their performance, and on the design of the algorithm itself.
  - **Horizontal ARAIM** (H-ARAIM) is a minor extension of today's RAIM architecture adding multi-constellation and dual-frequency capabilities. It is based on a static or quasi-static ISD to support horizontal navigation. ISD content is based upon Constellation Service Provider commitments to maintain certain level of performance and observational history.
  - **Offline ARAIM** to support horizontal and vertical navigation based on a monthly ISD from the ground to ensure that ISD parameters are consistent with up-to-date monitoring results. ISD parameters receive greater scrutiny than in the horizontal architecture due to the more stringent operation targets proposed for the offline architecture.

- **Online ARAIM** to support horizontal and vertical navigation based on an hourly ISD from the ground. In this way, Service Providers are given a larger control over GNSS performance.

- ARAIM assumptions and Feared Events: The ARAIM user algorithm needs to make certain assumptions about errors and threats and requires certain information to be provided by a specific ground segment to generate protection levels and provide integrity. In particular, the user ARAIM algorithm requires values for failure probabilities, the standard deviation of a distribution that bounds the orbit/clock error in the fault-free case and the nominal and maximum biases in fault-free conditions.
- User algorithm:
  - Fault Detection: Each failure mode defines a reduced-subset solution, which excludes the potentially faulty measurements. The physical separation distance between the all-in-view (AIV) solution and the subset solution is used as a fault detection test. Only if all separation tests are passed (i.e., all lie below the detection threshold) is the AIV solution accepted. A conventional chi-square test of the residuals is also performed for the AIV solution as a sanity check.
  - Protection Level calculation: The horizontal protection level is computed that considers all monitored failure modes, nominal errors, and nominal biases. As explained in [RD.50], PLs for this algorithm can be computed by two different considerations, MRAIM assuming Rayleigh distribution for horizontal error, or Maritime HRAIM assuming Gaussian distribution for East and North components ignoring the vertical. However, as explained in section 5.2.4, performance are almost identical and therefore same conclusions could be obtained for both, and therefore the assessment will be made only for one of them, the Maritime HRAIM assuming Gaussian distribution.
  -

Figure 3-3 and Figure 3-4 provide a high-level view of the rationale, inputs outputs and relationships of each of the functions detailed.

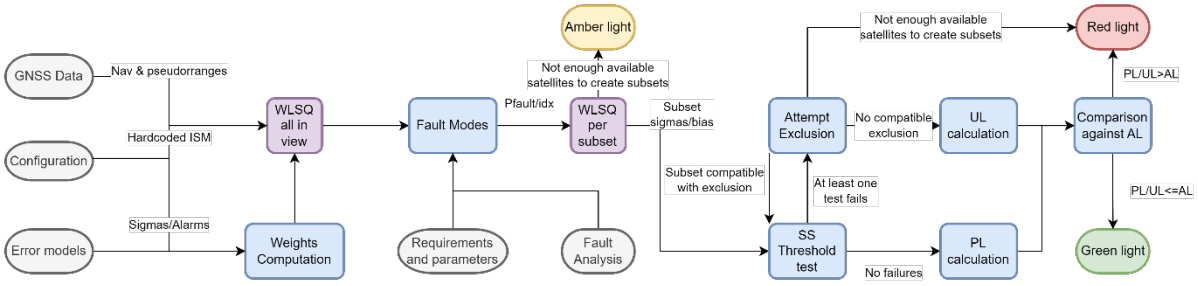

Figure 3-3. MRAIM offline conceptual flowchart

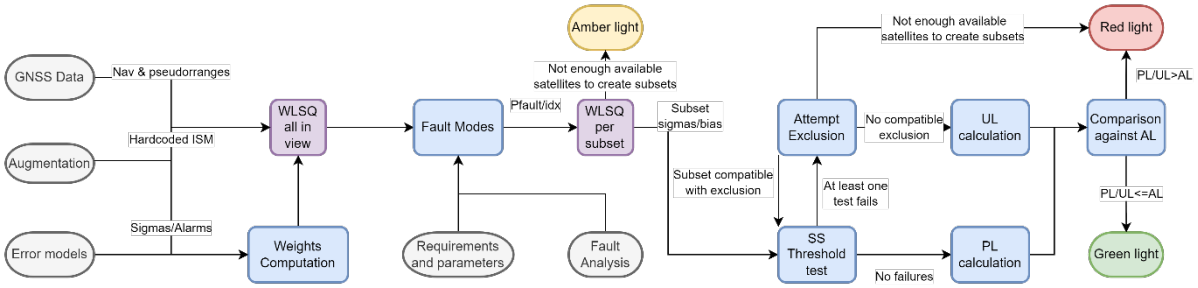

Figure 3-4. MRAIM online conceptual flowchart

Where:

- Grey bubbles are the required inputs
  - Particularly relevant are the ISD parameters required for the suitable tuning of the MRAIM algorithm
- Purple box is the PVT engine which computes the user estimated state vector.
- Blue boxes are the functions involved in the integrity algorithm:
  - Weights computation: computes satellite error models considered as nominal for the maritime environment.
  - Faults Mode calculation: the function that computes the required subsets to provide the desired level of integrity. According to the fault analysis, this function classifies the error that needs to be monitored to be included in the calculation.
  - Solution Separation Threshold test: the function that performs a threshold test for each subset and analyses if their separation is compatible with a failure. In that case, the faulty could be excluded to provide a safe positioning.
  - Attempt Exclusion: Fault exclusion could be performed if one of the Solution Separation Threshold tests fails. This function computes the compatible potential subsets and provides the compatible subset again to the Solution Separation Threshold test module as the subset is the new “all in view”.
  - Protection/Uncertainty Level calculation: the function that computes the Protection/Uncertainty Level according to the previously computed information.
- Red, amber and green light bubbles are integrity warning output information provided to mariners:
  - Red light: provided to the mariner when the HPL (no fault or fault excluded) or HUL (fault detected and not excluded) is computed and it is above the HAL.
  - Amber light: provided to the mariner when there is not enough satellite available to create subsets and provide a solution for every subset and the integrity requested.
  - Green light: provided to the mariner when the HPL (no fault or fault excluded) or HUL (fault detected and not excluded) is computed and it is below the HAL and no faults are detected.

4 DESCRIPTION OF ALGORITHM TESTING

This section presents an overview of the experimentation plan for the evaluation of the algorithm and a summary of the results of algorithm testing. The sections that follow then go into more detail on each element. The purpose of the experimentation is to assess the MGRAIM algorithm developed.

The experimentation consists of the following sequential stages:

- Data collection & generation
- Data processing
- Performance evaluation

These stages are discussed in the following subsections.

4.1 Data Generation and Data Processing

The functional testing and performance evaluation was executed based on the collection of real GNSS data (GPS and Galileo observables), using GMV facilities, in Nottingham.

4.1.1 GNSS Data

GNSS Data are measured with the Septentrio PolarRx5S. The PolaRx5S from Septentrio is a high-performance GNSS receiver capable of multi-constellation position solutions and logging, at a maximum of 100Hz. Supported constellations include GPS L1, L2, L5, Galileo E1, E5 (a, b, AltBoc) E6, BeiDou, B1, B, B3 and SBAS.

The PolaRx5S is currently located at the GMV offices in Nottingham as part of a receiver testbench in the lab. The receiver uses a single NAVX 3G+C antenna, which collects Static datasets from open sky, situated on the Sir Colin Campbell Building roof, which can receive all available GPS, Galileo, GLONASS, BeiDou and SBAS signals. Table 4-1 below provides a summary of the data collected for analysis. The data is approximately 1 hour which is suitable for testing the function of M(G)RAIM for Dual Frequency processing under failure.

Table 4-1 GPS Data collected for analysis

Date	Duration		Constellation/Frequency	File Format	Conversion Tool
	From	To			
2022/ 09 /28	10:15:00	11:00:16	GPS L1/L5 GAL E1/E5	RINEX	RTKCONV 2.4.3 (SBF to RINEX)

4.1.2 SBAS Data

The SBAS data used within this project was retrieved from GMV internal archive, in Rinex B format. The description of the Logbook format is provided in [RD.52].

Table 4-2 EGNOS Data collected for analysis

Date	Duration		PRN	File Format	Conversion Tool
	From	To			
2022/ 09 /28	10:00:00	11:00:00	123	RinexB	GMV Decoder

4.1.3 Simulation Data Generation

Simulated data provides an option to cover scenarios that would otherwise not be possible using field data alone. [RD.5] provides the specification for the Threats and Faults which are applicable to and will be used to develop the INSPIRe integrity solutions. To facilitate the analysis of these faults on the positioning solution, GMV has created a series of functions to introduce the errors to the RINEX files in a coherent way for a DF combination. Multiple faults for each of these scenarios are created by introducing ramps or biases or multipath on multiple satellites at the same time.

Table 4-3 Fault Injection

Fault	Baseline Function	Notes
Satellite Clock failure (ramp)	The fault injection tool applies a ramp error on a specified satellite	Standard clock failure on a single satellite – determined to be a steady clock ramp on one measurement.
Satellite Clock failure (bias)	The fault injection tool applies a bias value to a single SV	Clock failure on a single satellite leading to a bias/offset.
Satellite Bad Ephemeris Upload	Modification of parameters in the navigation message	Single satellite failure due to a bad ephemeris upload results in incorrect information.
Satellite multipath	The fault injection tool applies an elevation-dependent error is added to each pseudo range observation, with a random noise component included	Multipath induced error on a single satellite e.g., the introduction of oscillating bias error. Typical of a maritime environmental hazard.

4.1.4 Data Processing

The collected data will be processed off-line and in non-real time using the algorithm and several supporting tools. A set of algorithm performance test scenarios are defined in Section 5.2. The following high-level processing step shall be carried out:

- Run TPDF for each test scenario, configured according to test scenario definition.
  - Inputs:
    - RINEX observation file and navigation file
    - If SBAS legacy mode:
      - *.csv files output by EGNOS decoder for applicable calendar day.
  - Outputs:
    - PVT results files (.csv)
    - SBAS engine (Legacy)
    - MGRAIM / MRAIM engine
  - Residual data files (.csv)

4.2 Test Scenarios

A set of 24 test scenarios has been defined, as described in the table below.

Table 4-4 Test Scenarios

Test Scenario	Correction mode	Fault injection	Smoothing time constant
TS.01	MGRAIM	None	100s

Test Scenario	Correction mode	Fault injection	Smoothing time constant
TS.02	MRAIM	None	100s
TS.01a	MGRAIM (SBAS Enabled)	None	100s
TS.02a	MRAIM (SBAS Enabled)	None	100s
TS.03	MGRAIM	Single Satellite Clock failure (ramp) - High Elevation SV	100s
TS.04	MRAIM	Single Satellite Clock failure (ramp) - High Elevation SV	100s
TS.03a	MGRAIM (SBAS Enabled)	Single Satellite Clock failure (ramp) - High Elevation SV	100s
TS.04a	MRAIM (SBAS Enabled)	Single Satellite Clock failure (ramp) - High Elevation SV	100s
TS.05	MGRAIM	Single Satellite Clock failure (ramp) - Low Elevation SV	100s
TS.06	MRAIM	Single Satellite Clock failure (ramp) - Low Elevation SV	100s
TS.05a	MGRAIM (SBAS Enabled)	Single Satellite Clock failure (ramp) - Low Elevation SV	100s
TS.06a	MRAIM (SBAS Enabled)	Single Satellite Clock failure (ramp) - Low Elevation SV	100s
TS.07	MGRAIM	Multiple Satellite Clock failure (ramp) - High Elevation SV	100s
TS.08	MRAIM	Multiple Satellite Clock failure (ramp) - High Elevation SV	100s
TS.07a	MGRAIM (SBAS Enabled)	Multiple Satellite Clock failure (ramp) - High Elevation SV	100s
TS.08a	MRAIM (SBAS Enabled)	Multiple Satellite Clock failure (ramp) - High Elevation SV	100s
TS.09	MGRAIM	Single Satellite Clock failure (bias) - High Elevation SV	100s
TS.10	MRAIM	Single Satellite Clock failure (bias) - High Elevation SV	100s
TS.09a	MGRAIM (SBAS Enabled)	Single Satellite Clock failure (bias) - High Elevation SV	100s
TS.10a	MRAIM (SBAS Enabled)	Single Satellite Clock failure (bias) - High Elevation SV	100s
TS.11	MGRAIM	Single Satellite Clock failure (bias) -Low Elevation SV	100s
TS.12	MRAIM	Single Satellite Clock failure (bias) -Low Elevation SV	100s
TS.11a	MGRAIM (SBAS Enabled)	Single Satellite Clock failure (bias) -Low Elevation SV	100s
TS.12a	MRAIM (SBAS Enabled)	Single Satellite Clock failure (bias) -Low Elevation SV	100s
TS.013	MGRAIM	Multiple Satellite Clock failure (bias) - High Elevation SV	100s
TS.14	MRAIM	Multiple Satellite Clock failure (bias) - High Elevation SV	100s
TS.013a	MGRAIM (SBAS Enabled)	Multiple Satellite Clock failure (bias) - High Elevation SV	100s
TS.14a	MRAIM (SBAS Enabled)	Multiple Satellite Clock failure (bias) - High Elevation SV	100s

Test Scenario	Correction mode	Fault injection	Smoothing time constant
TS.15	MGRAIM	Single Satellite Bad Ephemeris Upload - High Elevation SV	100s
TS.16	MRAIM	Single Satellite Bad Ephemeris Upload - High Elevation SV	100s
TS.15a	MGRAIM (SBAS Enabled)	Single Satellite Bad Ephemeris Upload - High Elevation SV	100s
TS.16a	MRAIM (SBAS Enabled)	Single Satellite Bad Ephemeris Upload - High Elevation SV	100s
TS.17	MGRAIM	Multiple Satellite Bad Ephemeris Upload - High Elevation SV	100s
TS.18	MRAIM	Multiple Satellite Bad Ephemeris Upload - High Elevation SV	100s
TS.17a	MGRAIM (SBAS Enabled)	Multiple Satellite Bad Ephemeris Upload - High Elevation SV	100s
TS.18a	MRAIM (SBAS Enabled)	Multiple Satellite Bad Ephemeris Upload - High Elevation SV	100s
TS.19	MGRAIM	Single Satellite Multipath error - High Elevation SV	100s
TS.20	MRAIM	Single Satellite Multipath error Upload - Low Elevation SV	100s
TS.19a	MGRAIM (SBAS Enabled)	Single Satellite Multipath error - High Elevation SV	100s
TS.20a	MRAIM (SBAS Enabled)	Single Satellite Multipath error Upload - Low Elevation SV	100s
TS.21	MGRAIM	Multiple Satellite Multipath error - High Elevation SV	100s
TS.22	MRAIM	Multiple Satellite Multipath error Upload - Low Elevation SV	100s
TS.21a	MGRAIM (SBAS Enabled)	Multiple Satellite Multipath error - High Elevation SV	100s
TS.22a	MRAIM (SBAS Enabled)	Multiple Satellite Multipath error Upload - Low Elevation SV	100s
TS.23	MGRAIM	Single Satellite Ionospheric error - High Elevation SV	100s
TS.24	MRAIM	Single Satellite Ionospheric error - Low Elevation SV	100s
TS.23a	MGRAIM (SBAS Enabled)	Single Satellite Ionospheric error - High Elevation SV	100s
TS.24a	MRAIM (SBAS Enabled)	Single Satellite Ionospheric error - Low Elevation SV	100s

5 ASSESSMENT OF SUITABILITY OF ALGORITHM

This section contains an assessment of the suitability of the algorithm. The algorithm assessment was executed using the algorithm design described in Section 3 for both single and multiple satellite faults. Here the algorithms' ability to detect GNSS faults and where applicable exclude the faults as described in Section 4.1.3 and to raise the appropriate alert as defined in Section 3 was analysed.

Figure 5-1 depicts the satellite visibility for the selected dataset and the red, green and blue windows highlight the satellite and the period in which the faults were been injected on the high satellites G03 with an elevation of 64° and azimuth of 74° and low elevation satellites G12 with an elevation of 7° and azimuth of 336°. These satellites we used for executing the single fault test cases. For the satellites used the faults were injected at t=110s (SOW: 296228s) for a period of 300s to end at to t = 410s (SOW: 296528s). The results present here after are for single satellite fault case according to the test scenarios defined in Section 4.2. For the multiple satellite fault the was done using G03 and G06 (elevation of 45° and azimuth of 301°) and the faults were injected from t=110s (SOW: 296228s) to t = 410s (SOW: 296528s) and a second satellite from t=908s (SOW: 297026s) to t = 1208s (SOW: 297326s).

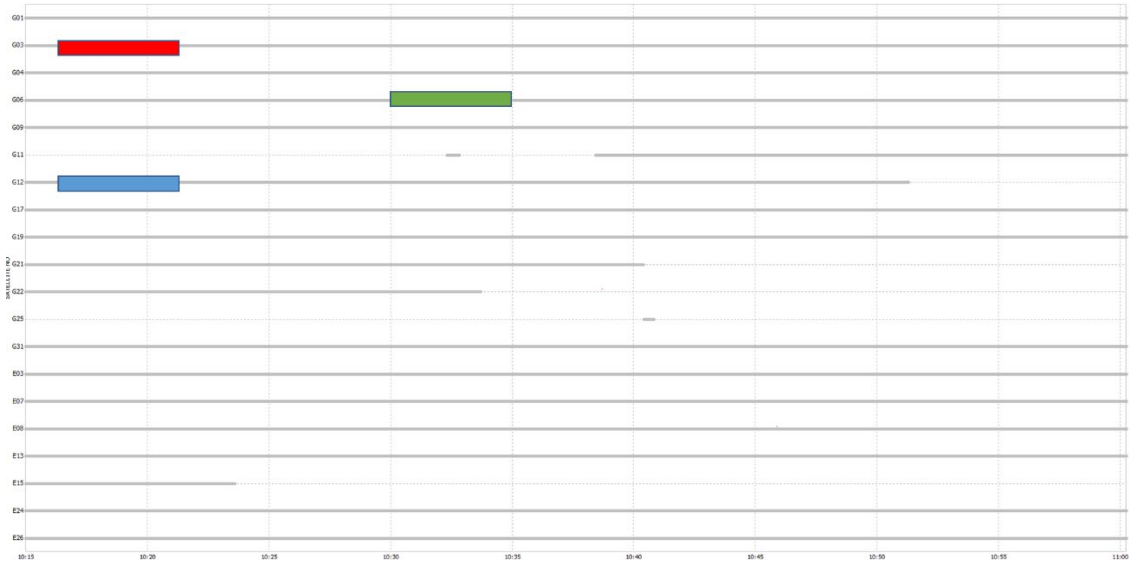

Figure 5-1 Satellite visibility condition and Fault injected on satellite G03, and G12 at time =110s to 410s and G06 at time = 908s to t = 1208s

It should be noted that for illustrative purposes for results where faults are injected, and the red integrity flag is raised the horizontal error is plotted to show the potential effect of the fault but the position is not provided in such a case.

The computation of the fault detection and FDE processes for the MGRAM and MRAIM algorithm respectively are described in full details in [RD.50]. The integrity warning outputs that are provided in the results plotted below illustrates one or a combination of the following traffic light indicators, the flag carry the following meaning:

- MGRAIM
  - Red light: provided to the mariner when at least one of the availability check or the fault detection test do not pass.
  - Amber light: provided to the mariner when geometry screening raises an alarm for at least one subset.

- Green light: provided to the mariner when all the tests are performed successfully, and the solution is therefore suitable for navigation.

- MRAIM
  - Red light: provided to the mariner when the HPL (no fault or fault excluded) or HUL (fault detected and not excluded) is computed and it is above the HAL.
  - Amber light: provided to the mariner when there is not enough satellite available to create subsets and provide a solution for every subset and the integrity requested.
  - Green light: provided to the mariner when the HPL (no fault or fault excluded) or HUL (fault detected and not excluded) is computed and it is below the HAL and no faults are detected.

5.1 Presentation of Experimentation and Evaluation results

5.1.1 Evaluation of a Fault-free Dataset

This subsection shows the results generated using a smoothing constant of 100 seconds based on the following test scenario:

Test Scenario	Correction mode	Fault injection
TS.01	MGRAIM DFMC	none
TS.02	MRAIM DFMC	none

5.1.1.1 TS01 – PVTI Performance Analysis (MGRAIM) - DFMC

Figure 5-2 show fault detection test results from Test Scenario 01 MGRAIM DFMC. Figure 5-2 illustrates test statistics and threshold values computed for the solution generated for the dataset. The test statistics and threshold values are used within Fault Detection Test as described in full details [RD.50]. It can be seen from the graph that the test statistic does not exceeds the detection threshold, when this occurs the “green light” integrity alarm/flag is raised, the average test statistic is 1.29 and the threshold is 6.49. Figure 5-3, shows integrity flags and the horizontal errors within the solution generated.

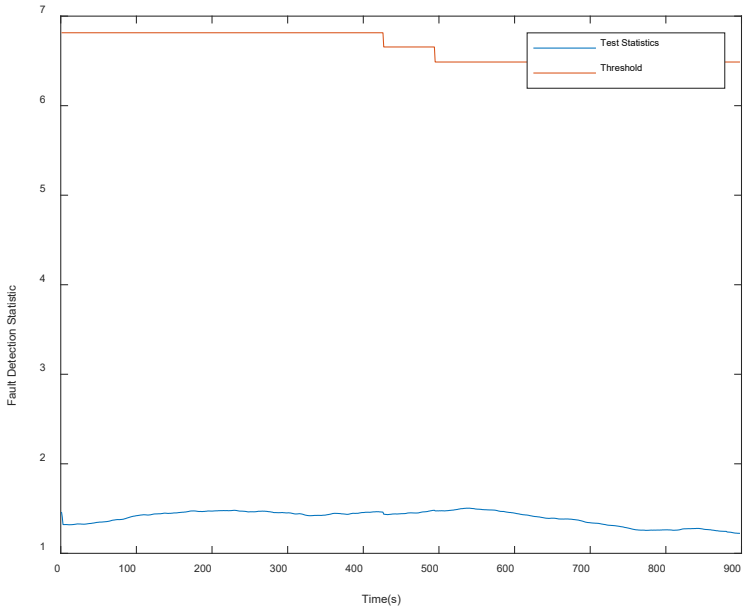

Figure 5-2 FD results from MGRAIM in fault-free case

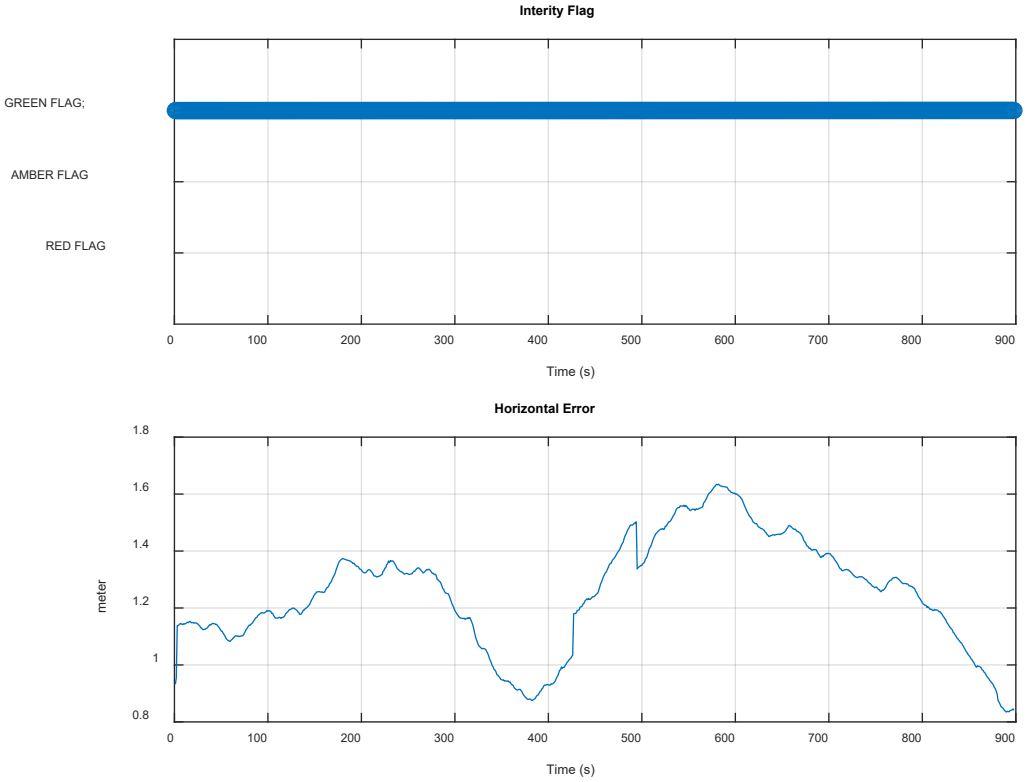

Figure 5-3 The MGRAIM Integrity Flag (above) and Horizontal Error

The solution performance is summarised in Table 5-1. For GPS L1/L5 and GAL E1/E5a the horizontal error is 1.44m with a percentile of 95%.

Table 5-1 TS01 - NEU and Horizontal error parameters for GPS L1/L5 and GAL E1/E5a

	MEAN (m)	STD (m)	95% (m)
North	0.045	0.239	0.393
East	1.076	0.209	1.404
Up	2.598	0.599	3.383
Horizontal	1.103	0.206	1.436

Figure 5-4 illustrate the number of satellites used to compute the PVT solution and the computed DOP.

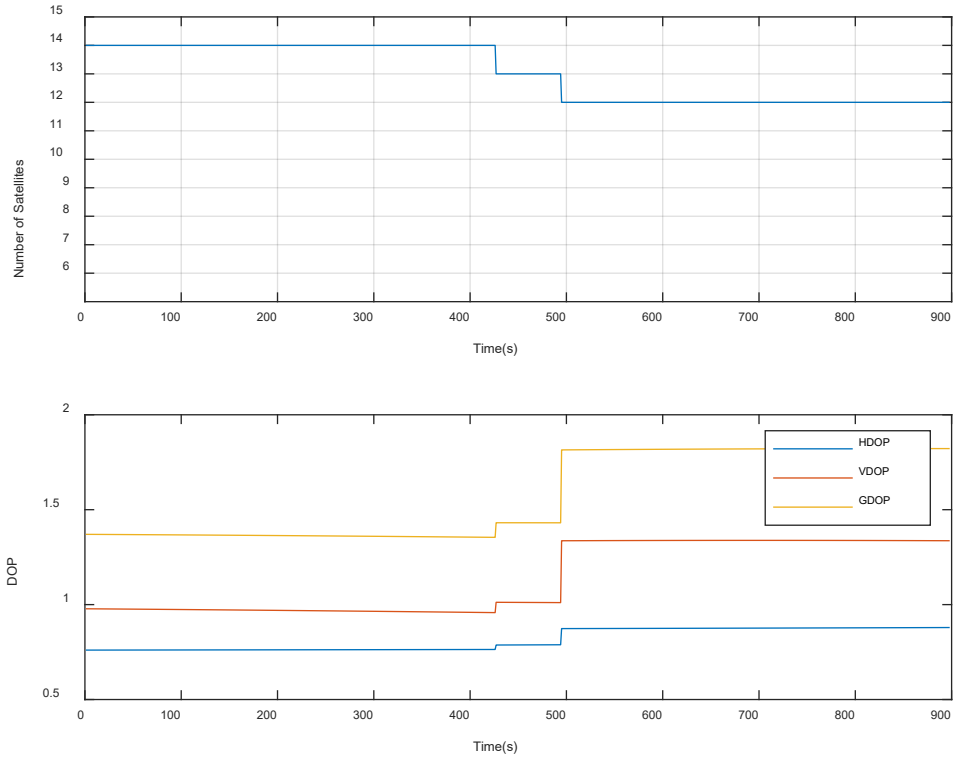

Figure 5-4 Number of SV used to generate the PVT solution and the DOP Values

5.1.1.2 TS02 – PVTI Performance Analysis (MRAIM) - DFMC

Figure 5-5, shows integrity flags, the horizontal errors and the protection level generated. It can be seen from the integrity flag plot that the GREEN flag is raised which in this case indicates that the following condition was met PL< AL, the alert limit is set to the value of 25 m.

All epochs shall be green due to a great AL value, under the MRAIM algorithm if the faults can be detected but could not be excluded, the uncertainty level is estimated and compare against the predefined AL. If the UL is less than the AL value GREEN flag raised otherwise Red Flag will be raised. This will be reflected in many of the results presented in this assessment since AL is set to 25m.

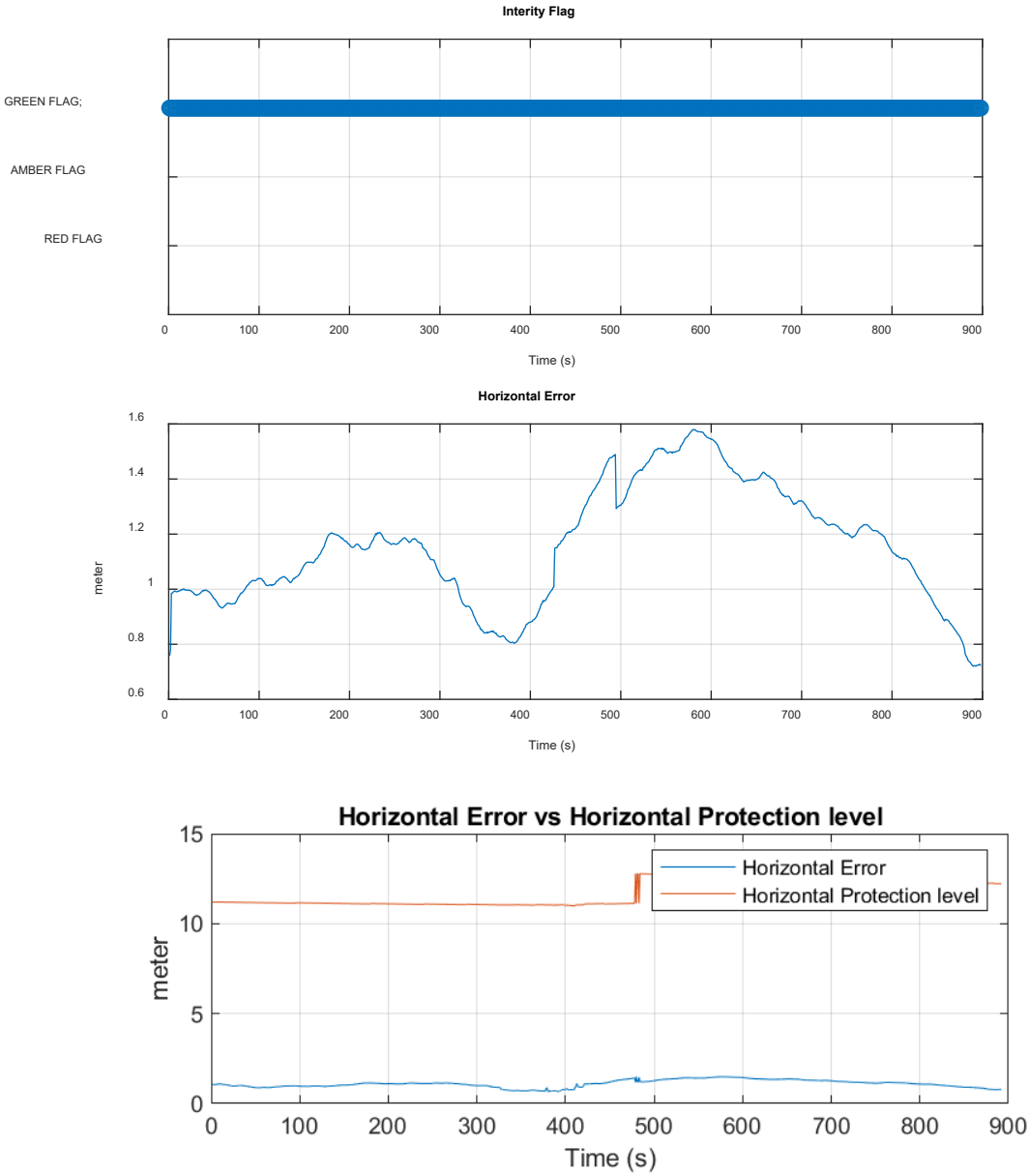

Figure 5-5 The MRAIM Integrity Flag (above), Horizontal Error(middle) and Horizontal Error vs HPL (below)

The solution performance is summarised in Table 5-2. For GPS L1/L5 and GAL E1/E5a the horizontal error is 1.44m with a percentile of 95%.

Table 5-2 TS02 - NEU and Horizontal error parameters for GPS L1/L5 and GAL E1/E5a

	MEAN (m)	STD (m)	95% (m)
North	0.045	0.239	0.393
East	1.076	0.209	1.404
Up	2.598	0.599	3.383
Horizontal	1.103	0.206	1.436

5.1.1.3 TS01a – PVTI Performance Analysis (MGRAIM) – DFMC SBAS

Figure 5-2 shows fault detection test results from Test Scenario 01a MGRAIM DFMC. Figure 5-6 illustrates test statistics and threshold values computed for the solution generated for the dataset. The test statistics and threshold values are used within Fault Detection Test as

described in full details [RD.50]. It can be seen from the graph that the test statistic does not exceed the detection threshold, when this occurs the “green light” integrity alarm/flag is raised, the average test statistic is 2.40 and the threshold is 6.48. Figure 5-7, shows integrity flags and the horizontal errors within the solution generated.

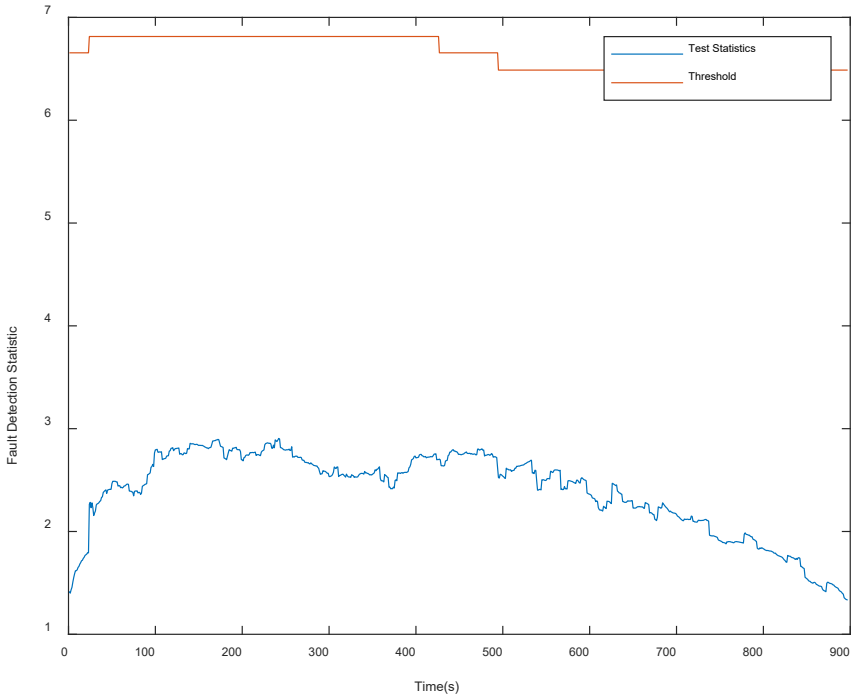

Figure 5-6 FD results from MRAIM in Ephemeris fault-free case

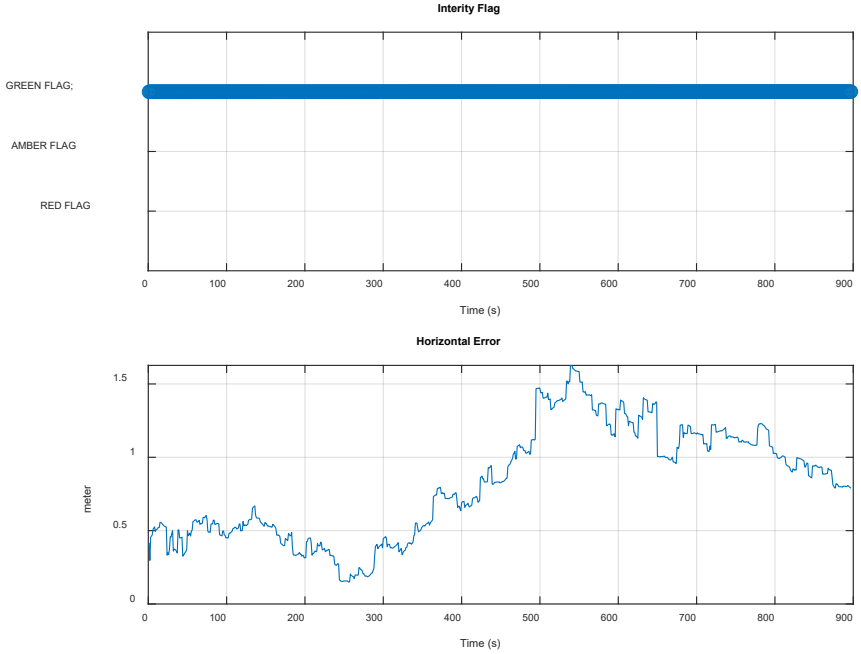

Figure 5-7 The MGRAIM Integrity Flag (above), Horizontal Error (below)

The solution performance is summarised in Table 5-1. For GPS L1/L5 and GAL E1/E5a the horizontal error is 1.44m with a percentile of 95%.

Table 5-3 TS01a - NEU and Horizontal error parameters for GPS L1/L5 and GAL E1/E5a

	MEAN (m)	STD (m)	95% (m)
North	0.045	0.239	0.393
East	1.076	0.209	1.404
Up	2.598	0.599	3.383
Horizontal	1.103	0.206	1.436

Figure 5-8 illustrate the number of satellites used to compute the PVT solution and the computed DOP.

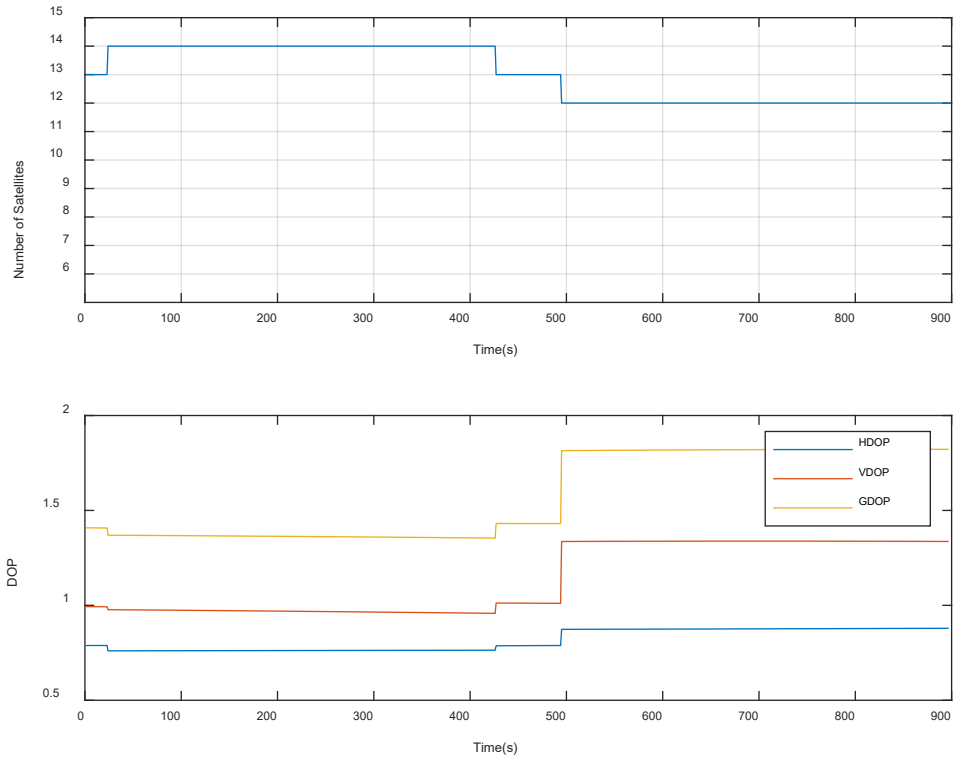

Figure 5-8 Number of SV used to generate the PVT solution and the DOP Values

5.1.1.4 TS02a – PVTI Performance Analysis (MRAIM) – DFMC SBAS

Figure 5-5, shows integrity flags, the horizontal errors and the protection level generated. It can be seen from the integrity flag plot that the GREEN flag is raised which in this case indicates that the following condition was met PL< AL, the alert limit is set to the value of 25 m.

All epochs shall be green due to a great AL value, under the MRAIM algorithm if the faults can be detected but could not be excluded, the uncertainty level is estimated and compare against the predefined AL. If the UL is less than the AL value GREEN flag raised otherwise Red Flag will be raised. This will be reflected in many of the results presented in this assessment since AL is set to 25.

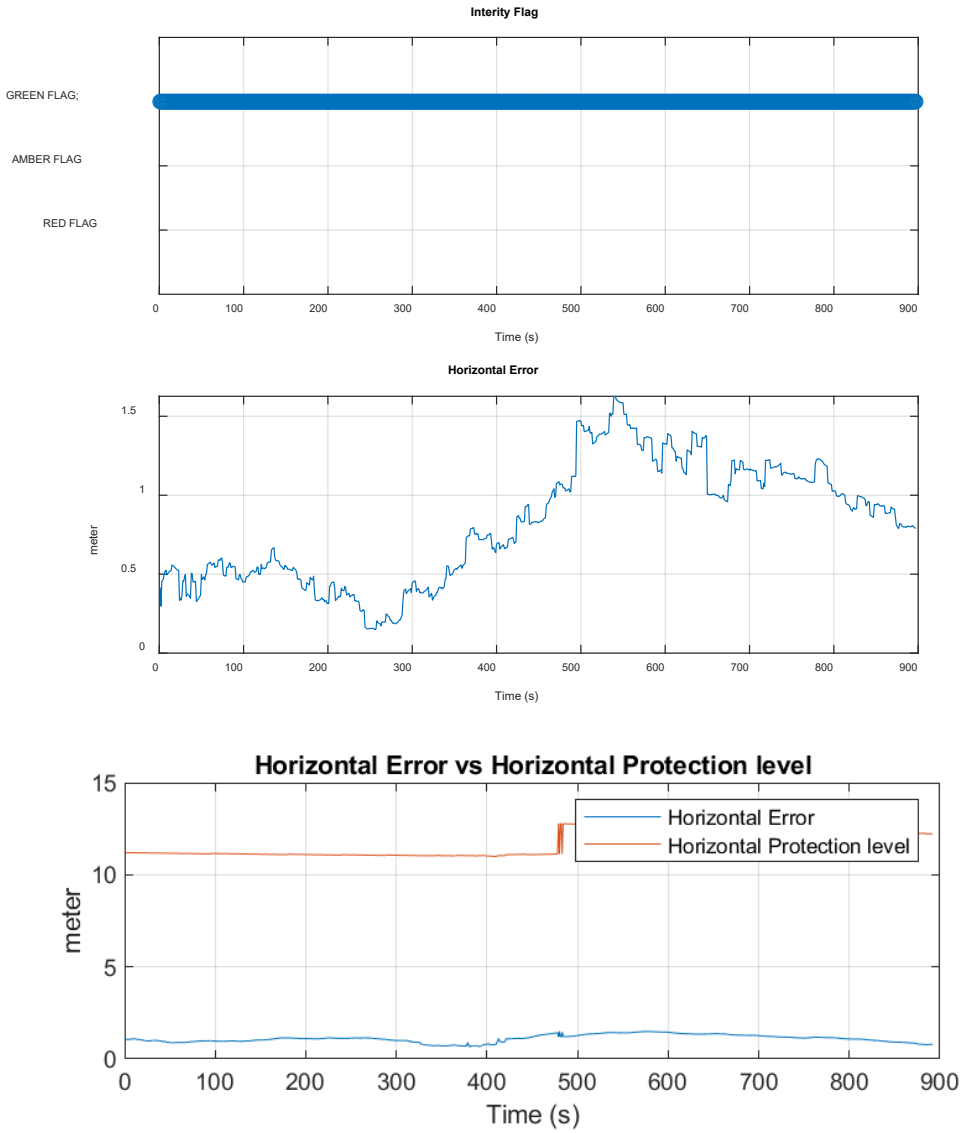

Figure 5-9 The MGRAIM Integrity Flag (above), Horizontal Error(middle) and Horizontal Error vs HPL (below)

The solution performance is summarised in Table 5-4. For GPS L1/L5 and GAL E1/E5a the horizontal error is 1.44m with a percentile of 95%.

Table 5-4 TS02a - NEU and Horizontal error parameters for GPS L1/L5 and GAL E1/E5a

	MEAN (m)	STD (m)	95% (m)
North	0.045	0.239	0.393
East	1.076	0.209	1.404
Up	2.598	0.599	3.383
Horizontal	1.103	0.206	1.436

5.1.2 Evaluation of GNSS Data with injected Ramp Error

5.1.2.1 Single High-elevation SV

The ramp-type fault refers to the slowly varying cumulative error which might be resulted in a jump in frequency and drift in the phase of the satellite clock. This subsection shows the results generated using a smoothing constant of 100 seconds based on the following test scenario:

Test Scenario	Correction mode	Fault injection	Comment
TS.03	MGRAIM DFMC	Single Satellite Clock failure (ramp) - High Elevation SV	apply ramp error on a single high-elevation SV
TS.04	MRAIM DFMC	Single Satellite Clock failure (ramp) - High Elevation SV	apply ramp error on a single high-elevation SV

Table 5-5 shows the configuration parameters and values used to create the ramp fault injection dataset. The ramp error at the speed of 0.4m/s is injected into the original pseudo-range of a single satellite from t=110s (SOW: 296228s) to t = 410s (SOW: 296528s).

Table 5-5 TS03/TS04 Configuration

Parameter	Value	Comment
Start time [GPS Week SOW]	[2229 296228];	represents the time and duration of the injection of the fault
End time [GPS Week SOW]	[2229 296528];	
Constellation	['G'];	The constellation which is affected
PRN	[3];	Satellites in which the fault was injected
Range drift	[0.4m/s]	

5.1.2.1.1 TS03 – PVTI Performance Analysis (MGRAM DFMC)

Figure 5-10 and Figure 5-11 show fault detection test results from Test Scenario 03 MGRAM DFMC. Figure 5-10 illustrates test statistics and threshold values computed for the solution generated for the dataset. The test statistics and threshold values are used within Fault Detection Test. It can be seen from the graph the point at which the test statistic exceeds the detection threshold at the point where the ramp error was injected into the file, when this occurs the “red light” integrity alarm/flag is raised. Figure 5-11, shows integrity flags and the horizontal errors within the solution generated.

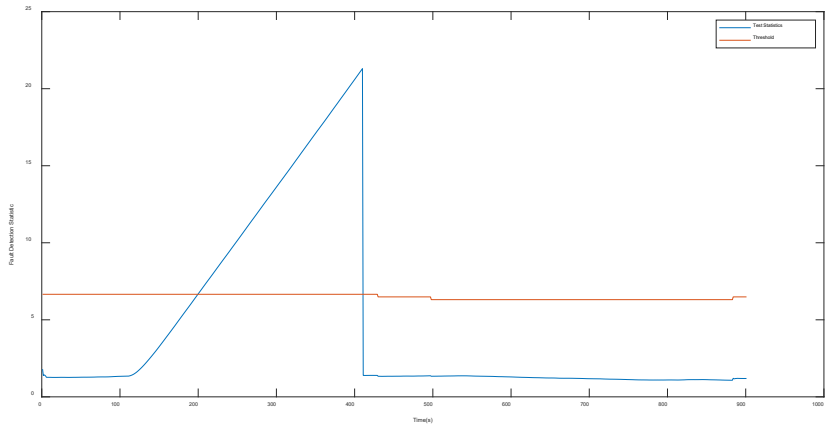

Figure 5-10 FD results from MGRAIM in ramp fault case

The results indicate that the algorithm has detected the injected fault, as the RED flag is raised, this occurred when the test-statistic exceeds the detection threshold ($t^2 > T^2$). The red flag was raised at time 200s where $t^2 = 6.682$ $T^2 = 6.656$ and ended at time 410s where $t^2 = 21.301$ $T^2 = 6.656$. The horizontal error values at these times were 15.74m and 55.78m respectively.

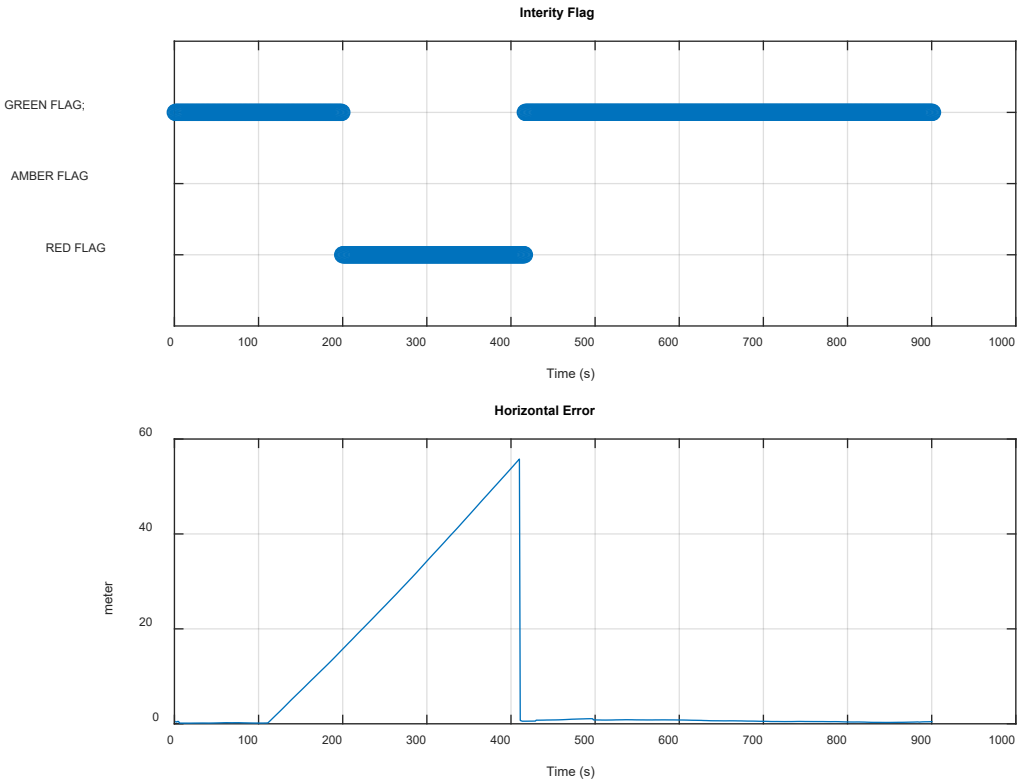

Figure 5-11 The MGRAIM Integrity Flag (above) and Horizontal Error (below).

The solution performance is summarised in Table 5-6. For GPS L1/L5 and GAL E1/E5a the horizontal error is 48.11m with a percentile of 95%.

Table 5-6 TS03 - NEU and Horizontal error parameters for GPS L1/L5 and GAL E1/E5a

	MEAN (m)	STD (m)	95% (m)
North	-7.545	13.319	39.653
East	-5.303	9.605	28.297
Up	-7.678	18.185	49.34
Horizontal	9.549	16.233	48.108

Figure 5-12 illustrate the number of satellites used to compute the PVT solution and the computed DOP.

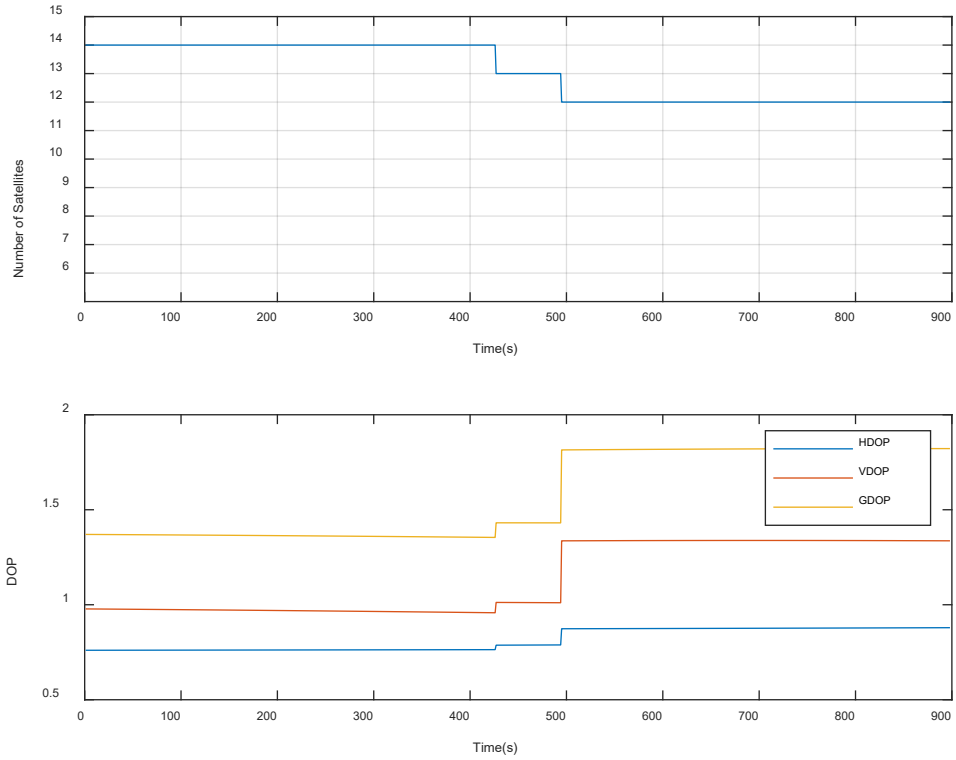

Figure 5-12 Number of SV used to generate the PVT solution and the DOP Values

5.1.2.1.2 TS04 – PVTI Performance Analysis (MRAIM DFMC)

Figure 5-13, shows integrity flags, the horizontal errors and the protection level generated using single high elevation satellite with the ramp error injected into the observation RINEX. It can be seen from the integrity flag plot that the GREEN flag is raised which in this case indicates that the following condition was met PL< AL, the alert limit is set to the value of 25 m.

It has been observed that the horizontal error produced a much smaller ramp error in magnitude and duration compared to the MGRAIM result. This can be attributed to the FDE process of the MRAIM where the Solution Separation Threshold test, the function that performs a threshold test for each subset and analyses if their separation is compatible with a failure. In that case where the configured threshold was met the faulty satellite was excluded to provide a safe positioning. Figure 5-14, shows the number of satellites is reduced due to the exclusion of the fault satellites The Positioning error generated is significantly reduced compared to MGRAIM approach.

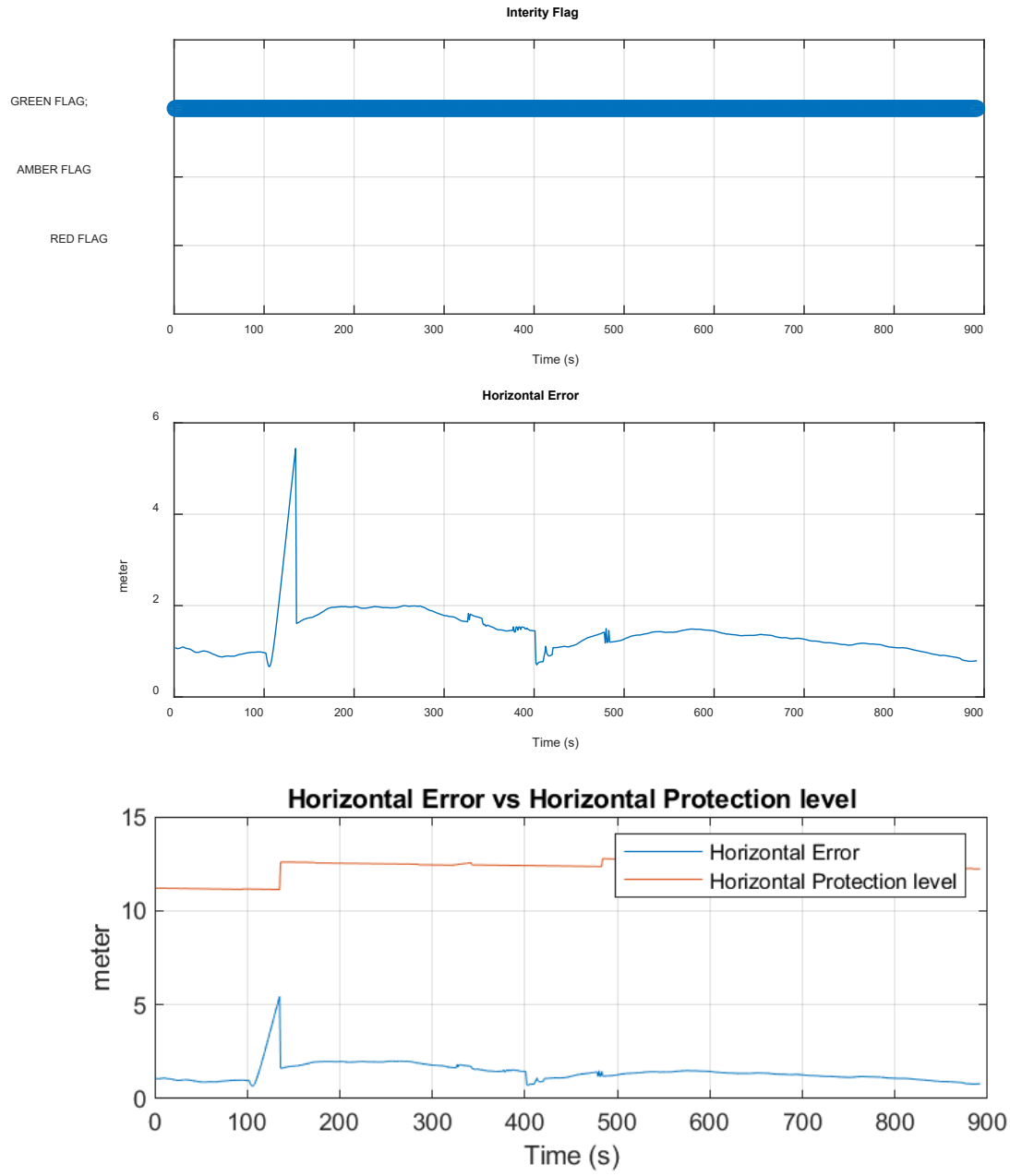

Figure 5-13 The MRAIM Integrity Flag (above), Horizontal Error (middle). and Horizontal Error vs HPL (below).

The solution performance is summarised in Table 5-7. For GPS L1/L5 and GAL E1/E5a the horizontal error is 1.98m with a percentile of 95%.

Table 5-7 TS04 - NEU and Horizontal error parameters for GPS L1/L5 and GAL E1/E5a

	MEAN (m)	STD (m)	95% (m)
North	0.169	0.781	1.158
East	1.164	0.492	1.632
Up	2.759	1.049	3.566
Horizontal	1.404	0.516	1.979

Figure 5-14 illustrate the number of satellites used to compute the PVT solution and the computed DOP.

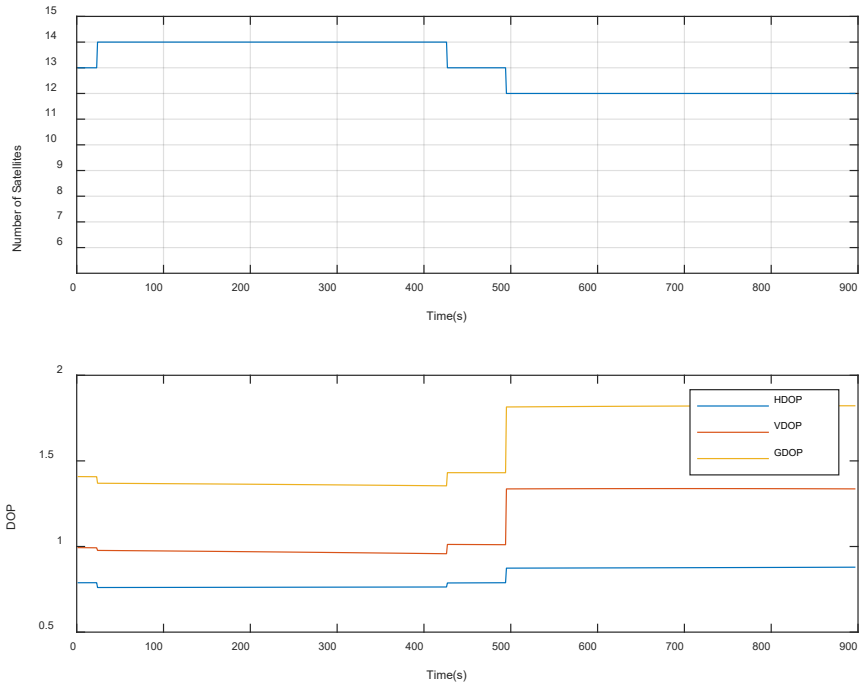

Figure 5-14 Number of SV used to generate the PVT solution and the DOP Values

5.1.2.1.3 TS03a – PVTI Performance Analysis (MGRAIM) – DFMC SBAS

Figure 5-15 and Figure 5-16 show fault detection test results from Test Scenario 03a MGRAM DFMC SBAS enabled. Figure 5-15 illustrates test statistics and threshold values computed for the solution generated for the dataset. The test statistics and threshold values are used within Fault Detection Test. It can be seen from the graph the point at which the test statistic exceeds the detection threshold at the point where the ramp error was injected into the file, when this occurs the “red light” integrity alarm/flag is raised. Figure 5-16, shows integrity flags and the horizontal errors within the solution generated.

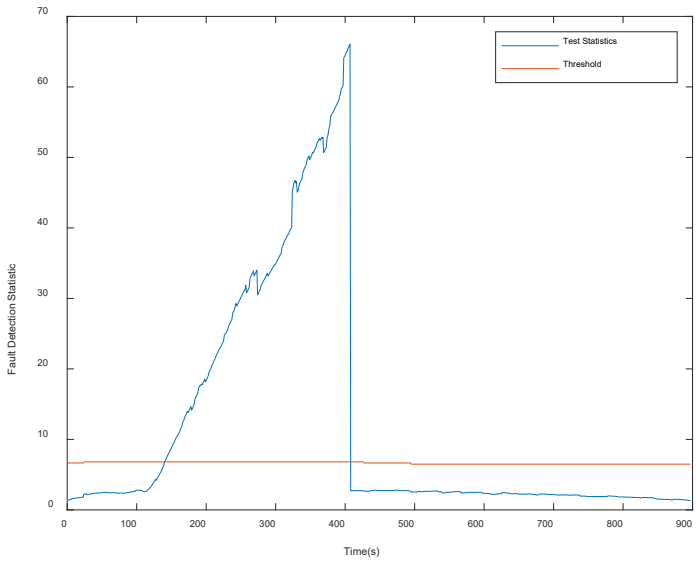

Figure 5-15 FD results from MGRAIM in ramp fault case

The results indicate that the algorithm has detected the injected fault.

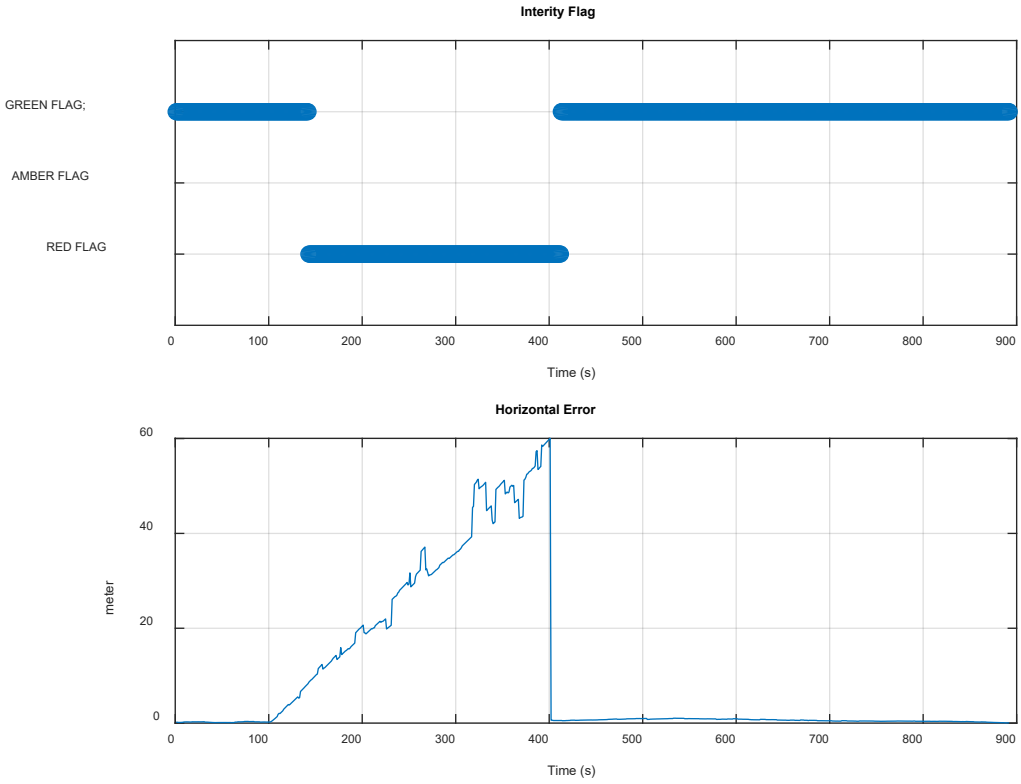

Figure 5-16 The MGRAIM Integrity Flag (above) Horizontal Error (below).

The solution performance is summarised in Table 5-8. For GPS L1/L5 and GAL E1/E5a the horizontal error is 50.08m with a percentile of 95%.

Table 5-8 TS03a - NEU and Horizontal error parameters for GPS L1/L5 and GAL E1/E5a

	MEAN (m)	STD (m)	95% (m)
North	-8.51	14.021	41.673
East	-4.876	8.981	26.999
Up	-3.888	10.111	22.978
Horizontal	9.988	16.543	50.081

Figure 5-17 illustrate the number of satellites used to compute the PVT solution and the computed DOP.

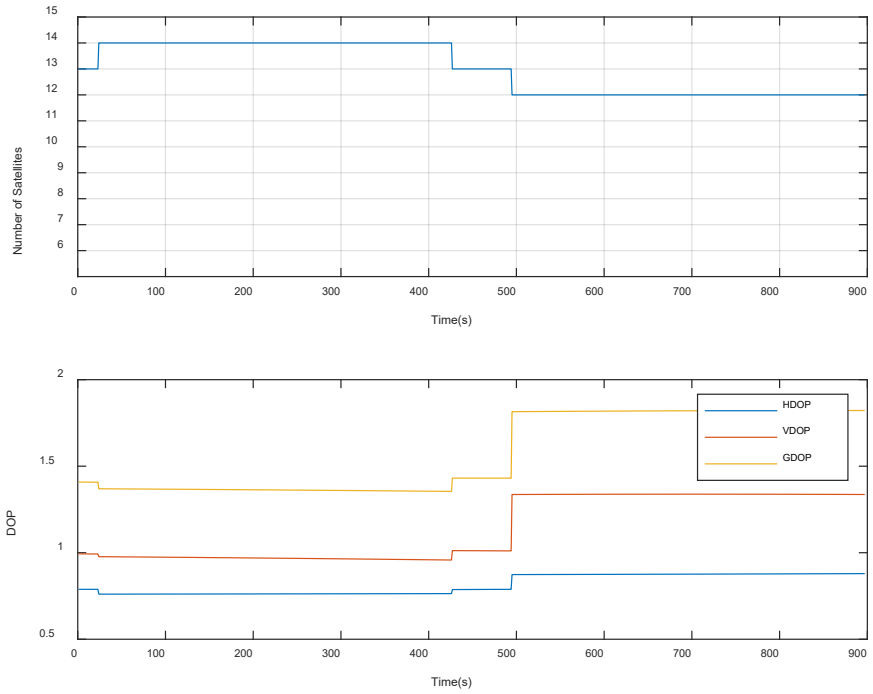

Figure 5-17 Number of SV used to generate the PVT solution and the DOP Values

5.1.2.1.4 TS04a – PVTI Performance Analysis (MRAIM) – DFMC SBAS

Figure 5-18, shows integrity flags, the horizontal errors and the protection level generated using single high elevation satellite with the ramp error injected into the observation RINEX. It can be seen from the integrity flag plot that the GREEN flag is raised which in this case indicates that the following condition was met PL< AL, the alert limit is set to the value of 25 m.

It has been observed that the horizontal error produced a much smaller ramp error in magnitude and duration compared to the MGRAIM result. This can be attributed to the FDE process of the MRAIM where the Solution Separation Threshold test, the function that performs a threshold test for each subset and analyses if their separation is compatible with a failure. In that case where the configured threshold was met the faulty satellite was excluded to provide a safe positioning. Figure 5-19, shows the number of satellites is reduced due to the exclusion of the fault satellites The Positioning error generated is significantly reduced compared to MGRAIM approach.

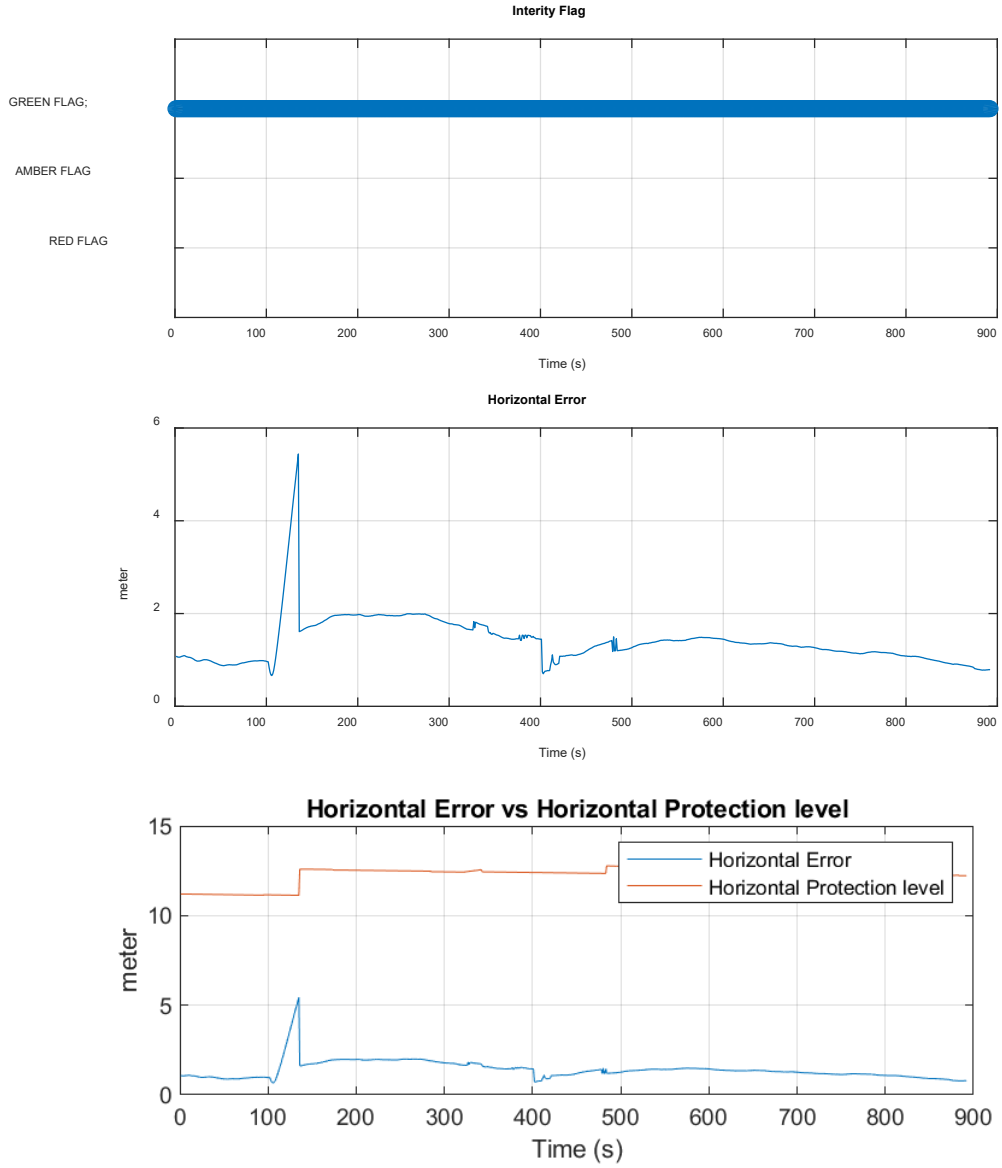

Figure 5-18 The MRAIM Integrity Flag (above), Horizontal Error (middle). and Horizontal Error vs HPL (below).

The solution performance is summarised in Table 5-9. For GPS L1/L5 and GAL E1/E5a the horizontal error is 1.98m with a percentile of 95%.

Table 5-9 TS04a - NEU and Horizontal error parameters for GPS L1/L5 and GAL E1/E5a

	MEAN (m)	STD (m)	95% (m)
North	0.169	0.781	1.158
East	1.164	0.492	1.632
Up	2.759	1.049	3.566
Horizontal	1.404	0.516	1.979

Figure 5-14 illustrate the number of satellites used to compute the PVT solution and the computed DOP.

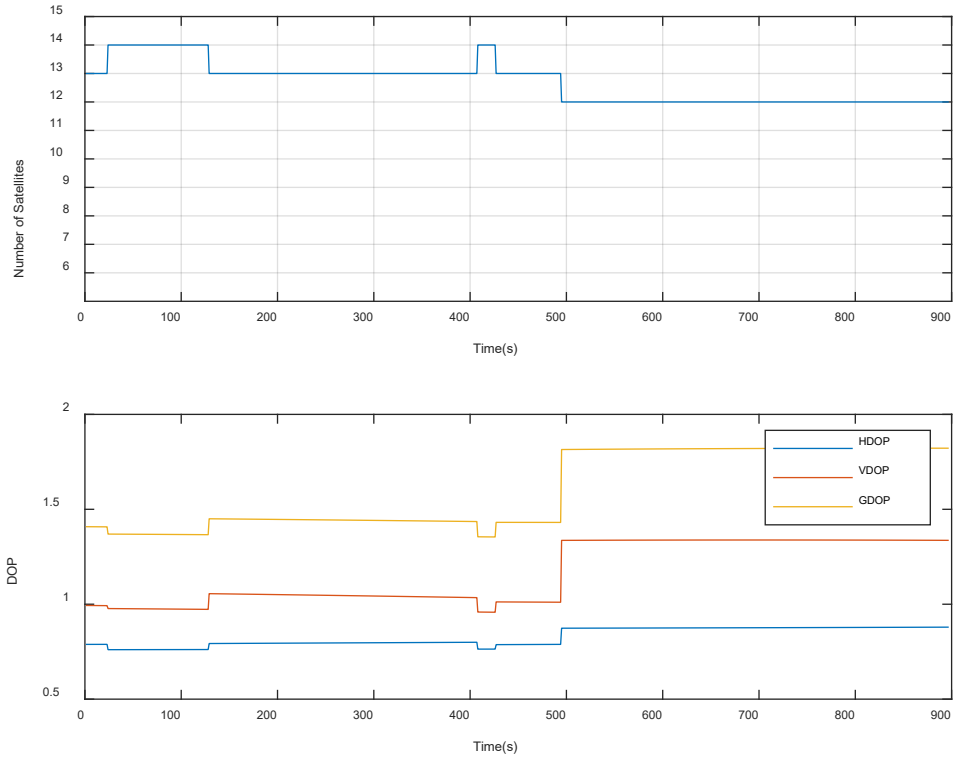

Figure 5-19 Number of SV used to generate the PVT solution and the DOP Values

5.1.2.2 Single Low-elevation SV

This subsection shows the results generated using a smoothing constant of 100 seconds for the following scenarios:

Test Scenario	Correction mode	Fault injection	Comment
TS.05	MGRAIM DFMC	Single Satellite Clock failure (ramp) - Low Elevation SV	apply ramp error on a single low-elevation SV
TS.06	MRAIM DFMC	Single Satellite Clock failure (ramp) - Low Elevation SV	apply ramp error on a single low-elevation SV

Table 5-10 shows the configuration parameters and values used to create the ramp fault injection dataset for a single low elevation satellite. The ramp error at the speed of 0.4m/s is injected into the original pseudo range of a single satellite from t=110s (SOW: 296228s) to t = 410s (SOW: 296528s).

Table 5-10 TS05/TS06 Configuration

Parameter	Value	Comment
Start time [GPS Week SOW]	[2229 296228];	represents the time and duration of the injection of the fault
End time [GPS Week SOW]	[2229 296528];	
Constellation	['G'];	The constellation on which is affected
PRN	[12];	Satellites in which the fault was injected
Range drift	[0.4m/s]	

5.1.2.2.1 TS05 – PVTI Performance Analysis (MGRAIM DFMC)

Figure 5-20 and Figure 5-21 show fault detection test results from Test Scenario 05 MGRAIM DFMC. Figure 5-20 illustrates test statistics and threshold values computed for the solution generated for the dataset. The test statistics and threshold values are used within Fault Detection Test. It can be seen from the graph that the test-statistic lies below the detection threshold $(t^2 \leq T^2)$ which indicates that all the screening process tests were performed successfully and therefore the solution is ok for use and the GREEN integrity flag is raised. Figure 5-21, shows integrity flags and the horizontal errors within the solution generated.

It has been observed that the ramp error injected on the low elevation was not detected by the MGRAIM DFMC algorithm this may be attributed to the low weighted placed on the low elevation satellite and the use of dual frequency multi-constellation signals.

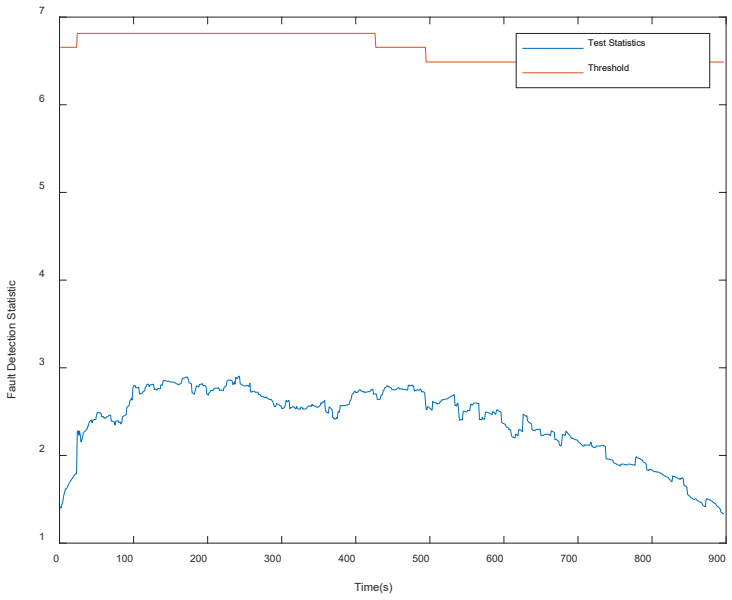

Figure 5-20 FD results from MGRAIM in ramp fault case

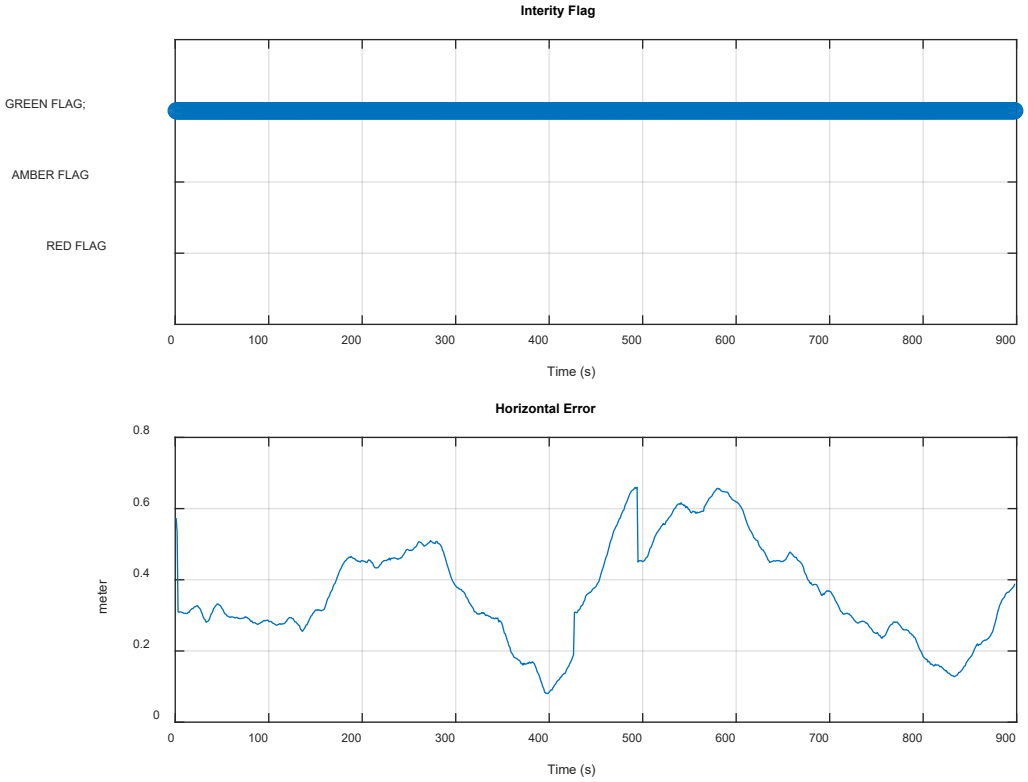

Figure 5-21 The MGRAIM Integrity Flag (above) and Horizontal Error vs HPL (below)

The solution performance is summarised in Table 5-11. For GPS L1/L5 and GAL E1/E5a the horizontal error is 0.524m with a percentile of 95%.

Table 5-11 TS05 - NEU and Horizontal error parameters for GPS L1/L5 and GAL E1/E5a

	MEAN (m)	STD (m)	95% (m)
North	0.145	0.239	0.476
East	0.127	0.209	0.455
Up	2.515	0.599	3.3
Horizontal	0.354	0.111	0.524

Figure 5-22 illustrates the number of satellites used to compute the PVT solution and the computed DOP.

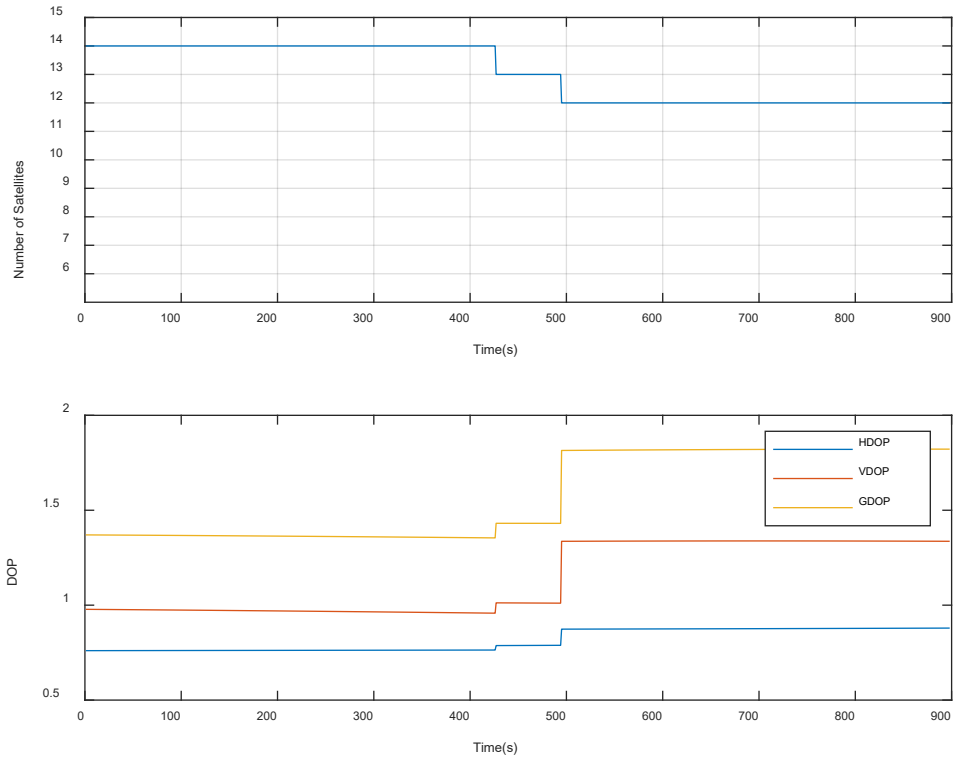

Figure 5-22 Number of SV used to generate the PVT solution and the DOP Values

5.1.2.2.2 TS06 – PVTI Performance Analysis (MRAIM DFMC)

Figure 5-23 show fault detection test results from Test Scenario 06 MRAIM DFMC, which included the integrity flags, the horizontal errors and the protection level generated. It can be seen from the integrity flag plot that the GREEN flag is raised which in this case indicates that the following condition was met PL< AL, the alert limit is set to the value of 25 m.

It has been observed that the ramp error injected on the low elevation was not detected by the MGRAIM DFMC algorithm this may be attributed to the low weighted placed on the low elevation satellite and the use of dual frequency multi-constellation signals.

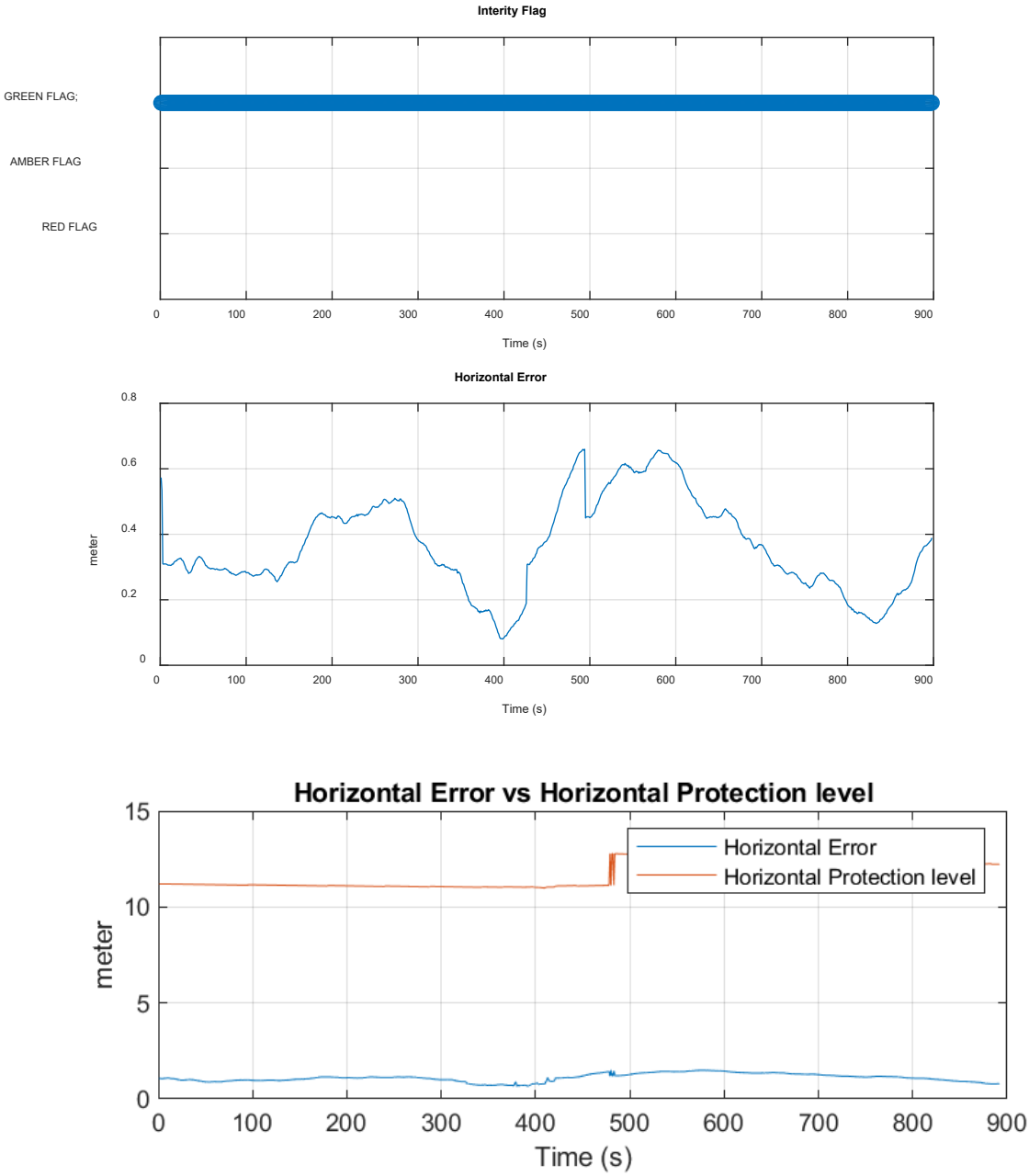

Figure 5-23 The MRAIM Integrity Flag (above) and Horizontal Error vs HPL (below)

The solution performance is summarised in Table 5-12. For GPS L1/L5 and GAL E1/E5a the horizontal error is 1.44m with a percentile of 95%.

Table 5-12 TS06 - NEU and Horizontal error parameters for GPS L1/L5 and GAL E1/E5a

	MEAN (m)	STD (m)	95% (m)
North	0.045	0.239	0.393
East	1.076	0.209	1.404
Up	2.598	0.599	3.383
Horizontal	1.103	0.206	1.436

5.1.2.2.3 TS05a – PVTI Performance Analysis (MGRAIM) – DFMC SBAS

Figure 5-24 and Figure 5-25 show fault detection test results from Test Scenario 05a MGRAIM DFMC. Figure 5-24 illustrates test statistics and threshold values computed for the solution generated for the dataset. The test statistics and threshold values are used within Fault Detection Test. It can be seen from the graph that the test-statistic lies below the detection threshold $(t^2 \leq T^2)$ which indicates that all the screening process tests were performed successfully and therefore the solution is ok for use and the GREEN integrity flag is raised. Figure 5-25, shows integrity flags and the horizontal errors within the solution generated.

It has been observed that the ramp error injected on the low elevation was not detected by the MGRAIM DFMC algorithm this may be attributed to the low weighted placed on the low elevation satellite and the use of dual frequency multi-constellation signals.

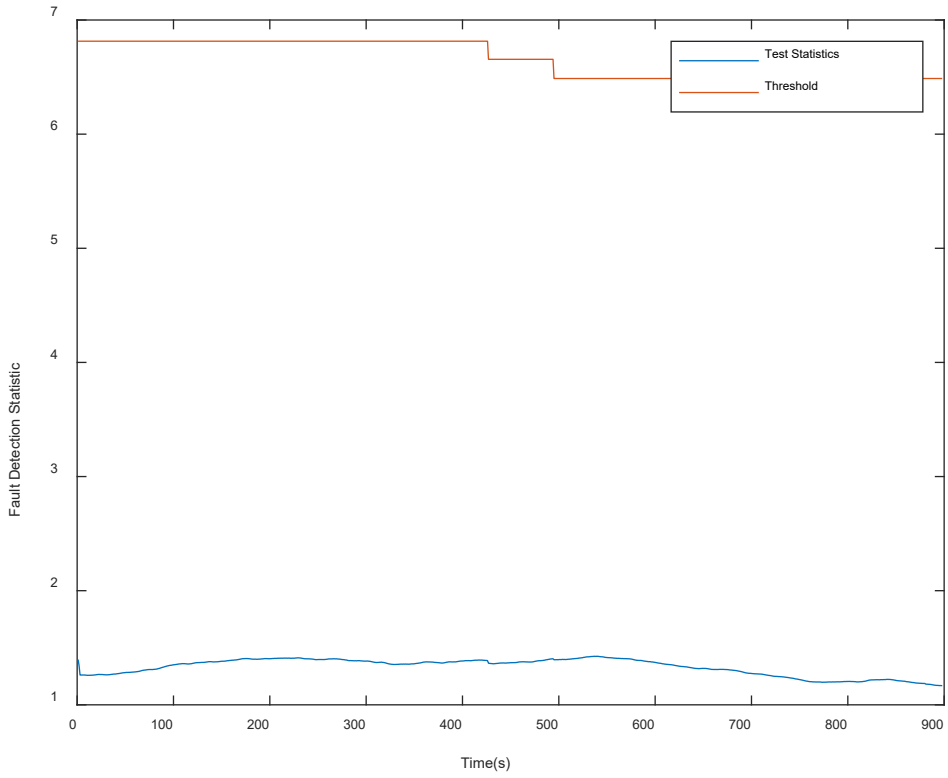

Figure 5-24 FD results from MGRAIM in ramp fault case

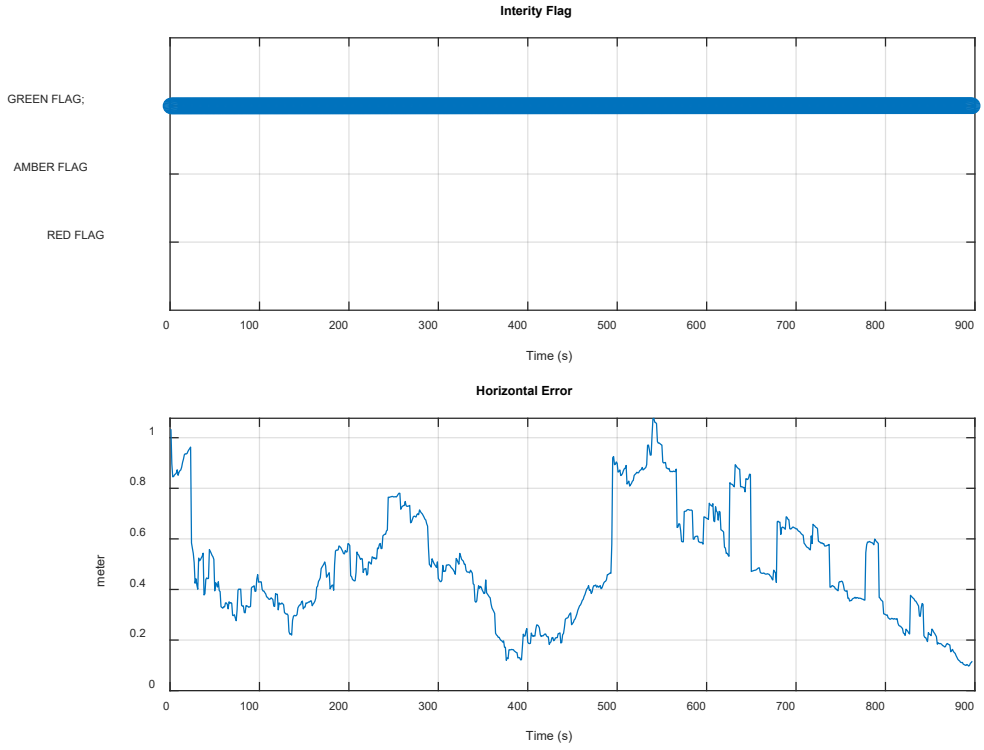

Figure 5-25 The MGRAIM Integrity Flag (above) and Horizontal Error (below)

The solution performance is summarised in Table 5-13. For GPS L1/L5 and GAL E1/E5a the horizontal error is 0.92m with a percentile of 95%.

Table 5-13 TS05a - NEU and Horizontal error parameters for GPS L1

	MEAN (m)	STD (m)	95% (m)
North	-0.357	0.27	0.837
East	0.246	0.11	0.416
Up	2.034	0.679	3.223
Horizontal	0.468	0.233	0.924

Figure 5-22 illustrates the number of satellites used to compute the PVT solution and the computed DOP.

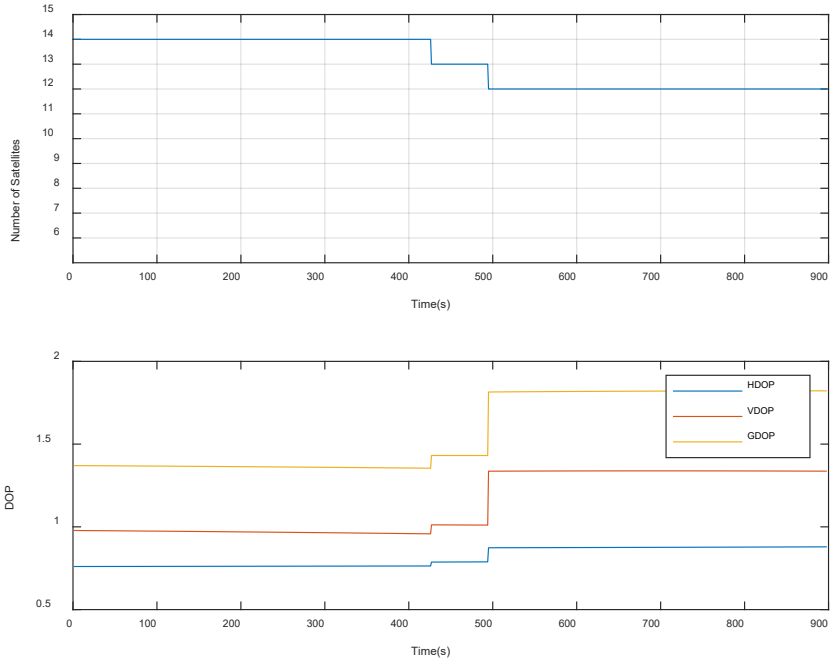

Figure 5-26 Number of SV used to generate the PVT solution and the DOP Values

5.1.2.2.4 TS06a – PVTI Performance Analysis (MRAIM) – DFMC SBAS

Figure 5-27 show fault detection test results from Test Scenario 06a MRAIM DFMC, which included the integrity flags, the horizontal errors and the protection level generated. It can be seen from the integrity flag plot that the GREEN flag is raised which in this case indicates that the following condition was met PL< AL, the alert limit is set to the value of 25 m.

It has been observed that the ramp error injected on the low elevation was not detected by the MRAIM DFMC algorithm this may be attributed to the low weighted placed on the low elevation satellite and the use of dual frequency multi-constellation signals.

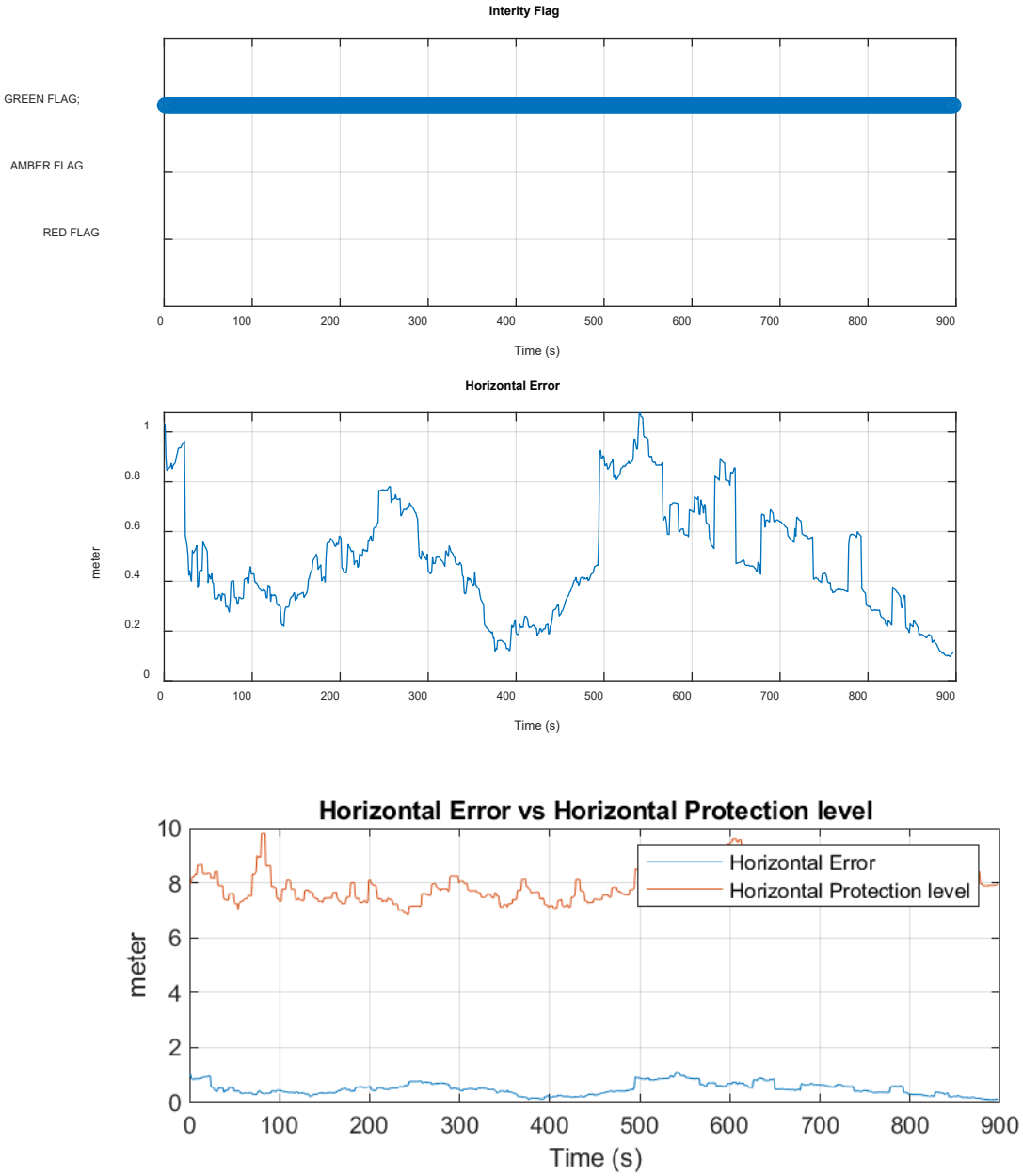

Figure 5-27 The MRAIM Integrity Flag (above) and Horizontal Error vs HPL (below)

The solution performance is summarised in Table 5-14. For GPS L1/L5 and GAL E1/E5a the horizontal error is 1.63m with a percentile of 95%.

Table 5-14 TS06a - NEU and Horizontal error parameters for GPS L1/L5 and GAL E1/E5a

	MEAN (m)	STD (m)	95% (m)
North	-0.457	0.27	0.936
East	1.195	0.11	1.364
Up	2.116	0.679	3.306
Horizontal	1.301	0.173	1.630

5.1.2.3 Multiple High-elevation SV

This subsection shows the results generated using a smoothing constant of 100 seconds based on the following test scenario:

Test Scenario	Correction mode	Fault injection	Comment
TS.07	MGRAIM DFMC	Multiple Satellite Clock failure (ramp) - High Elevation SV	apply ramp error on 2 high-elevation SV
TS.08	MGRAIM DFMC	Multiple Satellite Clock failure (ramp) - High Elevation SV	apply ramp error on a 2 high-elevation SV

Table 5-15 shows the configuration parameters and values used to create the ramp fault injection dataset. The ramp error at the speed of 0.4m/s is injected into the original pseudo-range of a satellite from t=110s (SOW: 296228s) to t = 410s (SOW: 296528s) and a second satellite from t=908s (SOW: 297026s) to t = 1208s (SOW: 297326s).

Table 5-15 TS07/TS08 Configuration

Parameter	Value	Comment
Start time [GPS Week SOW]	[2229 296228], [2229 297026];	represents the time and duration of the injection of the fault
End time [GPS Week SOW]	[2229 296528], [2229 297326];	
Constellation	['G'];	The constellation which is affected
PRN	[3], [6];	Satellites in which the fault was injected
Range drift	[0.4m/s]	

5.1.2.3.1 TS07– PVTI Performance Analysis (MGRAIM DFMC)

Figure 5-28 and Figure 5-29 show fault detection test results from Test Scenario 07 MGRAM DFMC. Figure 5-28 illustrates test statistics and threshold values computed for the solution generated for the dataset. The test statistics and threshold values are used within Fault Detection Test. It can be seen from the graph the point at which the test statistic exceeds the detection threshold at the point where the ramp error was injected into the file, when this occurs the “red light” integrity alarm/flag is raised. Figure 5-29, shows integrity flags and the horizontal errors within the solution generated.

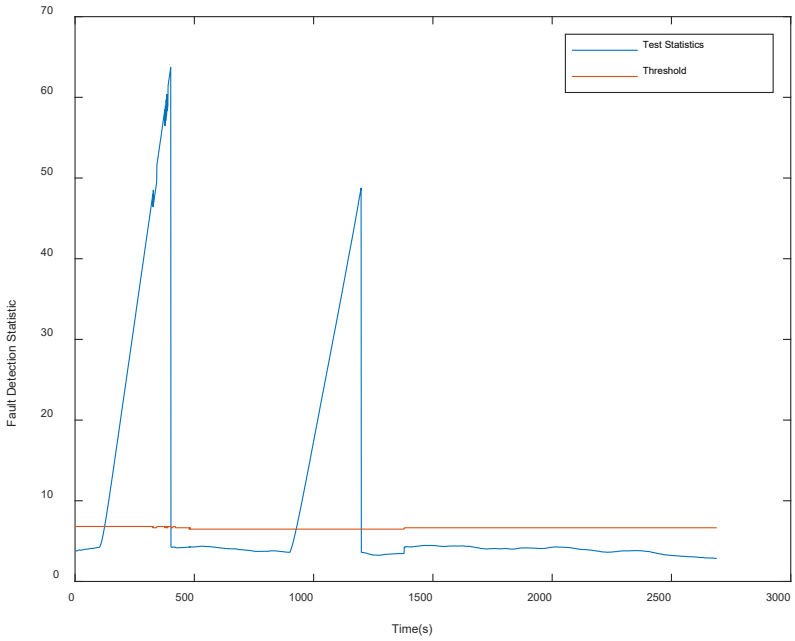

Figure 5-28 FD results from MGRAIM in ramp fault case

The results indicate that the algorithm has detected the injected fault, as the RED flag is raised, this occurred when the test-statistic exceeds the detection threshold ($t^2 > T^2$). The red flag was raised at time 211s where $t^2 = 6.834$ $T^2 = 6.814$ and ended at time 410s where $t^2 = 63.69$ $T^2 = 6.814$. The horizontal error values at these times were 3.427m and 56.440m respectively. The red flag was raised again at time 998s where $t^2 = 6.617$ $T^2 = 6.488$ and ended at time 1208s where $t^2 = 48.759$ $T^2 = 6.488$. The horizontal error values at these times were 5.239m and 52.187m respectively.

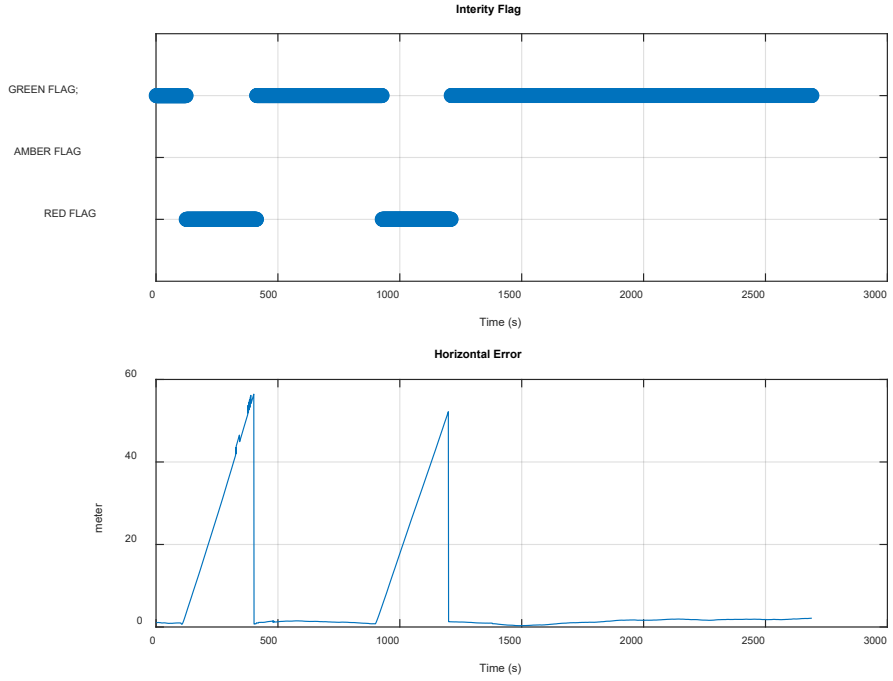

Figure 5-29 The MGRAIM Integrity Flag (above) and Horizontal Error (below).

The solution performance is summarised in Table 5-16. For GPS L1/L5 and GAL E1/E5a the horizontal error is 41.80m with a percentile of 95%.

Table 5-16 TS07 - NEU and Horizontal error parameters for GPS L1/L5 and GAL E1/E5a

	MEAN (m)	STD (m)	95% (m)
North	-3.587	9.949	27.777
East	1.432	10.241	28.705
Up	-0.193	11.785	30.485
Horizontal	7.012	13.023	41.795

Figure 5-30 illustrate the number of satellites used to compute the PVT solution and the computed DOP.

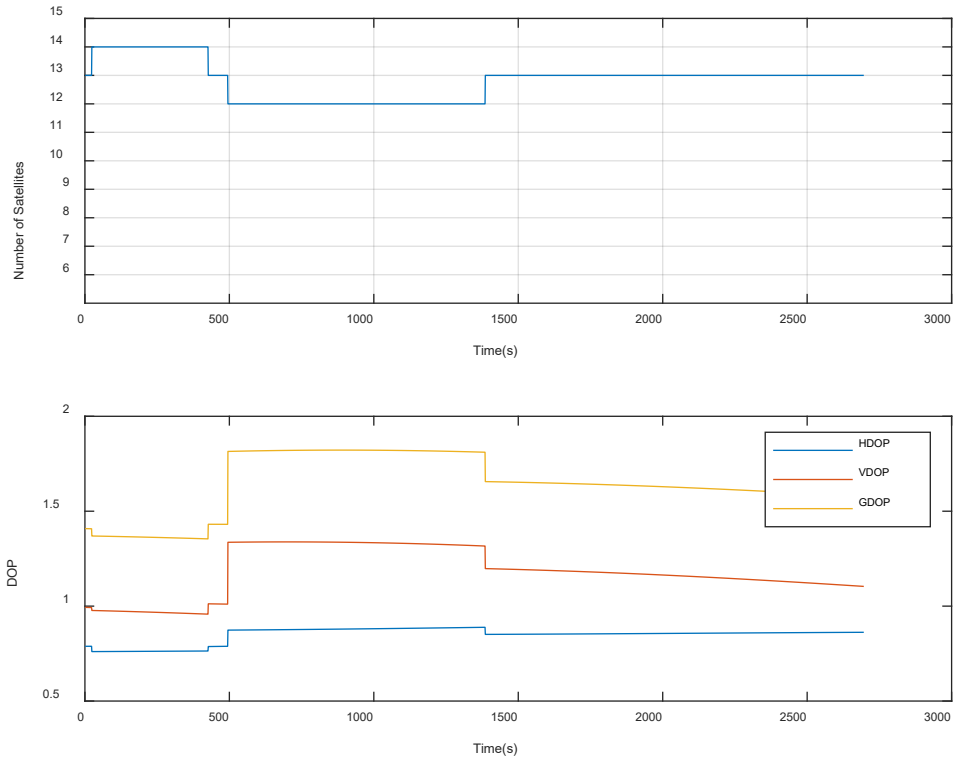

Figure 5-30 Number of SV used to generate the PVT solution and the DOP Values

5.1.2.3.2 TS08 – PVTI Performance Analysis (MRAIM DFMC)

Figure 5-31, shows integrity flags, the horizontal errors and the protection level generated. It can be seen from the integrity flag plot that the GREEN flag is raised which in this case indicates that the following condition was met PL< AL, the alert limit is set to the value of 25 m.

It has been observed that the horizontal error produced a much smaller ramp error in magnitude and duration compared to the MGRAIM result, also the second fault has been eliminated. This can be attributed to the FDE process of the MRAIM where the Solution Separation Threshold test, the function that performs a threshold test for each subset and analyses if their separation is compatible with a failure. In that case where the configured threshold was met the faulty satellite was excluded to provide a safe positioning. Figure 5-32, shows the number of satellites is reduced due to the exclusion of the fault satellites The Positioning error generated is significantly reduced compared to MGRAIM approach.

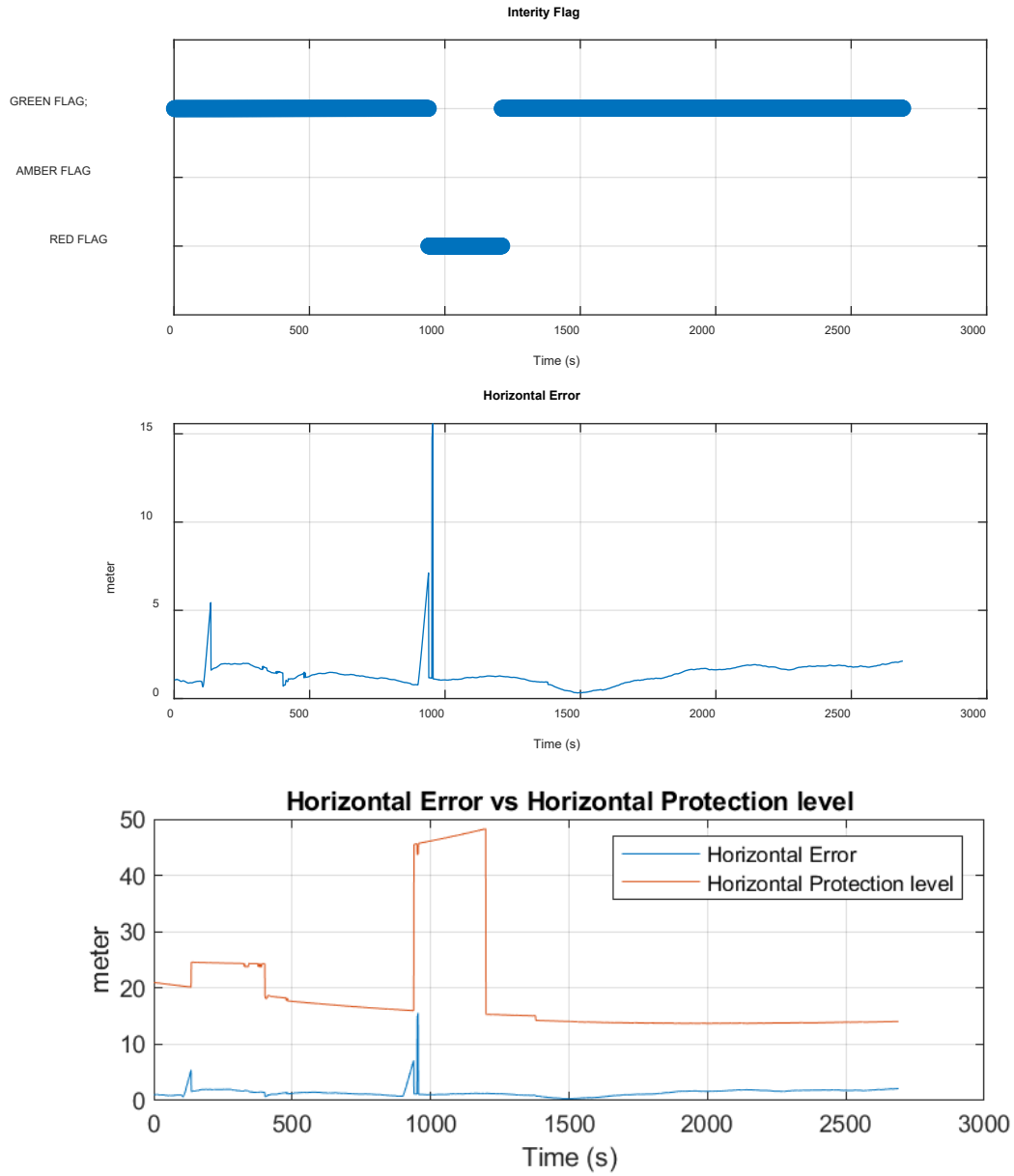

Figure 5-31 The MRAIM Integrity Flag (above), Horizontal Error (middle). and Horizontal Error vs HPL (below).

The solution performance is summarised in Table 5-17. For GPS L1/L5 and GAL E1/E5a the horizontal error is 1.98m with a percentile of 95%.

Table 5-17 TS08 - NEU and Horizontal error parameters for GPS L1/L5 and GAL E1/E5a

	MEAN (m)	STD (m)	95% (m)
North	+0.709	0.937	1.526
East	+0.943	0.646	1.618
Up	+3.325	1.678	6.482
Horizontal	1.422	0.816	1.977

Figure 5-32 illustrate the number of satellites used to compute the PVT solution and the computed DOP.

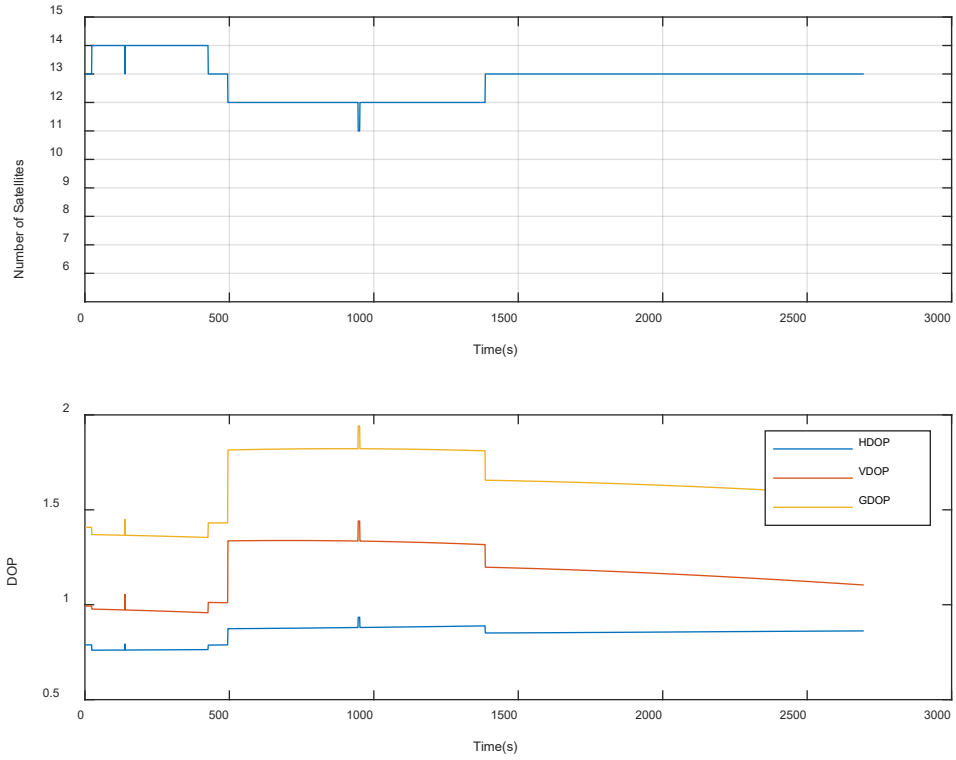

Figure 5-32 Number of SV used to generate the PVT solution and the DOP Values

5.1.2.3.3 TS07a – PVTI Performance Analysis (MGRAIM) – DFMC SBAS

Figure 5-33 and Figure 5-34 show fault detection test results from Test Scenario 07a MGRAM DFMC. v illustrates test statistics and threshold values computed for the solution generated for the dataset. The test statistics and threshold values are used within Fault Detection Test. It can be seen from the graph the point at which the test statistic exceeds the detection threshold at the point where the ramp error was injected into the file, when this occurs the “red light” integrity alarm/flag is raised. Figure 5-34, shows integrity flags and the horizontal errors within the solution generated.

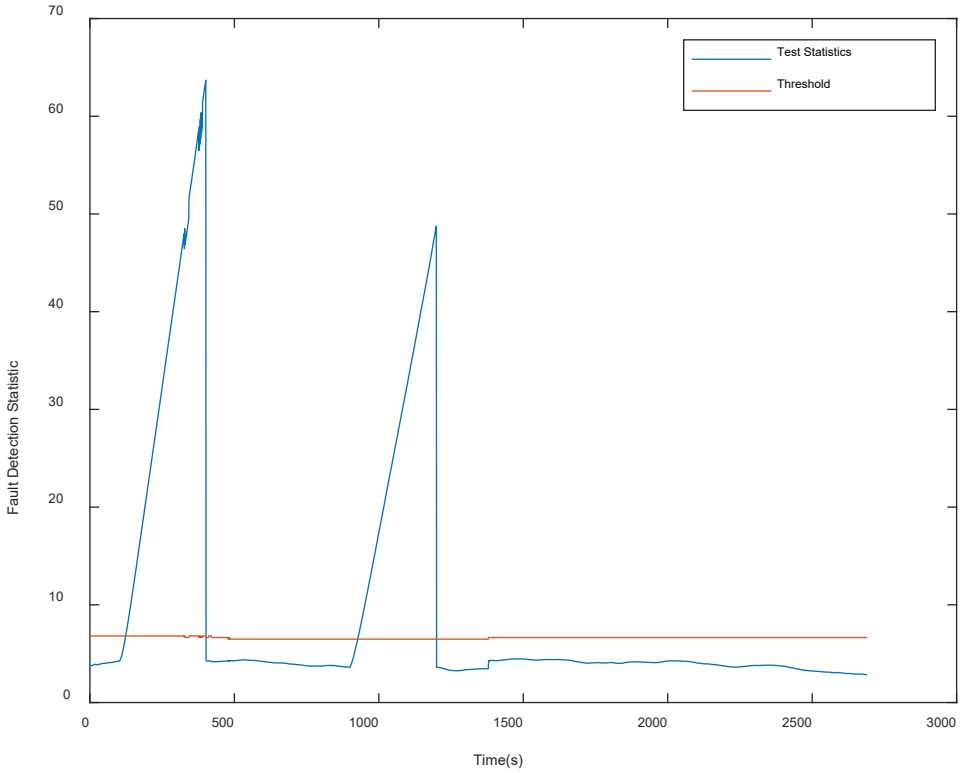

Figure 5-33 FD results from MGRAIM in ramp fault case

The results indicate that the algorithm has detected the injected fault, as the RED flag is raised, this occurred when the test-statistic exceeds the detection threshold ($t^2 > T^2$). The red flag was raised at time 211s where $t^2 = 6.834$ $T^2 = 6.814$ and ended at time 410s where $t^2 = 63.69$ $T^2 = 6.814$. The horizontal error values at these times were 3.427m and 56.440m respectively. The red flag was raised again at time 998s where $t^2 = 6.617$ $T^2 = 6.488$ and ended at time 1208s where $t^2 = 48.759$ $T^2 = 6.488$. The horizontal error values at these times were 5.239m and 52.187m respectively.

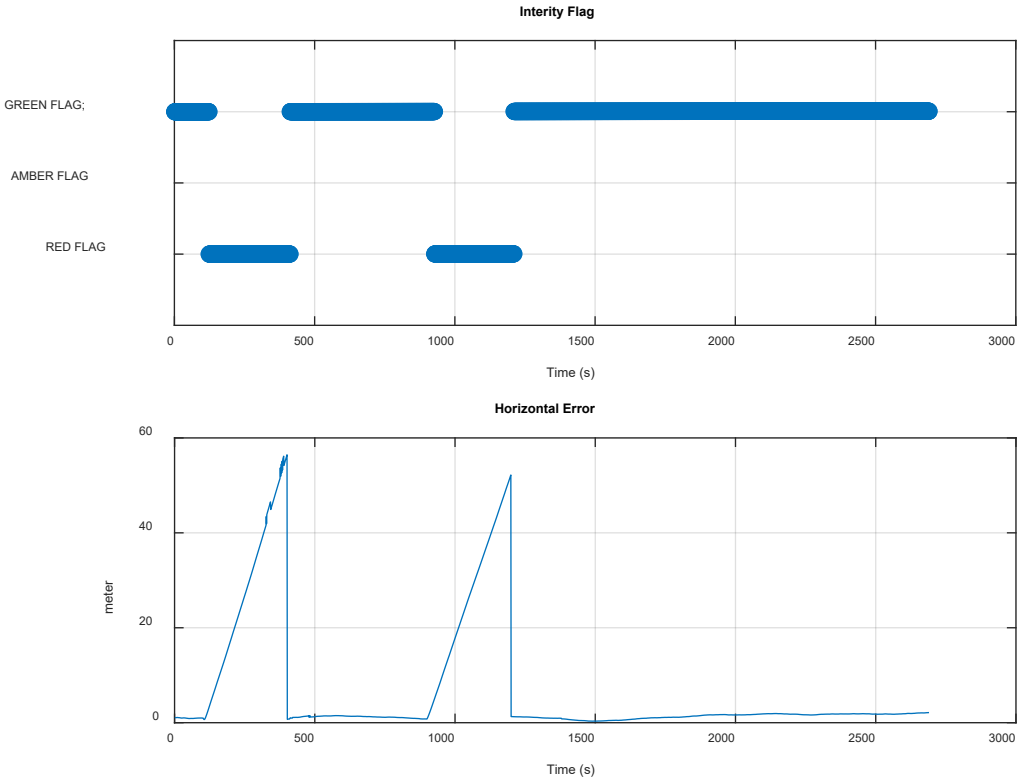

Figure 5-34 The MGRAIM Integrity Flag (above) and Horizontal Error (below).

The solution performance is summarised in Table 5-18. For GPS L1/L5 and GAL E1/E5a the horizontal error is 41.80m with a percentile of 95%.

Table 5-18 TS07a - NEU and Horizontal error parameters for GPS L1/L5 and GAL E1/E5a

	MEAN (m)	STD (m)	95% (m)
North	-3.587	9.949	27.777
East	1.432	10.241	28.705
Up	-0.193	11.785	30.485
Horizontal	7.012	13.023	41.795

Figure 5-35 illustrate the number of satellites used to compute the PVT solution and the computed DOP.

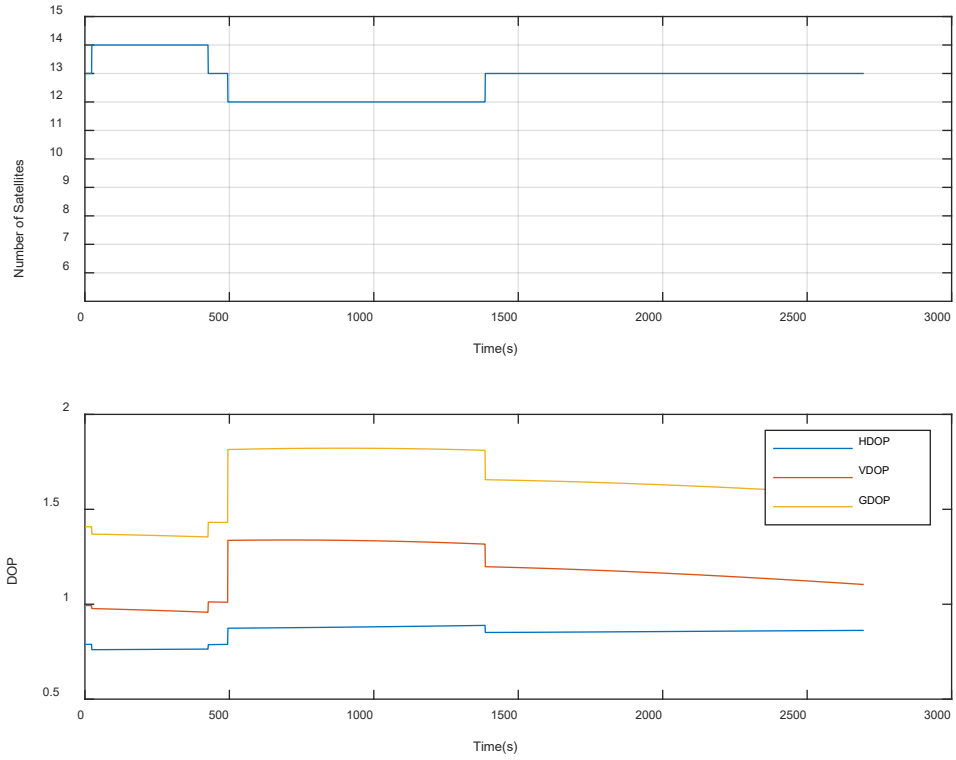

Figure 5-35 Number of SV used to generate the PVT solution and the DOP Values

5.1.2.3.4 TS08a – PVTI Performance Analysis (MRAIM) – DFMC SBAS

Figure 5-36, shows integrity flags, the horizontal errors and the protection level generated. It can be seen from the integrity flag plot that the GREEN flag is raised which in this case indicates that the following condition was met PL< AL, the alert limit is set to the value of 25m. Figure 5-37, shows the number of satellites is reduced due to the exclusion of the fault satellites.

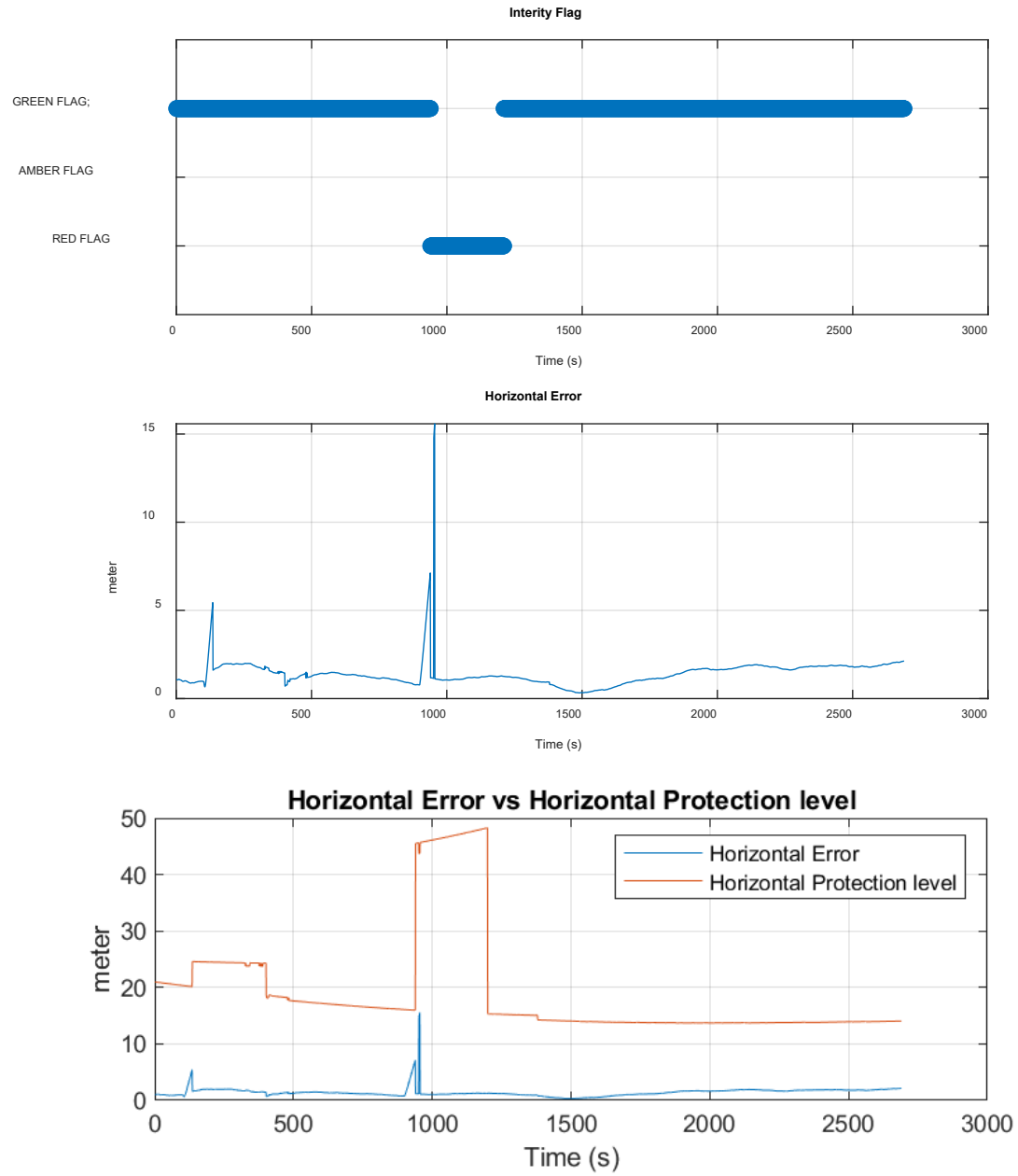

Figure 5-36 The MRAIM Integrity Flag (above), Horizontal Error (middle). and Horizontal Error vs HPL (below).

The solution performance is summarised in Table 5-7. For GPS L1/L5 and GAL E1/E5a the horizontal error is 1.98m with a percentile of 95%.

Table 5-19 TS04 - NEU and Horizontal error parameters for GPS L1/L5 and GAL E1/E5a

	MEAN (m)	STD (m)	95% (m)
North	+0.709	0.937	1.526
East	+0.943	0.646	1.618
Up	+3.325	1.678	6.482
Horizontal	1.422	0.816	1.977

Figure 5-14 illustrate the number of satellites used to compute the PVT solution and the computed DOP.

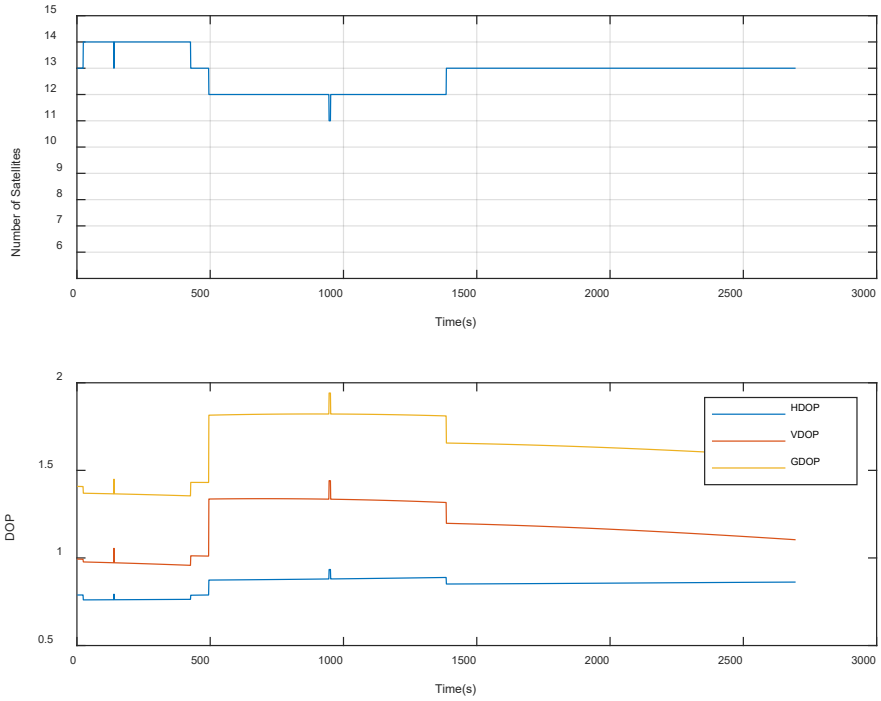

Figure 5-37 Number of SV used to generate the PVT solution and the DOP Values

5.1.3 Evaluation of GNSS Data with injected Bias Error

5.1.3.1 Single High-elevation SV

The bias fault is a basic class of GNSS anomaly, which is usually caused by the phase jump of satellite clocks or another additive fault like signal multipath. It may lead to a substantial, virtually instant shift in the user's position even by hundreds of meters.

This subsection shows the results generated using a smoothing constant of 100 seconds based on the following test scenario:

Test Scenario	*Correction mode*	*Fault injection*	*Comment*
TS.09	MGRAIM DFMC	Single Satellite Clock failure (bias) - High Elevation SV	Applying a bias error on a single high-elevation SV
TS.10	MRAIM DFMC	Single Satellite Clock failure (bias) - High Elevation SV	apply bias error on a single high-elevation SV

The subsection will look at the results generated using the minimum and a large detectable bias error that will raise a RED integrity flag as well as a bias value that will raise GREEN flag these values were extracted from the ramp error analysis conducted in [RD.49]. Table 5-20 shows the configuration parameters and values used to create the bias fault injection dataset. A fault bias of 35m, 36.8m and 100m was injected at times t=110s, t=908s and t =1808s in a high-elevation satellite G03.

Table 5-20 TS09/TS10 Configuration MGRAIM DFMC case

Parameter	*Value*	*Comment*
Start time [SOW]	[297026, 296228, 297926]	represents the time and duration of the injection of the fault
End time [SOW]	[297326, 296528, 298226]	
Constellation	['G'];	The constellation on which is affected
PRN	[3];	Satellites in which the fault was injected
Range bias	[35, 36.8, 100];	fault bias values injected into the RINEX file.

5.1.3.1.1 TS09– PVTI Performance Analysis (MGRAIM DFMC)

Figure 5-38 and Figure 5-39 show fault detection test results from Test Scenario 09 MGRAIM DFMC. Figure 5-38 illustrates test statistics and threshold values computed for the solution generated for the dataset. The test statistics and threshold values are used within Fault Detection Test. It can be seen from the graph the point at which the test statistic exceeds the detection threshold, when this occurs the "red light" integrity alarm/flag is raised. Figure 5-39, shows integrity flags and the horizontal errors within the solution generated.

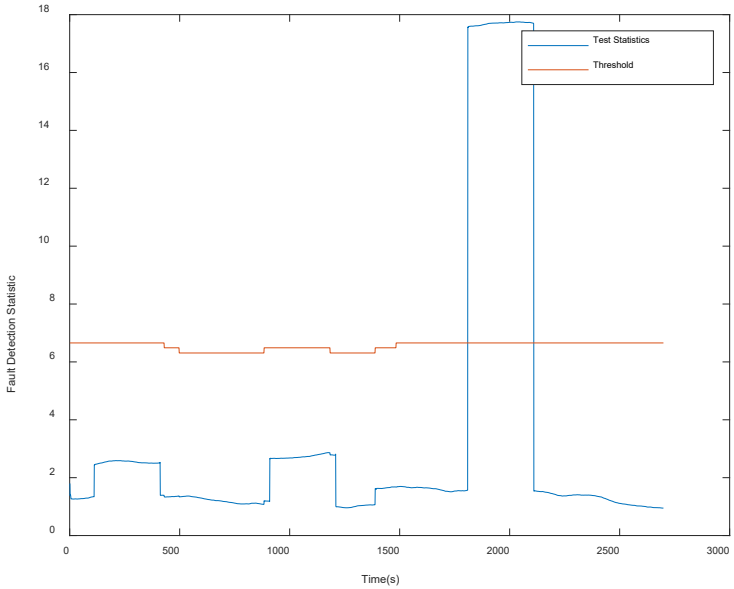

Figure 5-38 FD results from MGRAIM in bias fault case

The results indicate that the algorithm has detected the injected fault. It has been observed that the fault biases of 35m, 36.8m were detected but as seen from Figure 5-38 the test-statistic lies below the detection threshold ($t^2 \leq T^2$) raising a GREEN integrity flag. However, in the case of the fault bias of 100m a RED flag was raised, this occurs when the test statistic exceeds the detection threshold ($t^2 > T^2$). The red flag was raised at time 1807s where $t^2 = 17.57 > T^2 = 6.66$ and ended at time 2106s where $t^2 = 17.69 > T^2 = 6.66$ .. Figure 5-39, shows integrity flags and the horizontal errors within the solution generated.

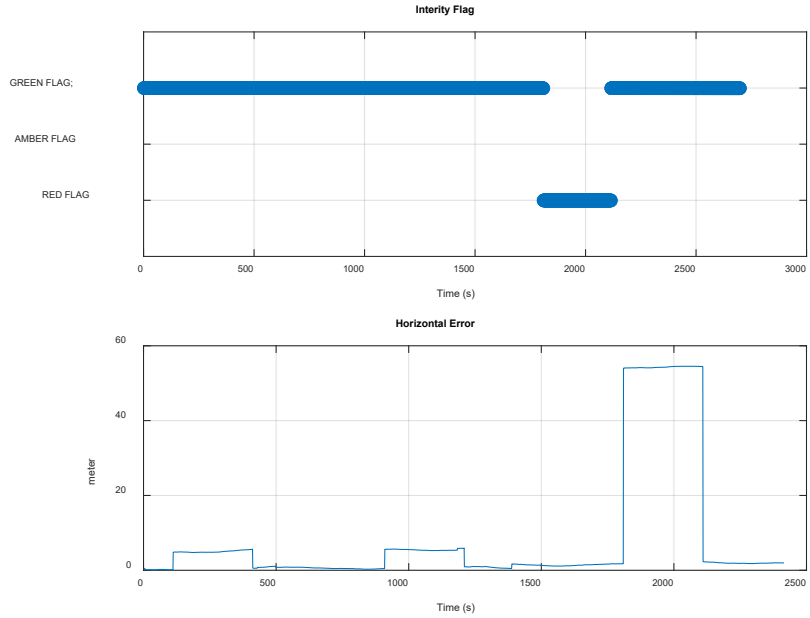

Figure 5-39 The MGRAIM Integrity Flag (above) and Horizontal Error vs HPL (below)

The solution performance is summarised in Table 5-21. For GPS L1/L5 and GAL E1/E5a the horizontal error is 54.43m with a percentile of 95%.

Table 5-21 TS09 - NEU and Horizontal error parameters for GPS L1/L5 and GAL E1/E5a

	MEAN (m)	STD (m)	95% (m)
North	-4.505	10.422	35.176
East	-5.925	13.09	41.709
Up	-2.087	9.844	37.225
Horizontal	8.194	16.378	54.427

Figure 5-40 illustrate the number of satellites used to compute the PVT solution and the computed DOP.

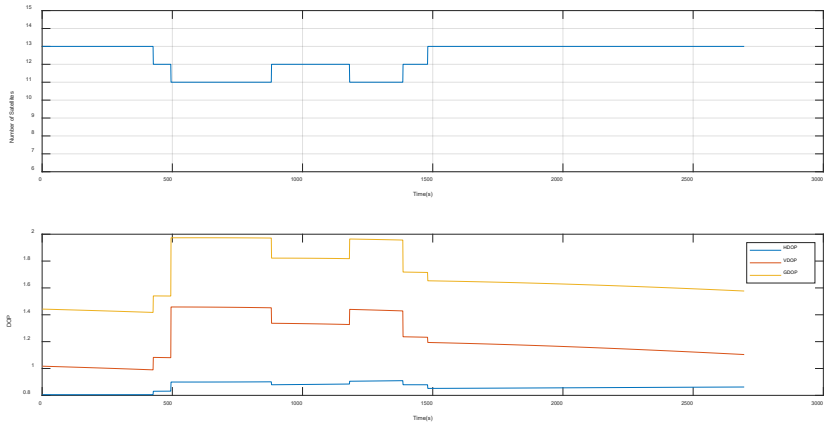

Figure 5-40 Number of SV used to generate the PVT solution and the DOP Values

5.1.3.1.2 TS10 – PVTI Performance Analysis (MRAIM DFMC)

Figure 5-41, show fault detection test results from Test Scenario 10 MRAIM DFMC, which included the integrity flags, the horizontal errors and the protection level generated. It can be seen from the integrity flag plot that the GREEN flag is raised which in this case indicates that the following condition was met PL< AL, the alert limit is set to the value of 25 m.

It has been observed that the horizontal error produced a much smaller bias error in magnitude and duration compared to the MGRAIM result. This can be attributed to the FDE process of the MRAIM where the Solution Separation Threshold test, the function that performs a threshold test for each subset and analyses if their separation is compatible with a failure. In that case where the configured threshold was met the faulty satellite was excluded to provide a safe positioning. Figure 5-14, shows the number of satellites is reduced due to the exclusion of the fault satellites The Positioning error generated is significantly reduced compared to MGRAIM approach.

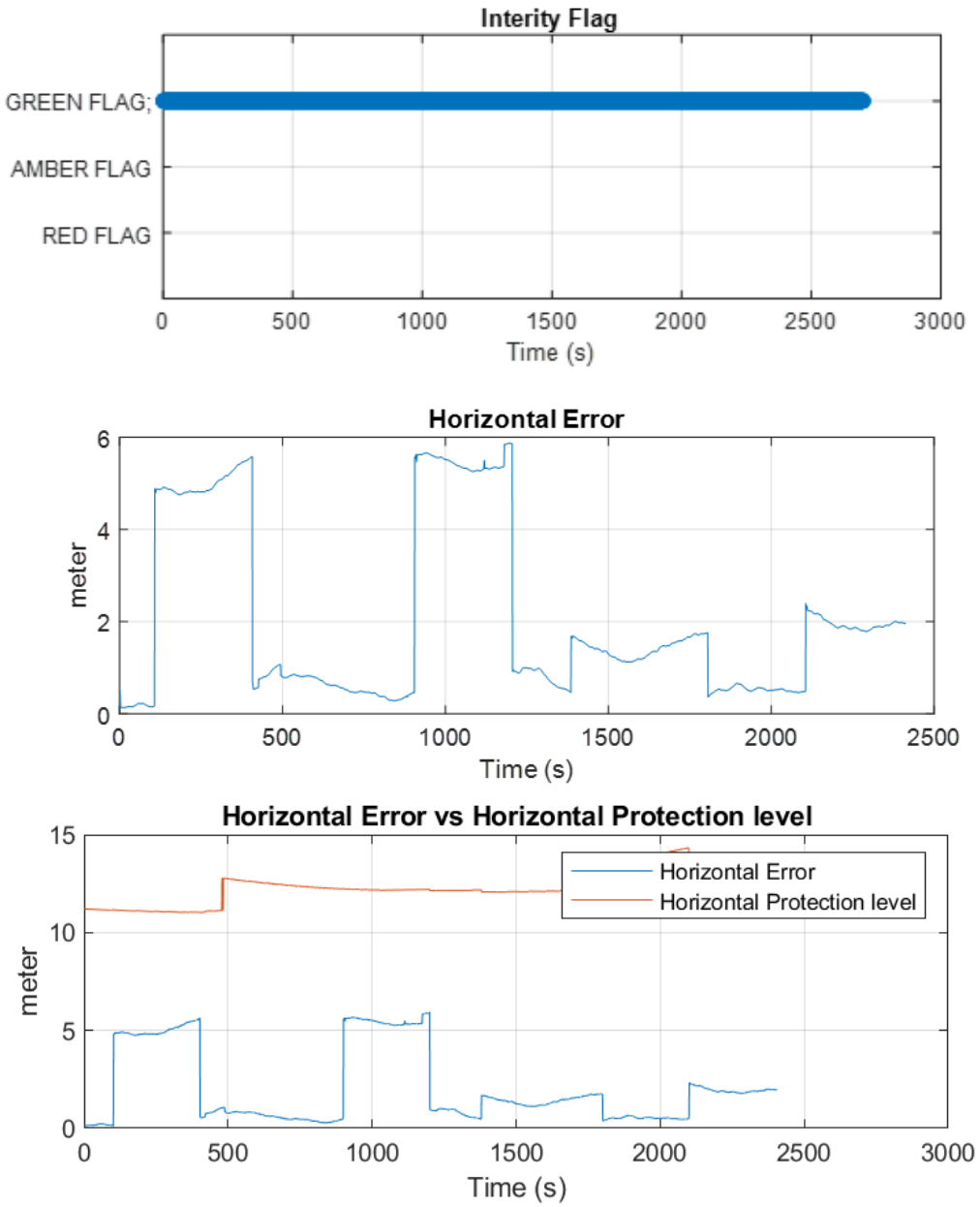

Figure 5-41 The MRAIM Integrity Flag (above), Horizontal Error (middle) and Horizontal Error vs HPL (below)

The solution performance is summarised in Table 5-22. For GPS L1/L5 and GAL E1/E5a the horizontal error is 5.6m with a percentile of 95%.

Table 5-22 TS08 - NEU and Horizontal error parameters For GPS L1/L5 and GAL E1/E5a

	MEAN (m)	STD (m)	95% (m)
North	0.071	2.275	4.156
East	-0.475	1.731	3.845
Up	2.173	3.104	7.641
Horizontal	2.057	2.043	5.600

Figure 5-42 illustrate the number of satellites used to compute the PVT solution and the computed DOP.

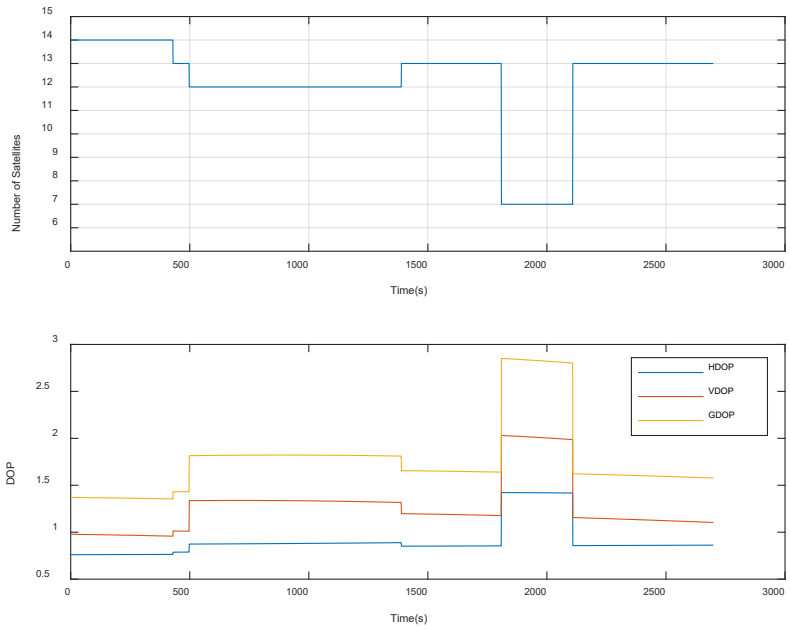

Figure 5-42 Number of SV used to generate the PVT solution and the DOP Values

5.1.3.1.3 TS09a – PVTI Performance Analysis (MGRAIM) – DFMC SBAS

Figure 5-43 and Figure 5-44 show fault detection test results from Test Scenario 09a MGRAIM DFMC. Figure 5-43 illustrates test statistics and threshold values computed for the solution generated for the dataset. The test statistics and threshold values are used within Fault Detection Test. It can be seen from the graph the point at which the test statistic exceeds the detection threshold, when this occurs the “red light” integrity alarm/flag is raised. Figure 5-44, shows integrity flags and the horizontal errors within the solution generated.

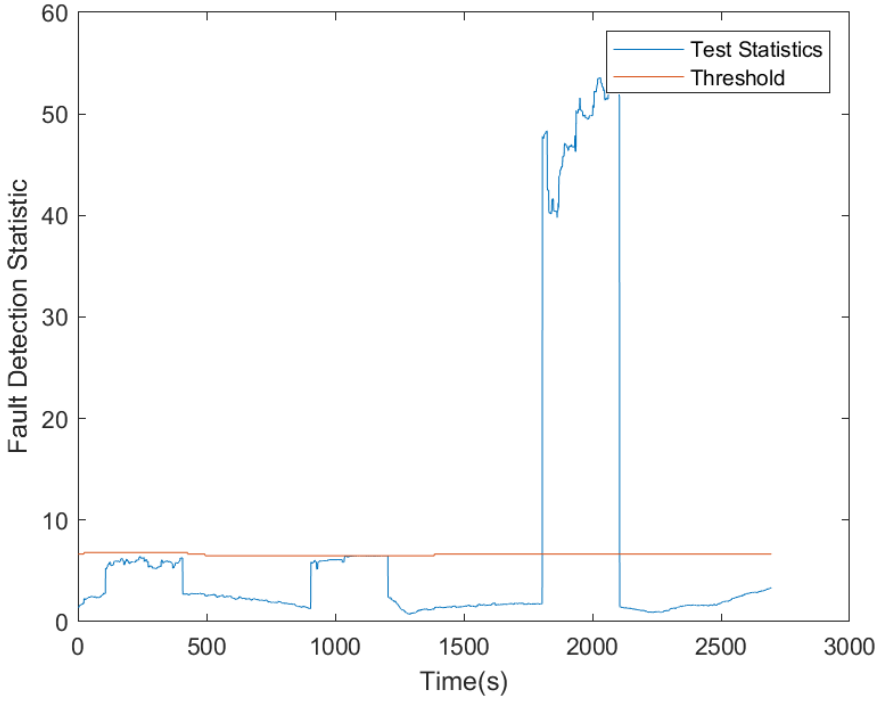

Figure 5-43 FD results from MGRAIM in ramp fault case

The results indicate that the algorithm has detected the injected fault. It has been observed that the fault biases of 35m, 36.8m were detected but as seen from Figure 5-43 the test-statistic lies below the detection threshold ($t^2 \leq T^2$) raising a GREEN integrity flag. However, in the case of the fault bias of 100m a RED flag was raised, this occurs when the test statistic exceeds the detection threshold ($t^2 > T^2$). The red flag was raised at time 1807s where $t^2 = 38.040 > T^2 = 6.56$ and ended at time 2106s where $t^2 = 40.83 > T^2 = 6.66$. Figure 5-44, shows integrity flags and the horizontal errors within the solution generated.

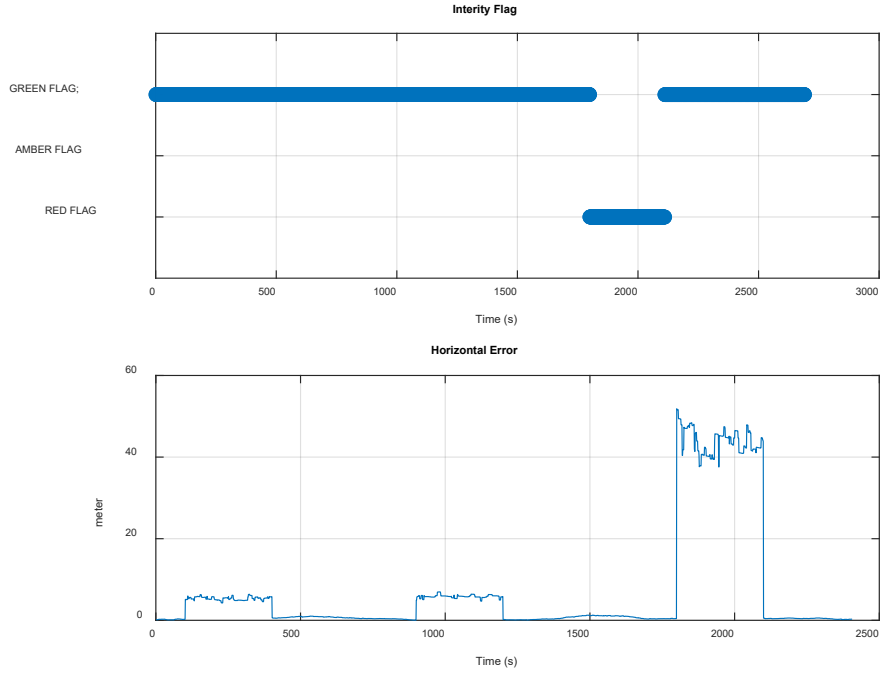

Figure 5-44 The MGRAIM Integrity Flag (above) and Horizontal Error (below)

The solution performance is summarised in Table 5-23. For GPS L1/L5 and GAL E1/E5a the horizontal error is 45.06m with a percentile of 95%.

Table 5-23 TS09a - NEU and Horizontal error parameters for GPS L1/L5 and GAL E1/E5a

	MEAN (m)	STD (m)	95% (m)
North	-4.254	7.304	23.456
East	-5.381	12.225	37.324
Up	5.368	11.699	35.237
Horizontal	7.194	14.075	45.064

Figure 5-45 illustrate the number of satellites used to compute the PVT solution and the computed DOP.

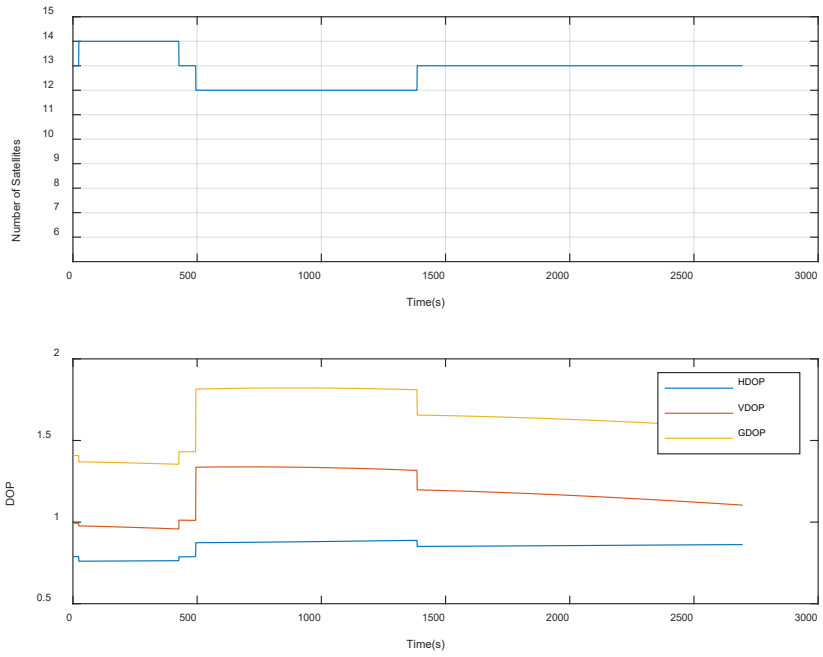

Figure 5-45 Number of SV used to generate the PVT solution and the DOP Values

5.1.3.1.4 TS010a – PVTI Performance Analysis (MRAIM) – DFMC SBAS

Figure 5-46, show fault detection test results from Test Scenario 10a MRAIM DFMC, which included the integrity flags, the horizontal errors and the protection level generated. It can be seen from the integrity flag plot that the GREEN flag is raised which in this case indicates that the following condition was met PL< AL, the alert limit is set to the value of 25 m.

It has been observed that the horizontal error produced a much smaller bias error in magnitude and duration compared to the MGRAIM result. This can be attributed to the FDE process of the MRAIM where the Solution Separation Threshold test, the function that performs a threshold test for each subset and analyses if their separation is compatible with a failure. In that case where the configured threshold was met the faulty satellite was excluded to provide a safe positioning. Figure 5-47, shows the number of satellites is reduced due to the exclusion of the fault satellites The Positioning error generated is significantly reduced compared to MGRAIM approach.

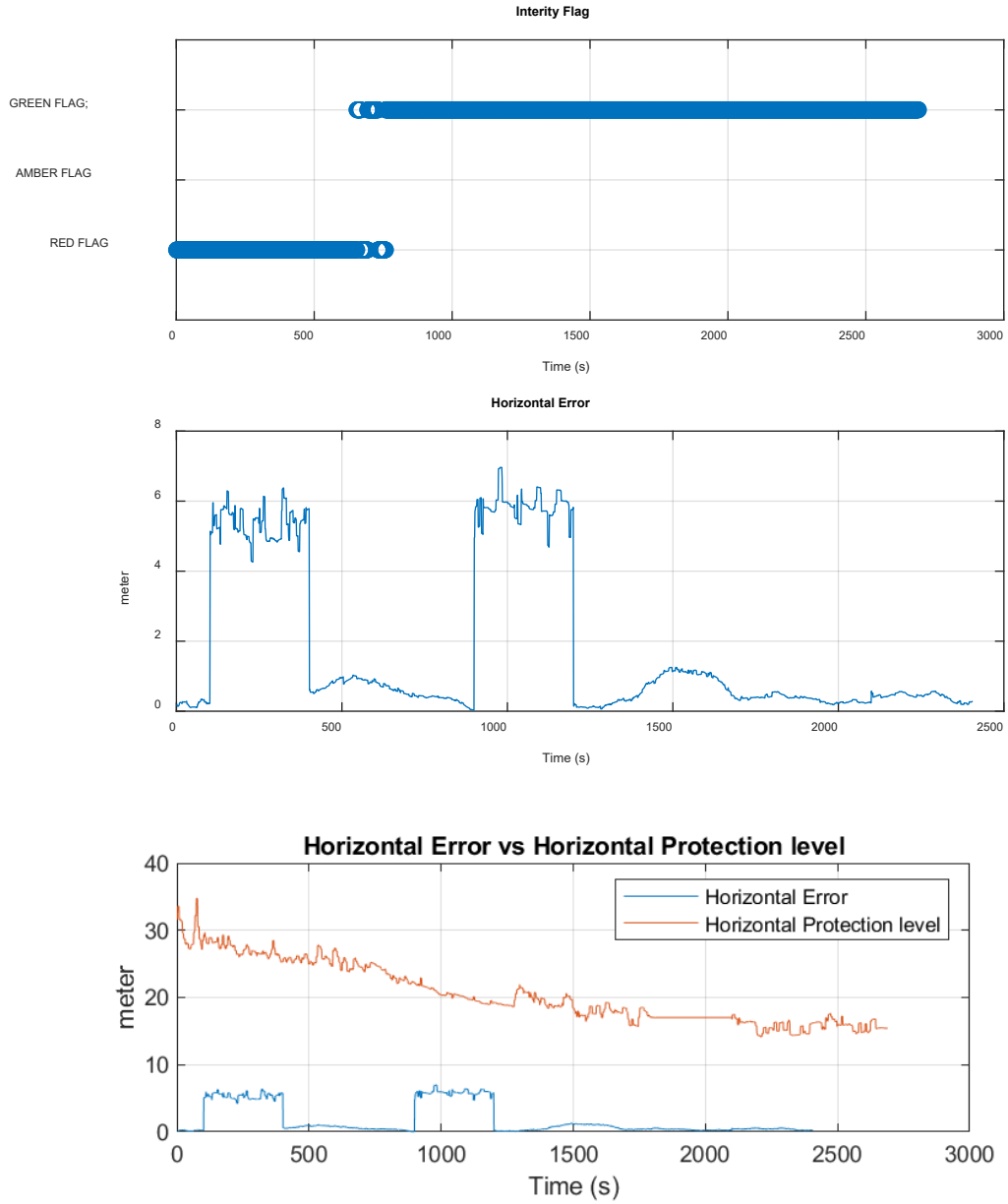

Figure 5-46 The MRAIM Integrity Flag (above), Horizontal Error (middle) and Horizontal Error vs HPL (below)

The solution performance is summarised in Table 5-24. For GPS L1/L5 and GAL E1/E5a the horizontal error is 5.97 with a percentile of 95%.

Table 5-24 TS10a - NEU and Horizontal error parameters For GPS L1/L5 and GAL E1/E5a

	MEAN (m)	STD (m)	95% (m)
North	-1.394	1.802	4.854
East	-0.687	1.566	4.134
Up	1.33	1.954	4.538
Horizontal	1.768	2.233	5.972

Figure 5-47 illustrate the number of satellites used to compute the PVT solution and the computed DOP.

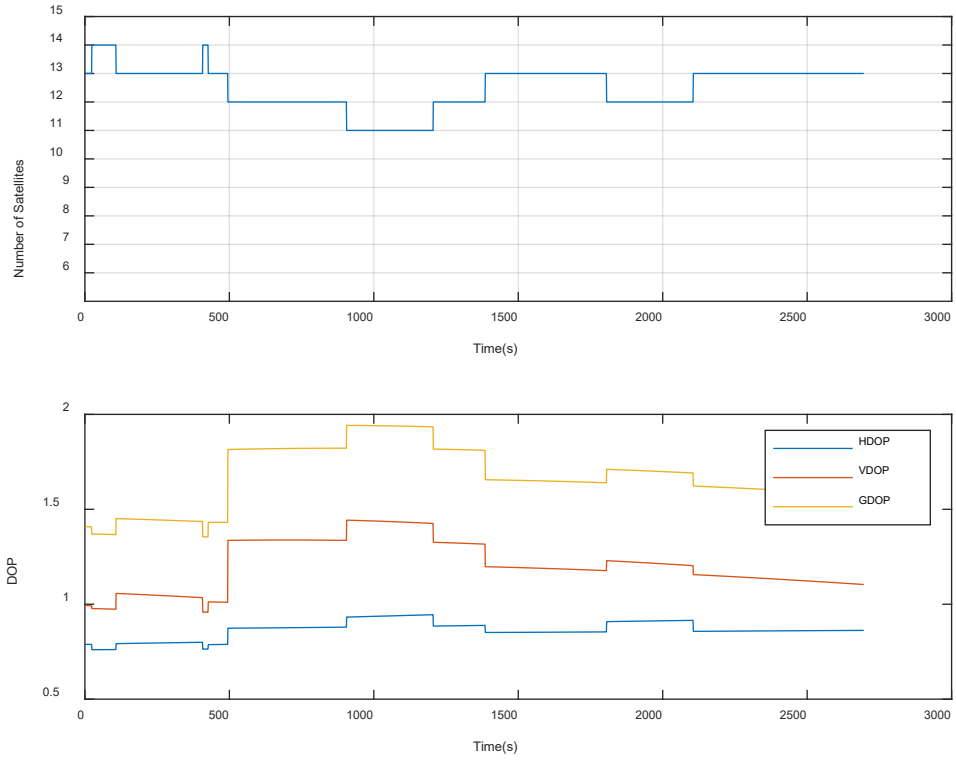

Figure 5-47 Number of SV used to generate the PVT solution and the DOP Values

5.1.3.2 Single Low-Elevation SV

The bias fault is a basic class of GNSS anomaly, which is usually caused by the phase jump of satellite clocks or another additive fault like signal multipath. It may lead to a substantial, virtually instant shift in the user's position even by hundreds of meters.

This subsection shows the results generated using a smoothing constant of 100 seconds based on the following test scenario:

Test Scenario	*Correction mode*	*Fault injection*	*Comment*
TS.11	MGRAIM DFMC	Single Satellite Clock failure (bias) -Low Elevation SV	Applying a bias error on a single high-elevation SV
TS.12	MRAIM DFMC	Single Satellite Clock failure (bias) -Low Elevation SV	apply bias error on a single high-elevation SV

The subsection will look at the results generated using the minimum and a large detectable bias error that will raise a RED integrity flag as well as a bias value that will raise GREEN flag these values were extracted from the ramp error analysis conducted [RD.49]. These values were extracted from the ramp error analysis conducted in the previous subsection. Table 5-25 shows the configuration parameters and values used to create the bias fault injection dataset. A fault bias of 50m, 56.4m, and 100m was injected at times t=110s, t=908s and t =1808s in a low-elevation satellite G12.

Table 5-25 TS11/TS12 Configuration MGRAIM DFMC

Parameter	Value	Comment
Start time [SOW]	[297026, 296228, 297926]	represents the time and duration of the injection of the fault
End time [SOW]	[297326, 296528, 298226]	
Constellation	['G'];	The constellation on which is affected
PRN	[12];	Satellites in which the fault was injected
Range bias	[50, 56.4,100];	fault bias values injected into the RINEX file.

5.1.3.2.1 TS11 – PVTI Performance Analysis (MGRAIM) DFMC

This subsection looks at the results generated using a minimum and maximum detectable bias errors. Figure 5-48 and Figure 5-49 show fault detection test results from Test Scenario 11 MGRAIM DFMC. Figure 5-48 illustrates test statistics and threshold values computed for the solution generated for the dataset. The test statistics and threshold values are used within Fault Detection Test. It can be seen from the graph that the test-statistic lies below the detection threshold $(t^2 \leq T^2)$ which indicates that all the screening process tests were performed successfully and therefore the solution is ok for use. Figure 5-49, shows integrity flags and the horizontal errors within the solution generated.

It has been observed that the bias error injected on the low elevation was not detected by the MGRAIM DFMC algorithm this may be attributed to the low weighted placed on the low elevation satellite and the available to more satellites with the inclusion of the Galileo satellites.

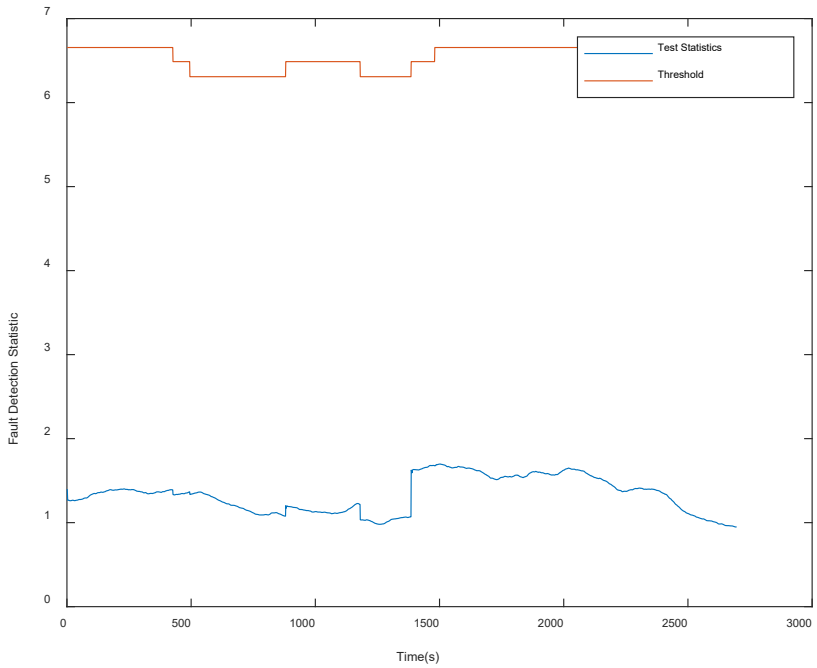

Figure 5-48 FD results from MGRAIM in Bias fault case

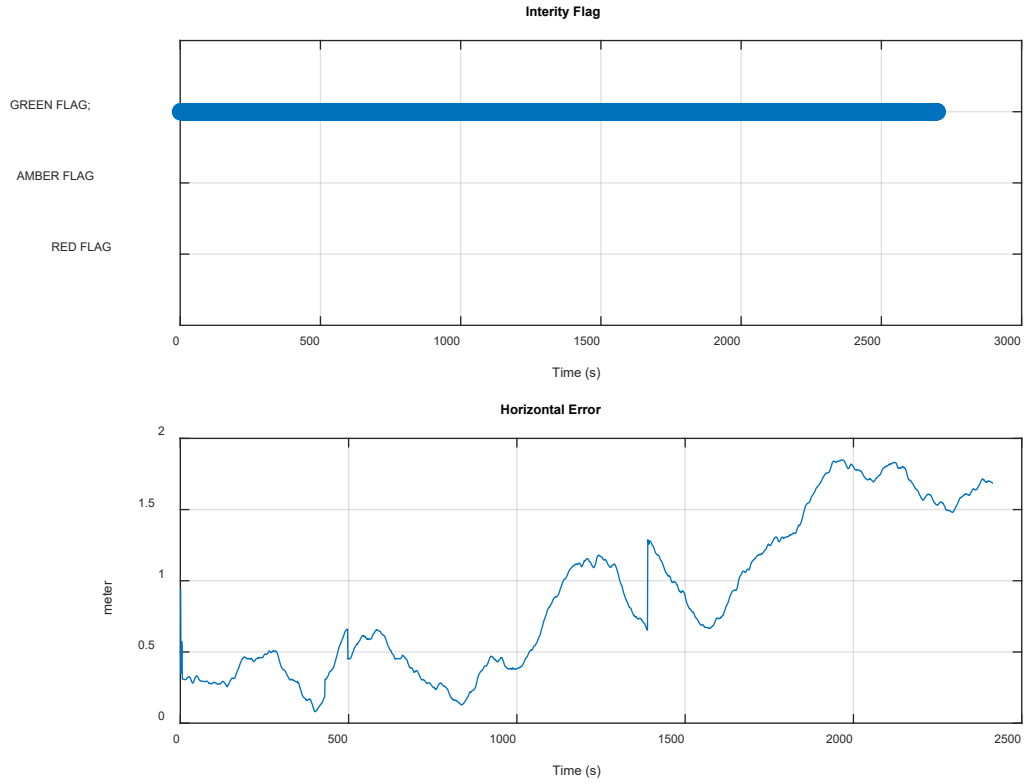

Figure 5-49 The MGRAIM Integrity Flag (above) and Horizontal Error (below)

The solution performance is summarised in Table 5-26. For GPS L1/L5 and GAL E1/E5a the horizontal error is 2.17m with a percentile of 95%.

Table 5-26 TS11 - NEU and Horizontal error parameters for GPS L1/L5 and GAL E1/E5a

	MEAN (m)	STD (m)	95% (m)
North	0.692	0.926	2.058
East	-0.355	0.384	1.06
Up	3.497	2.261	7.367
Horizontal	1.066	0.687	2.169

Figure 5-50 illustrate the number of satellites used to compute the PVT solution and the computed DOP.

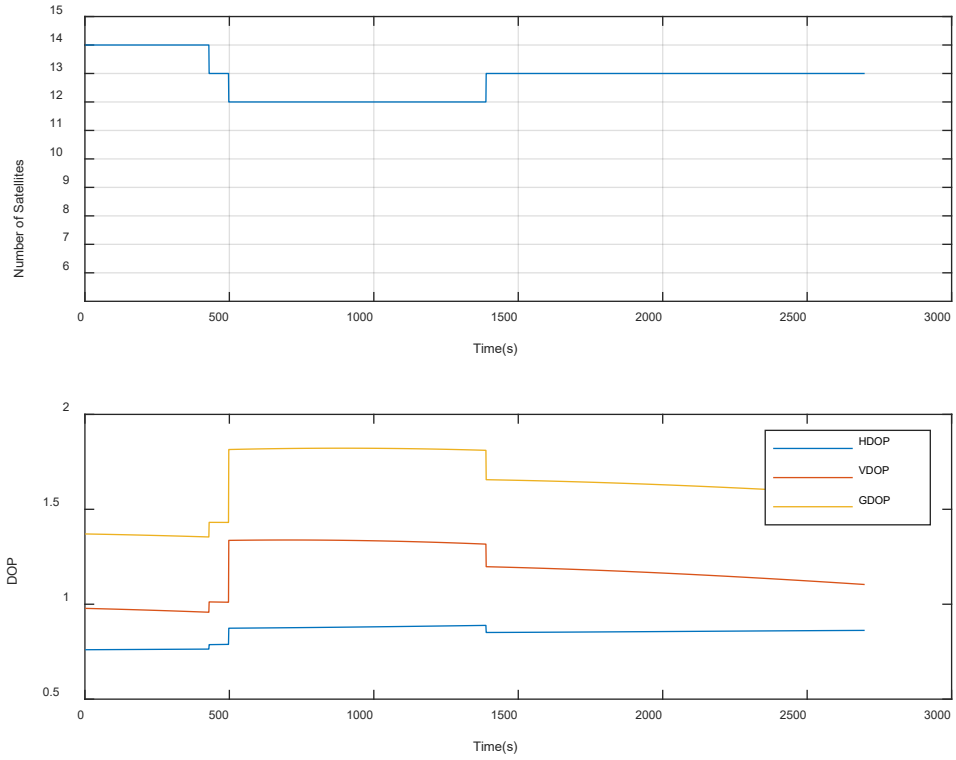

Figure 5-50 Number of SV used to generate the PVT solution and the DOP Values

5.1.3.2.2 TS.12 – PVTI Performance Analysis (MRAIM DFMC)

Figure 5-51 show fault detection test results from Test Scenario 12 MRAIM DFMC, which included the integrity flags, the horizontal errors and the protection level generated. It can be seen from the integrity flag plot that the GREEN flag is raised which in this case indicates that the following condition was met PL< AL, the alert limit is set to the value of 25 m.

It has been observed that the ramp error injected on the low elevation was not detected by the MGRAIM DFMC algorithm this may be attributed to the low weighted placed on the low elevation satellite and the available to more satellites with the inclusion of the Galileo satellites.

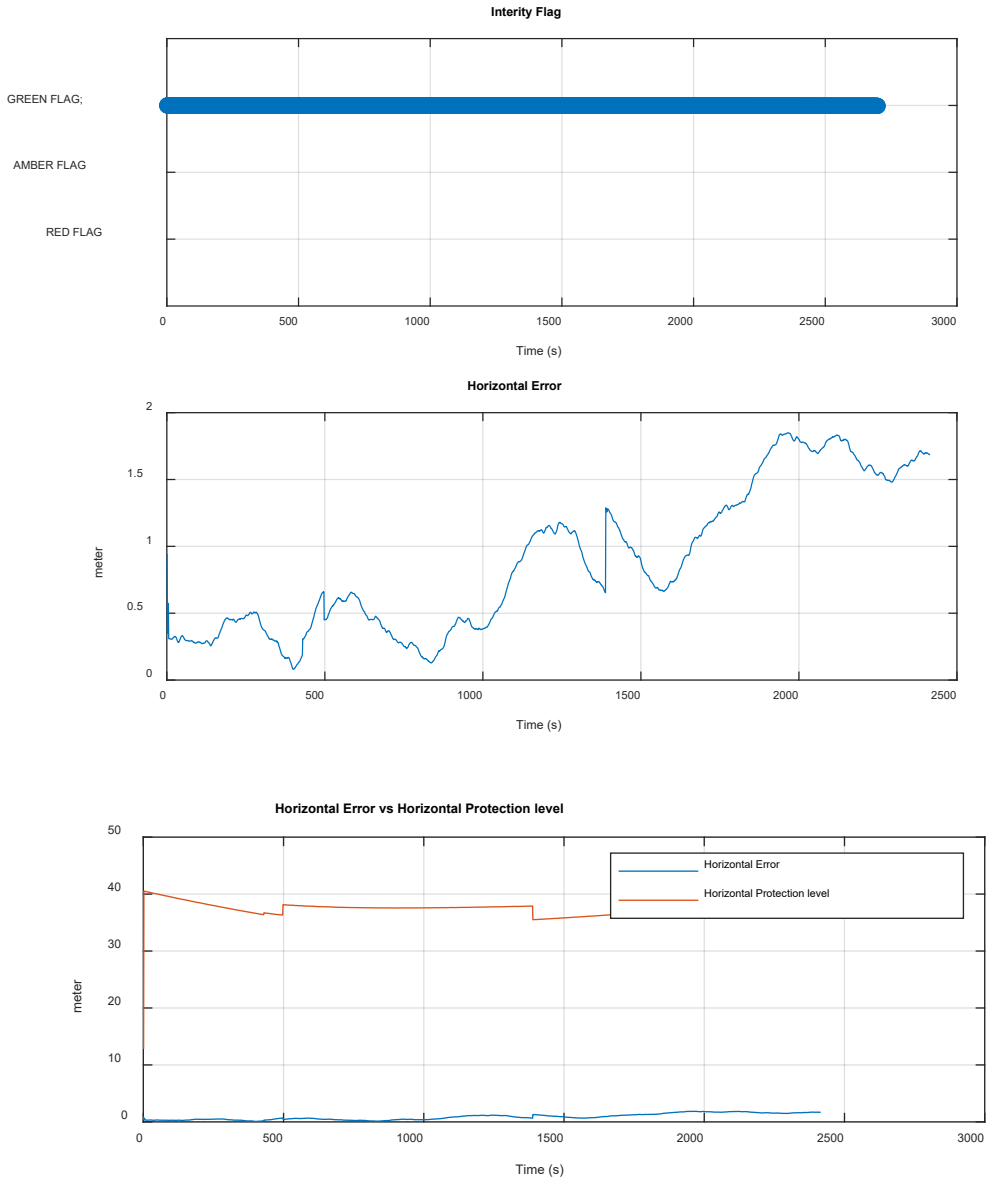

Figure 5-51 The MRAIM Integrity Flag (above) and Horizontal Error (middle) and HPL (below)

The solution performance is summarised in Table 5-27. For GPS L1/L5 and GAL E1/E5a the horizontal error is 2.17m with a percentile of 95%.

Table 5-27 TS12 - NEU and Horizontal error parameters for GPS L1

	MEAN (m)	STD (m)	95% (m)
North	0.692	0.926	2.058
East	-0.355	0.384	1.06
Up	3.497	2.261	7.367
Horizontal	1.066	0.687	2.169

Figure 5-52 illustrate the number of satellites used to compute the PVT solution and the computed DOP.

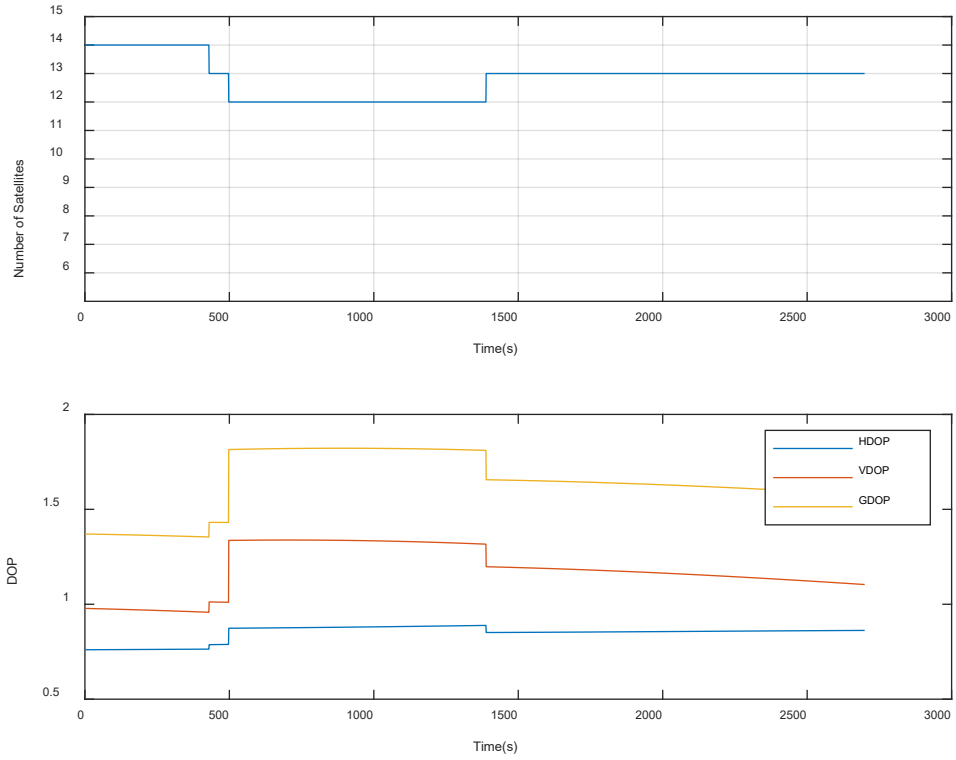

Figure 5-52 Number of SV used to generate the PVT solution and the DOP Values

5.1.3.2.3 TS11a – PVTI Performance Analysis (MGRAIM) DFMC SBAS

This subsection looks at the results generated using a minimum and maximum detectable bias errors. Figure 5-53 and Figure 5-54 show fault detection test results from Test Scenario 11a MGRAIM DFMC. Figure 5-53 illustrates test statistics and threshold values computed for the solution generated for the dataset. The test statistics and threshold values are used within Fault Detection Test. It can be seen from the graph that the test-statistic lies below the detection threshold $(t^2 \leq T^2)$ which indicates that all the screening process tests were performed successfully and therefore the solution is ok for use. Figure 5-54, shows integrity flags and the horizontal errors within the solution generated.
It has been observed that the ramp error injected on the low elevation was not detected by the MGRAIM DFMC algorithm this may be attributed to the low weighted placed on the low elevation satellite and the available to more satellites with the inclusion of the Galileo satellites.

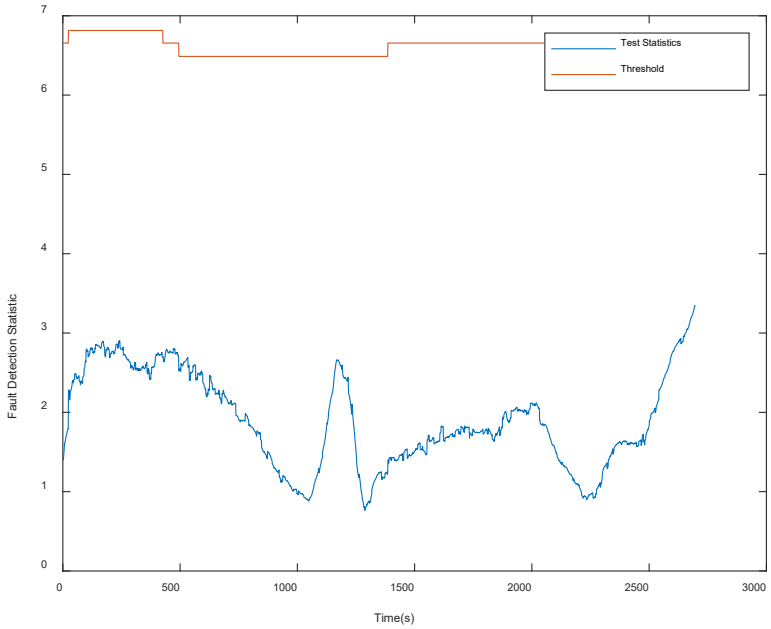

Figure 5-53 FD results from MGRAIM in ramp fault case

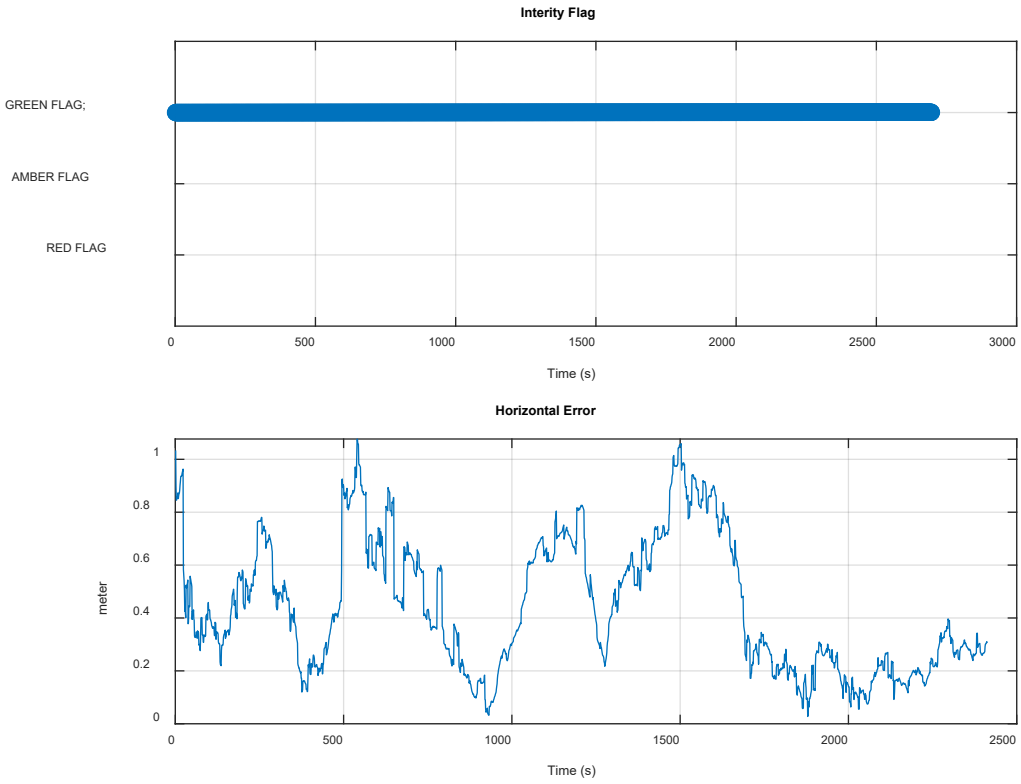

Figure 5-54 The MGRAIM Integrity Flag (above) and Horizontal Error (below)

The solution performance is summarised in Table 5-28 For GPS L1/L5 and GAL E1/E5a the horizontal error is 0.89m with a percentile of 95%.

Table 5-28 TS11a - NEU and Horizontal error parameters for GPS L1/L5 and GAL E1/E5a

	MEAN (m)	STD (m)	95% (m)
North	-0.07	0.377	0.795
East	0.124	0.31	0.597
Up	-0.404	1.139	2.46
Horizontal	0.442	0.25	0.891

Figure 5-55 illustrate the number of satellites used to compute the PVT solution and the computed DOP.

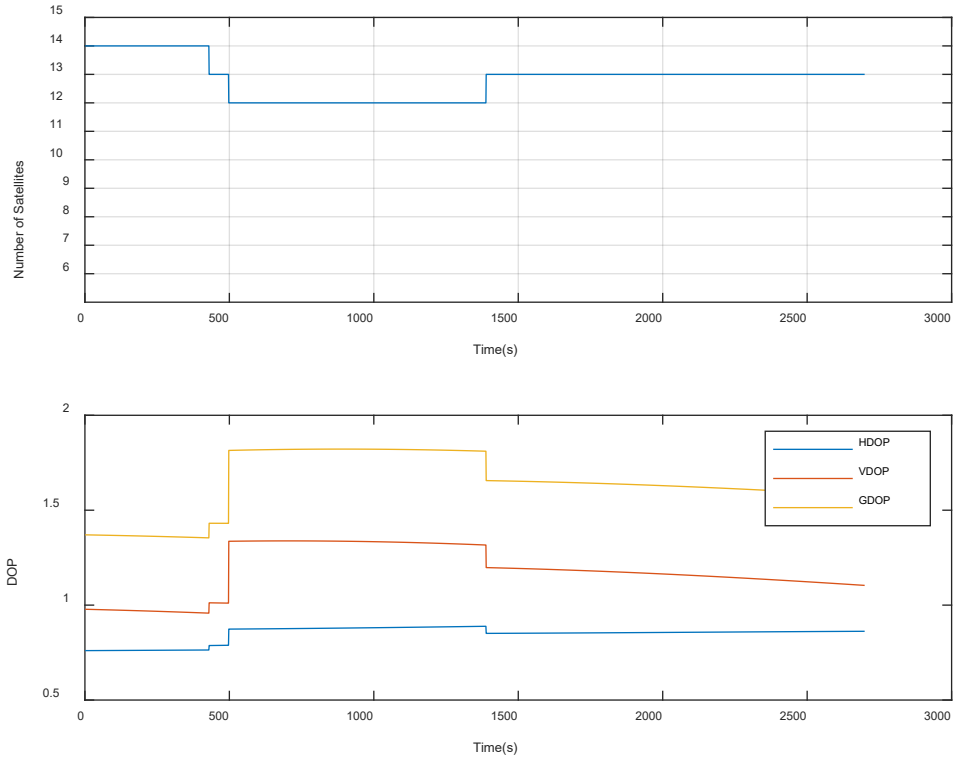

Figure 5-55 Number of SV used to generate the PVT solution and the DOP Values

5.1.3.2.4 TS.12a – PVTI Performance Analysis (MRAIM) DFMC SBAS

Figure 5-56 show fault detection test results from Test Scenario 12a MRAIM DFMC, which included the integrity flags, the horizontal errors and the protection level generated. It can be seen from the integrity flag plot that the GREEN flag is raised which in this case indicates that the following condition was met PL< AL, the alert limit is set to the value of 25 m.

It has been observed that the ramp error injected on the low elevation was not detected by the MGRAIM DFMC algorithm this may be attributed to the low weighted placed on the low elevation satellite and the available to more satellites with the inclusion of the Galileo satellites.

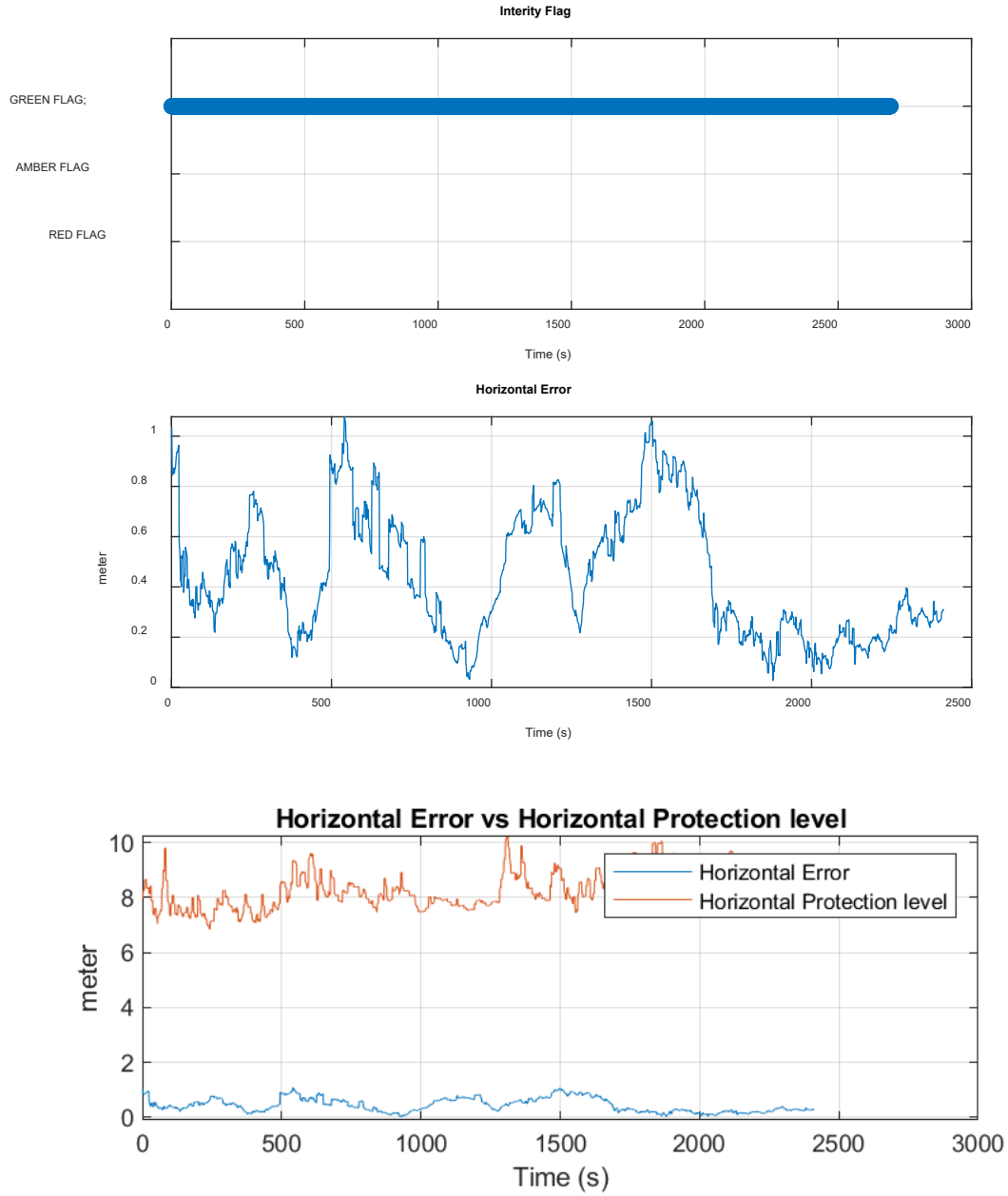

Figure 5-56 The MRAIM Integrity Flag (above) and Horizontal Error (middle) and HPL (below)

The solution performance is summarised in Table 5-29. For GPS L1/L5 and GAL E1/E5a the horizontal error is 0.89m with a percentile of 95%.

Table 5-29 TS12a - NEU and Horizontal error parameters for GPS L1

	MEAN (m)	STD (m)	95% (m)
North	-0.07	0.377	0.795
East	0.124	0.31	0.597
Up	-0.404	1.139	2.46
Horizontal	0.442	0.25	0.891

Figure 5-57 illustrate the number of satellites used to compute the PVT solution and the computed DOP.

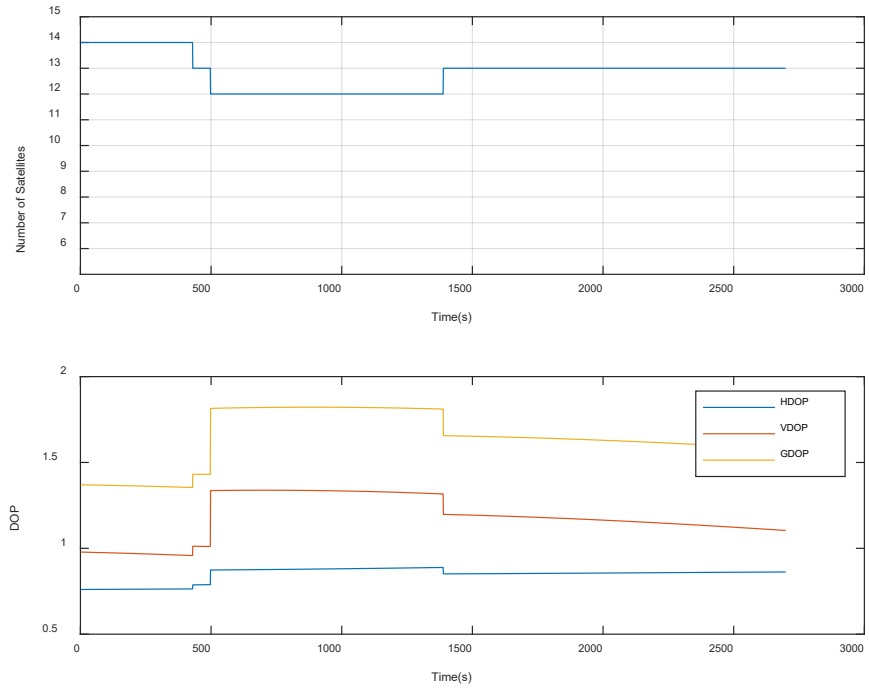

Figure 5-57 Number of SV used to generate the PVT solution and the DOP Values

5.1.3.3 Multiple High-elevation SV

This subsection shows the results generated using a smoothing constant of 100 seconds based on the following test scenario:

Test Scenario	Correction mode	Fault injection	Comment
TS.13	MGRAIM DFMC	Multiple Satellite Clock failure (bias) - High Elevation SV	Applying a bias error on 2 high-elevation SV
TS.14	MGRAIM DFMC	Multiple Satellite Clock failure (bias) - High Elevation SV	apply bias error on 2 high-elevation SV

Table 5-30 shows the configuration parameters and values used to create the bias fault injection dataset. A large bias fault of 100m was injected into the original pseudo-range of GPS satellite G04 and G06 from t=110s (SOW: 296228s) to t = 410s (SOW: 296528s) and a second satellite from t=908s (SOW: 297026s) to t = 1208s (SOW: 297326s).

Table 5-30 TS13/TS14 Configuration

Parameter	Value	Comment
Start time [GPS Week SOW]	[2229 296228]; [2229 297026];	represents the time and duration of the injection of the fault
End time [GPS Week SOW]	[2229 296528]; [2229 297326]	
Constellation	['G'];	The constellation which is affected
PRN	[3], [6];	Satellites in which the fault was injected
Range bias	[100,100];	fault bias values injected into the RINEX file.

5.1.3.3.1 TS13– PVTI Performance Analysis (MGRAIM DFMC)

Figure 5-58 and Figure 5-59 show fault detection test results from Test Scenario 13 MGRAM DFMC. Figure 5-58 illustrates test statistics and threshold values computed for the solution generated for the dataset. The test statistics and threshold values are used within Fault Detection Test. It can be seen from the graph the point at which the test statistic exceeds the detection threshold at the point where the ramp error was injected into the file, when this occurs the “red light” integrity alarm/flag is raised. Figure 5-59, shows integrity flags and the horizontal errors within the solution generated.

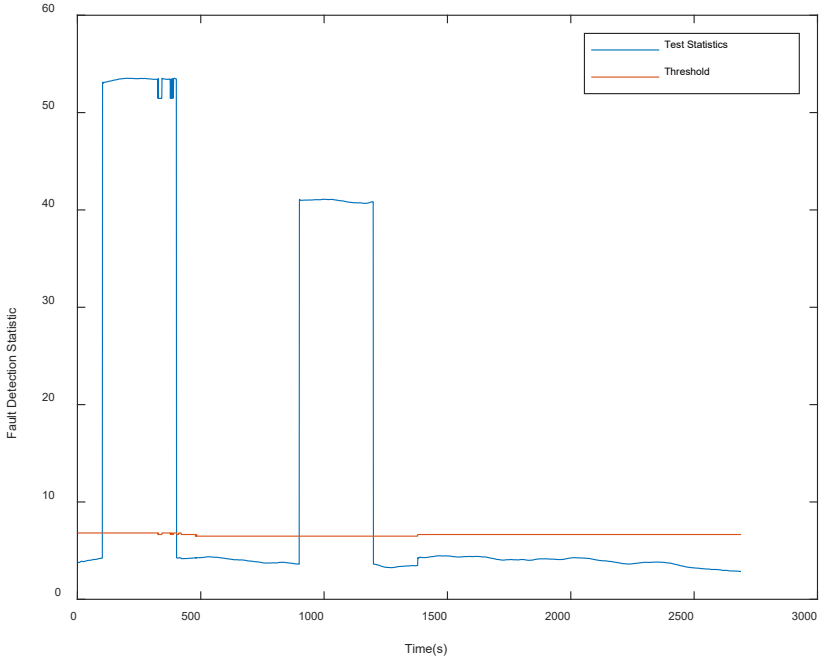

Figure 5-58 FD results from MGRAIM in Bias fault case

The results indicate that the algorithm has detected the injected fault, as the RED flag is raised, this occurred when the test-statistic exceeds the detection threshold ($t^2 > T^2$). The red flag was raised at time 111s where $t^2 = 53.122$ $T^2 = 6.814$ and ended at time 410s where $t^2 = 53.457$ $T^2 = 6.814$. The horizontal error values at these times were 45.191m and 47.106m respectively. The red flag was raised again at time 909s where $t^2 = 41.072$ $T^2 = 6.488$ and ended at time 1208s where $t^2 = 40.841$ $T^2 = 6.488$ The horizontal error values at these times were 43.102m and 43.650m respectively.

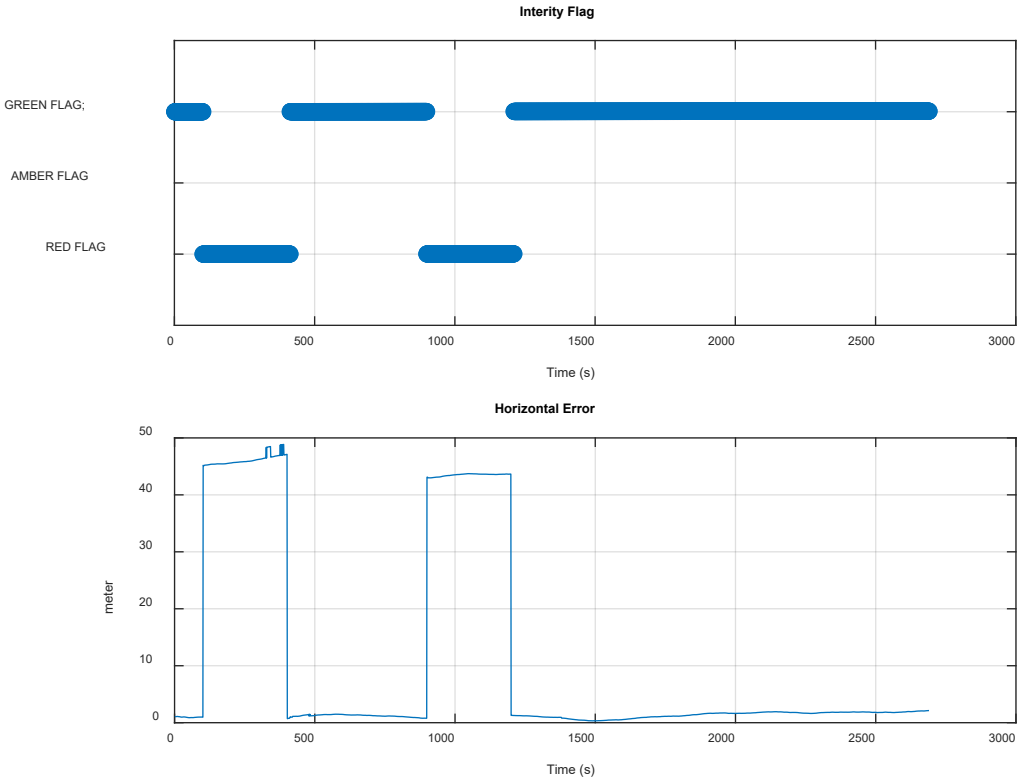

Figure 5-59 The MGRAIM Integrity Flag (above) and Horizontal Error (below).

The solution performance is summarised in Table 5-31. For GPS L1/L5 and GAL E1/E5a the horizontal error is 45.90m with a percentile of 95%.

Table 5-31 TS13 - NEU and Horizontal error parameters for GPS L1/L5 and GAL E1/E5a

	MEAN (m)	STD (m)	95% (m)
North	6.403	13.758	37.613
East	1.796	14.672	35.868
Up	-2.482	16.515	48.086
Horizontal	10.989	18.111	45.898

Figure 5-60 illustrate the number of satellites used to compute the PVT solution and the computed DOP.

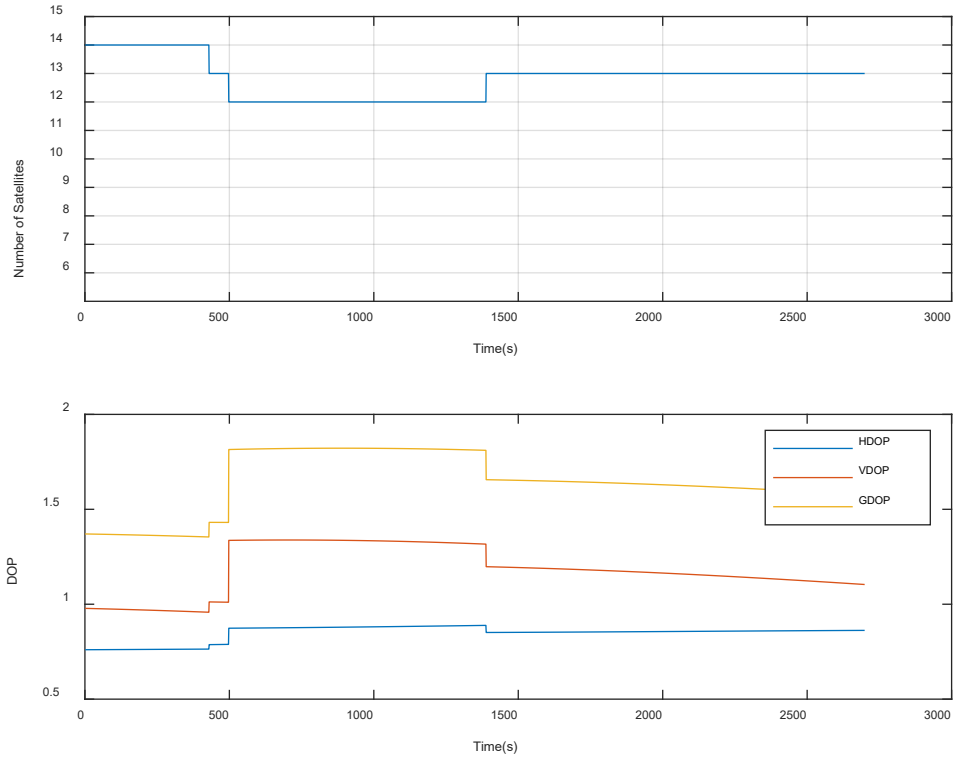

Figure 5-60 Number of SV used to generate the PVT solution and the DOP Values

5.1.3.3.2 TS14 – PVTI Performance Analysis (MRAIM) DFMC

Figure 5-61, shows integrity flags, the horizontal errors and the protection level generated. It can be seen from the integrity flag plot that the GREEN flag is raised which in this case indicates that the following condition was met PL< AL, the alert limit is set to the value of 100 m.

The large errors caused by the bias are removed compared to the MGRAIM result in TS13. This can be attributed to the FDE process of the MRAIM where the Solution Separation Threshold test, the function that performs a threshold test for each subset and analyses if their separation is compatible with a failure. In that case where the configured threshold was met the faulty satellite was excluded to provide a safe positioning. Figure 5-62 shows the number of satellites is reduced due to the exclusion of the fault satellites The Positioning error generated is significantly reduced compared to MGRAIM approach.

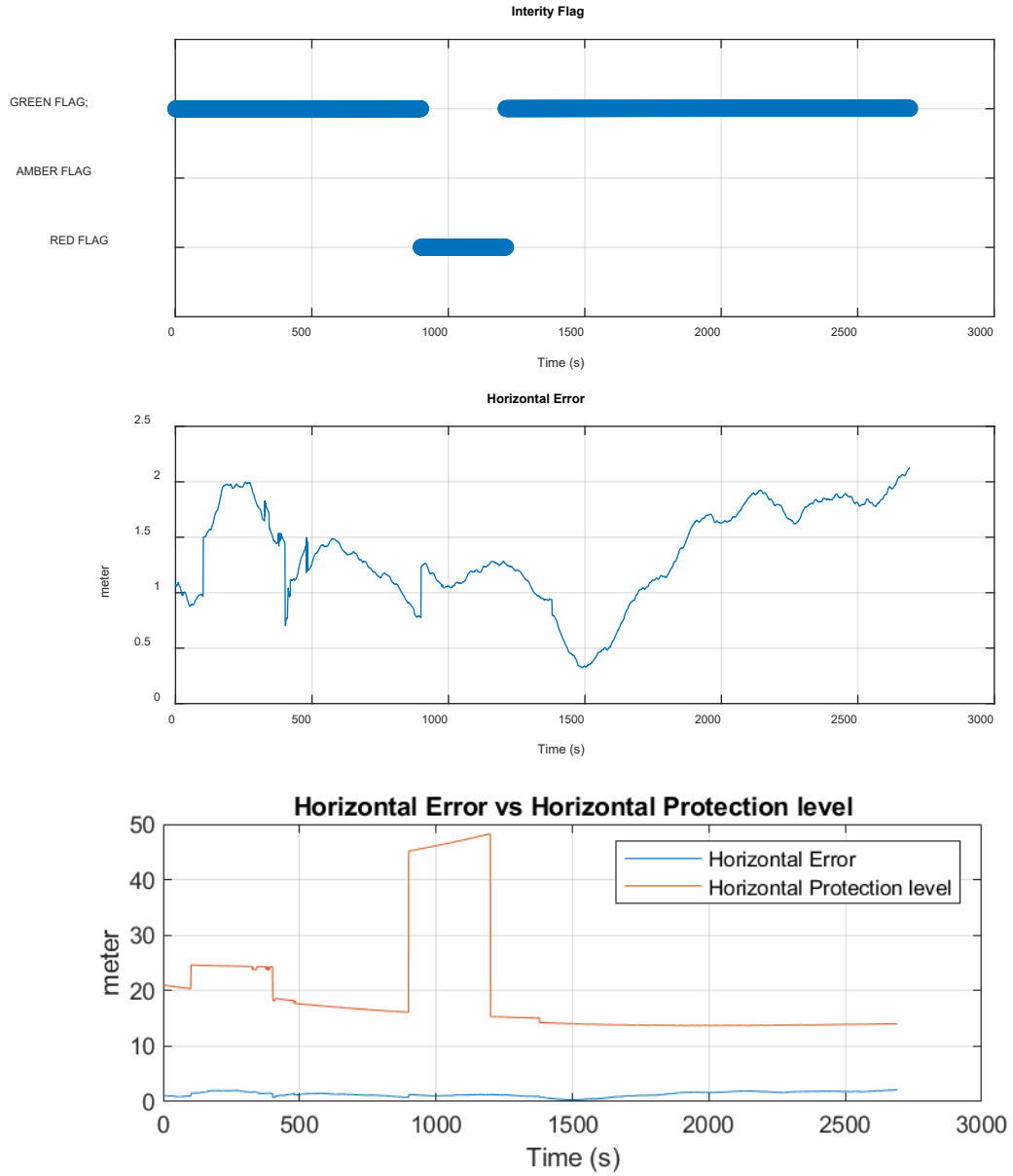

Figure 5-61 The MRAIM Integrity Flag (above), Horizontal Error (middle). and Horizontal Error vs HPL (below).

The solution performance is summarised in Table 5-7. For GPS L1/L5 and GAL E1/E5a the horizontal error is 1.96m with a percentile of 95%.

Table 5-32 TS14 - NEU and Horizontal error parameters for GPS L1/L5 and GAL E1/E5a

	MEAN (m)	STD (m)	95% (m)
North	0.811	0.574	1.492
East	0.900	0.461	1.582
Up	3.341	1.243	6.450
Horizontal	1.349	0.438	1.958

Figure 5-14 illustrate the number of satellites used to compute the PVT solution and the computed DOP.

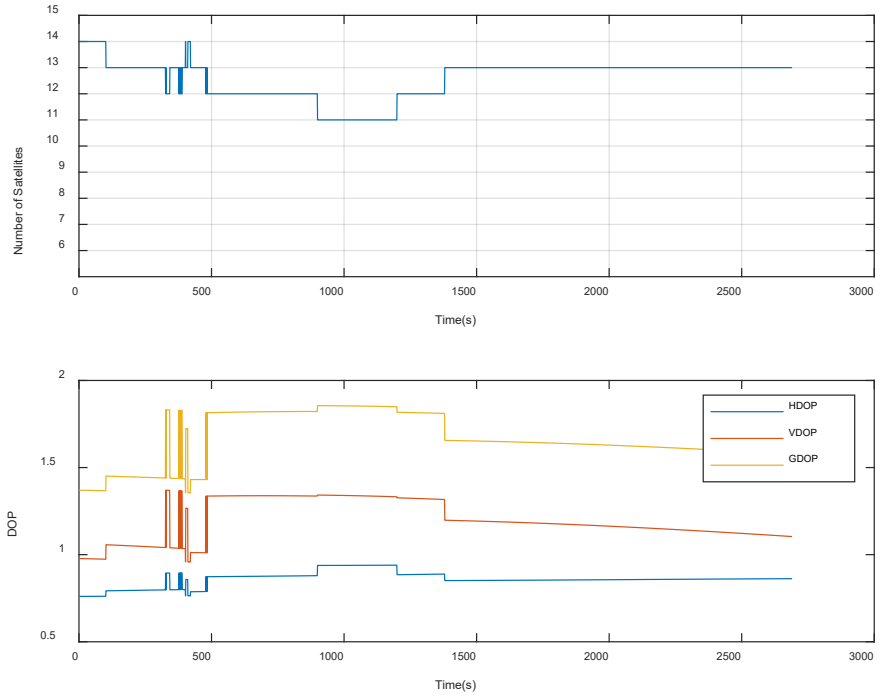

Figure 5-62 Number of SV used to generate the PVT solution and the DOP Values

5.1.3.3.3 TS13a– PVTI Performance Analysis (MGRAIM) DFMC SBAS

Figure 5-63 and Figure 5-64 show fault detection test results from Test Scenario 13a MGRAM DFMC. Figure 5-63 illustrates test statistics and threshold values computed for the solution generated for the dataset. The test statistics and threshold values are used within Fault Detection Test. It can be seen from the graph the point at which the test statistic exceeds the detection threshold at the point where the ramp error was injected into the file, when this occurs the “red light” integrity alarm/flag is raised. Figure 5-64, shows integrity flags and the horizontal errors within the solution generated.

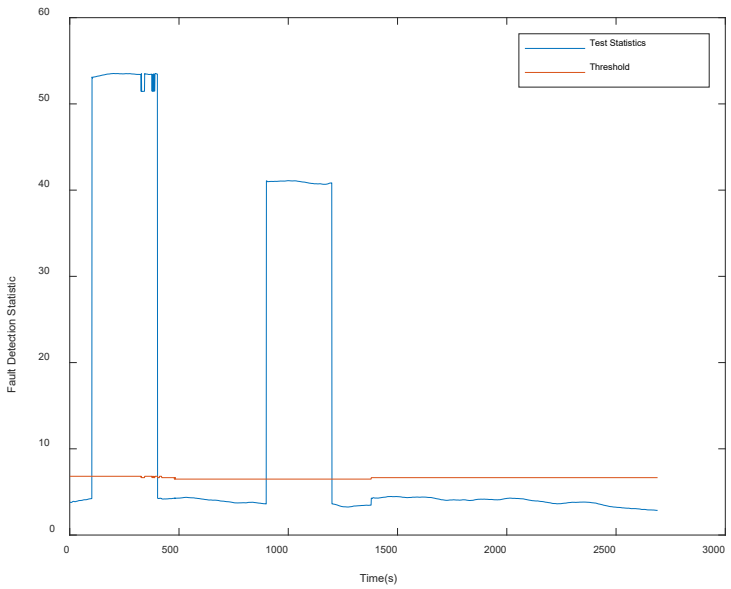

Figure 5-63 FD results from MGRAIM in ramp fault case

The results indicate that the algorithm has detected the injected fault, as the RED flag is raised, this occurred when the test-statistic exceeds the detection threshold ($t^2 > T^2$). The red flag was raised at time 111s where $t^2 = 53.122$ $T^2 = 6.814$ and ended at time 410s where $t^2 = 53.457$ $T^2 = 6.814$. The horizontal error values at these times were 45.191m and 47.106m respectively. The red flag was raised again at time 909s where $t^2 = 41.072$ $T^2 = 6.488$ and ended at time 1208s where $t^2 = 40.841$ $T^2 = 6.488$ The horizontal error values at these times were 43.102m and 43.650m respectively.

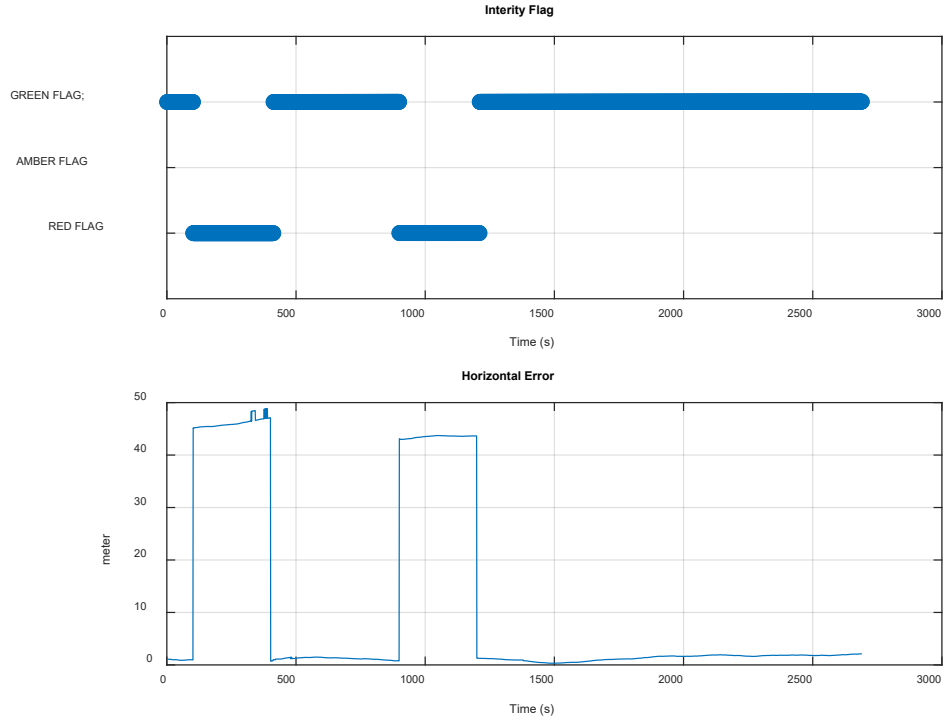

Figure 5-64 The MGRAIM Integrity Flag (above) and Horizontal Error (below).

The solution performance is summarised in Table 5-33. For GPS L1/L5 and GAL E1/E5a the horizontal error is 45.90m with a percentile of 95%.

Table 5-33 TS13a - NEU and Horizontal error parameters for GPS L1/L5 and GAL E1/E5a

	MEAN (m)	STD (m)	95% (m)
North	6.403	13.758	37.613
East	1.796	14.672	35.868
Up	-2.482	16.515	48.086
Horizontal	10.989	18.111	45.898

Figure 5-65 illustrate the number of satellites used to compute the PVT solution and the computed DOP.

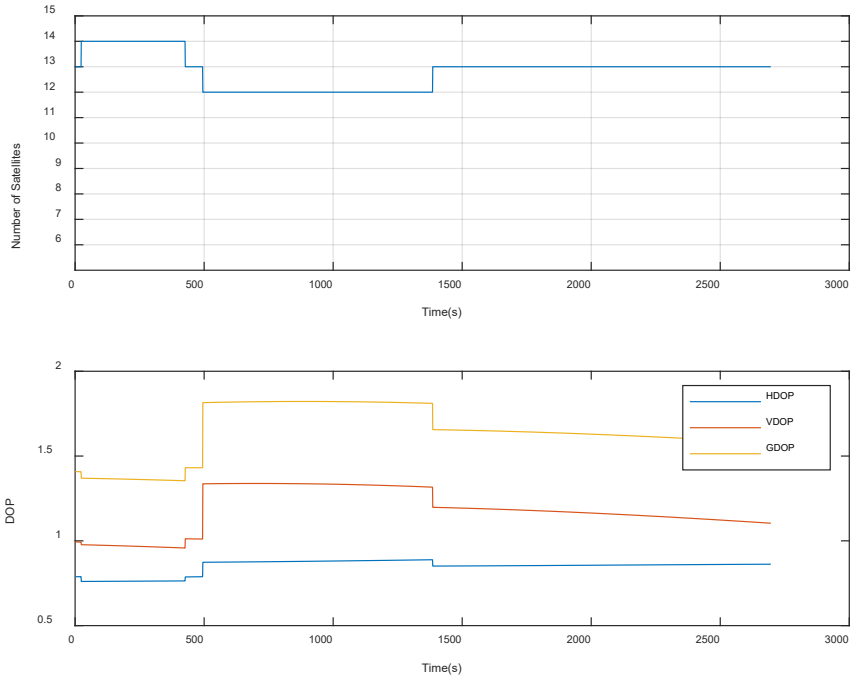

Figure 5-65 Number of SV used to generate the PVT solution and the DOP Values

5.1.3.3.4 TS14a – PVTI Performance Analysis (MRAIM) DFMC SBAS

Figure 5-66, shows integrity flags, the horizontal errors and the protection level generated. It can be seen from the integrity flag plot that the GREEN flag is raised which in this case indicates that the following condition was met PL< AL, the alert limit is set to the value of 25 m.

The large errors caused by the bias are removed compared to the MGRAIM result in TS14a. This can be attributed to the FDE process of the MRAIM where the Solution Separation Threshold test, the function that performs a threshold test for each subset and analyses if their separation is compatible with a failure. In that case where the configured threshold was met the faulty satellite was excluded to provide a safe positioning. Figure 5-67 shows the number of satellites is reduced due to the exclusion of the fault satellites The Positioning error generated is significantly reduced compared to MGRAIM approach.

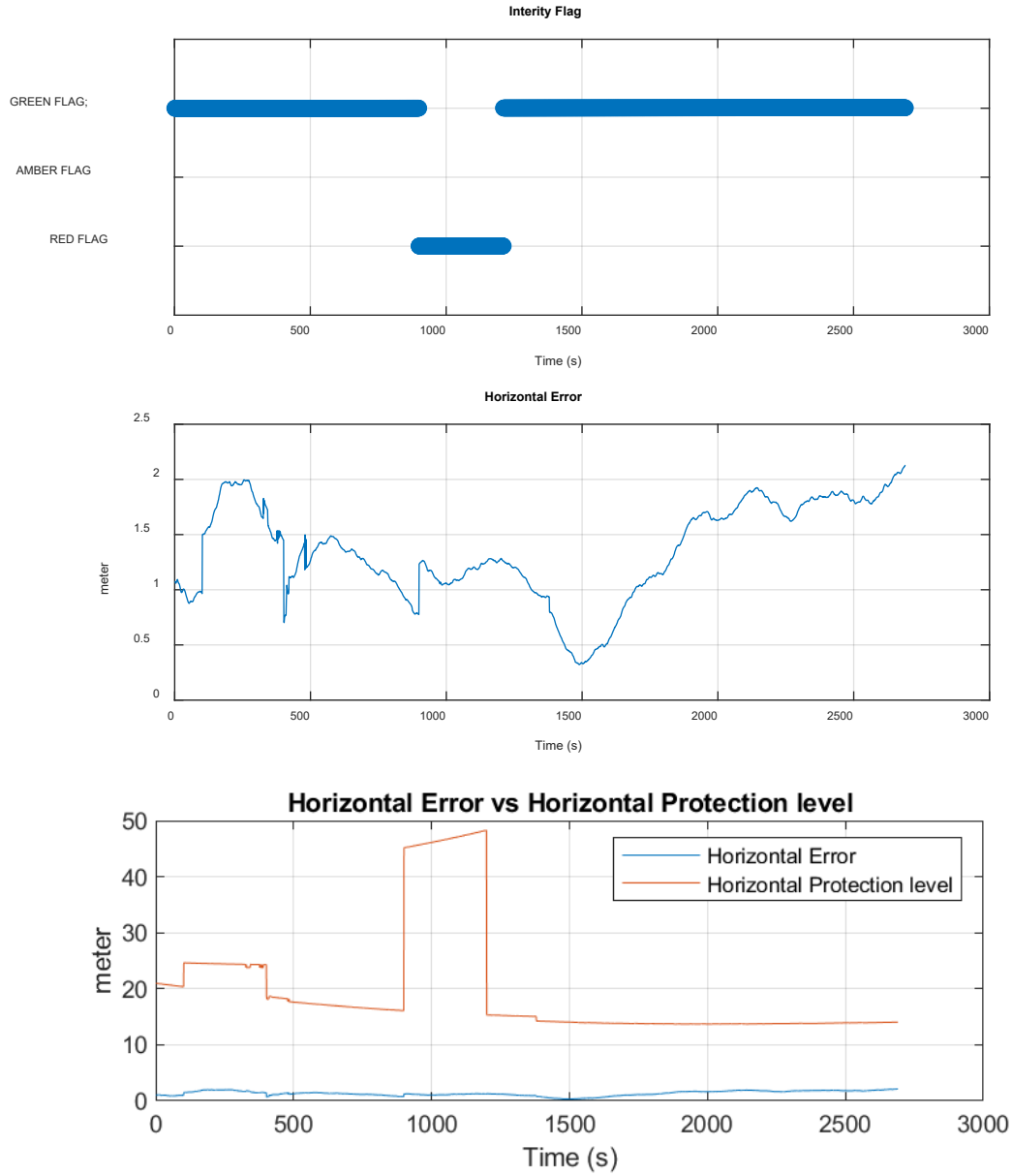

Figure 5-66 The MRAIM Integrity Flag (above), Horizontal Error (middle). and Horizontal Error vs HPL (below).

The solution performance is summarised in Table 5-34. For GPS L1/L5 and GAL E1/E5a the horizontal error is 1.96m with a percentile of 95%.

Table 5-34 TS14a - NEU and Horizontal error parameters for GPS L1/L5 and GAL E1/E5a

	MEAN (m)	STD (m)	95% (m)
North	0.811	0.574	1.492
East	0.900	0.461	1.582
Up	3.341	1.243	6.450
Horizontal	1.349	0.438	1.958

Figure 5-67 illustrate the number of satellites used to compute the PVT solution and the computed DOP.

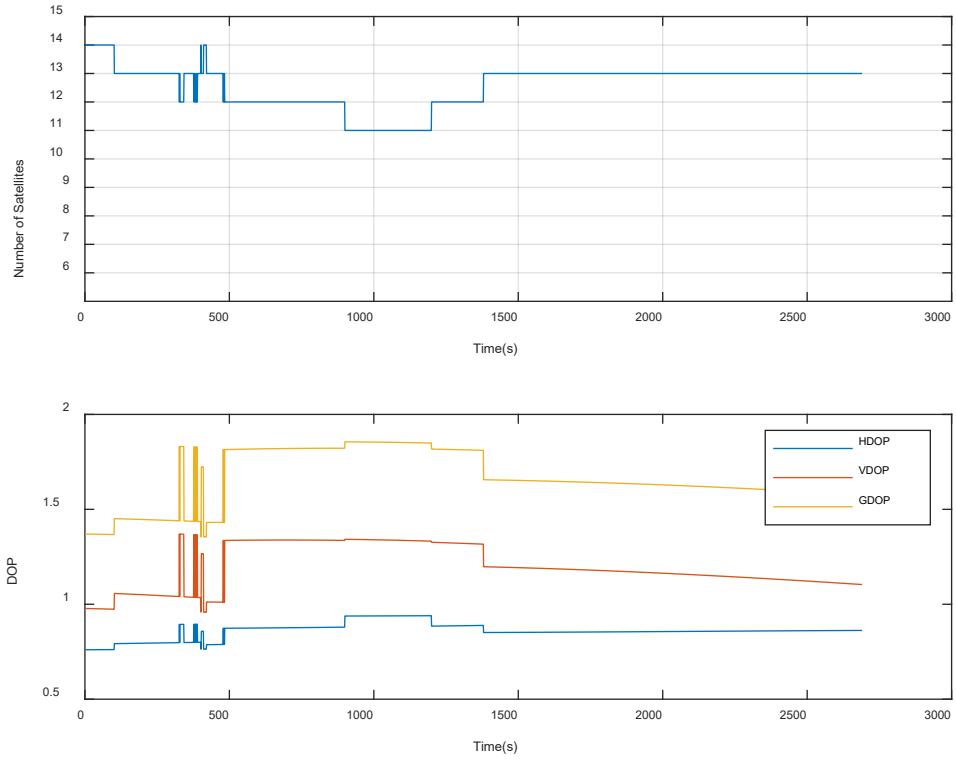

Figure 5-67 Number of SV used to generate the PVT solution and the DOP Values

5.1.4 Evaluation of GNSS Data with injected Ephemeris Error

5.1.4.1 Single high-elevation SV

The ephemeris is the satellite coordinate system. It tells the receiver where the satellite is at an instant of time. GPS receivers calculate coordinates relative to the known locations of satellites in space, a complex task that involves knowing the shapes of satellite orbits as well as their velocities, neither of which is constant. The GPS Control Segment monitors satellite locations at all times, calculates orbit eccentricities, and compiles these deviations in documents called ephemerides. An ephemeris is compiled for each satellite and broadcast with the satellite signal. There is always a certain amount of age in the ephemerides and that means that the position of the satellite expressed in its ephemeris at the moment of observation cannot be perfect. So orbital bias could be thought of as the error in the broadcast ephemeris. Even with the corrections from the GNSS ground control system, there are still small errors in the orbit that can result in up to ±2.5 metres of position error.

This subsection shows the results generated using a smoothing constant of 100 seconds based on the following test scenario:

Test Scenario	*Correction mode*	*Fault injection*	*Comment*
TS.15	MGRAIM DFMC	Single Satellite Bad Ephemeris Upload - High Elevation SV	Manually edit an ephemeris parameter within the Broadcast Navigation Message (e.g., the longitude of the ascending node (LAAN) value)
TS.16	MRAIM DFMC	Single Satellite Bad Ephemeris Upload - High Elevation SV	

Table 5-35 shows the configuration parameters and values used to create the bias fault injection dataset. For this test scenario the longitude of the ascending node parameter on a high elevation was modified within the broadcast navigation message from its original value .248039365746D+01 to .148039365746D+01

Table 5-35 TS.15/TS.16 Configuration

Parameter	*Value*	*Comment*
Constellation	['G'];	The constellation on which is affected
PRN	[4];	Satellites in which the fault was injected
Ephemeris – The longitude of the ascending node Ω_0)	*From:0.248039365746D+01 to 0.148039365746D+01;*	The LAAN one of the orbital elements used to specify the orbit of an object in space.

5.1.4.1.1 TS15 – PVTI Performance Analysis (MGRAIM) DFMC

Figure 5-68 and Figure 5-69 show fault detection test results from Test Scenario 15 MGRAIM DFMC. Figure 5-68 illustrates test statistics and threshold values computed for the solution generated for the dataset. The test statistics and threshold values are used within Fault Detection Test. It can be seen from the graph the point at which the test statistic exceeds the detection threshold, when this occurs the “red light” integrity alarm/flag is raised. Figure 5-69, shows integrity flags and the horizontal errors within the solution generated.

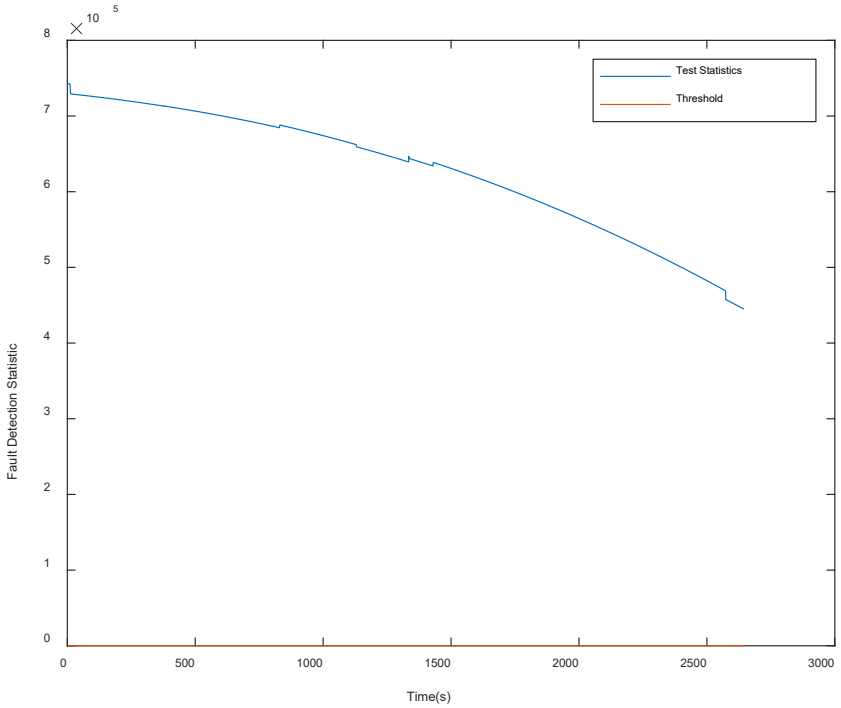

Figure 5-68 FD results from MGRAIM in Ephemeris fault case

The results indicate that the algorithm has detected the injected fault, as the RED flag is raised, this occurs when the test statistic exceeds the detection threshold ($t^2 > T^2$). The red flag was raised for the entire duration of the dataset as the test statistics exceed the threshold value of 6.40.

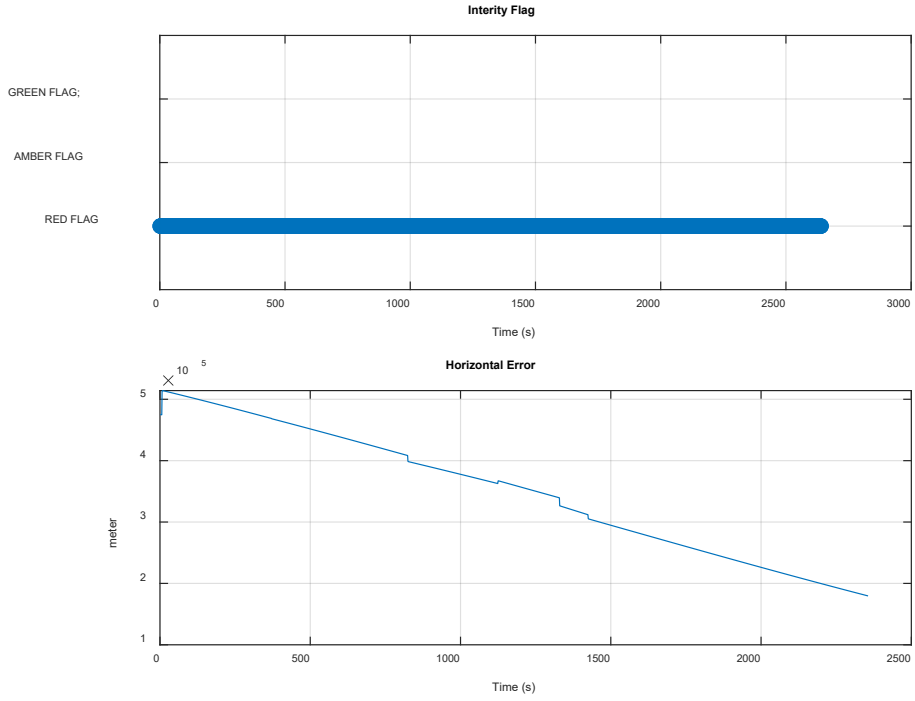

Figure 5-69 The MGRAIM Integrity Flag (above) and Horizontal Error (below)

The solution performance is summarised in Table 5-36, for GPS L1/L5 and GAL E1/5a.

Table 5-36 TS15 - NEU and Horizontal error parameters for GPS L1/L5 and GAL E1/E5a

	MEAN (m)	STD (m)	95% (m)
North	-44666.1	43542.75	117610.8
East	-348156	96935.8	486960.7
Up	308513.9	47600.18	352158.4
Horizontal	352465.4	101330	499849.6

Figure 5-70 illustrate the number of satellites used to compute the PVT solution and the computed DOP.

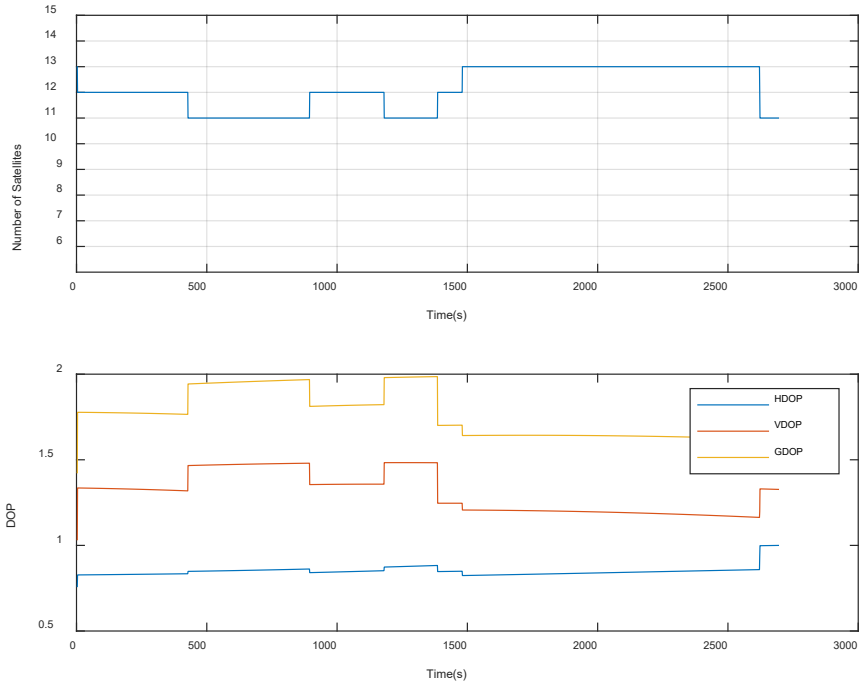

Figure 5-70 Number of SV used to generate the PVT solution and the DOP Values

5.1.4.1.2 TS16 – PVTI Performance Analysis (MRAIM) DFMC

Figure 5-71, shows integrity flags, the horizontal errors and the protection level generated. It's been observed that the fault was detected and where possible eliminated, and the integrity RED and GREEN flags were raised accordingly. The RED flag indicates to the user at least one of the SS tests fails, and the error is not excluded and/or the PL/UL is over the AL, while the GREEN flag indicates that all the tests are performed successfully and therefore the solution is ok for use. Figure 5-72, shows the number of satellites is reduced due to the exclusion of the fault satellites The Positioning error generated is significantly reduced compared to MGRAIM approach.

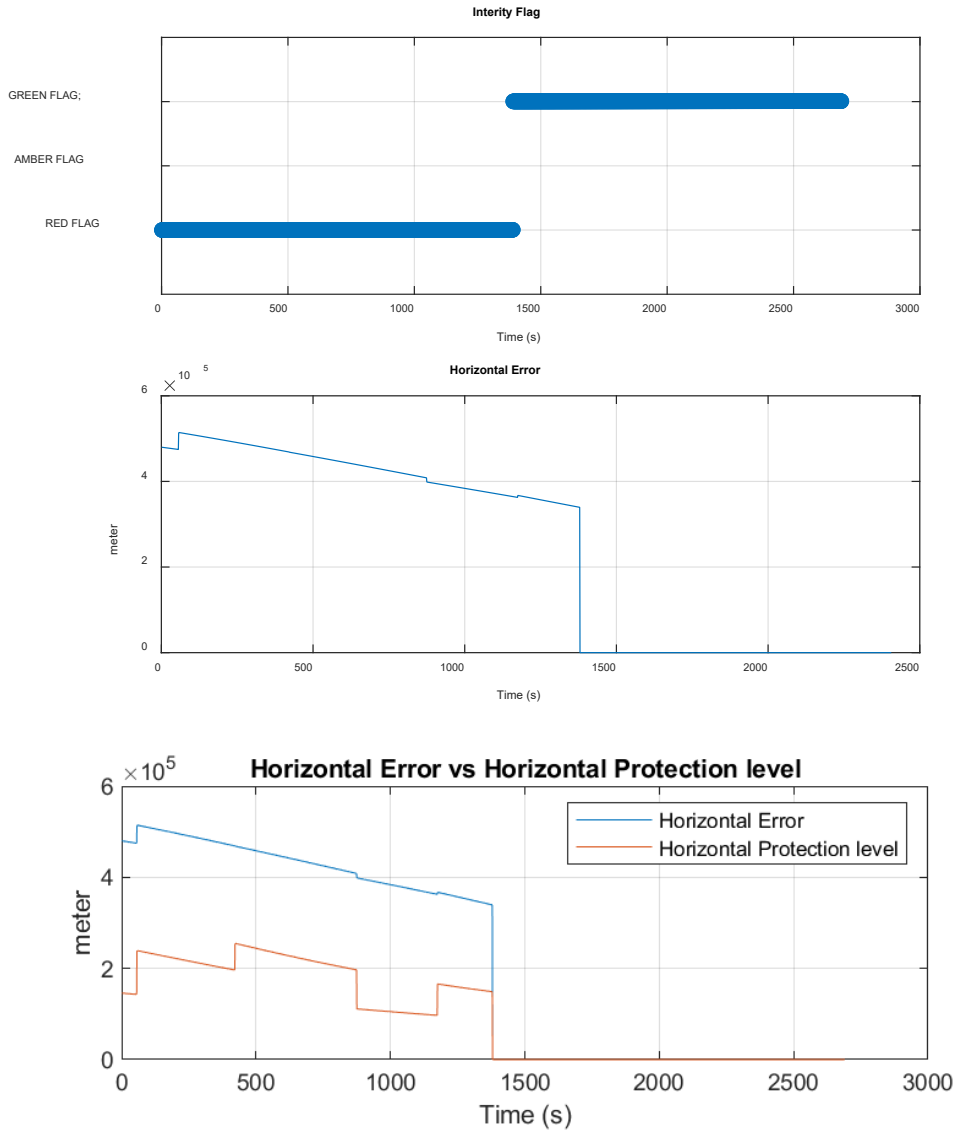

Figure 5-71 The MRAIM Integrity Flag (above), Horizontal Error (middle) and HPL (below)

The solution performance is summarised in Table 5-37 for GPS L1/L5 and GAL E1/5a.

Table 5-37 TS12 - NEU and Horizontal error parameters for GPS L1/L5 and GAL E1/5a.

	MEAN (m)	STD (m)	95% (m)
North	-41870.9	44987.17	117610.8
East	-242652	211763.2	486960.7
Up	170131.8	151552.2	351995.2
Horizontal	246765.5	215887.1	499849.6

Figure 5-72 illustrate the number of satellites used to compute the PVT solution and the computed DOP.

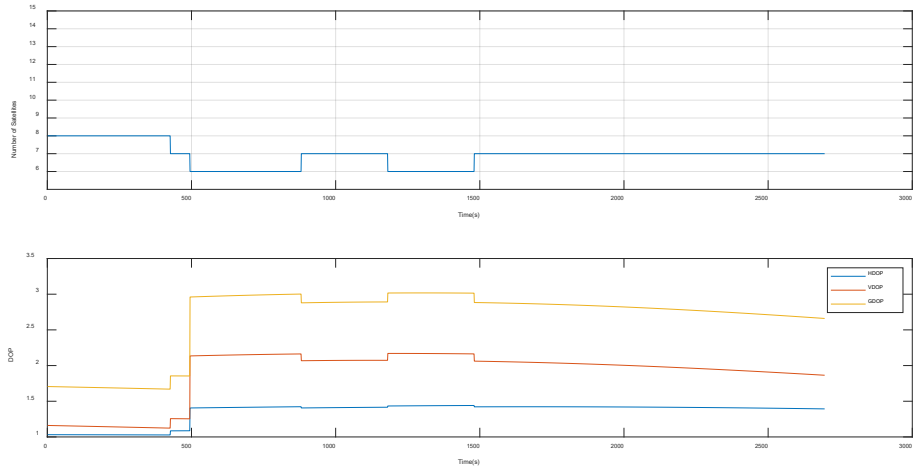

Figure 5-72 Number of SV used to generate the PVT solution and the DOP Values

5.1.4.1.3 TS15a – PVTI Performance Analysis (MGRAIM) DFMC SBAS

Figure 5-73 and Figure 5-74 show fault detection test results from Test Scenario 15 MGRAIM DFMC. Figure 5-73 illustrates test statistics and threshold values computed for the solution generated for the dataset. The test statistics and threshold values are used within Fault Detection Test. It can be seen from the graph the point at which the test statistic exceeds the detection threshold, when this occurs the “red light” integrity alarm/flag is raised. Figure 5-74, shows integrity flags and the horizontal errors within the solution generated.

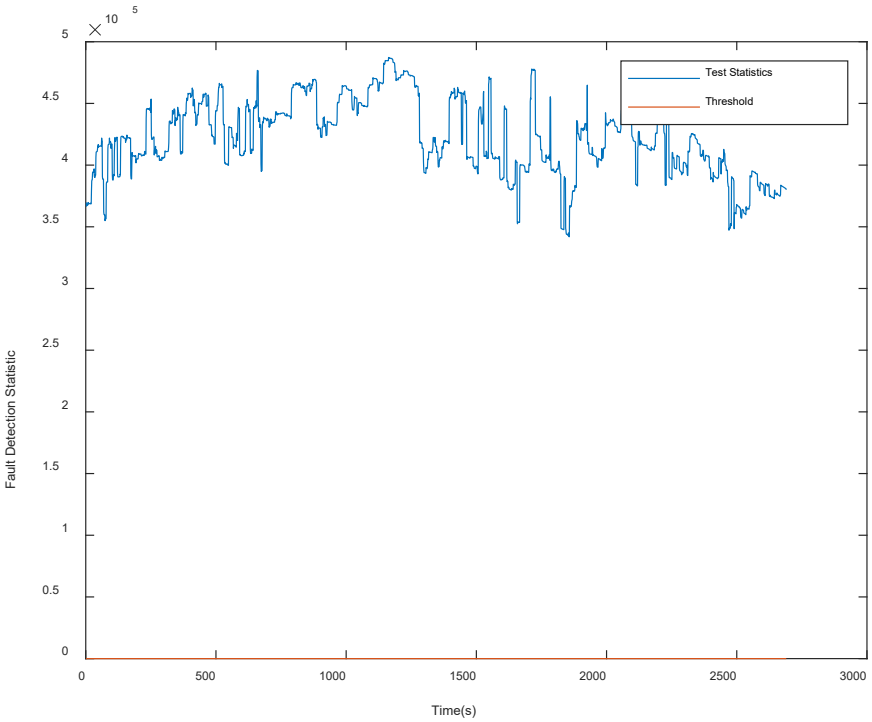

Figure 5-73 FD results from MGRAIM in Ephemeris fault case

The results indicate that the algorithm has detected the injected fault, as the RED flag is raised, this occurs when the test statistic exceeds the detection threshold ($t^2 > T^2$). The red flag was raised for the entire duration of the dataset as the test statistics exceed the threshold value of 6.40.

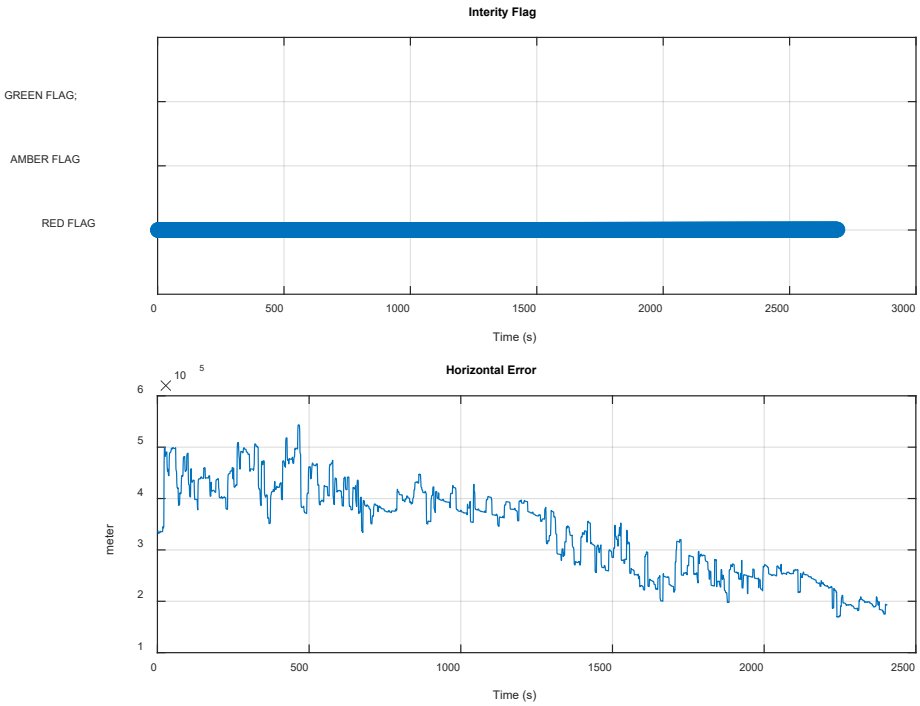

Figure 5-74 The MGRAIM Integrity Flag (above) and Horizontal Error (below)

The solution performance is summarised in Table 5-38, for GPS L1/L5 and GAL E1/5a.

Table 5-38 TS16 - NEU and Horizontal error parameters for GPS L1/L5 and GAL E1/E5a

	MEAN (m)	STD (m)	95% (m)
North	-94395.1	54600.38	184146.8
East	-323094	79068.52	444689.9
Up	301673	173564.5	570875.5
Horizontal	338639.2	88633.66	478246.5

Figure 5-75 illustrate the number of satellites used to compute the PVT solution and the computed DOP.

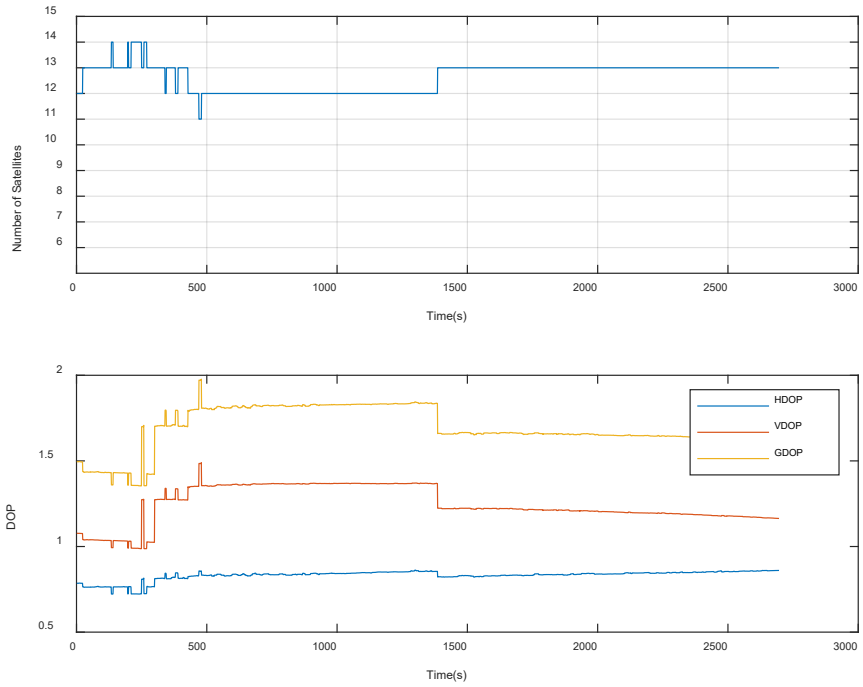

Figure 5-75 Number of SV used to generate the PVT solution and the DOP Values

5.1.4.1.4 TS16a – PVTI Performance Analysis (MRAIM) DFMC SBAS

Figure 5-76, shows integrity flags, the horizontal errors and the protection level generated. It's been observed that the fault was detected and where possible eliminated, and the integrity RED and GREEN flags were raised accordingly. The RED flag indicates to the user at least one of the SS tests fails and the error is not excluded and/or the PL/UL is over the AL, while the GREEN flag indicates that all the tests are performed successfully and therefore the solution is ok for use. Figure 5-77, shows the number of satellites is reduced due to the exclusion of the fault satellites The Positioning error generated is significantly reduced compared to MGRAIM approach.

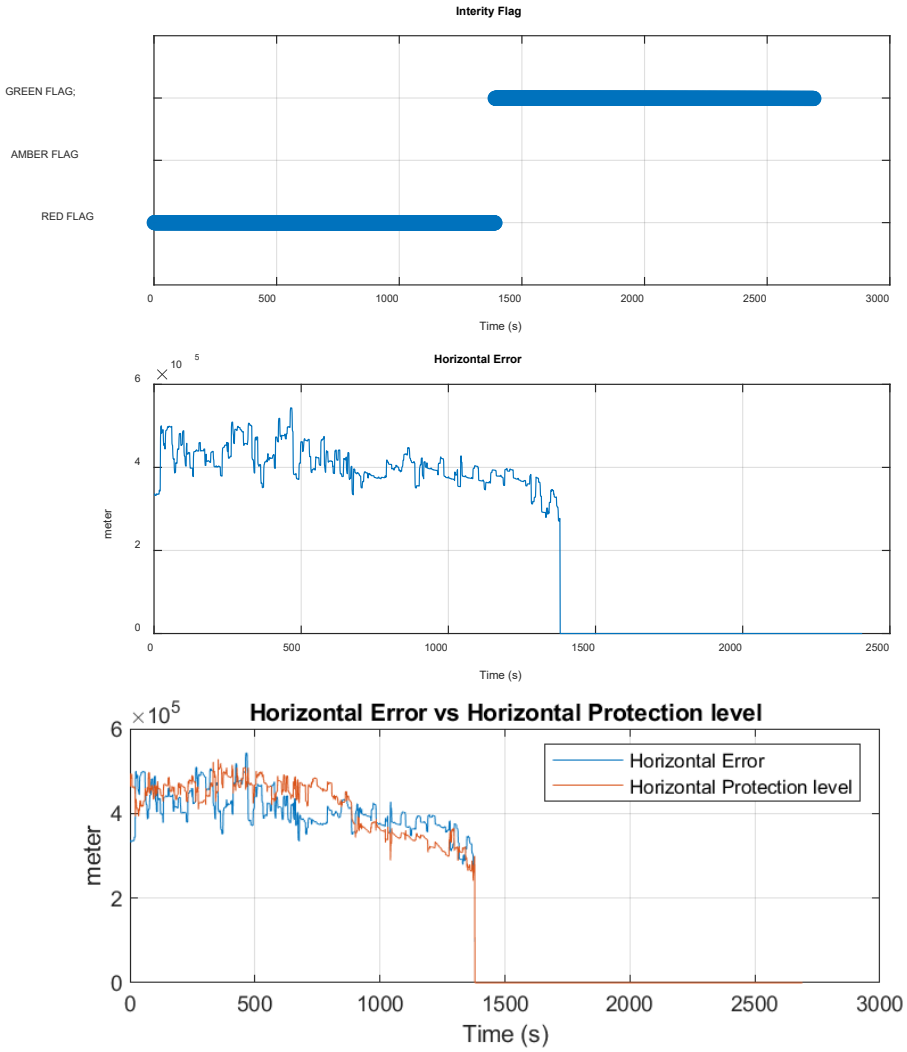

Figure 5-76 The MRAIM Integrity Flag (above), Horizontal Error (middle) and HPL (below)

The solution performance is summarised in Table 5-39 for GPS L1/L5 and GAL E1/5a.

Table 5-39 TS16a - NEU and Horizontal error parameters for GPS L1/L5 and GAL E1/5a.

	MEAN (m)	STD (m)	95% (m)
North	-75816	69987.7	184146.8
East	-219484	191504.5	444689.9
Up	113970.3	141513.8	360564.8
Horizontal	232631	203411.2	478246.5

Figure 5-77 illustrate the number of satellites used to compute the PVT solution and the computed DOP.

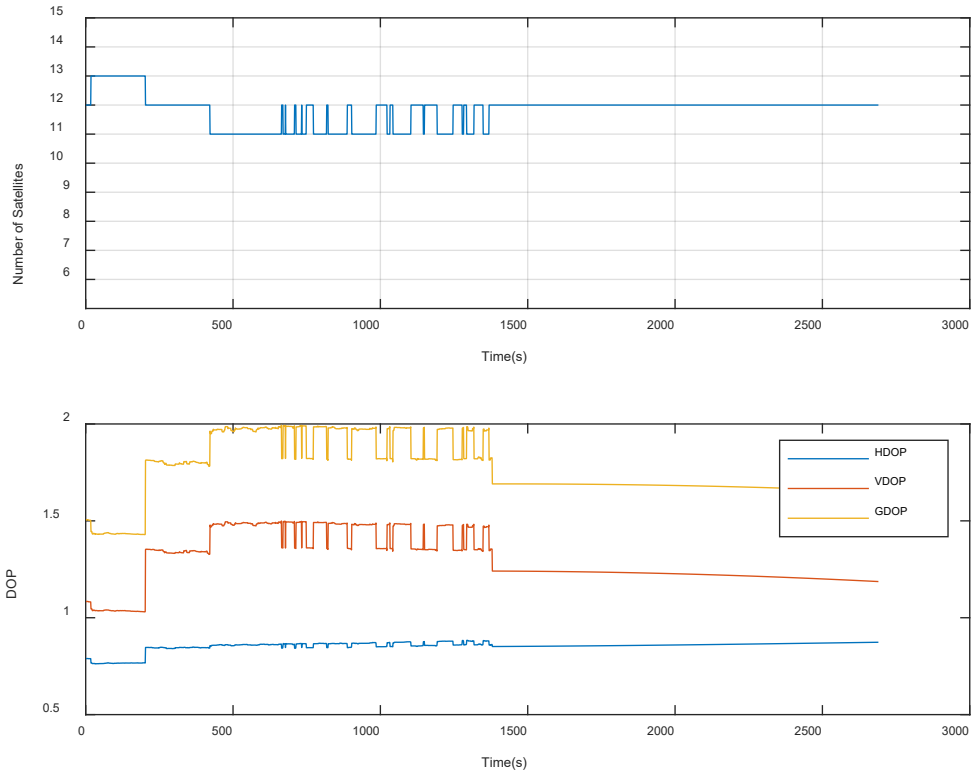

Figure 5-77 Number of SV used to generate the PVT solution and the DOP Values

5.1.4.2 Multiple High-elevation SV

This subsection shows the results generated using a smoothing constant of 100 seconds based on the following test scenario:

This subsection shows the results generated using a smoothing constant of 100 seconds based on the following test scenario:

Test Scenario	*Correction mode*	*Fault injection*	*Comment*
TS.17	MGRAIM DFMC	Single Satellite Bad Ephemeris Upload - High Elevation SV	Manually edit an ephemeris parameter within the Broadcast Navigation Message (e.g. the longitude of the ascending node (LAAN) value)
TS.18	MRAIM DFMC	Single Satellite Bad Ephemeris Upload - High Elevation SV	

Table 5-40 shows the configuration parameters and values used to create the bias fault injection dataset. For this test scenario the longitude of the ascending node parameter on a high elevation satellite was modified within the broadcast navigation message from its original value.

Table 5-40 TS.11/TS.12 Configuration

Parameter	*Value*	*Comment*
Constellation	['G'];	The constellation on which is affected
PRN	[3]; [6];	Satellites in which the fault was injected
Ephemeris – The longitude of the ascending node Ω_0)	*From:0.248039365746D+01 to 0.148039365746D+01;* *From: 0.357628910851D+00 to 0.257628910851D+00*	The LAAN is the orbital elements used to specify the orbit of an object in space.

5.1.4.2.1 TS17– PVTI Performance Analysis (MGRAIM) DFMC

Figure 5-78 and Figure 5-79 show fault detection test results from Test Scenario 17 MGRAIM DFMC. Figure 5-78 illustrates test statistics and threshold values computed for the solution generated for the dataset. The test statistics and threshold values are used within Fault Detection Test. It can be seen from the graph the point at which the test statistic exceeds the detection threshold, when this occurs the “red light” integrity alarm/flag is raised. Figure 5-79, shows integrity flags and the horizontal errors within the solution generated.

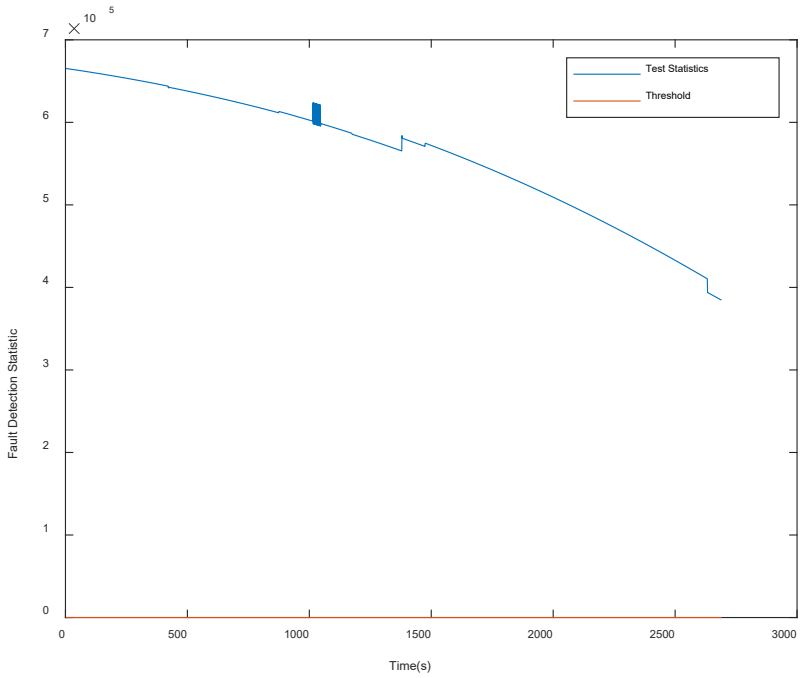

Figure 5-78 FD results from MGRAIM in Ephemeris fault case

The results indicate that the algorithm has detected the injected fault, as the RED flag is raised, this occurred when the test-statistic exceeds the detection threshold ($t^2 > T^2$). The red flag was raised for the entire duration of the dataset as the test statistics exceed the threshold value of 5.39.

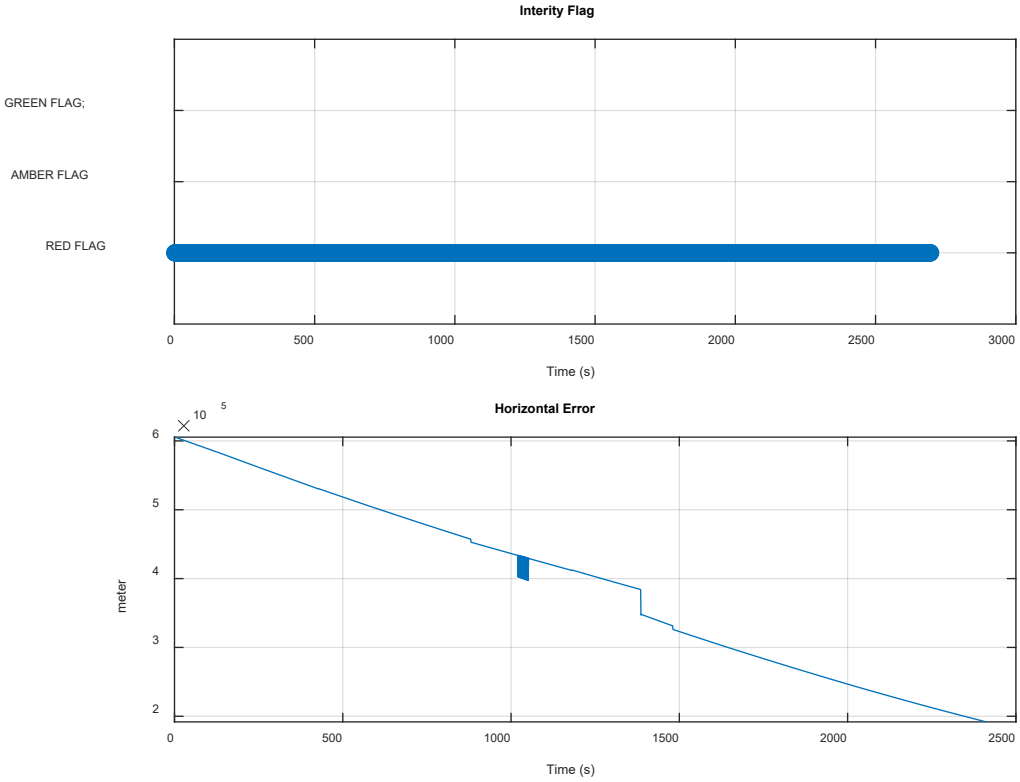

Figure 5-79 The MGRAIM Integrity Flag (above) and Horizontal Error (below).

The solution performance is summarised in Table 5-41 for GPS L1/L5 and GAL E1/E5a .

Table 5-41 TS17 - NEU and Horizontal error parameters for GPS L1/L5 and GAL E1/E5a

	MEAN (m)	STD (m)	95% (m)
North	34501.13	40463.46	84726.35
East	-400848	109690.5	556776
Up	369574.6	58133.31	438229.1
Horizontal	405538.1	105243.7	558354.2

Figure 5-80 illustrate the number of satellites used to compute the PVT solution and the computed DOP.

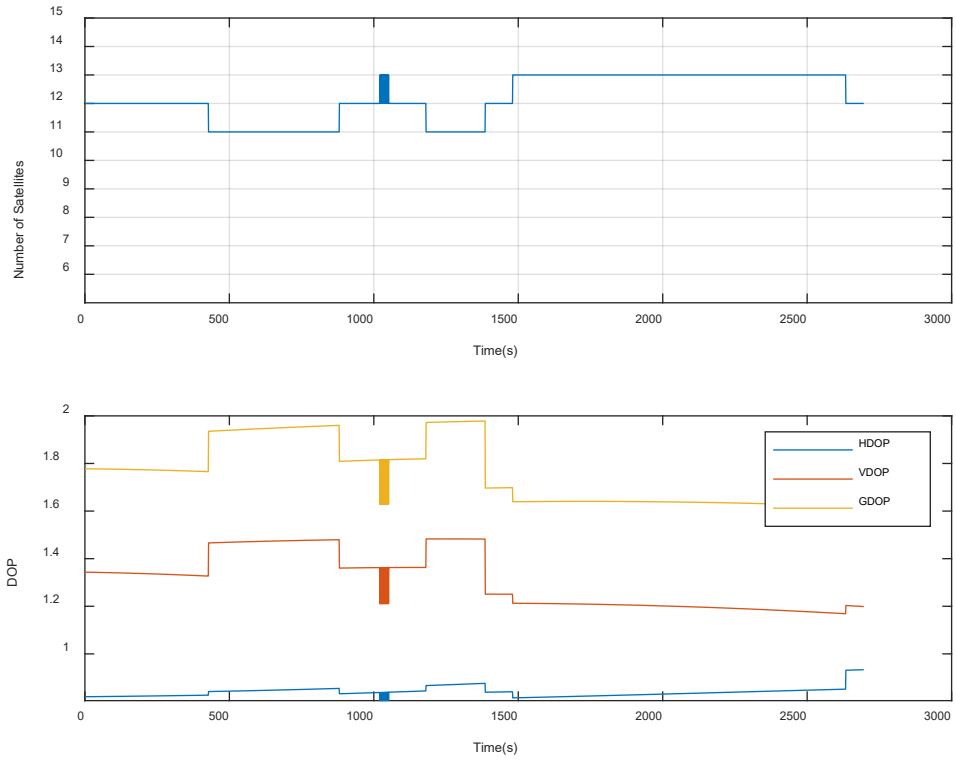

Figure 5-80 Number of SV used to generate the PVT solution and the DOP Values

5.1.4.2.2 TS18 – PVTI Performance Analysis (MRAIM) DFMC

Figure 5-81 shows integrity flags, the horizontal errors and the protection level generated. It's been observed that the fault was detected and eliminated, and the integrity RED and GREEN flags were raised accordingly. The RED flag indicates to the user at least one of the SS test fails and the error is not excluded and/or the PL/UL is over the AL, while the GREEN flag indicates that all the tests are performed successfully and therefore the solution is ok for use. Figure 5-102, shows the number of satellites is reduced due to the exclusion of the fault satellites The Positioning error generated is significantly reduced compared to MGRAIM approach.

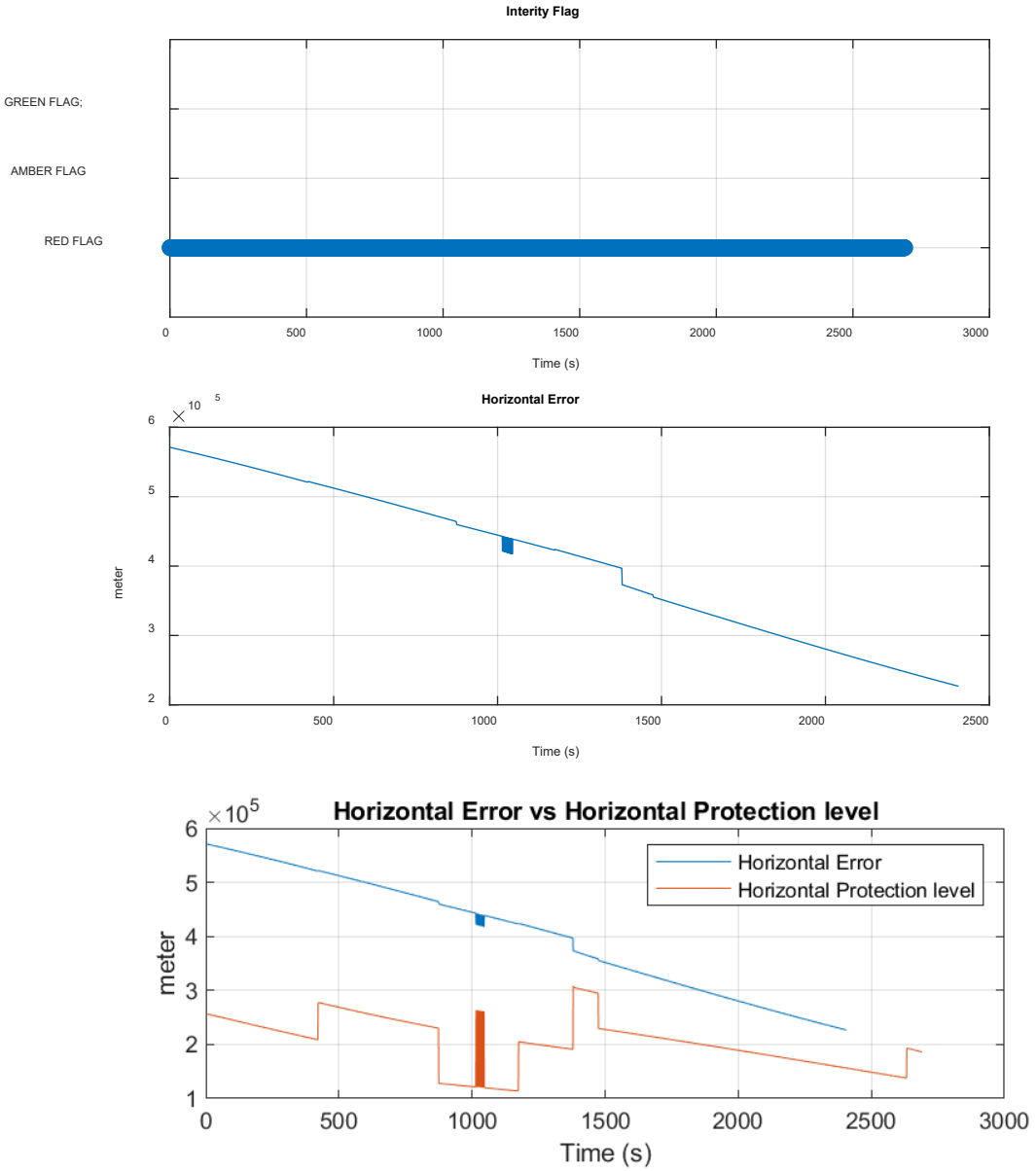

Figure 5-81 The MRAIM Integrity Flag (above), Horizontal Error (middle). and Horizontal Error vs HPL (below).

The solution performance is summarised in Table 5-42 for GPS L1/L5 and GAL E1/E5a.

Table 5-42 TS18 - NEU and Horizontal error parameters for GPS L1/L5 and GAL E1/E5a

	MEAN (m)	STD (m)	95% (m)
North	84726.35	40463.46	84726.35
East	556776	109690.5	556776
Up	438229.1	58133.31	438229.1
Horizontal	558354.2	105243.7	558354.2

Figure 5-102 illustrate the number of satellites used to compute the PVT solution and the computed DOP.

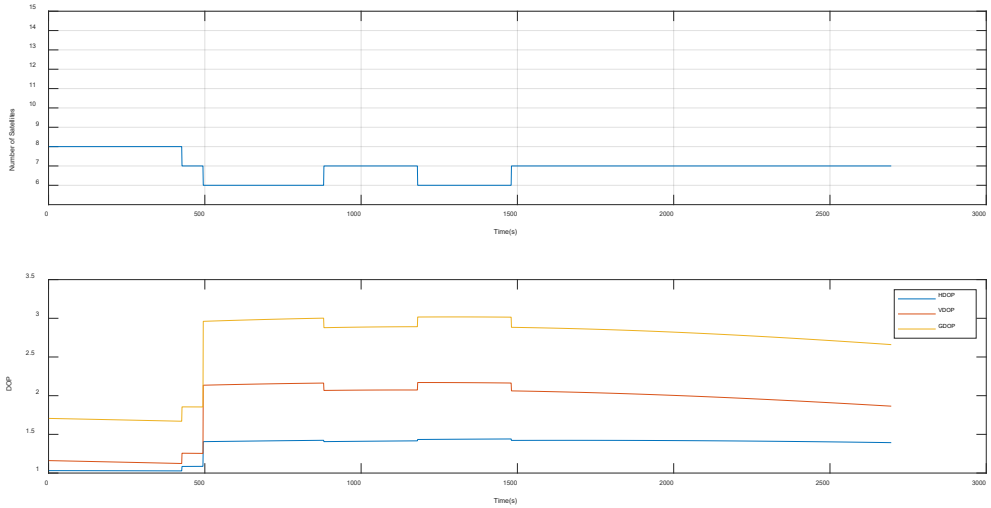

Figure 5-82 Number of SV used to generate the PVT solution and the DOP Values

5.1.4.2.3 TS17a– PVTI Performance Analysis (MGRAIM) DFMC SBAS

Figure 5-83 and Figure 5-84 show fault detection test results from Test Scenario 17 MGRAIM DFMC. Figure 5-83 illustrates test statistics and threshold values computed for the solution generated for the dataset. The test statistics and threshold values are used within Fault Detection Test. It can be seen from the graph the point at which the test statistic exceeds the detection threshold, when this occurs the “red light” integrity alarm/flag is raised. Figure 5-84, shows integrity flags and the horizontal errors within the solution generated.

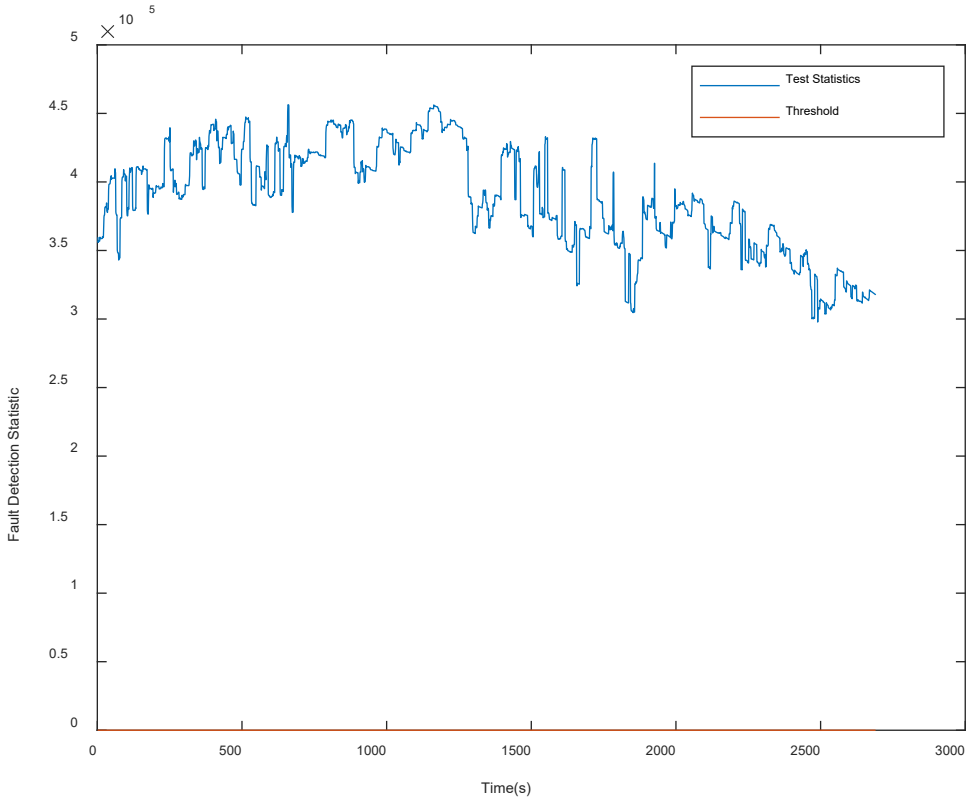

Figure 5-83 FD results from MGRAIM in Ephemeris fault case

The results indicate that the algorithm has detected the injected fault, as the RED flag is raised, this occurred when the test-statistic exceeds the detection threshold ($t^2 > T^2$). The red flag was raised for the entire duration of the dataset as the test statistics exceed the threshold value of 5.39.

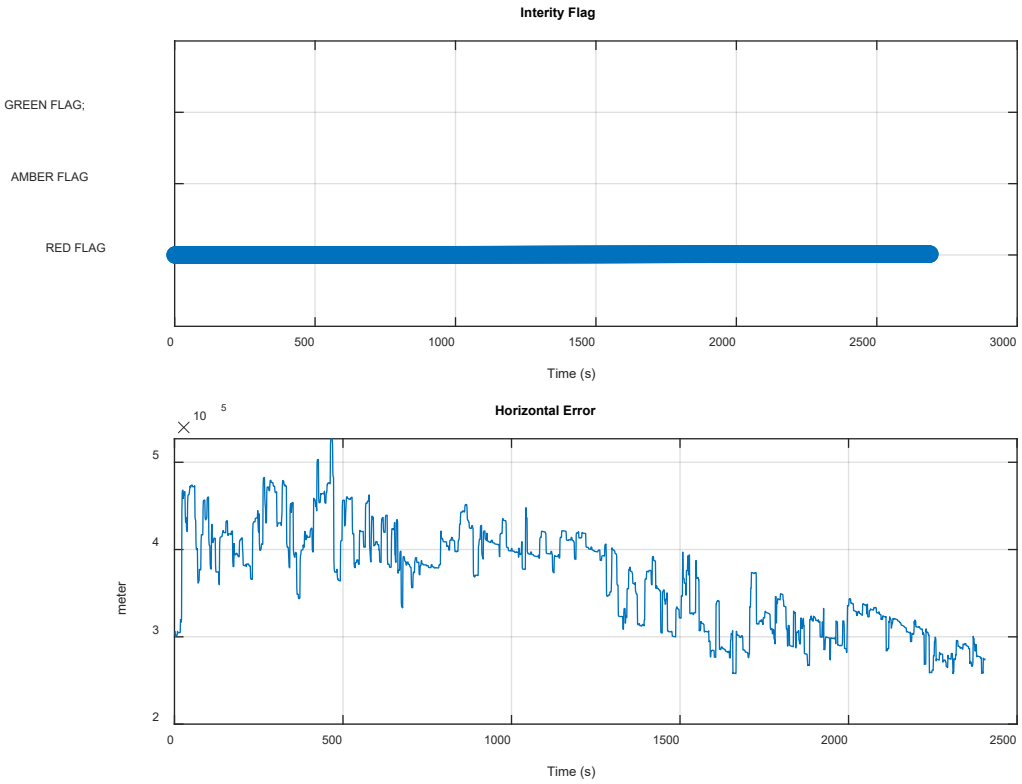

Figure 5-84 The MGRAIM Integrity Flag (above) and Horizontal Error (below).

The solution performance is summarised in Table 5-43. For GPS L1/L5 and GAL E1/E5a the horizontal error is 37.885m with a percentile of 95%.

Table 5-43 TS17a - NEU and Horizontal error parameters for GPS L1/L5 and GAL E1/E5a

	MEAN (m)	STD (m)	95% (m)
North	-1883.05	60173.12	111741
East	-360630	59495.61	454445
Up	29065.33	211391.7	381089.1
Horizontal	365884.8	57836.96	460513.2

Figure 5-85 illustrate the number of satellites used to compute the PVT solution and the computed DOP.

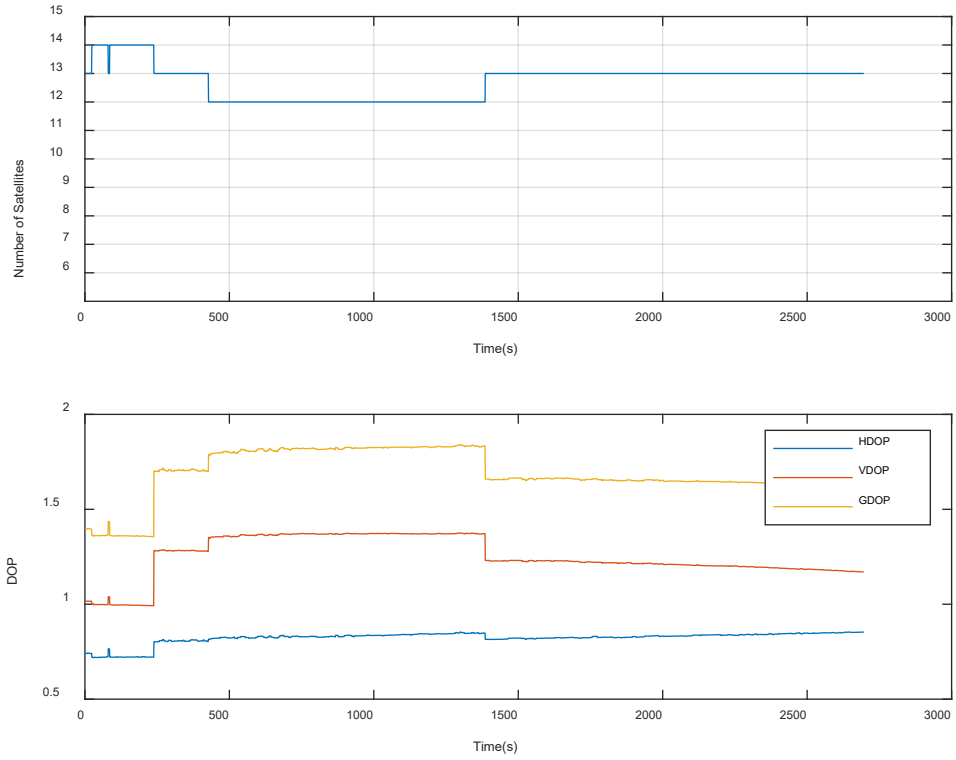

Figure 5-85 Number of SV used to generate the PVT solution and the DOP Values

5.1.4.2.4 TS18a – PVTI Performance Analysis (MRAIM) DFMC SBAS

Figure 5-86 shows integrity flags, the horizontal errors and the protection level generated. The RED flag indicates to the user at least one of the SS test fails and the error is not excluded and/or the PL/UL is over the AL, while the GREEN flag indicates that all the tests are performed successfully and therefore the solution is ok for use. Figure 5-87, shows the number of satellites is reduced due to the exclusion of the fault satellites The Positioning error generated is significantly reduced compared to MGRAIM approach.

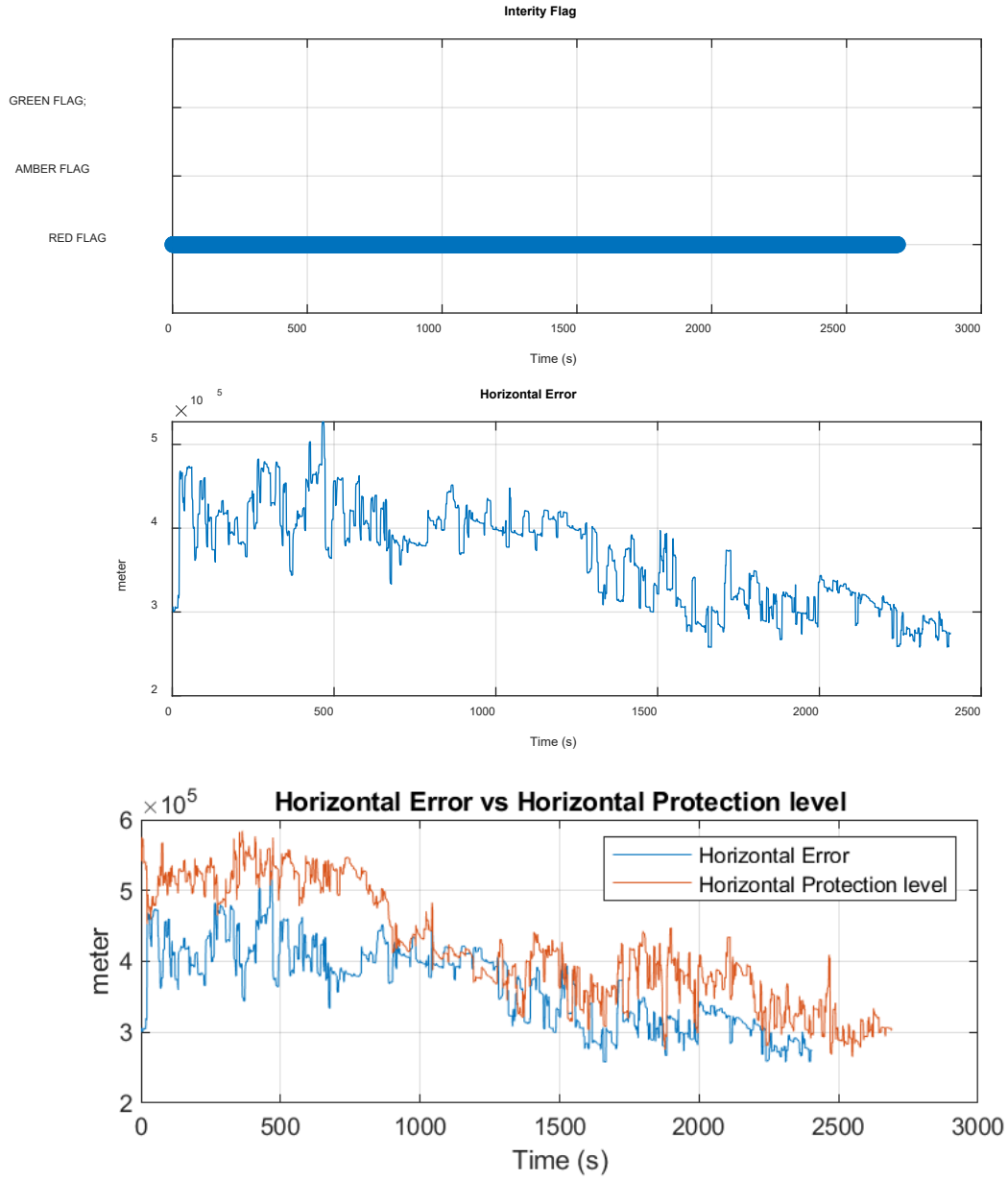

Figure 5-86 The MRAIM Integrity Flag (above), Horizontal Error (middle). and Horizontal Error vs HPL (below).

The solution performance is summarised in Table 5-44 for GPS L1/L5 and GAL E1/E5a.

Table 5-44 TS18a - NEU and Horizontal error parameters for GPS L1/L5 and GAL E1/E5a

	MEAN (m)	STD (m)	95% (m)
North	-1883.05	60173.12	111741
East	-360630	59495.61	454445
Up	29065.33	211391.7	381089.1
Horizontal	365884.8	57836.96	460513.2

Figure 5-87 illustrate the number of satellites used to compute the PVT solution and the computed DOP.

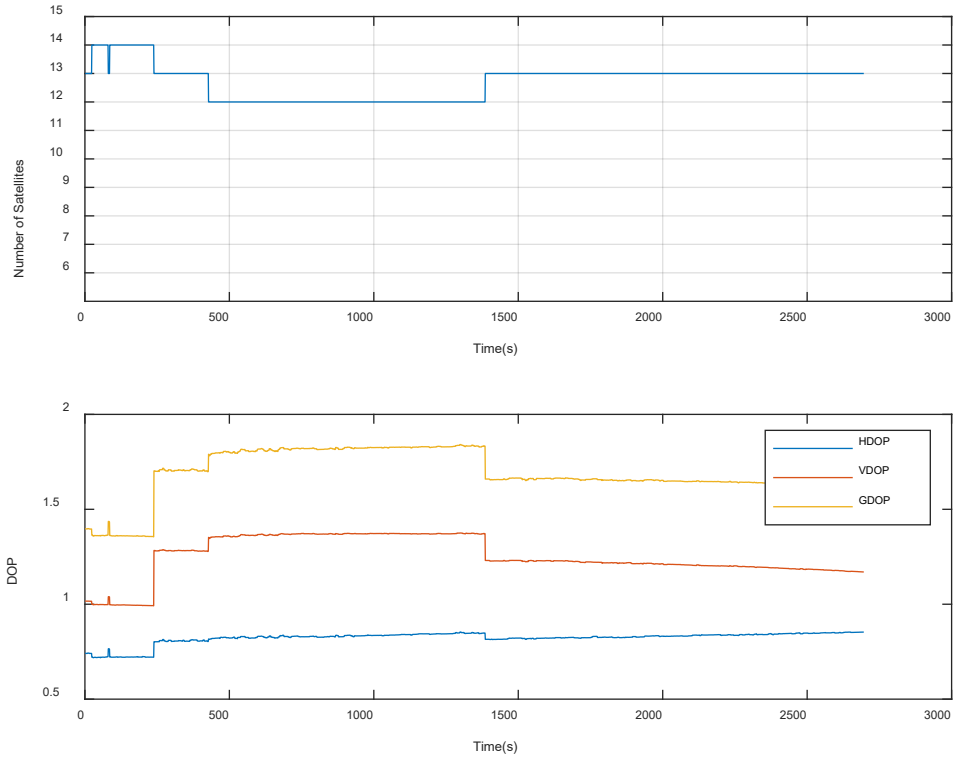

Figure 5-87 Number of SV used to generate the PVT solution and the DOP Values

5.1.5 Evaluation of GNSS Data with injected Multipath Error

5.1.5.1 Single high elevation SV

Multipath is a very localised effect, which depends only on the local environment surrounding the antenna. GNSS multipath is caused by the reception of signals arrived not only directly from satellites, but also reflected or diffracted the local objects. These signal components arrive with a certain delay, phase, and amplitude difference relative to the line-of-sight (LOS) component Multipath results in an error in pseudo range measurements and thus affects the positioning accuracy since the multipath signal takes a longer path than the direct signal resulting in pseudorange (code phase) errors of tens of metres.

This subsection shows the results generated using a smoothing constant of 100 seconds based on the following test scenario:

Test Scenario	*Correction mode*	*Fault injection*
TS.19	MGRAIM DFMC	Applying multipath error on a single high-elevation SV
TS.20	MRAIM DFMC	Applying multipath error on a single high-elevation SV

Table 5-45 shows the configuration parameters and values used to create the multipath fault injection dataset. A fault bias of 36.8m was injected into the original pseudo-range of a single high elevation (G03) satellite from t=110s (SOW: 296228s) to t = 410s (SOW: 296528s), with an amplitude of 5m.

Table 5-45 TS19/TS20 Configuration

Parameter	*Value*	*Comment*
Start time [SOW]	[296228];	represents the time and duration of the injection of the fault
End time [SOW]	[296528];	
Constellation	['G'];	The constellation on which is affected
PRN	[4]	Satellites in which the fault was injected
Bias	[36.8]	fault bias values injected into the RINEX file.
Amplitude	[5]	Multipath components
Period	[30]	

5.1.5.1.1 TS19– PVTI Performance Analysis (MGRAIM) DFMC

Figure 5-88 and Figure 5-89 show fault detection test results from Test Scenario 19 MGRAIM DFMC. Figure 5-88 illustrates test statistics and threshold values computed for the solution generated for the dataset. It can be seen from the graph that the test statistic does not exceeds the detection threshold, when this occurs the “GREEN light” integrity alarm/flag is raised.

It has been observed that the multipath error injected with a bias value of 36.8 was not detected by the MGRAIM DFMC algorithm this may be attributed to the use of dual frequency multi-constellation signals.

Figure 5-89, shows integrity flags and the horizontal errors within the solution generated.

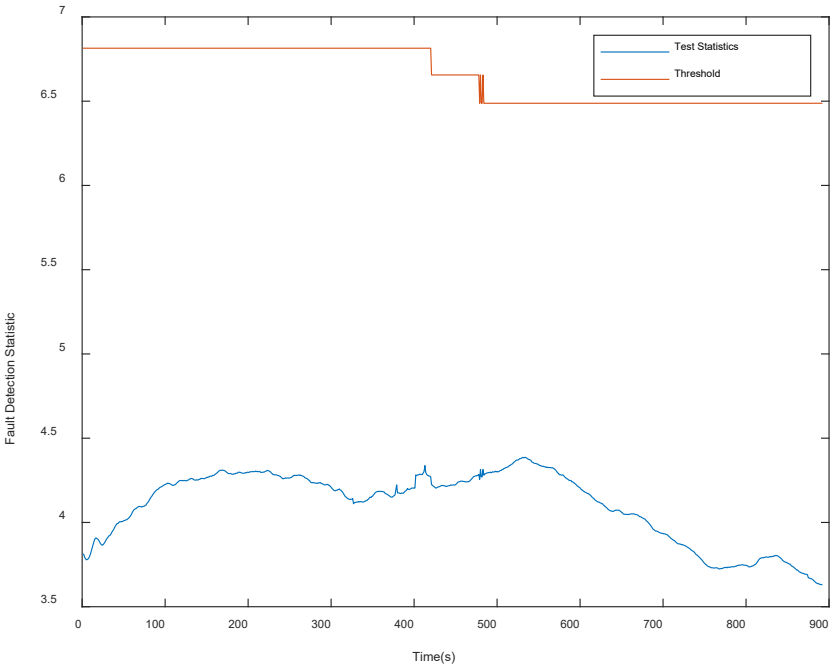

Figure 5-88 FD results from MGRAIM in Multipath fault case

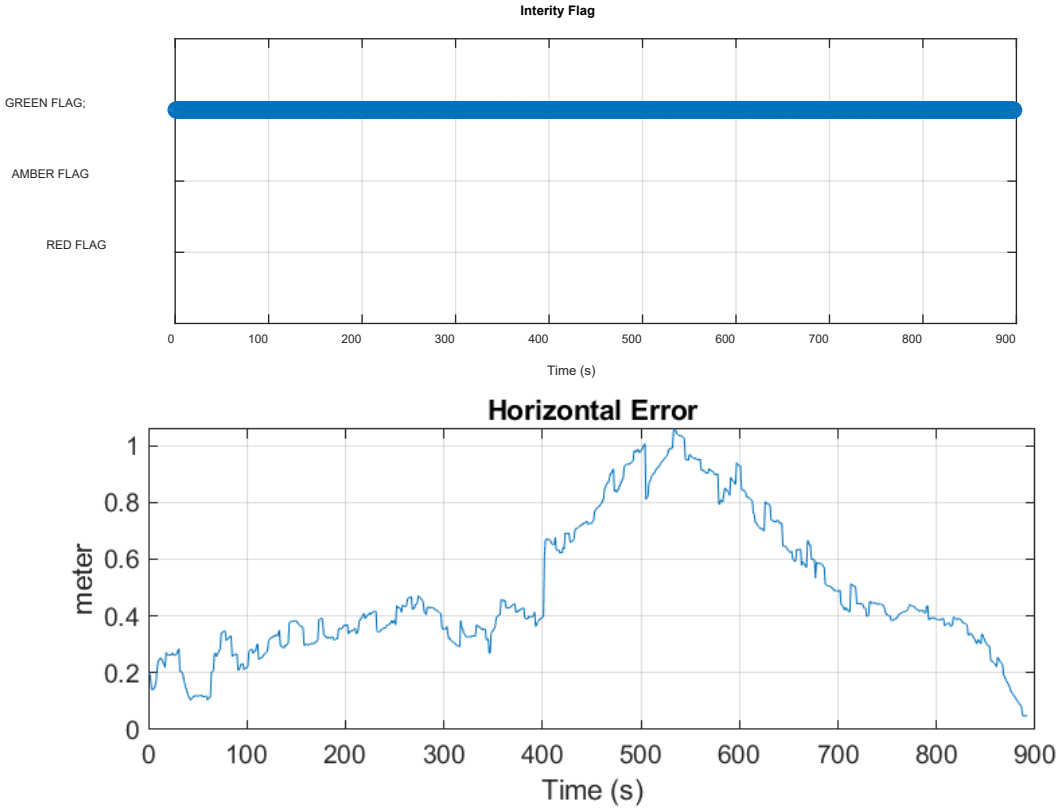

Figure 5-89 The MGRAIM Integrity Flag (above) and Horizontal Error (below)

The solution performance is summarised in Table 5-7. For GPS L1/L5 and GAL E1/5a the horizontal error is 0.57m with a percentile of 95%.

Table 5-46 TS19 - NEU and Horizontal error parameters for GPS L1

	MEAN (m)	STD (m)	95% (m)
North	0.147	0.284	0.536
East	0.128	0.201	0.438
Up	2.515	0.586	3.297
Horizontal	0.379	0.123	0.574

Figure 5-90 illustrate the number of satellites used to compute the PVT solution and the computed DOP.

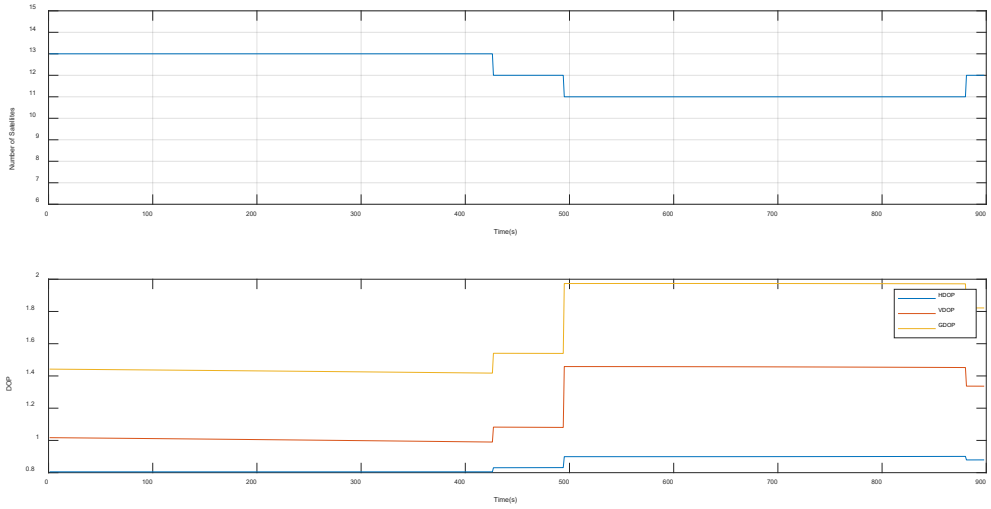

Figure 5-90 Number of SV used to generate the PVT solution and the DOP Values

5.1.5.1.2 TS20– PVTI Performance Analysis (MRAIM) DFMC

Figure 5-91 show fault detection test results from Test Scenario 14 MRAIM DFMC, which included the integrity flags, the horizontal errors and the protection level generated. It can be seen from the integrity flag plot that the GREEN flag is raised which in this case indicates that the following condition was met PL< AL, the alert limit is set to the value of 25 m.

It has been observed that the horizontal error produced a much smaller ramp error in magnitude and duration compared to the MGRAIM result. This can be attributed to the FDE process of the MRAIM where the Solution Separation Threshold test, the function that performs a threshold test for each subset and analyses if their separation is compatible with a failure. In that case where the configured threshold was met the faulty satellite was excluded to provide a safe positioning. Figure 5-14, shows the number of satellites is reduced due to the exclusion of the fault satellites The Positioning error generated is significantly reduced compared to MGRAIM approach.

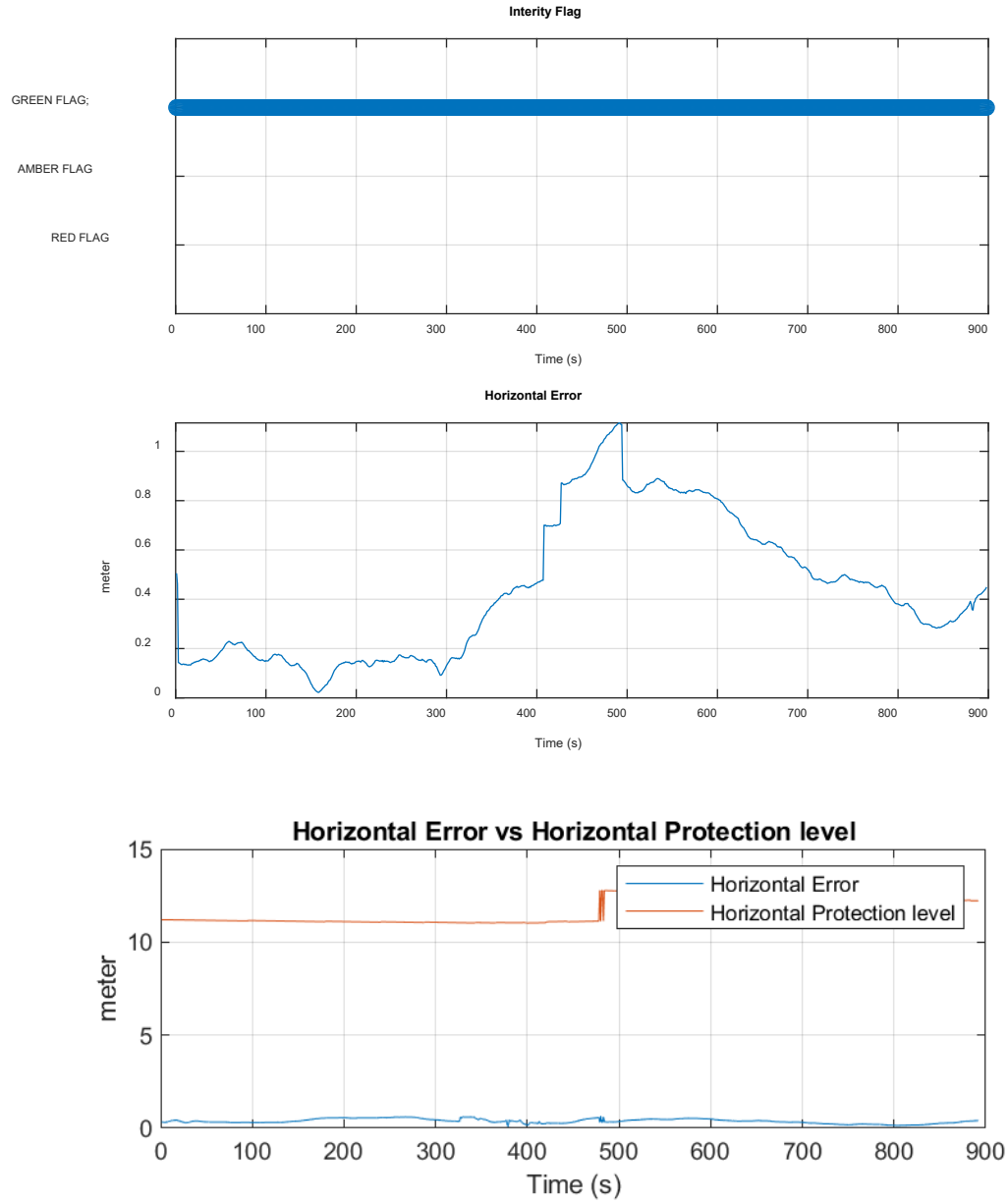

Figure 5-91 The MRAIM Integrity Flag (above) and Horizontal Error (middle) HPL (below)

The solution performance is summarised in Table 5-47. For GPS L1/L5 and GAL E1/5a the horizontal error is 0.57m with a percentile of 95%.

Table 5-47 TS20 - NEU and Horizontal error parameters for GPS L1

	MEAN (m)	STD (m)	95% (m)
North	0.147	0.284	0.536
East	0.128	0.201	0.438
Up	2.515	0.586	3.297
Horizontal	0.379	0.123	0.574

Figure 5-92 illustrate the number of satellites used to compute the PVT solution and the computed DOP.

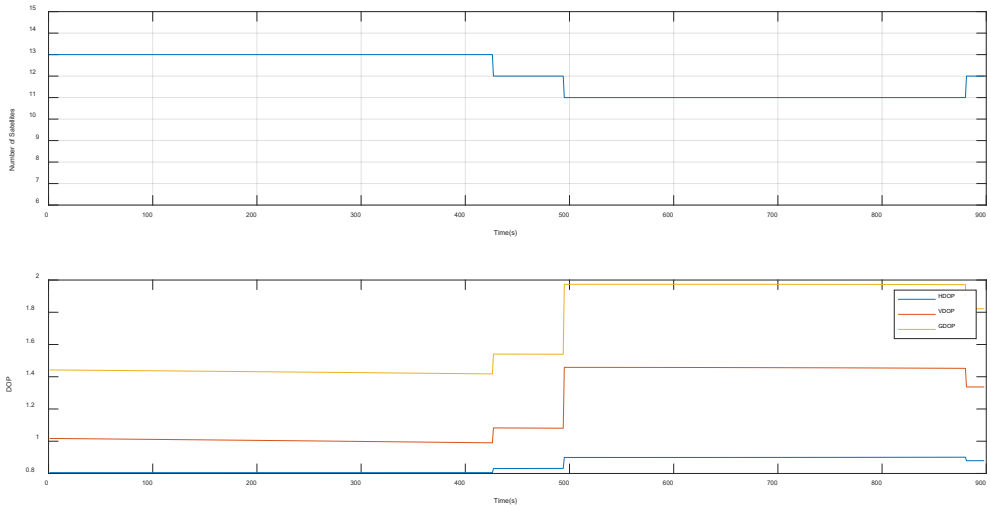

Figure 5-92 Number of SV used to generate the PVT solution and the DOP Values

5.1.5.1.3 TS19a– PVTI Performance Analysis (MGRAIM)) DFMC SBAS

Figure 5-93 and Figure 5-94 show fault detection test results from Test Scenario 19a MGRAIM DFMC. Figure 5-93 illustrates test statistics and threshold values computed for the solution generated for the dataset. It can be seen from the graph that the test statistic does not exceeds the detection threshold, when this occurs the “GREEN light” integrity alarm/flag is raised.

It has been observed that the multipath error injected with a bias value of 36.8 was not detected by the MGRAIM DFMC algorithm this may be attributed to the use of dual frequency multi-constellation signals.

Figure 5-94, shows integrity flags and the horizontal errors within the solution generated.

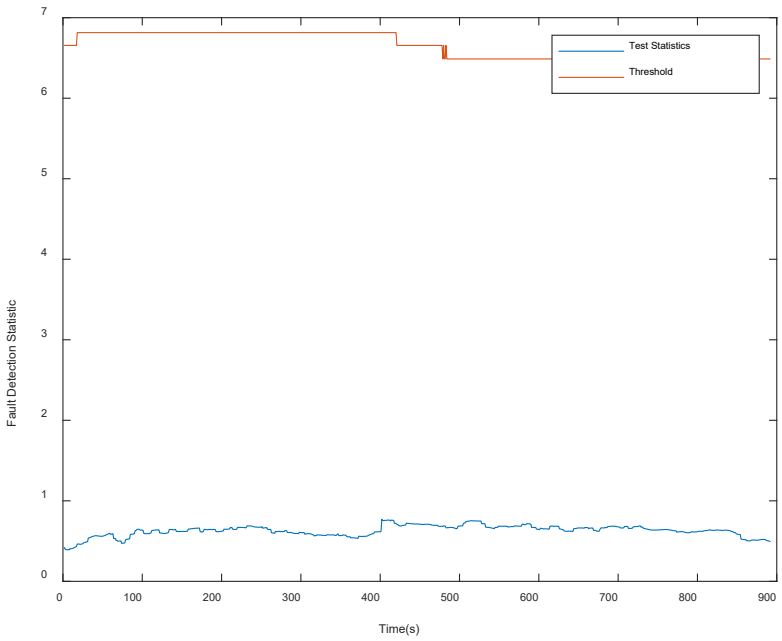

Figure 5-93 FD results from MGRAIM in Multipath fault case

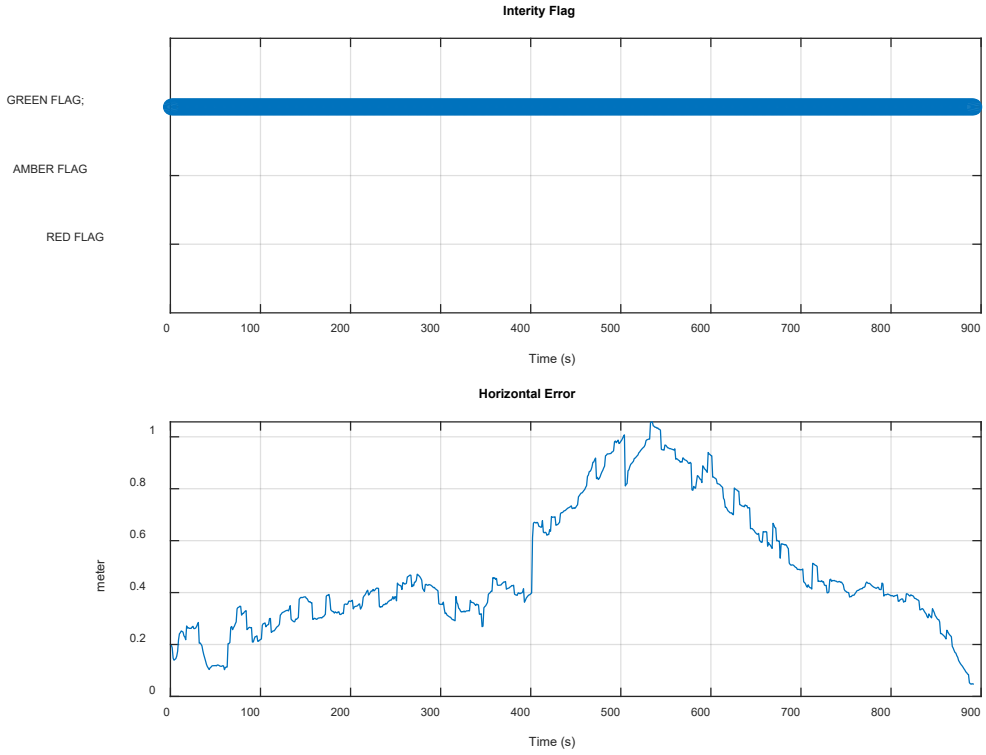

Figure 5-94 The MGRAIM Integrity Flag (above) and Horizontal Error (below)

The solution performance is summarised in Table 5-48. For GPS L1/L5 and GAL E1/5a the horizontal error is 0.95m with a percentile of 95%.

Table 5-48 TS19a - NEU and Horizontal error parameters for GPS L1

	MEAN (m)	STD (m)	95% (m)
North	-0.354	0.31	0.884
East	0.247	0.114	0.428
Up	2.047	0.667	3.206
Horizontal	0.485	0.245	0.951

Figure 5-95 illustrate the number of satellites used to compute the PVT solution and the computed DOP.

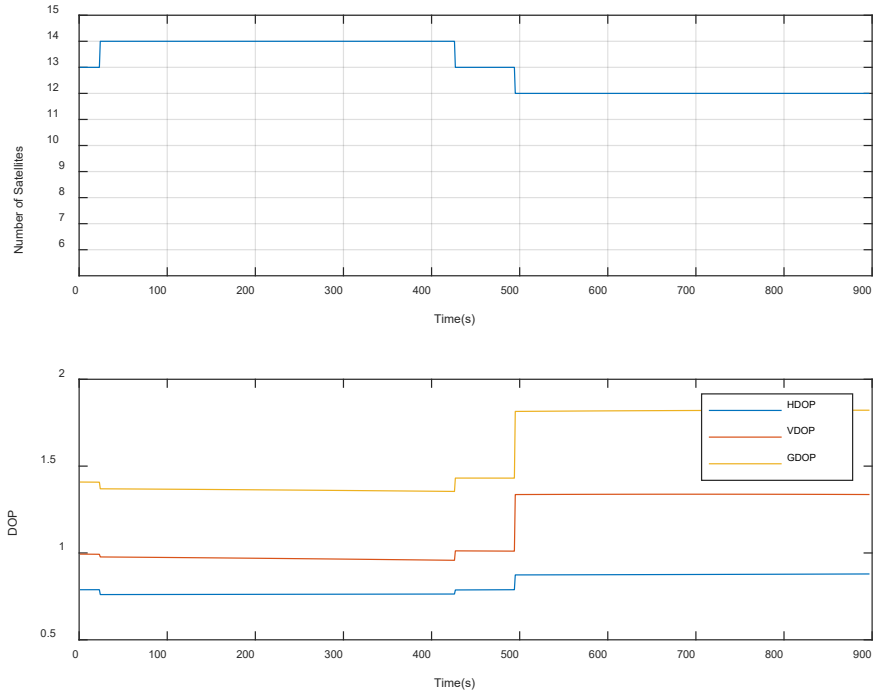

Figure 5-95 Number of SV used to generate the PVT solution and the DOP Values

5.1.5.1.4 TS20a – PVTI Performance Analysis (MRAIM) DFMC SBAS

Figure 5-96 show fault detection test results from Test Scenario 20a MRAIM DFMC, which included the integrity flags, the horizontal errors and the protection level generated. It can be seen from the integrity flag plot that the GREEN flag is raised which in this case indicates that the following condition was met PL< AL, the alert limit is set to the value of 25 m.

It has been observed that the horizontal error produced a much smaller ramp error in magnitude and duration compared to the MGRAIM result. This can be attributed to the FDE process of the MRAIM where the Solution Separation Threshold test, the function that performs a threshold test for each subset and analyses if their separation is compatible with a failure. In that case where the configured threshold was met the faulty satellite was excluded to provide a safe positioning. Figure 5-97, shows the number of satellites is reduced due to the exclusion of the fault satellites The Positioning error generated is significantly reduced compared to MGRAIM approach.

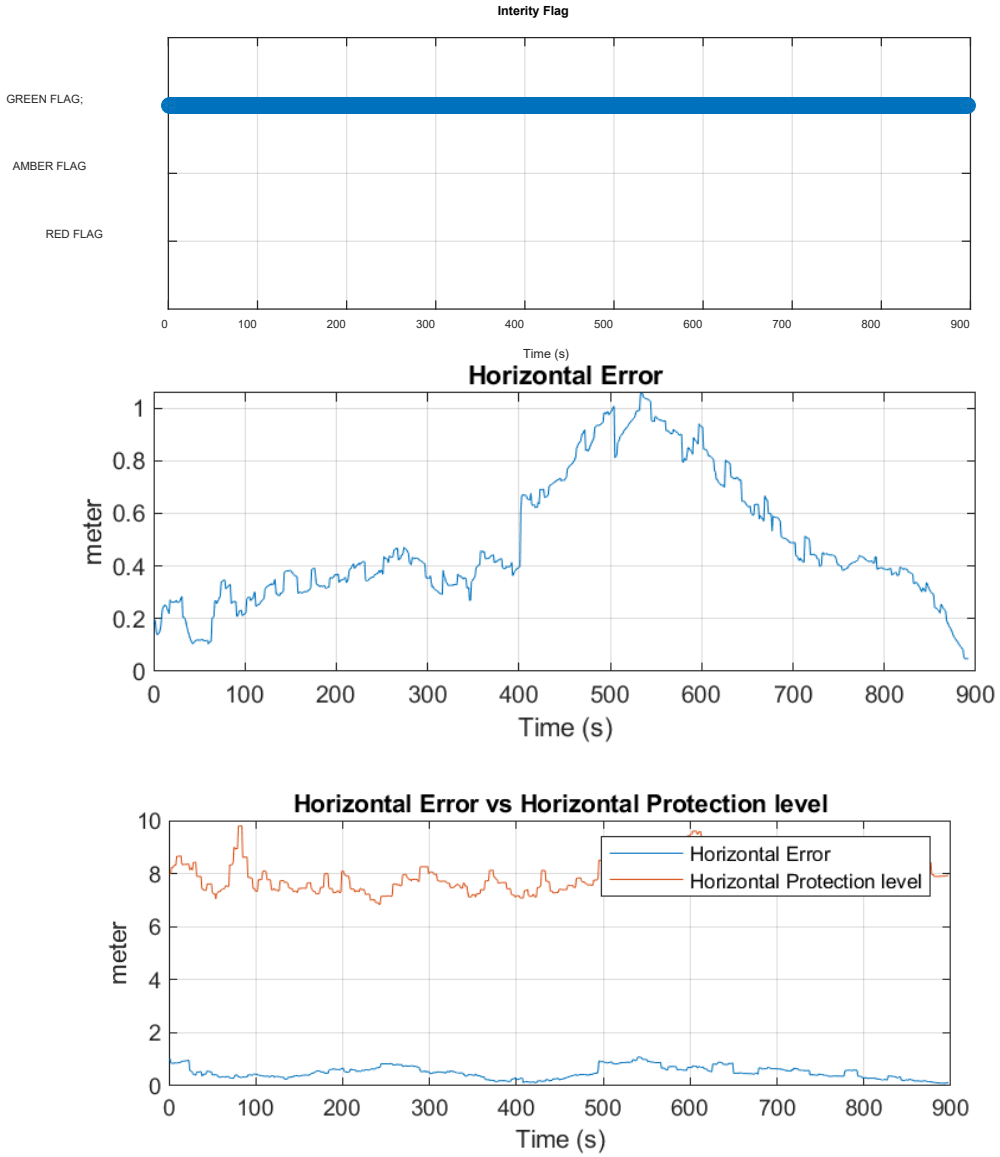

Figure 5-96 The MRAIM Integrity Flag (above) and Horizontal Error (middle) HPL (below)

The solution performance is summarised in Table 5-49. For GPS L1/L5 and GAL E1/5a the horizontal error is 0.95m with a percentile of 95%.

Table 5-49 TS20a - NEU and Horizontal error parameters for GPS L1

	MEAN (m)	STD (m)	95% (m)
North	-0.354	0.31	0.884
East	0.247	0.114	0.428
Up	2.047	0.667	3.206
Horizontal	0.485	0.245	0.951

Figure 5-92 illustrate the number of satellites used to compute the PVT solution and the computed DOP.

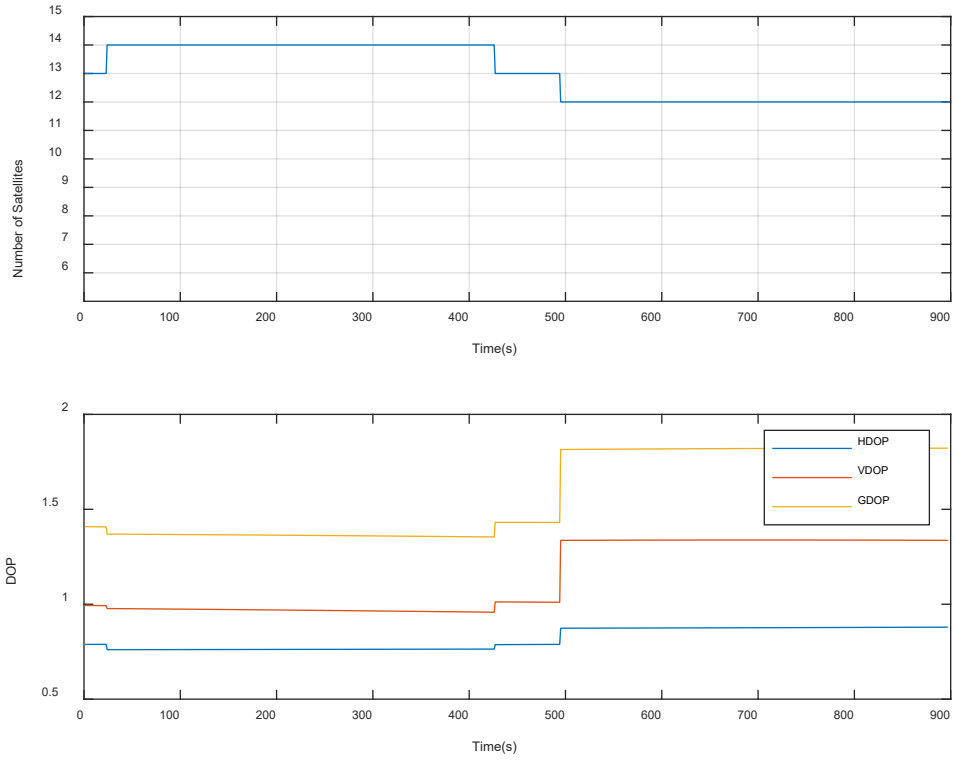

Figure 5-97 Number of SV used to generate the PVT solution and the DOP Values

5.1.5.2 Multiple High-elevation SV

This subsection shows the results generated using a smoothing constant of 100 seconds based on the following test scenario:

Test Scenario	Correction mode	Fault injection
TS.21	MGRAIM DFMC	Applying multipath error on a Multiple GPS high-elevation SV
TS.22	MRAIM DFMC	Applying multipath error on a Multiple GPS high-elevation SV

Table 5-50 shows the configuration parameters and values used to create the bias fault injection dataset. A large bias fault of 100m was injected into the original pseudo-range of GPS satellite G04 and G06 from t=110s (SOW: 296228s) to t = 410s (SOW: 296528s) and a second satellite from t=908s (SOW: 297026s) to t = 1208s (SOW: 297326s).

Table 5-50 TS21/TS22 Configuration

Parameter	*Value*	*Comment*
Start time [SOW]	[2229 297026,2229 296228];	represents the time and duration of the injection of the fault
End time [SOW]	[2229 297326,2229 296528];	
Constellation	['G', 'G'];	The constellation on which is affected
PRN	[3, 6];	Satellites in which the fault was injected
Bias	[100, 100]	fault bias values injected into the RINEX file.
Amplitude	[5, 5];	Multipath components
Period	[30, 30];	

5.1.5.2.1 TS21– PVTI Performance Analysis (MRAIM) DFMC

Figure 5-98 and Figure 5-99 show fault detection test results from Test Scenario 21 MGRAIM DFMC. Figure 5-98 illustrates test statistics and threshold values computed for the solution generated for the dataset. The test statistics and threshold values are used within Fault Detection Test. It can be seen from the graph the point at which the test statistic exceeds the detection threshold, when this occurs the “RED” integrity flag is raised. Figure 5-99, shows integrity flags and the horizontal errors within the solution generated.

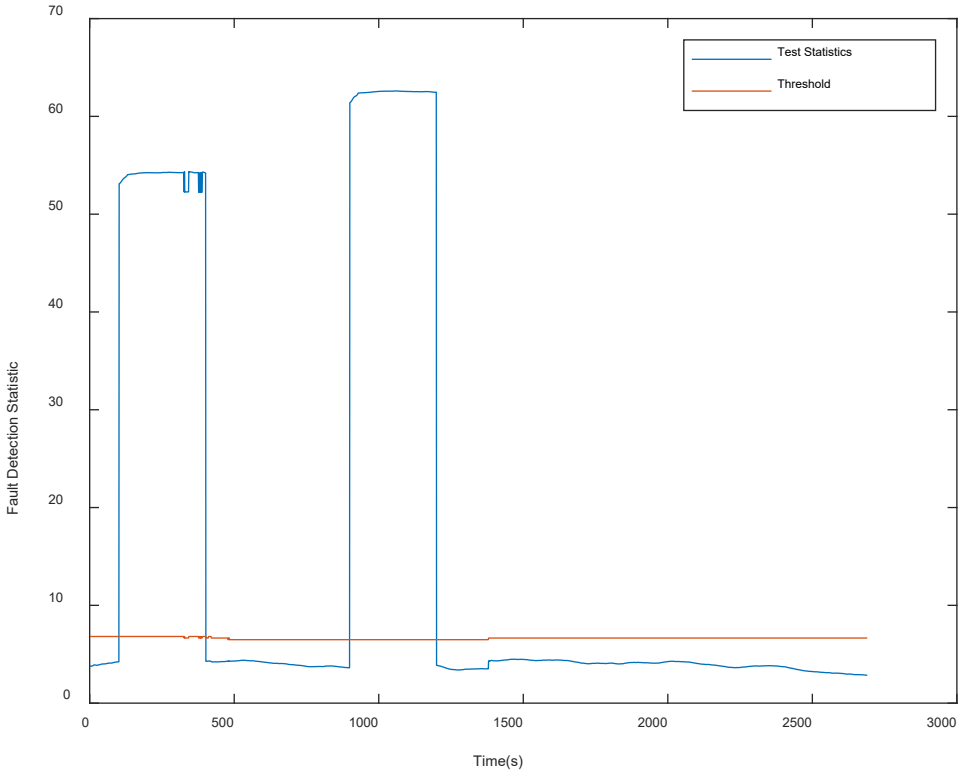

Figure 5-98 FD results from MGRAIM in Multipath fault case

The results indicate that the algorithm has detected the injected fault, as the RED flag is raised, this occurred when the test-statistic exceeds the detection threshold ($t^2 > T^2$). The red flag was raised at time 111s where $t^2 = 53.122$ $T^2 = 6.814$ and ended at time 410s where $t^2 = 53.457$ $T^2 = 6.814$. The horizontal error values at these times were 45.191m and 47.801m respectively. The red flag was raised again at time 909s where $t^2 = 41.072$ $T^2 = 6.488$ and ended at time 1208s where $t^2 = 40.841$ $T^2 = 6.488$ The horizontal error values at these times were 5.638m and 1.281 respectively.

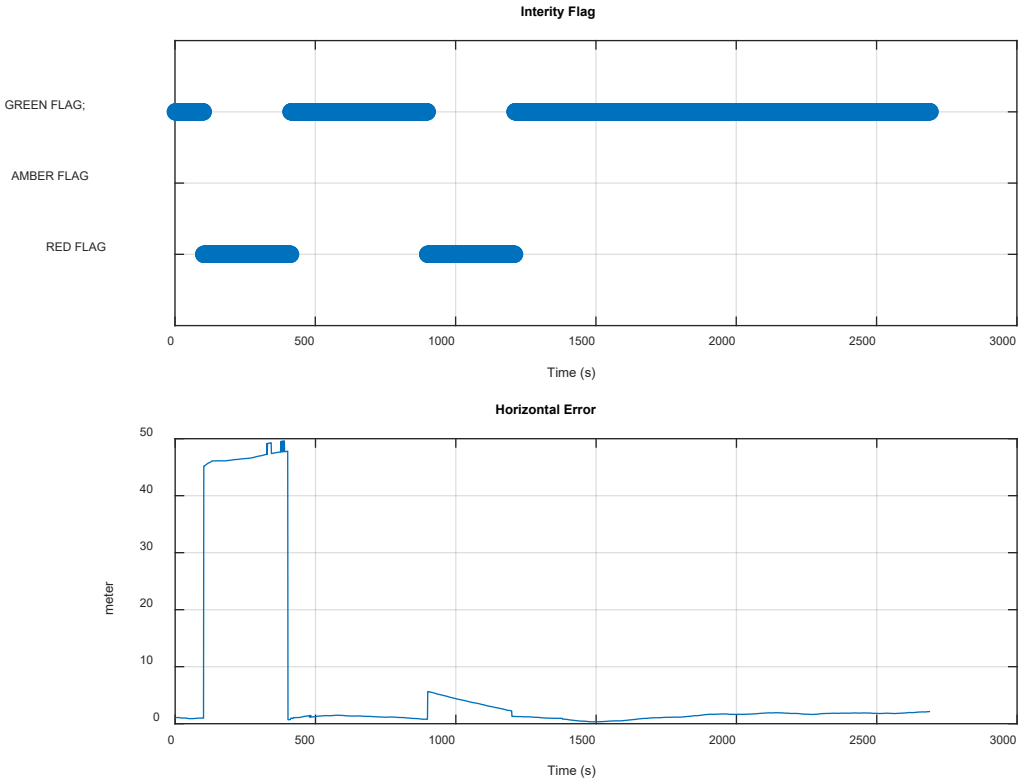

Figure 5-99 The MGRAIM Integrity Flag (above) and Horizontal Error (below)

The solution performance is summarised in Table 5-51. For GPS L1/L5 and GAL E1/5a the horizontal error is 46.59m with a percentile of 95%.

Table 5-51 TS21 - NEU and Horizontal error parameters for GPS L1

	MEAN (m)	STD (m)	95% (m)
North	-3.319	12.538	38.141
East	-2.073	8.636	26.656
Up	-9.771	24.25	60.482
Horizontal	6.656	14.24	46.586

Figure 5-100 illustrate the number of satellites used to compute the PVT solution and the computed DOP.

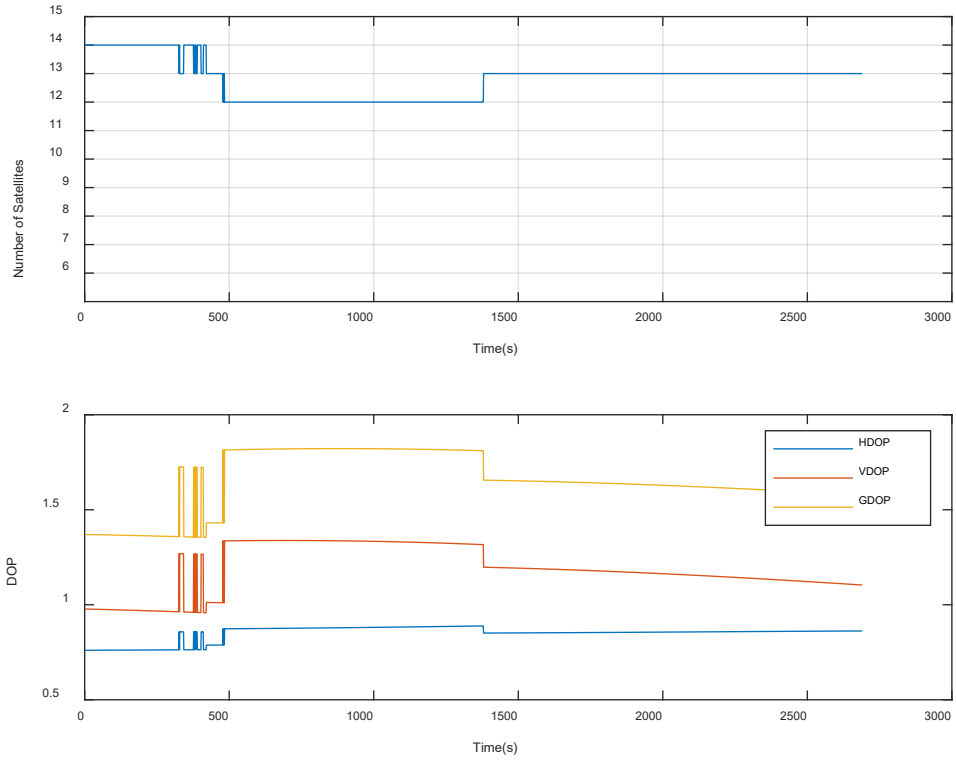

Figure 5-100 Number of SV used to generate the PVT solution and the DOP Values

5.1.5.2.2 TS22– PVTI Performance Analysis (MRAIM) DFMC

Figure 5-101 show fault detection test results from Test Scenario 22 MRAIM DFMC, which included the integrity flags, the horizontal errors and the protection level generated. It can be seen from the integrity flag plot that the GREEN flag is raised which in this case indicates that the following condition was met PL< AL, the alert limit is set to the value of 100 m. The large errors caused by the bias are removed compared to the MGRAIM result in TS21. This can be attributed to the FDE process of the MRAIM where the Solution Separation Threshold test, the function that performs a threshold test for each subset and analyses if their separation is compatible with a failure. In that case where the configured threshold was met the faulty satellite was excluded to provide a safe positioning. Figure 5-102, shows the number of satellites is reduced due to the exclusion of the fault satellites The Positioning error generated is significantly reduced compared to MGRAIM approach.

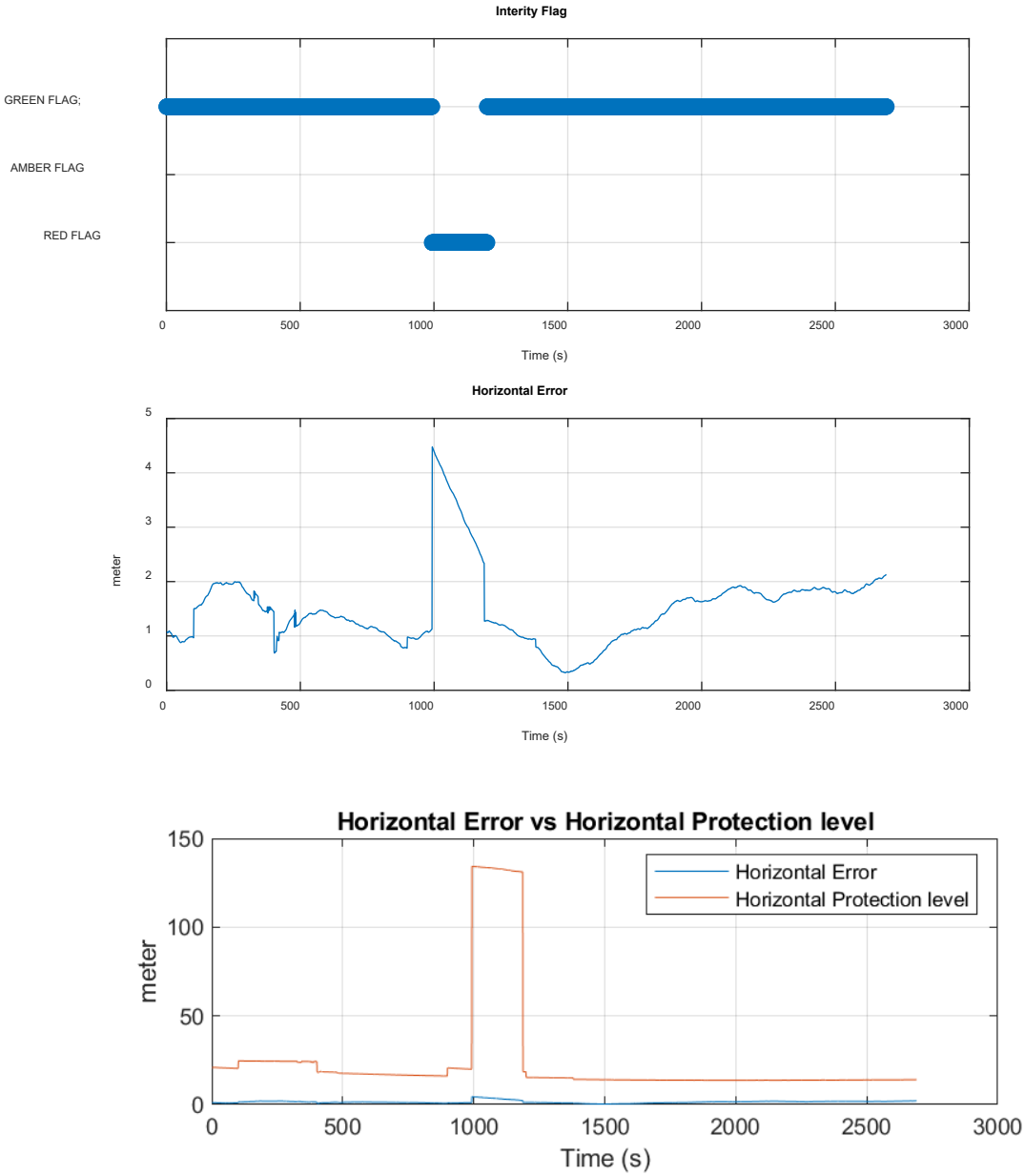

Figure 5-101 The MRAIM Integrity Flag (above) and Horizontal Error (middle) HPL (below)

The solution performance is summarised in Table 5-52. For GPS L1/L5 and GAL E1/5a the horizontal error is 2.99m with a percentile of 95%.

Table 5-52 TS22 - NEU and Horizontal error parameters for GPS L1

	MEAN (m)	STD (m)	95% (m)
North	0.94	0.866	2.939
East	0.979	0.408	1.621
Up	-1.561	16.455	60.281
Horizontal	1.503	0.707	2.99

Figure 5-102 illustrate the number of satellites used to compute the PVT solution and the computed DOP.

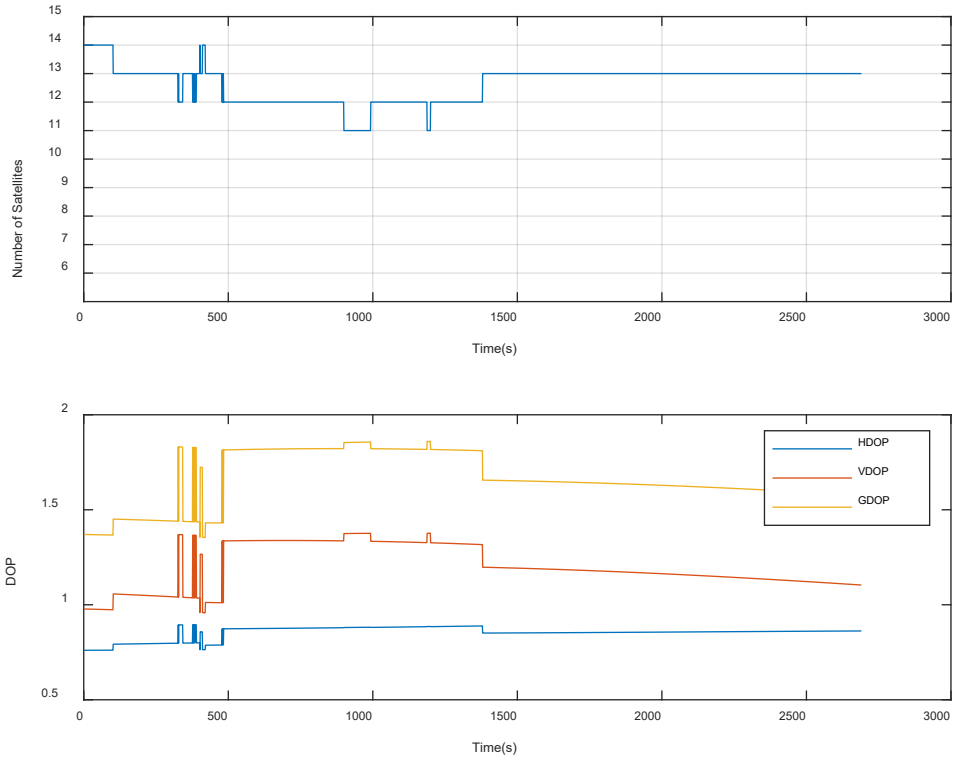

Figure 5-102 Number of SV used to generate the PVT solution and the DOP Values

5.1.5.2.3 TS21a– PVTI Performance Analysis (MGRAIM) DFMC SBAS

Figure 5-103 and Figure 5-104 shows the fault detection test results from Test Scenario 21a MGRAIM DFMC. Figure 5-103 illustrates test statistics and threshold values computed for the solution generated for the dataset. The test statistics and threshold values are used within Fault Detection Test. It can be seen from the graph the point at which the test statistic exceeds the detection threshold, when this occurs the “RED” integrity flag is raised. Figure 5-104, shows integrity flags and the horizontal errors within the solution generated.

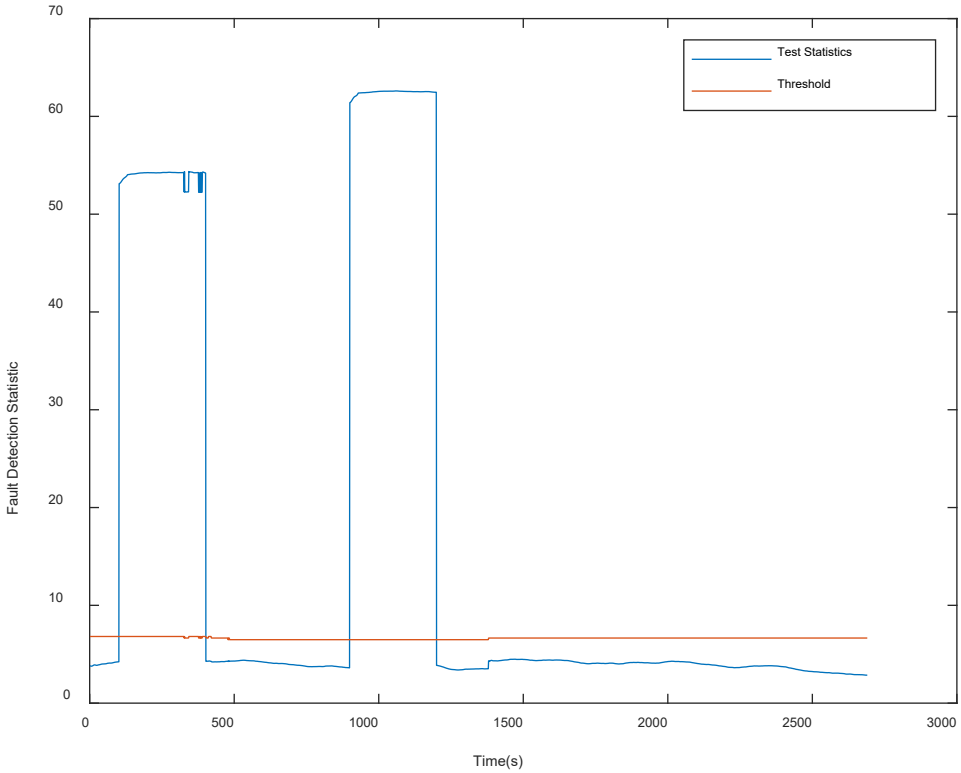

Figure 5-103 FD results from MGRAIM in Multipath fault case

The results indicate that the algorithm has detected the injected fault, as the RED flag is raised, this occurred when the test-statistic exceeds the detection threshold ($t^2 > T^2$). The red flag was raised at time 111s where $t^2 = 53.122$ $T^2 = 6.814$ and ended at time 410s where $t^2 = 53.457$ $T^2 = 6.814$. The horizontal error values at these times were 45.191m and 47.801m respectively. The red flag was raised again at time 909s where $t^2 = 41.072$ $T^2 = 6.488$ and ended at time 1208s where $t^2 = 40.841$ $T^2 = 6.488$ The horizontal error values at these times were 5.638m and 1.281 respectively.

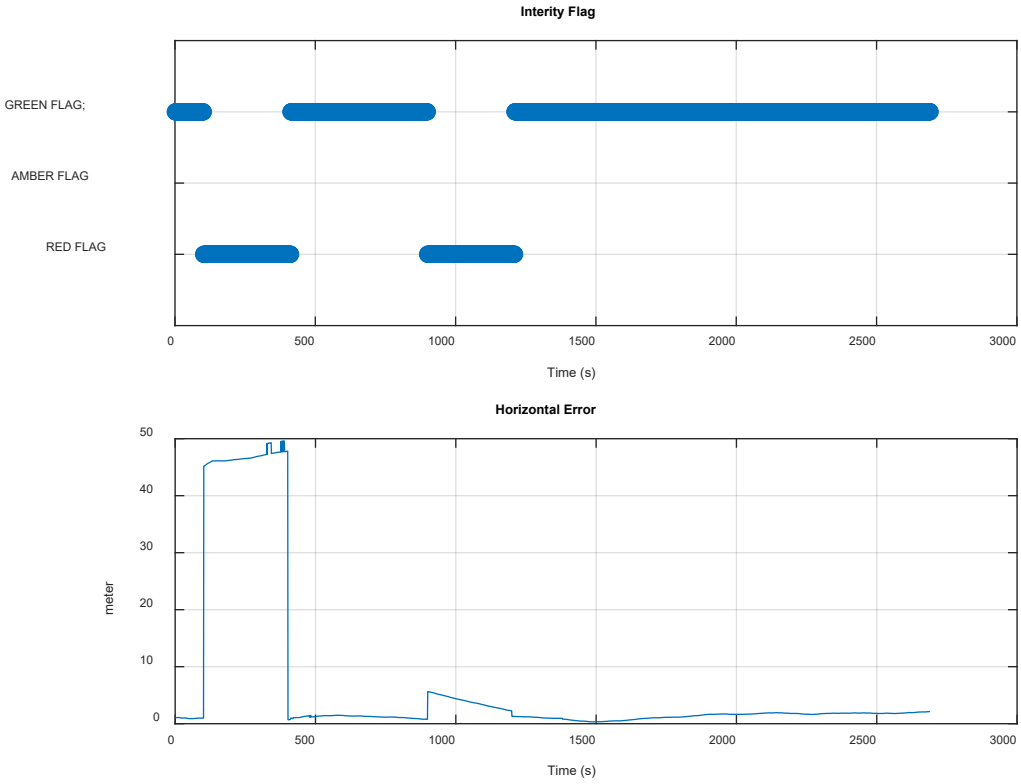

Figure 5-104 The MGRAIM Integrity Flag (above) and Horizontal Error (below)

The solution performance is summarised in Table 5-53. For GPS L1/L5 and GAL E1/5a the horizontal error is 46.59m with a percentile of 95%.

Table 5-53 TS21a - NEU and Horizontal error parameters for GPS L1

	MEAN (m)	STD (m)	95% (m)
North	-3.319	12.538	38.141
East	-2.073	8.636	26.656
Up	-9.771	24.25	60.482
Horizontal	6.656	14.24	46.586

Figure 5-105 illustrate the number of satellites used to compute the PVT solution and the computed DOP.

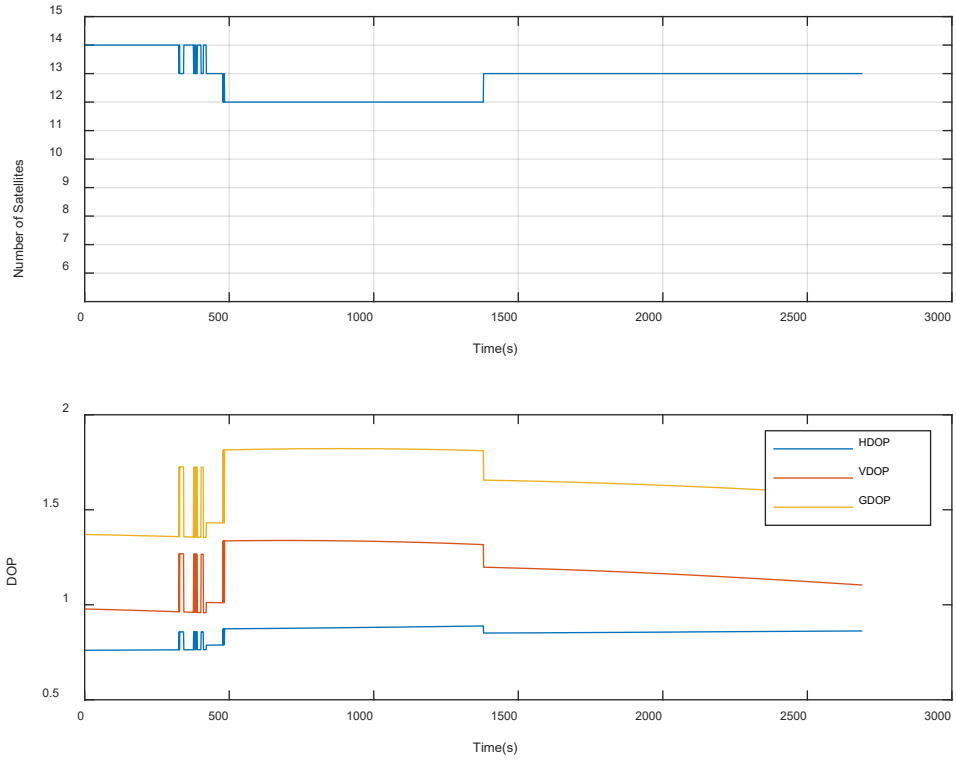

Figure 5-105 Number of SV used to generate the PVT solution and the DOP Values

5.1.5.2.4 TS22a– PVTI Performance Analysis (MRAIM) DFMC SBAS

Figure 5-106 show fault detection test results from Test Scenario 22a MRAIM DFMC, which included the integrity flags, the horizontal errors and the protection level generated. It can be seen from the integrity flag plot that the GREEN flag is raised which in this case indicates that the following condition was met PL< AL, the alert limit is set to the value of 100 m. The large errors caused by the bias are removed compared to the MGRAIM result in TS21a. This can be attributed to the FDE process of the MRAIM where the Solution Separation Threshold test, the function that performs a threshold test for each subset and analyses if their separation is compatible with a failure. In that case where the configured threshold was met the faulty satellite was excluded to provide a safe positioning. Figure 5-107, shows the number of satellites is reduced due to the exclusion of the fault satellites The Positioning error generated is significantly reduced compared to MGRAIM approach.

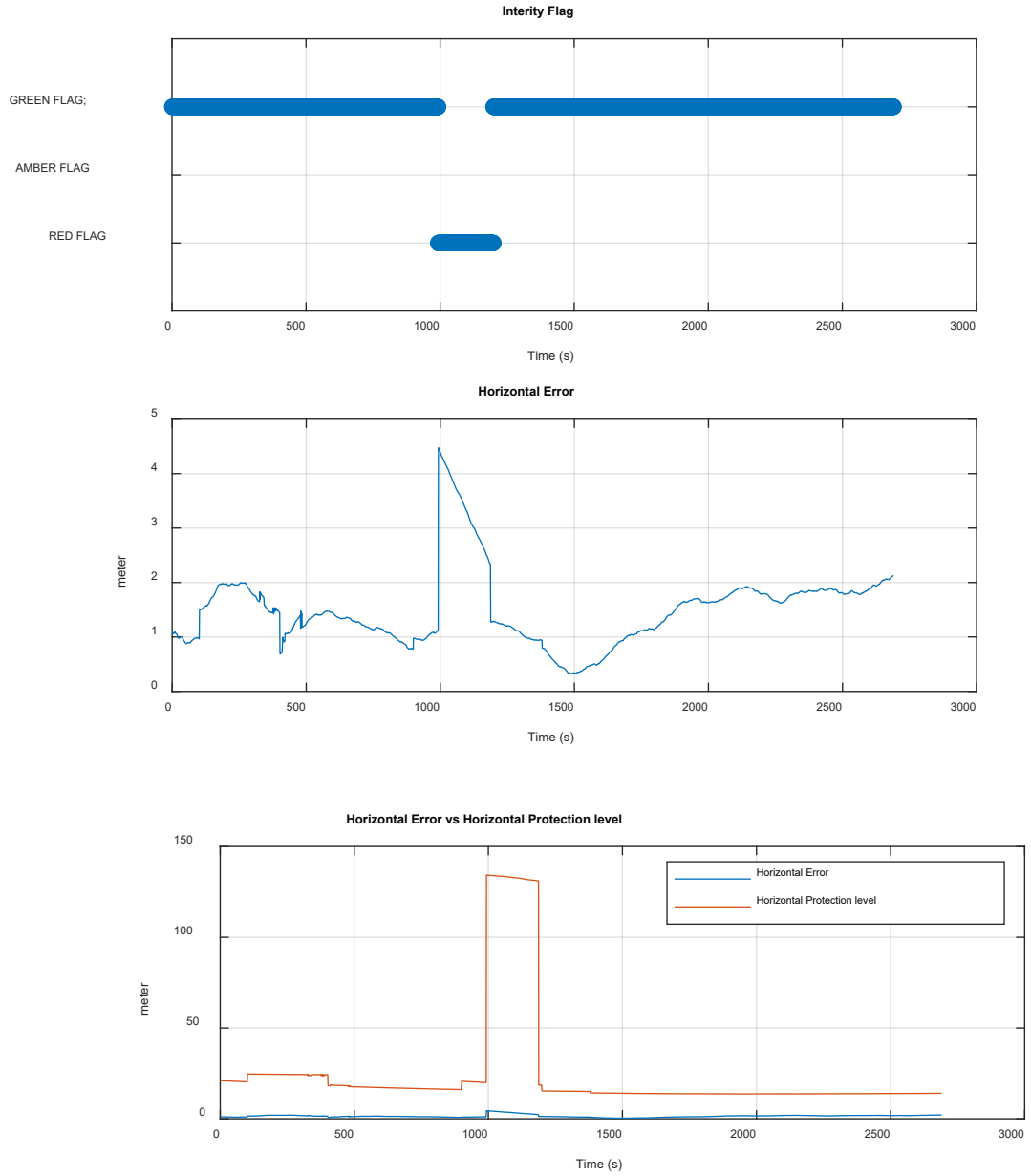

Figure 5-106 The MRAIM Integrity Flag (above) and Horizontal Error (middle) HPL (below)

The solution performance is summarised in Table 5-54. For GPS L1/L5 and GAL E1/5a the horizontal error is 2.99m with a percentile of 95%.

Table 5-54 TS22a - NEU and Horizontal error parameters for GPS L1

	MEAN (m)	STD (m)	95% (m)
North	0.94	0.866	2.939
East	0.979	0.408	1.621
Up	-1.561	16.455	60.281
Horizontal	1.503	0.707	2.99

Figure 5-102 illustrate the number of satellites used to compute the PVT solution and the computed DOP.

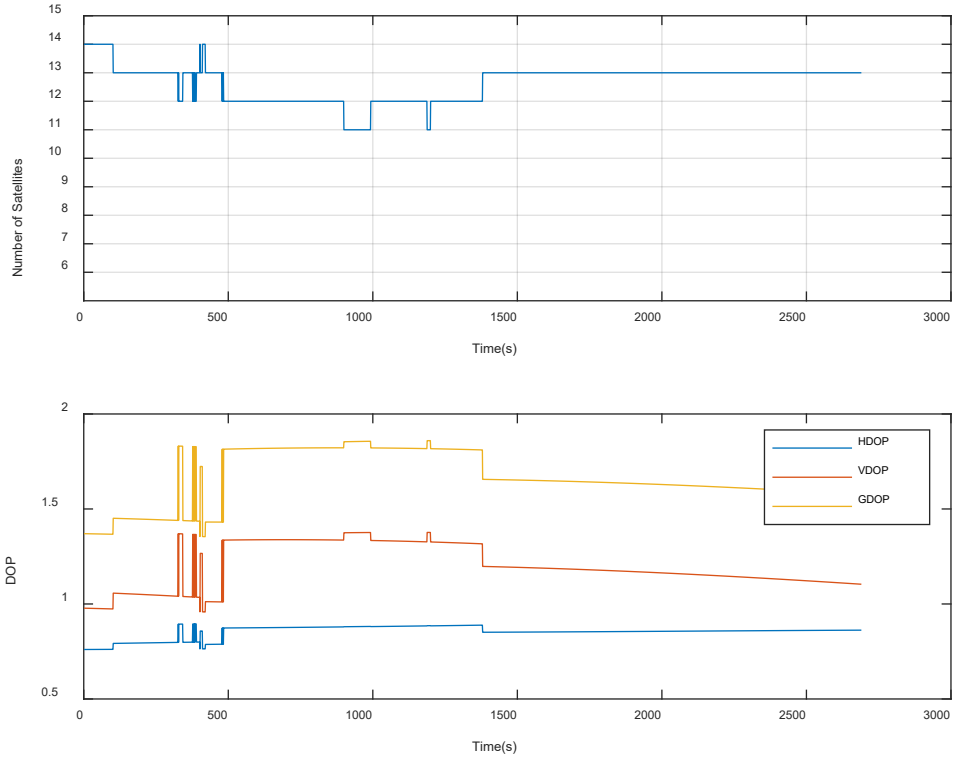

Figure 5-107 Number of SV used to generate the PVT solution and the DOP Values

5.1.6 Evaluation of an Ionosphere Error on a single High-elevation SV

One of the largest errors in GNSS positioning is attributable to the atmosphere. Through both refraction and diffraction, the atmosphere alters the apparent speed and, to a lesser extent, the direction of the signal. This causes an apparent delay in the signal's transit from the satellite to the receiver. The ionospheric delay varies with solar activity, time of year, season, time of day and location. This makes it very difficult to predict how much ionospheric delay is impacting the calculated position. The radio frequency of the signal passing through the ionosphere also varies with the ionospheric delay. Dual Frequency receiver can by comparing the measurements for L1 to the measurements for L2 determine the amount of ionospheric delay and remove this error from the calculated position. However, for single frequency receiver ionospheric models (e.g. Klobuchar Ionospheric Model and NeQuick Ionospheric Model) are used to reduce ionospheric delay errors.

This subsection shows the results generated using a smoothing constant of 100 seconds based on the following test scenario:

Test Scenario	Correction mode	Fault injection
TS.23	MGRAIM (DFMC)	Applying Ionospheric delay on a single high-elevation SV
TS.24	MRAIM (DFMC)	Applying Ionospheric delay on a single low -elevation SV

Table 5-55 shows the configuration parameters and values used to create the Ionospheric fault injection dataset. A fault bias of 36.8m and drift of 0.4m/s was injected into the original pseudo range of a single high elevation (G03) satellite from t=110s (SOW: 296228s) to t = 410s (SOW: 296528s).

Table 5-55 TS15/TS16 Configuration

Parameter	Value	Comment
Start time [SOW]	[296228];	represents the time and duration of the injection of the fault
End time [SOW]	[296528];	
Constellation	['G'];	The constellation on which is affected
Bias	[36.8]	fault bias values injected into the RINEX file.
Drift	[0.4]	

5.1.6.1 TS23 – PVTI Performance Analysis (MGRAIM) DFMC

Figure 5-108 and Figure 5-109 show fault detection test results from Test Scenario 15 EGNOS disabled. Figure 5-108 illustrates test statistics and threshold values computed for the solution generated for the dataset. The test statistics and threshold values are used within Fault Detection Test. It can be seen from the graph that the test-statistic lies below the detection threshold $(t^2 \leq T^2)$ which indicates that all the screening process tests were performed successfully and therefore the solution is ok for use. Figure 5-109, shows integrity flags and the horizontal errors within the solution generated. The AMBER integrity flag indicated that the geometry screening raised an alarm for at least one subset and cannot be guaranteed there is not a problem.

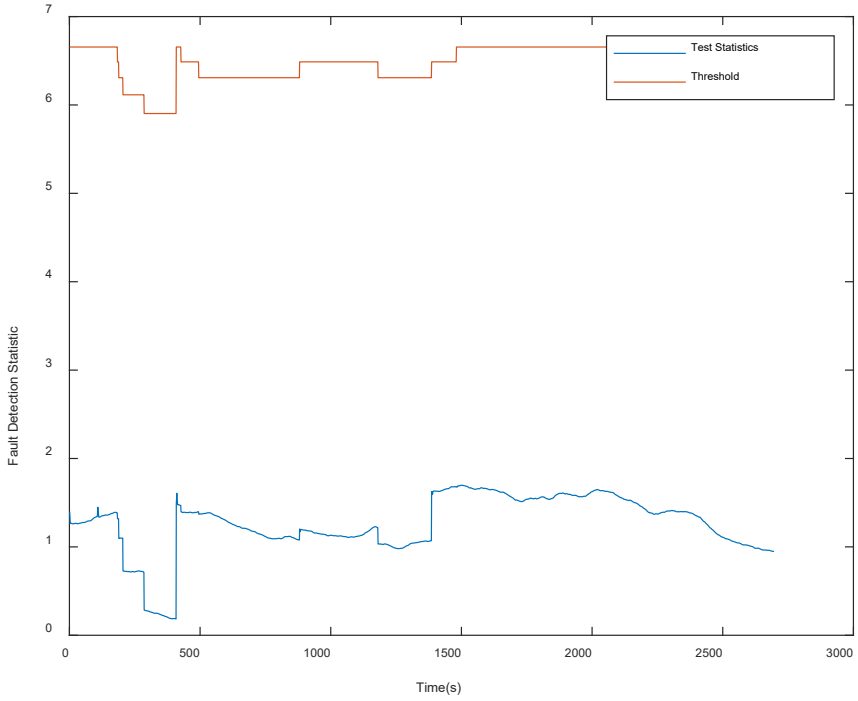

Figure 5-108 FD results from MGRAIM in Ionosphere fault case

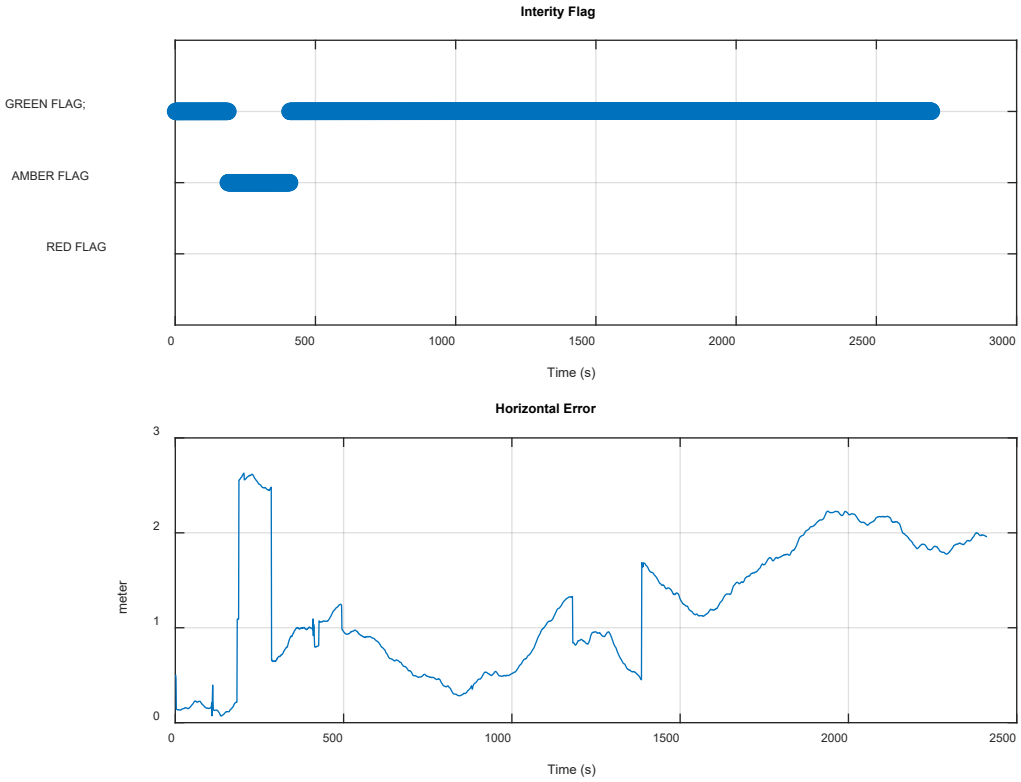

Figure 5-109 The MGRAIM Integrity Flag (above) and Horizontal Error (below)

The solution performance is summarised in Table 5-56. For GPS L1/L5 and GAL E1/E5a the horizontal error is 1.66m with a percentile of 95%.

Table 5-56 TS23 - NEU and Horizontal error parameters for GPS L1/L5 and GAL E1/E5a

	MEAN (m)	STD (m)	95% (m)
North	0.432	0.864	1.636
East	-0.261	0.451	0.953
Up	3.335	2.187	6.993
Horizontal	0.966	0.521	1.661

Figure 5-110 illustrate the number of satellites used to compute the PVT solution and the computed DOP.

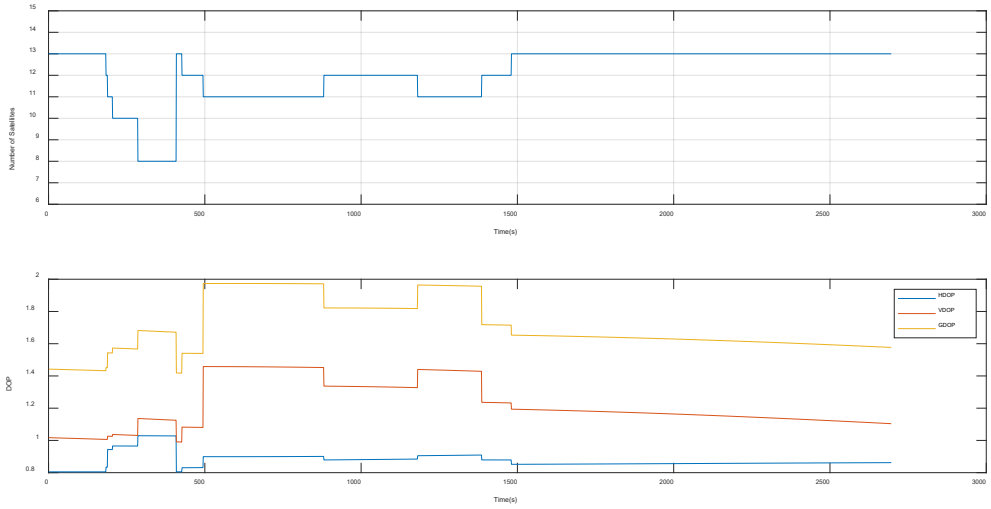

Figure 5-110 Number of SV used to generate the PVT solution and the DOP Values

5.1.6.2 TS24 – PVTI Performance Analysis (MRAIM) DFMC

Figure 5-111 shows integrity flags and the horizontal errors within the solution generated, which includes the integrity flags, the horizontal errors and the protection level generated. It can be seen from the integrity flag plot that the GREEN flag is raised which in this case indicates that the following condition was met PL< AL, the alert limit is set to the value of 100 m.

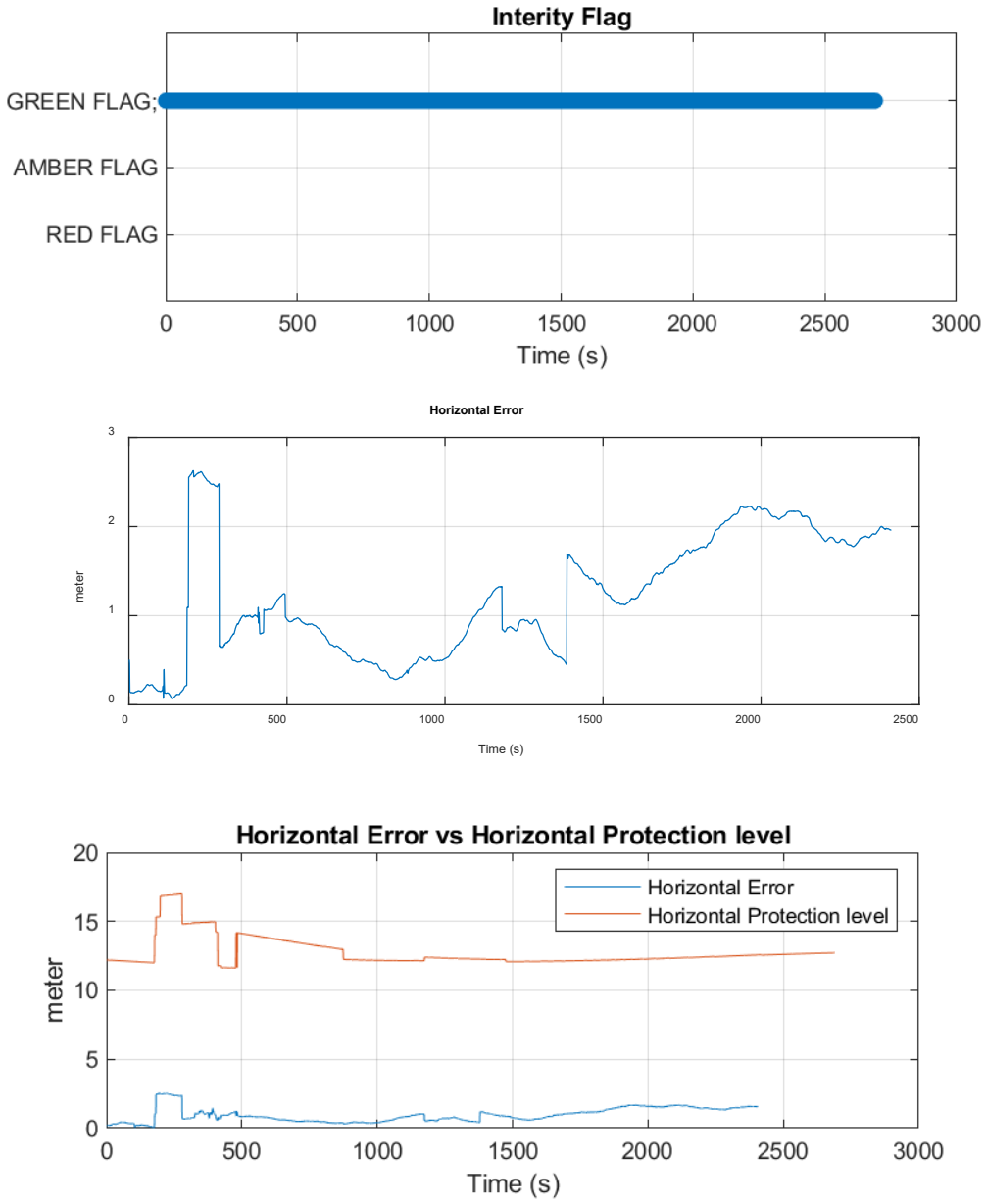

Figure 5-111 The MRAIM Integrity Flag (above) Horizontal Error (middle) and HPL (below)

The solution performance is summarised in Table 5-57. For GPS L1/L5 and GAL E1/E5a the horizontal error is 1.66m with a percentile of 95%.

Table 5-57 TS24 - NEU and Horizontal error parameters for GPS L1/L5 and GAL E1/E5a

	MEAN (m)	STD (m)	95% (m)
North	0.432	0.864	1.636
East	-0.261	0.451	0.953
Up	3.335	2.187	6.993
Horizontal	0.966	0.521	1.661

Figure 5-110 illustrate the number of satellites used to compute the PVT solution and the computed DOP.

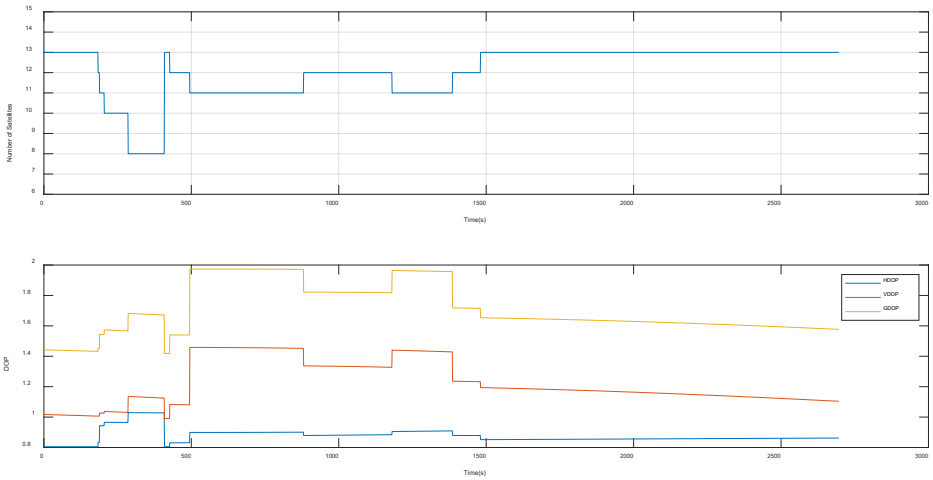

Figure 5-112 Number of SV used to generate the PVT solution and the DOP Values

5.1.6.3 TS23a – PVTI Performance Analysis (MGRAIM) DFMC SBAS

Figure 5-113 and Figure 5-114 shows the fault detection test results from Test Scenario 15 EGNOS disabled. Figure 5-113 illustrates test statistics and threshold values computed for the solution generated for the dataset. The test statistics and threshold values are used within Fault Detection Test.

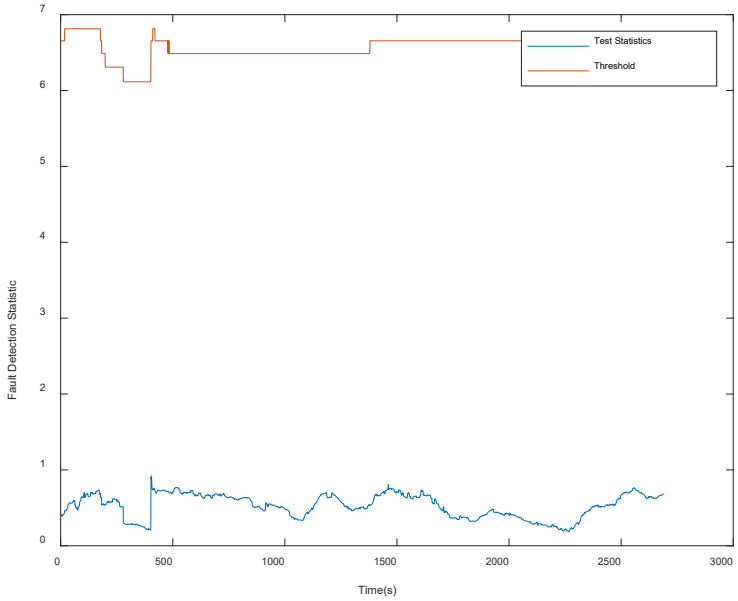

Figure 5-113 FD results from MGRAIM in Ionosphere fault case

It can be seen from the graph that the test-statistic lies below the detection threshold ($t^2 \leq T^2$) which indicates that all the screening process tests were performed successfully and therefore the solution is ok for use. Figure 5-114, shows integrity flags and the horizontal errors within the solution generated. The AMBER integrity flag indicated that the geometry screening raised an alarm for at least one subset and cannot be guaranteed there is not a problem.

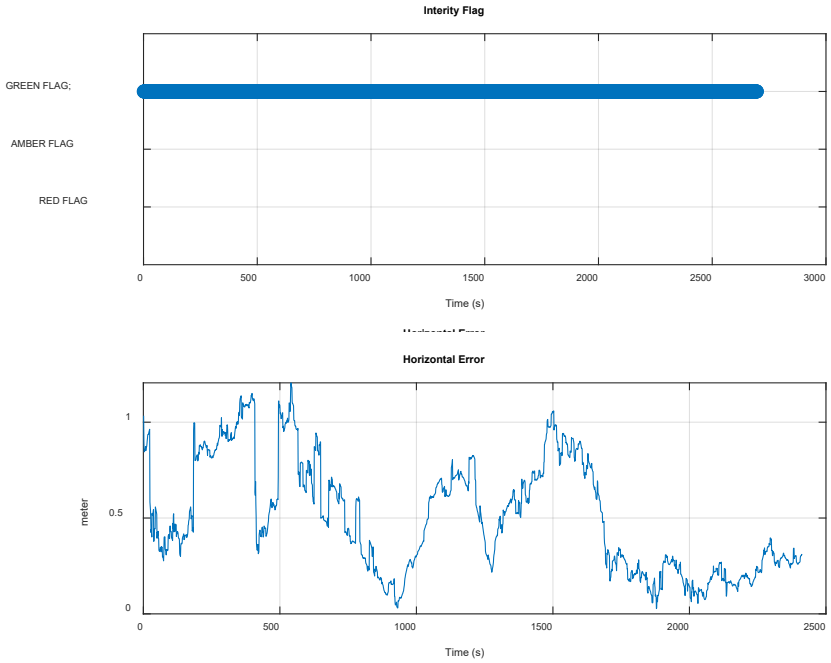

Figure 5-114 The MGRAIM Integrity Flag (above) and Horizontal Error (below)

The solution performance is summarised in Table 5-58. For GPS L1/L5 and GAL E1/E5a the horizontal error is 1.076m with a percentile of 95%.

Table 5-58 TS23a - NEU and Horizontal error parameters for GPS L1/L5 and GAL E1/E5a

	MEAN (m)	STD (m)	95% (m)
North	-0.277	0.413	1.07
East	0.143	0.156	0.408
Up	1.438	1.153	3.098
Horizontal	0.437	0.318	1.076

Figure 5-115 illustrates the number of satellites used to compute the PVT solution and the computed DOP.

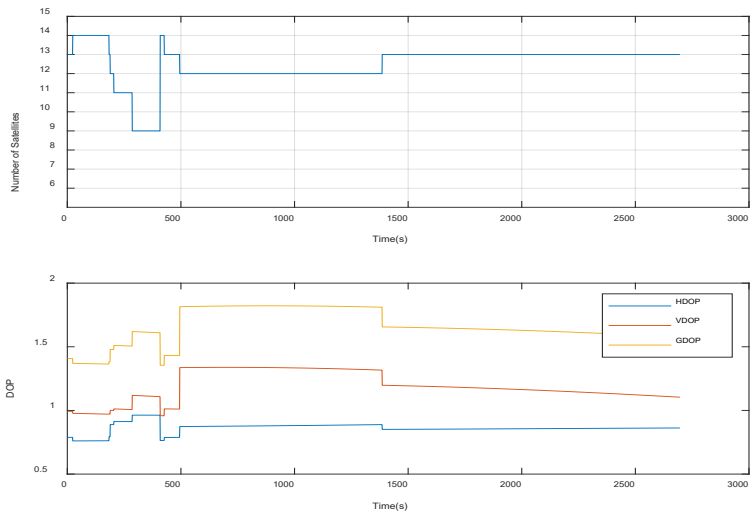

Figure 5-115 Number of SV used to generate the PVT solution and the DOP Values

5.1.6.4 TS24a– PVTI Performance Analysis (MRAIM) DFMC SBAS

Figure 5-116 shows integrity flags and the horizontal errors within the solution generated, which includes the integrity flags, the horizontal errors and the protection level generated. It can be seen from the integrity flag plot that the GREEN flag is raised which in this case indicates that the following condition was met PL< AL, the alert limit is set to the value of 25 m.

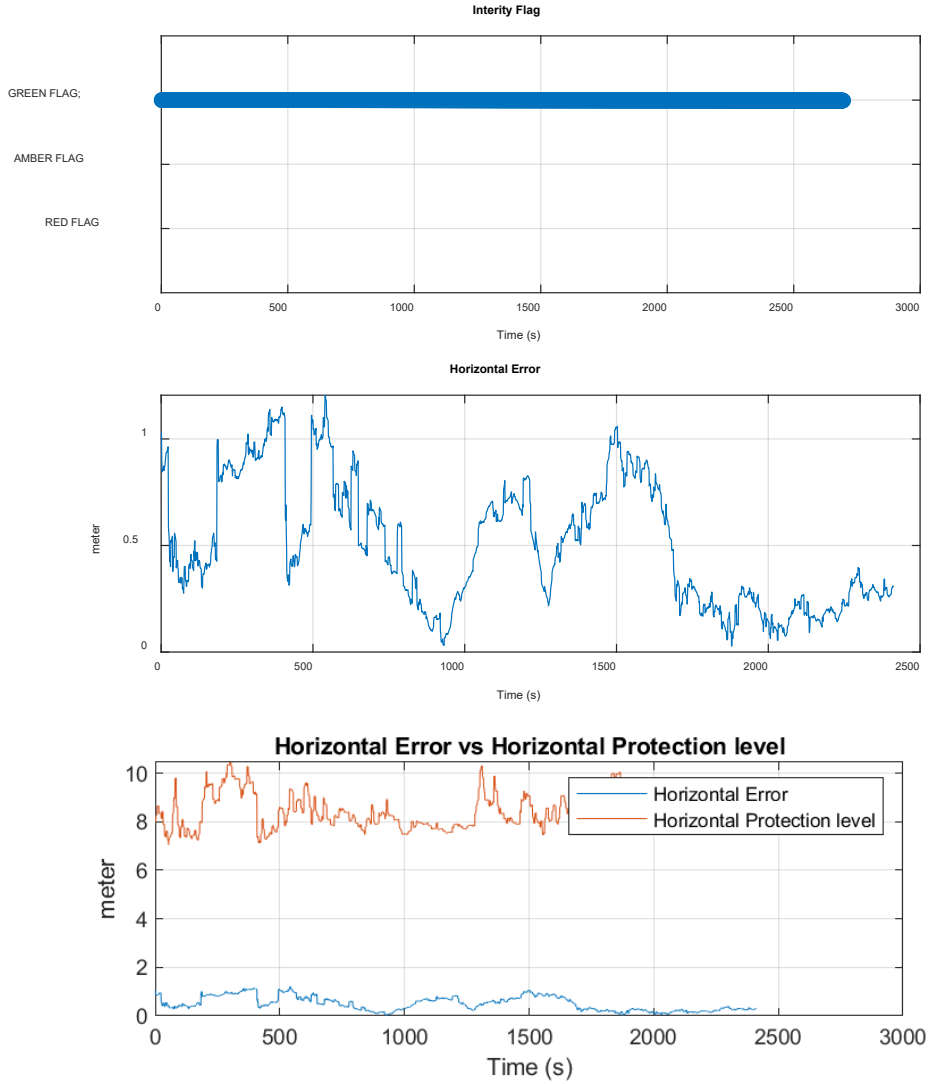

Figure 5-116 The MRAIM Integrity Flag (above) Horizontal Error (middle) and HPL (below)

The solution performance is summarised in Table 5-59. For GPS L1/L5 and GAL E1/E5a the horizontal error is 1.076m with a percentile of 95%.

Table 5-59 TS23a - NEU and Horizontal error parameters for GPS L1/L5 and GAL E1/E5a

	MEAN (m)	STD (m)	95% (m)
North	-0.277	0.413	1.07
East	0.143	0.156	0.408
Up	1.438	1.153	3.098
Horizontal	0.437	0.318	1.076

Figure 5-117 illustrate the number of satellites used to compute the PVT solution and the computed DOP.

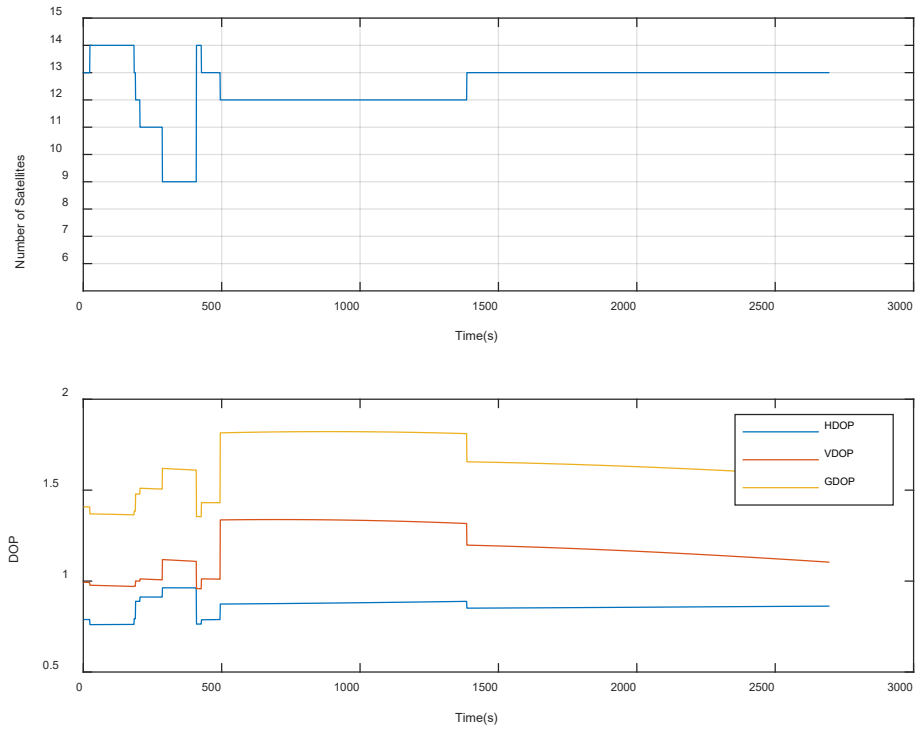

Figure 5-117 Number of SV used to generate the PVT solution and the DOP Values

5.1.7 Summary

The section examined the PVT solution generated using the algorithm described in Section 4, which focused on fault detection in the case of M(G)RAIM and fault detection and exclusion in MRAIM. Functional testing and performance evaluation were conducted based on the collection of real GNSS data (GPS and Galileo observables) using GMV facilities in Nottingham. Comparisons were made to the integrity algorithm developed with EGNOS V3 enabled. To evaluate the algorithm's ability to detect and, where applicable, exclude faults, simulated data was used with faults injected into the RINEX file. The simulated data provided an option to cover scenarios that would otherwise not be possible using field data alone.

The results presented within this section are for faults applied on single and multiple satellites and have shown that the algorithm is able to compute a PVT solution using the MGRAIM and MRAIM concepts. It has been observed that the MGRAIM algorithm is able to detect the fault and raise the appropriate integrity status flag as defined in Table 4.2. While the MRAIM algorithm can detect and exclude the fault and compute the related HPL.

In this iteration of the assessment results presented, the focus was on evaluating the functionality of the DFMC M(G)RAIM and MRAIM algorithms developed and comparing the output of both algorithms against each other. It should be noted that for illustrative purposes for results where faults are injected, and the red integrity flag is raised the horizontal error is plotted to show the potential effect of the fault but the position is not provided in such a case.

Section 5.2 provides a deeper analysis of the MGRAIM and MRAIM algorithms, comparing their performance for fault-free and faulted cases in DFMC and DFMC+EGNOS scenarios using Monte-Carlo simulations.

5.2 Monte-Carlo Simulation

5.2.1 Introduction

The experimentation in Section 5 above has shown for some real data and example faults the fault detection capability in DFMC case for both MGRAIM (developed in WP2 [RD.49]) and MRAIM (developed in WP3 as described in [RD.50]) for DFMC (GPS+GAL) and DFMC+SBAS processing. Those tests validate the functionality of the algorithm and compare the detection capability of GPS and GPS+EGNOS cases for different types of faults.

In these Monte Carlo simulations, we show some further analysis to investigate algorithm performance and highlight advantages and disadvantages of the algorithms. The idea of the Monte Carlo simulation is that they are configured with general parameters for the scenario:

- Time period range
- Location range (max/min lat/lon/ht)
- Number of samples
- UERE budget
- Nav file
  - Apply EGNOS or not

- Elevation mask

In addition, configure it with specific settings for the scenario under test:

- Probability of false alarm
- Accuracy / DOP thresholds
- Whether the simulation should include satellite faults or not
- MRAIM integrity parameters

The Monte Carlo simulation then works in the following way:

- Loop for number of samples
  - Choose random time within the configured range
  - Choose random location within the location range
  - Use nav file and elevation mask to work out which sats in view
  - Form design matrix and weight matrix
  - Generate random error for each satellite range based on normal distribution with standard deviation based on current UERE value (for elevation of satellite)
  - If a fault case
    - Add on a random fault (from 0 to max fault value) for a random satellite
  - Compute snapshot weighted least squares position solution
  - In MGAIM case
    - Do MGRAIM check to identify faulty cases and set integrity flag (red / amber / green)
  - Else in MRAIM case
    - Do MRAIM checks and compute HPL and set integrity flag (red / amber / green)
  - Keep track of stats (max errors, number of epochs where pos error > threshold, etc.)
- End loop
- Output stats and plots

Simulations have been executed for DFMC and DFMC+SBAS cases for coastal requirements covering fault-free and faulted cases. Both the MRAIM and MGRAIM algorithms are processed. The results are shown in the following sections.

5.2.2 MGRAIM Simulation Results

5.2.2.1 General Parameters

In the first instance, the MGRAIM algorithm (developed in WP2 [RD.49]) is re-analysed using DFMC measurements rather than GPS L1 only. All simulations have been run with the following general parameters.

Table 5-60: Monte Carlo Simulation Configuration Values Common to All Simulations

Parameter	Value	Description
numSamples	100000	Number of samples to simulation in the simulation
StartTime	[2229 295200]	Start time (weeks and seconds of week) of period in which samples will be generated. Chosen to align with the data used in algorithm testing (10:00 on 28/09/22)

EndTime	[2229 302400]	End time (weeks and seconds of week) of period in which samples will be generated. Chosen to align with the data used in algorithm testing (12:00 on 28/09/22)
minLat	48	Latitude defining southern boundary of area to be considered in sample generation.
maxLat	62	Latitude defining northern boundary of area to be considered in sample generation.
minLon	-10	Longitude defining western boundary of area to be considered in sample generation.
maxLon	4	Longitude defining eastern boundary of area to be considered in sample generation.
minHt	90	Height used for locations in sample generation
maxHt	90	Height used for locations in sample generation
elevMask	5	Elevation mask to use for solution
pfa	1e-5	Probability of false alarm to use in algorithm
maxHDOP	4	HDOP threshold check for MGRAIM algorithm
maxGDOP	6	GDOP threshold check for MGRAIM algorithm

In terms of the constellation, two options are used. In both cases, the actual nav messages reflecting the operational GPS and Galileo constellation on 28th Sep 2022 are used. However, in one case only those GPS satellites that have L5 measurements are used (which is only a subset of the full constellation) to reflect the current situation, whereas in the second option all GPS satellites are used (representing the future case when all GPS satellites will have L5 measurements).

5.2.2.2 Coastal Scenarios

We only show the coastal scenario because we could see from WP2 [RD.49] that GPS L1 only was ok for the ocean case and so the use of DFMC to potentially improve performance in the Coastal scenario is more interesting.

In coastal mode, the 95% horizontal accuracy threshold is 10m.

Firstly, we consider the DFMC only case (GPS + Galileo). In this case the following UERE is assumed (considering small residual ionosphere, troposphere, multipath/noise and orbit/clock errors).

- For orbit/clock SIS errors, Satellite URA is used "as-broadcast" from the GNSS satellite, typically this is:

$$\sigma_{URA} = 2m \text{ for GPS}$$

$$\sigma_{URA} = 6m \text{ for Galileo}$$

- The residual noise from the corrected troposphere is defined in [RD.4] as 0.12m (12cm), scaled according to the elevation (θ) of the satellite:

$$\sigma_{tropo} = 0.12m \times S(\theta)$$

$$S(\theta) = \sqrt{\frac{1.001}{0.002 + \sin^2(\theta)}}$$

- The ionosphere error is mainly removed through combination of dual frequency. The following model for residual errors is obtained from ARAIM ADD V3.1 [RD.15]:

$$\sigma_{ionoDF} = 0.018 + \frac{40}{261 + elevation^2}$$

- For noise and multipath, it is explained in [RD.50] that an appropriate model for a maritime receiver is:

$$\sigma_{mp} = 0.017 + 3.087 \cdot e^{(-0.042 \cdot \theta[deg])}$$

  Note that this includes both noise and multipath and is for unsmoothed code measurements. Assuming that the receiver will apply 100s smoothing, we then reduce the multipath and noise by a factor of 2 as an approximation of the improvement that would be expected. However, the noise and multipath models for DFMC should be modified in order to overbound these errors, accounting for the fact that the linear combination of dual frequency data will inflate these errors. The factor should be applied as defined in ARAIM ADD V3.1 [RD.15]:

$$\sigma_{mpDF} = \sqrt{\frac{f_{L1}^4 + f_{L5}^4}{(f_{L1}^2 - f_{L5}^2)^2}} \cdot \sigma_{mpSF}$$

This leads to the following elevation dependent UERE (considering ionosphere, troposphere, multipath/noise and orbit/clock errors).

Table 5-61: UERE Budget, GPS L1/L5 (metres)

	Ionosphere	Troposphere	Multipath / Noise	Orbit/Clock	Total
5	0.16	1.23	3.26	2	4.02
10	0.13	0.67	2.65	2	3.39
15	0.10	0.46	2.15	2	2.97
20	0.08	0.35	1.75	2	2.68
30	0.05	0.24	1.16	2	2.32
40	0.04	0.19	0.77	2	2.15
50	0.03	0.16	0.51	2	2.07
60	0.03	0.14	0.34	2	2.03
90	0.02	0.12	0.11	2	2.01

Table 5-62: UERE Budget, Galileo E1/E5a (metres)

	Ionosphere	Troposphere	Multipath / Noise	Orbit/Clock	Total
5	0.16	1.23	3.26	6	6.94
10	0.13	0.67	2.65	6	6.59
15	0.10	0.46	2.15	6	6.39

20	0.08	0.35	1.75	6	6.26
30	0.05	0.24	1.16	6	6.12
40	0.04	0.19	0.77	6	6.05
50	0.03	0.16	0.51	6	6.02
60	0.03	0.14	0.34	6	6.01
90	0.02	0.12	0.11	6	6.00

Fault-Free

First, the fault free case is run. The intention is to check the performance in terms of false alarms and nominal accuracy and availability.

In the GPS L1 case it was seen there were a number of occasions where that level of performance cannot be achieved and so there were epoch samples with red and amber integrity flags – even in the fault free case. This was because the reported 95% horizontal accuracy was larger than the threshold of 10m for some of the all-in-view solution, or some subsets.

With DFMC, we are improving the geometry of the solution (by providing more satellites) and reducing some of the actual and expected errors (due to use of dual frequency to remove ionospheric errors). Therefore, we should improve both the reported 95% horizontal accuracy and the actual positioning errors.

For the DFMC case with current GPS (i.e., with not all satellites having L5) the performance improvement over GPS L1 only will be more limited. In this case, we do have smaller maximum error than in GPS L1 case and more samples with green flag, but we still do not have 100% availability. Overall, the maximum error is 16.46m and there are:

- 0.001% of epoch samples with red flag
- 3.11% of epoch samples with amber flag
- 96.89% of epoch samples with green flag

The amber flag is for those epochs where at least one subset has estimated 95% horizontal accuracy great than 10m. This means that currently for DFMC GNSS if we used this approach for checking the validity of the solution, even in the fault-free case we get a lower availability of a valid solution (green integrity flag) than we would require. This is partly because of assumptions for orbit/clock errors (which may be overly pessimistic for Galileo) and partly because the solution geometry is not the best it could be due to not all GPS satellites being used.

The plots below show the errors vs estimated 95% accuracy for all results, all but red status, and green only.

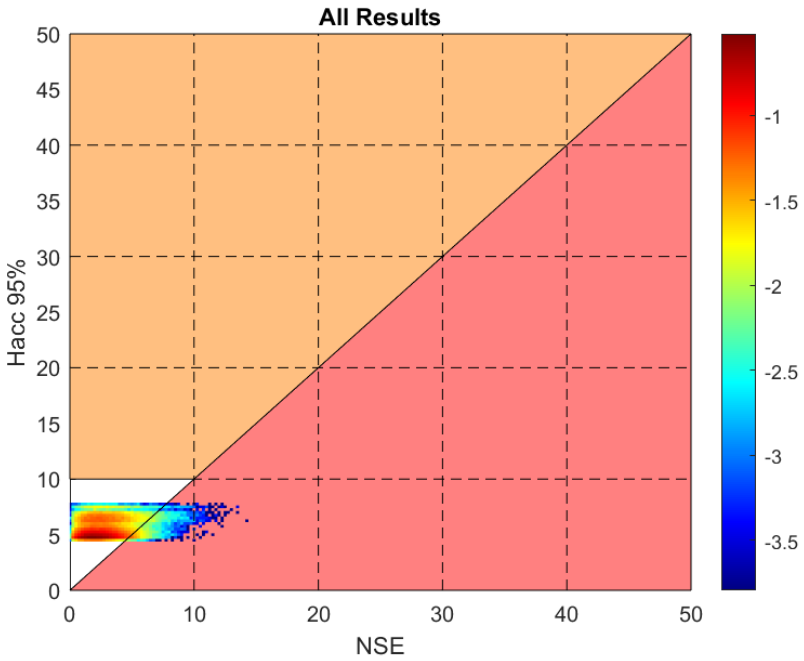

Figure 5-118: Plot of Computed Horizontal Position Error vs 95% Horizontal Accuracy in Coastal Scenario current DFMC Fault-Free Case – all samples

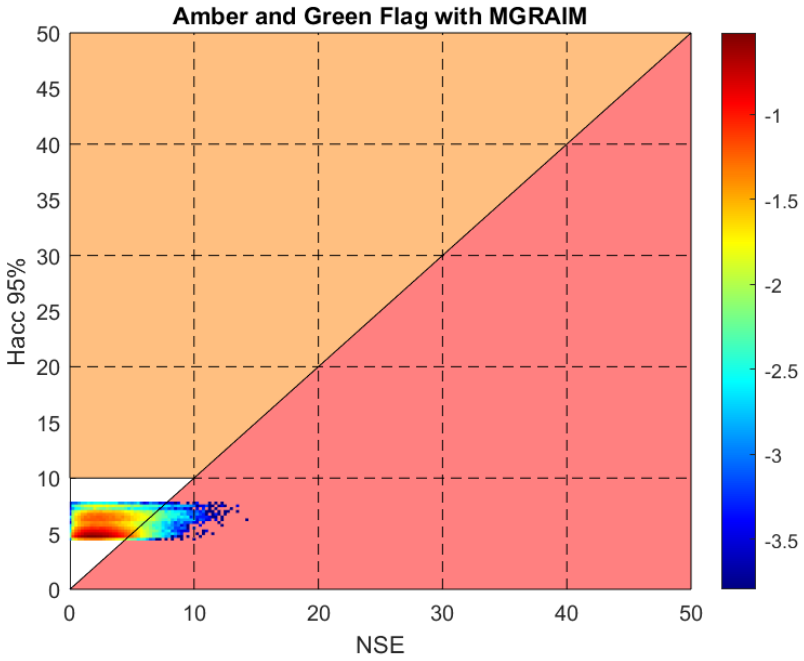

Figure 5-119: Plot of Computed Horizontal Position Error vs 95% Horizontal Accuracy in Coastal Scenario current DFMC Fault-Free Case – amber and green status only

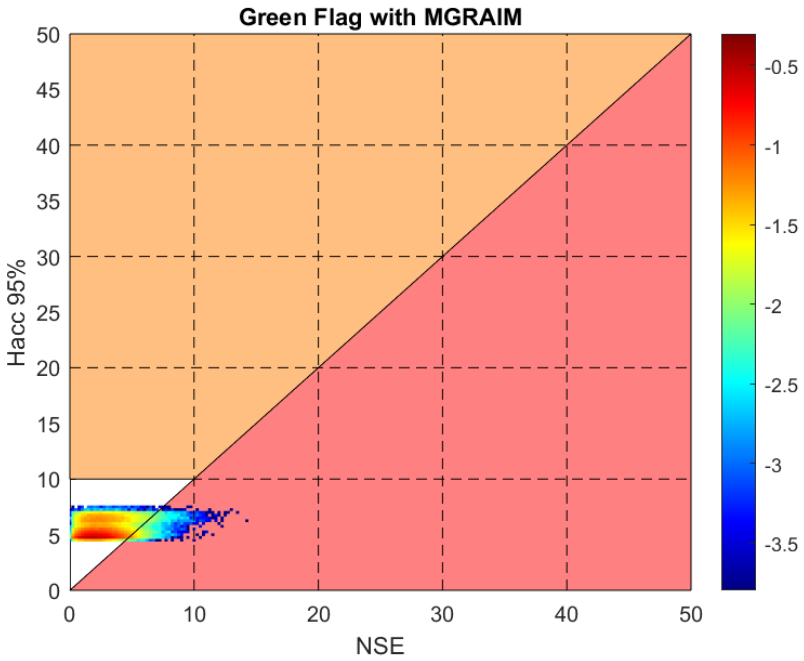

Figure 5-120: Plot of Computed Horizontal Position Error vs 95% Horizontal Accuracy in Coastal Scenario current DFMC Fault-Free Case - green status only

The different checks in effect remove those solutions with the worst geometries, although this does not necessarily remove the largest horizontal accuracy values. The maximum horizontal error is 14.17m when considering all samples and also for those with green status. This also means there are still some cases (0.11%) where the position error is larger than 10m, and there are of course still 5% of cases where the position error exceeds the reported 95% horizontal position accuracy. So, there is some benefit in the fault free case of including these different checks, but it comes at the expense of solution availability.

If we consider all GPS satellites to have L5 (as will be the case in the future) then the solution geometry is greatly improved, and this feeds through to the position accuracy and the MGRAIM performance. In this case we have 99.999% of solutions with green status and the maximum horizontal position error is 10.43m. This means the coastal requirements are met 99.999% of the time in this scenario, although of course 5% of the values are still bigger than the reported 95% horizontal accuracy statistics.

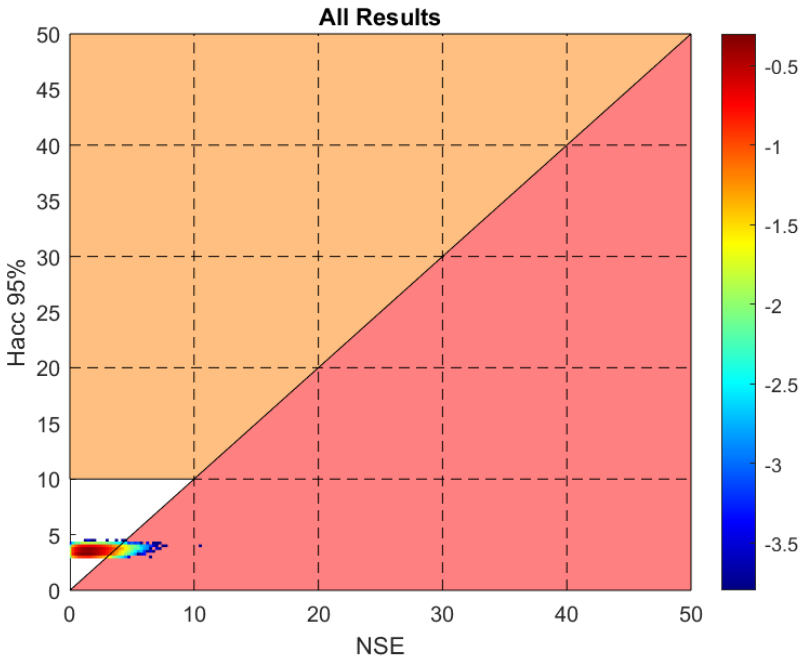

Figure 5-121: Plot of Computed Horizontal Position Error vs 95% Horizontal Accuracy in Coastal Scenario future DFMC Fault-Free Case – all samples

We can also check the performance when DFMC EGNOS corrections are applied. This will provide better orbit/clock products, and accordingly smaller uncertainty values to form the UERE. For EGNOS we assume the following UERE.

- For tropospheric and ionospheric errors, we assume the same as in the GPS+Galileo DF uncorrected case;
- For orbit/clock SIS errors, we assume that typical broadcast sigma UDRE is 1.37m (i.e., same as for legacy case),
- For multipath, we assume the same as in the uncorrected DFMC case.

Table 5-63: UERE Budget, GPS+Galileo DFMC EGNOS (metres)

	Ionosphere	Troposphere	Multipath / Noise	Orbit/Clock	Total
5	0.16	1.23	3.26	1.37	3.75
10	0.13	0.67	2.65	1.37	3.06
15	0.10	0.46	2.15	1.37	2.59
20	0.08	0.35	1.75	1.37	2.25
30	0.05	0.24	1.16	1.37	1.81
40	0.04	0.19	0.77	1.37	1.58
50	0.03	0.16	0.51	1.37	1.47
60	0.03	0.14	0.34	1.37	1.42
90	0.02	0.12	0.11	1.37	1.38

In this case – unlike in the SF EGNOS case – we do not impose a check on the pierce point being in the usual IGP grid because ionospheric errors are corrected through use of dual-frequency measurements.

For the current DFMC case (with only some satellites having L5 measurements), when using those settings in the fault-free costal scenario we 100% availability of solutions with green flag and a maximum error of just 6.88m. This is an improvement over the GPS L1 EGNOS case – partly due to improved geometry and partly due to the reduced uncertainty in ionospheric errors (because they are now removed through the ionosphere-free combination).

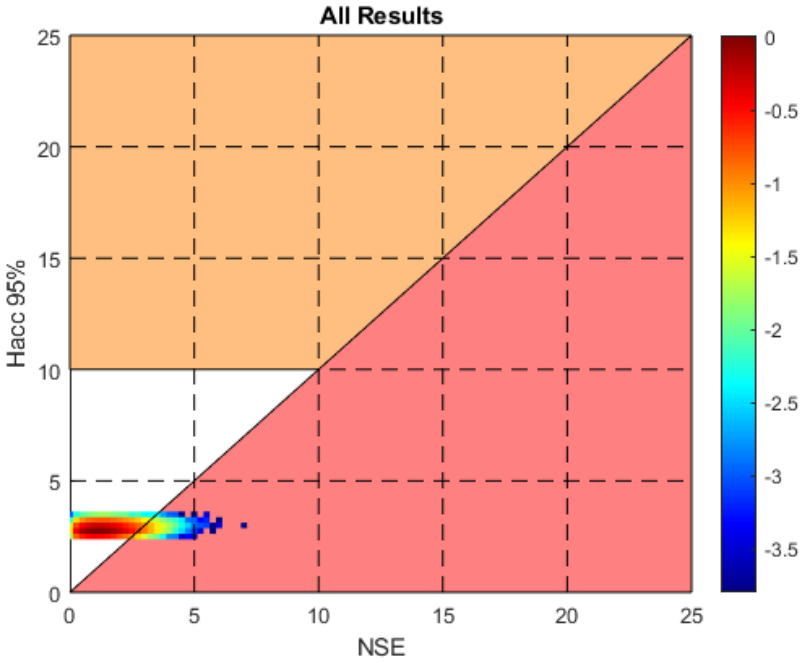

Figure 5-122: Plot of Computed Horizontal Position Error vs 95% Horizontal Accuracy in Coastal Scenario current DFMC EGNOS Fault-Free Case – all samples

When considering the future DFMC case (where all GPS satellites have L5) then we see 100% availability of solutions with green flag and a maximum error of just 4.91m, which is well within the 10m requirement.

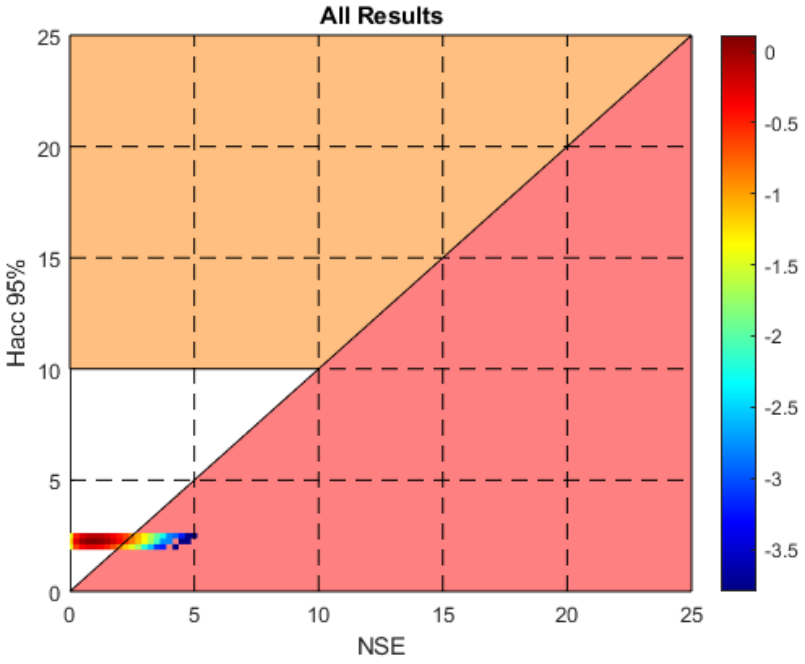

Figure 5-123: Plot of Computed Horizontal Position Error vs 95% Horizontal Accuracy in Coastal Scenario full DFMC EGNOS Fault-Free Case – all samples

Faulty Cases

To investigate the fault detection capability and impact of faults, we run the DFMC cases with a single fault added. Like in the SF analysis, on each sample epoch a random fault of between 0 and 50m is added to a random satellite (in view) on each sample epoch.

For the current GPS case (with only a subset of satellites having L5) we expect to see some improvement over GPS L1, but not the full benefit of DFMC. In this case we see that without any fault detection, the maximum horizontal position error reaches 59.82m and there are 24.5% of epochs where the position error exceeds 10m. Also, there are 43.2% of sample epochs where the actual position error exceeds the reported 95% horizontal accuracy value.

From these figures, it can be seen that the general level of error is lower than in the GPS L1 case but there are more extreme outliers in this scenario.

It can also be seen that 38.26% of epochs are marked as red, i.e., a fault is detected. This is a higher % of fault detections than in the GPS L1 case. However, even after all the checks there are still 6.01% of epochs where the position error is greater than 10m but the status is green, although this is a much smaller % than in the GPS L1 case.

The plots showing the errors vs 95% horizontal accuracy are shown below for all sample epochs and those just with green integrity flag.

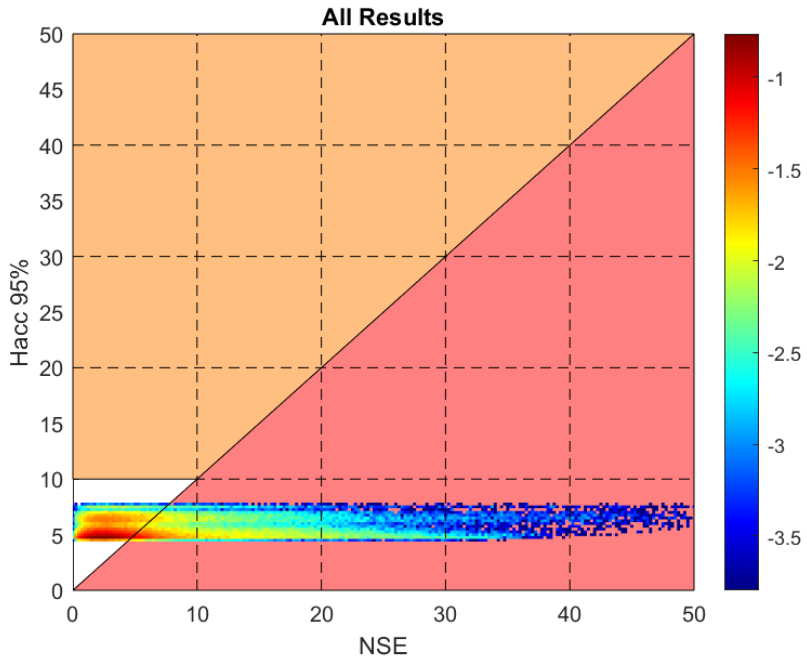

Figure 5-124: Plot of Computed Horizontal Position Error vs 95% Horizontal Accuracy in Coastal Scenario current DFMC Single Fault case (up to 50m) – all samples

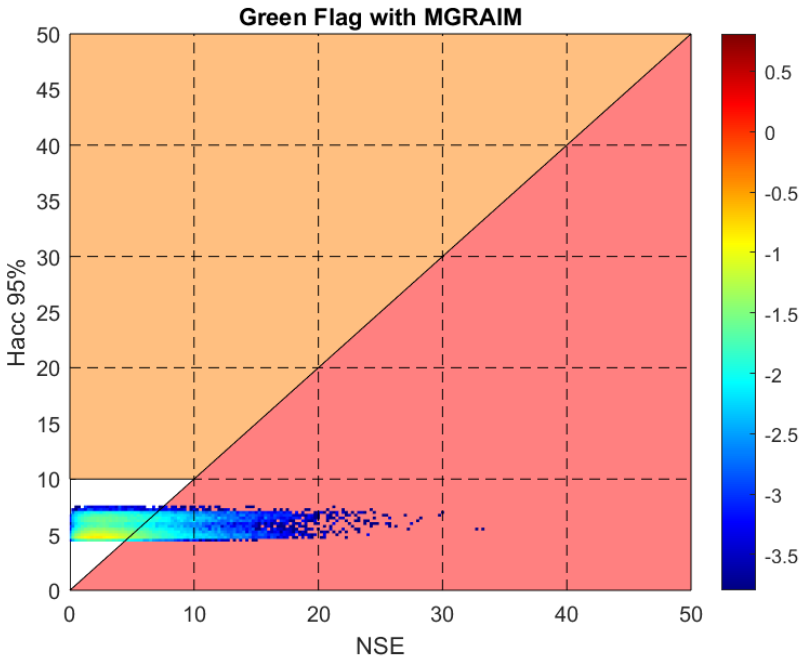

Figure 5-125: Plot of Computed Horizontal Position Error vs 95% Horizontal Accuracy in Coastal Scenario current DFMC Single Fault case (up to 50m) – only green samples

In the future scenario where we consider all GPS satellites as having L5 measurements then we see a further improvement. In this case we see that without any fault detection, the maximum horizontal position error reaches 26.26m and there are 11.5% of epochs where the position error exceeds 10m. Also, there are 45.37% of sample epochs where the actual position error exceeds the reported 95% horizontal accuracy value.

If we consider the MGRAIM checks then we see that 45.17% of epochs are marked as red, i.e., a fault is detected, and there are now only 0.1% of epochs that have green status and horizontal error > 10m, which is much smaller than in the current GPS DFMC case and the GPS L1 case. This demonstrates the improvement in integrity through additional measurements and improved geometry.

The plots showing the errors vs 95% horizontal accuracy are shown below for all sample epochs and for those just with green integrity flag.

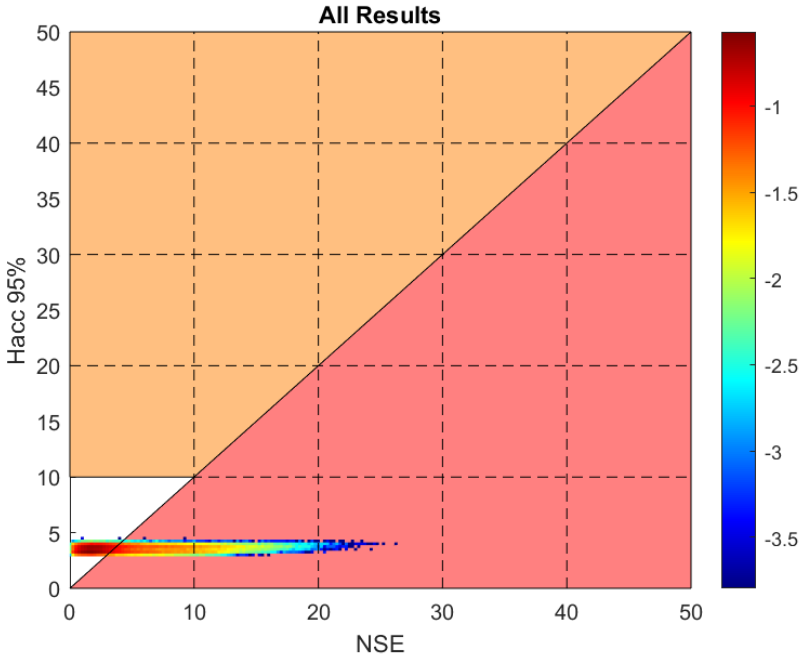

Figure 5-126: Plot of Computed Horizontal Position Error vs 95% Horizontal Accuracy in Coastal Scenario future DFMC Single Fault case (up to 50m) – all samples

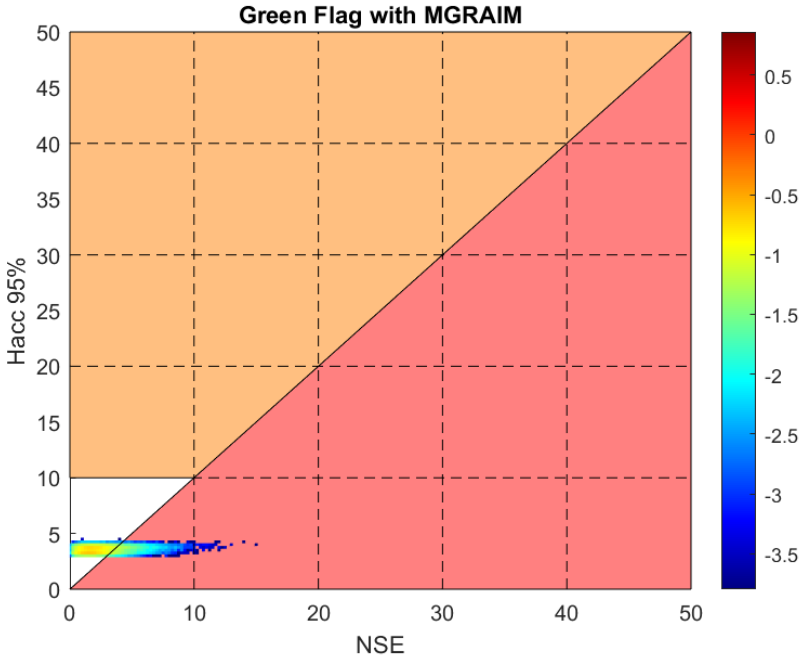

Figure 5-127: Plot of Computed Horizontal Position Error vs 95% Horizontal Accuracy in Coastal Scenario future DFMC Single Fault case (up to 50m) – only green samples

Finally, we perform a coastal scenario with single fault (up to 50m) for the DFMC EGNOS case. We saw in the fault-free case that this gave some smaller errors and horizontal accuracy that in the DFMC only case, and so again we might expect the fault detection capability to be improved.

Firstly, we present the current DFMC case (with not all satellites having L5 measurements).

In this simulation we see that without any fault detection, the maximum horizontal position error for DFMC + EGNOS reaches 32.3m and there are 22.6% of epochs where the position error exceeds 10m. The fault detection is quite successful, and the red flag is raised on 73.16% of

epochs. All of these show the application of DFMC EGNOS detecting more faults (i.e., detecting them earlier) than in the current DFMC only case, although it is also noted that 28% of epochs have horizontal error that exceed the reported horizontal accuracy and there are 0.43% of epochs with green status where position error exceeds 10m.

The plots showing the errors vs 95% horizontal accuracy are shown below for all sample epochs and those just with green integrity flag.

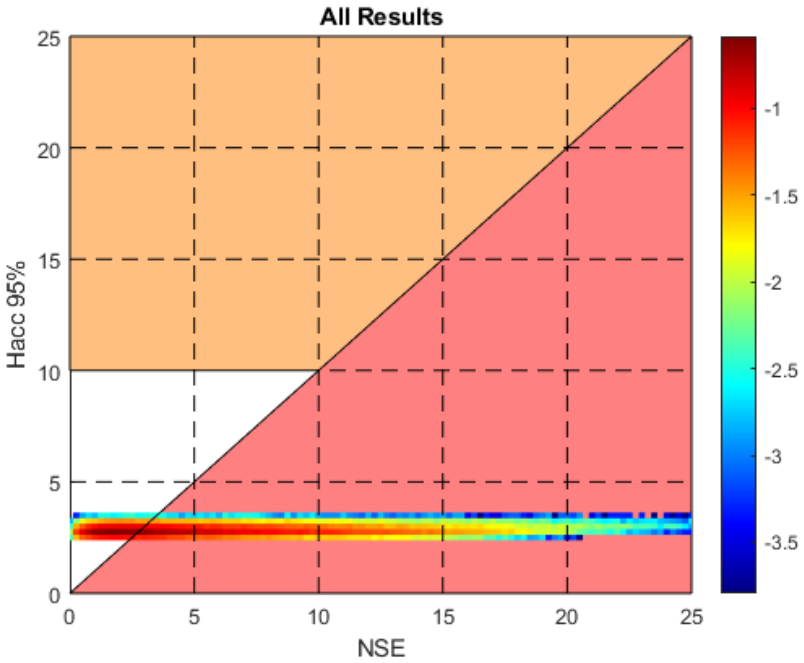

Figure 5-128: Plot of Computed Horizontal Position Error vs 95% Horizontal Accuracy in Coastal Scenario current DFMC+EGNOS Single Fault case (up to 50m) – all samples

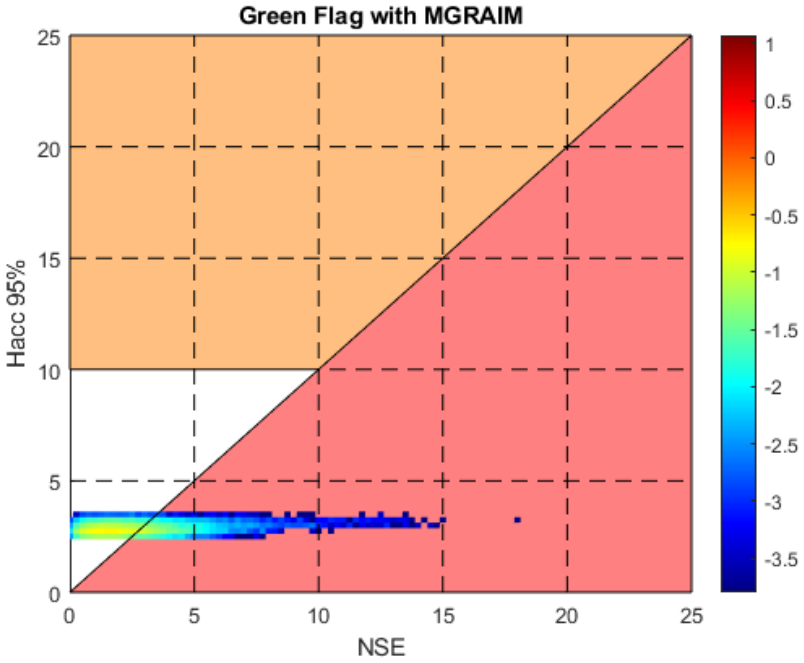

Figure 5-129: Plot of Computed Horizontal Position Error vs 95% Horizontal Accuracy in Coastal Scenario current DFMC+EGNOS Single Fault case (up to 50m) – only valid (green) sample epochs

If we consider the future DFMC case with all GPS satellites having L5 measurements, then the results are improved further. In this case the maximum error (without any fault detection) is just 20.2m and there are 7% of samples with position error >10m. With fault detection then this marks 71.7% of epochs as faulty (red flag) and the remaining maximum error is only 7.3m. Plots of these results are shown below.

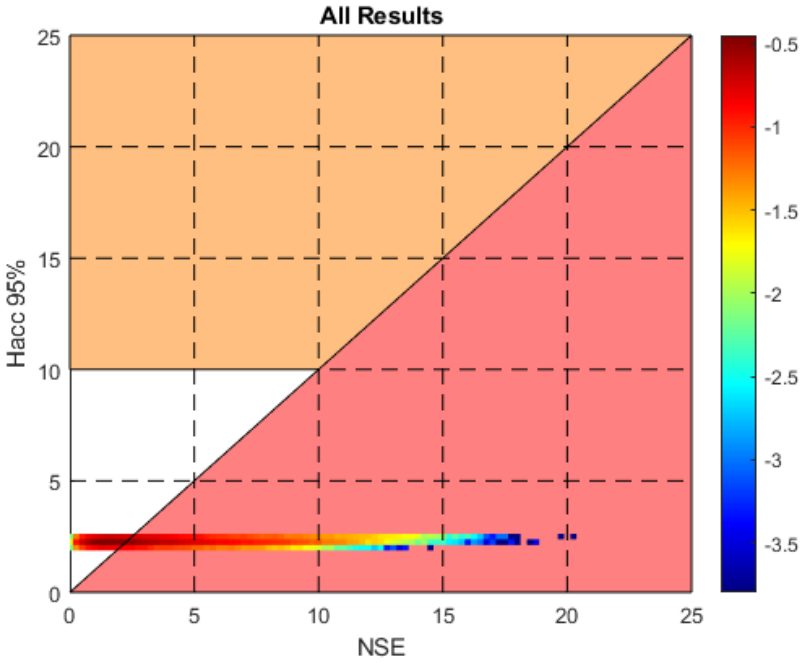

Figure 5-130: Plot of Computed Horizontal Position Error vs 95% Horizontal Accuracy in Coastal Scenario future DFMC+EGNOS Single Fault case (up to 50m) – all samples

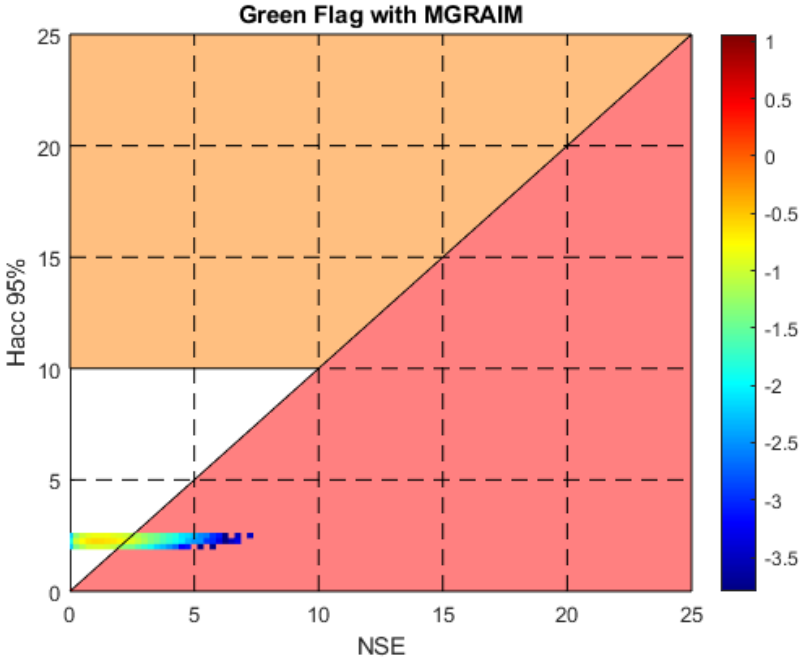

Figure 5-131: Plot of Computed Horizontal Position Error vs 95% Horizontal Accuracy in Coastal Scenario future DFMC+EGNOS Single Fault case (up to 50m) – only valid (green) sample epochs

5.2.2.3 Summary

The key results from the different MGRAIM scenarios (all for Coastal requirements) are summarised in the following table.

Table 5-64: Summary of Key Results from Different Monte Carlo Simulation Scenarios for DFMC MGRAIM

Constellations	GPS	Faults	Max Hz Err	Mx valid Hz Err	Red flag %	Amber flag %	Green flag %	% Valid Hz Err > Hacc 95%	% Valid Hz Err > Hacc threshold
GPS+GAL DF	Current	Fault Free	14.17m	14.17m	0.001	3.11	96.89	5.8	0.11
GPS+GAL DF	Future	Fault Free	10.43m	10.43m	0.001	0.0	99.999	5.2	0.001
GPS+GAL DF	Current	Single fault – up to 50m	59.82m	33.19m	38.26	1.9	59.82	24.8	6.07
GPS+GAL DF	Future	Single fault – up to 50m	26.26m	14.99m	45.17	0.0	54.83	18.67	0.12
GPS+GAL + DFMC EGNOS	Current	Fault Free	6.88m	6.88m	0.0	0.0	100.0	5.3	0.0
GPS+GAL + DFMC EGNOS	Future	Fault Free	4.91m	4.91m	0.0	0.0	100.0	5.1	0.0
GPS+GAL + DFMC EGNOS	Current	Single fault – up to 50m	32.3m	18.0m	73.17	0.0	26.83	28.18	0.43
GPS+GAL + DFMC EGNOS	Future	Single fault – up to 50m	20.19m	7.34m	71.75	0.0	28.25	22.6	0.0

Note that the equivalent results for GPS L1 MGRAIM from WP2 are shown in the following table.

Table 5-65: Summary of Key Results from Different Monte Carlo Simulation Scenarios for GPS L1 MGRAIM (from WP2)

Constellations	Operation	Faults	Max Hz Err	Mx valid Hz Err	Red flag %	Amber flag %	Green flag %	% Valid Hz Err > Hacc 95%	% Valid Hz Err > Hacc threshold
GPS L1	Coastal	Fault Free	17.08 m	16.36 m	0.06	15.35	84.59	5.18	0.71
GPS L1	Coastal	Single fault – up to 50m	39.61 m	27.49 m	28.99	10.98	60.03	29.82	13.91
GPS L1 + EGNOS	Coastal	Fault Free	9.3m	9.3m	0.0	0.0	100.0	5.2	0.0
GPS L1 + EGNOS	Coastal	Single fault – up to 50m	32.04 m	19.42 m	64.015	0.0	35.985	33.17	0.686

In addition, the cumulative distributions of the horizontal safety index for each scenario are shown. In this case (for the MGRAIM algorithm) the horizontal safety index is defined as the ratio between the actual horizontal error and the applicable horizontal performance indicator (95% horizontal accuracy metric). In the first plot the values are generated considering all solutions, no matter what the value of the integrity flag.

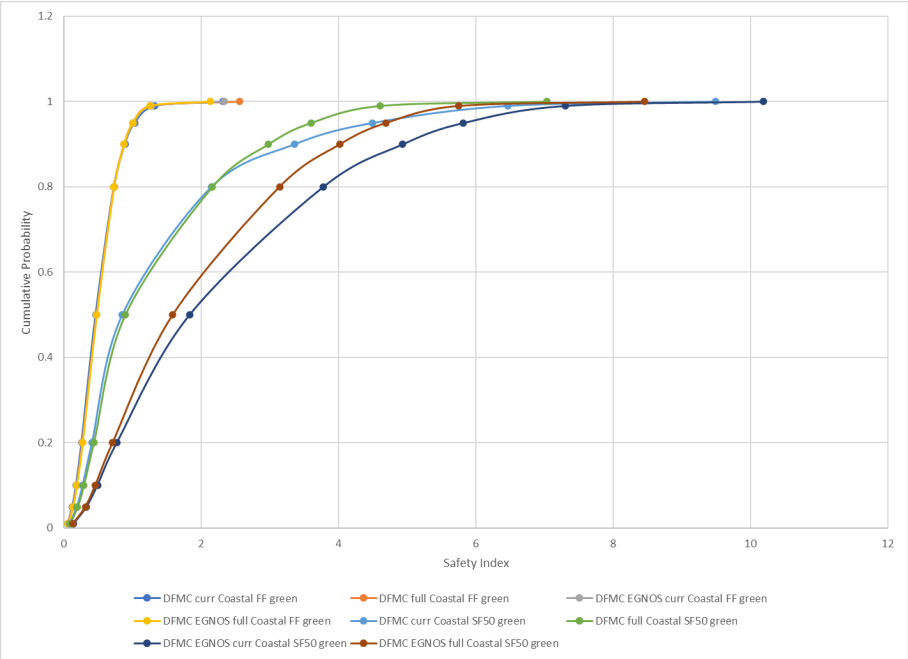

Figure 5-132: Cumulative Distribution of Horizontal Safety Index for DFMC MGRAIM Scenarios (all results)

The equivalent for WP2 (single constellation, single frequency) is also shown.

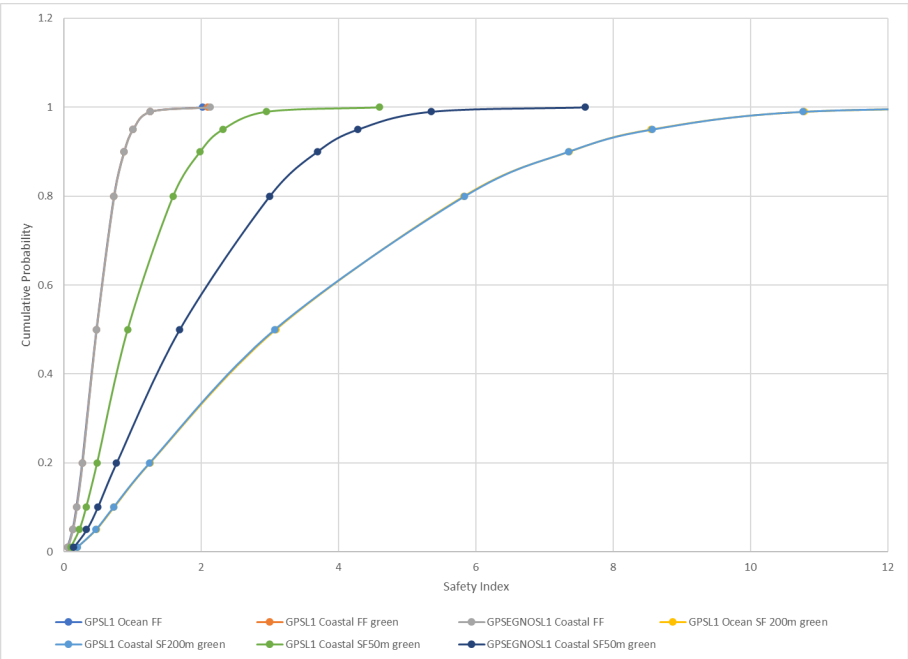

Figure 5-133: Cumulative Distribution of Horizontal Safety Index for Single Frequency MGRAIM Scenarios (all results)

It can be seen from the plot that the cumulative distributions are almost identical for the fault-free cases, and that they reach 95% for a safety index of 1, which is expected because the performance indicator is 95% horizontal accuracy. However, in the faulty cases we see that there is very low cumulative % for a safety index of 1, i.e. the horizontal 95% accuracy is not

bounding the actual errors with any degree of confidence, and there are longer tails to the distribution (i.e. larger errors as we get to the extremes) for the DFMC case compared to the single frequency case.

If we look at the results considering only those with green integrity flag status then we see the following results.

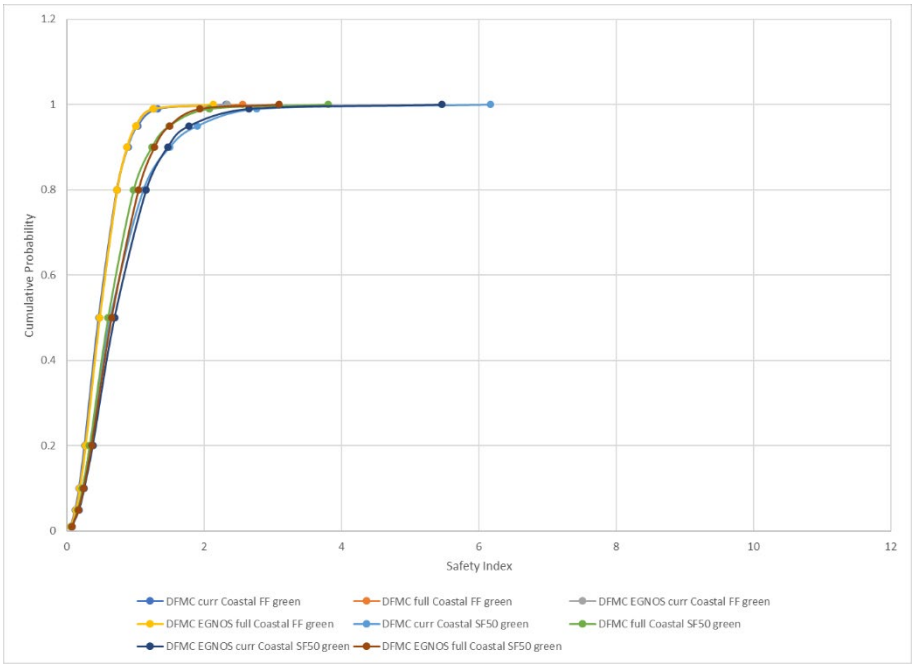

Figure 5-134: Cumulative Distribution of Horizontal Safety Index for DFMC MGRAIM Scenarios (green integrity flag)

Again, the single frequency results from WP2 are also shown for comparison.

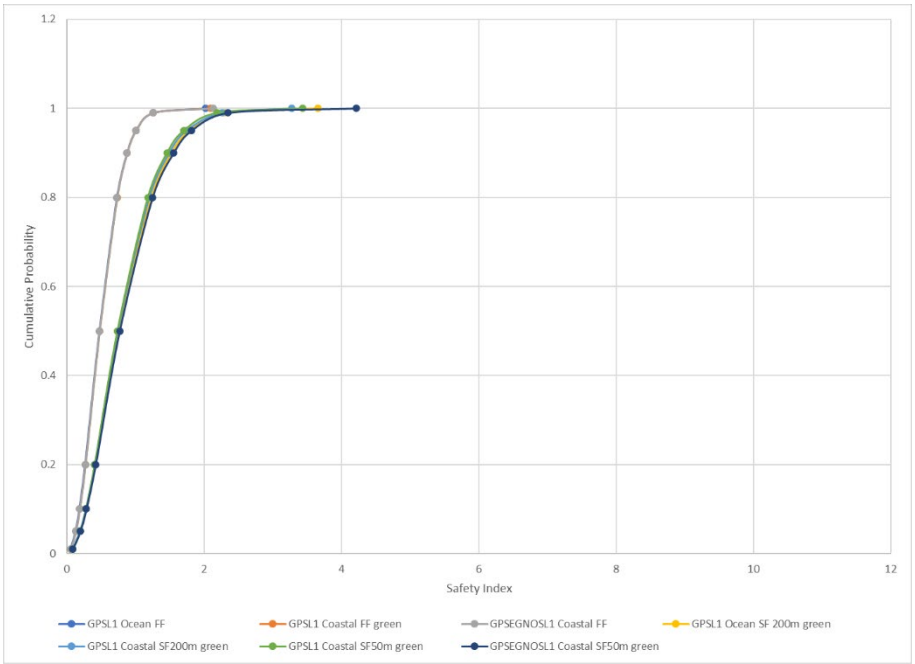

Figure 5-135: Cumulative Distribution of Horizontal Safety Index for Single Frequency MGRAIM Scenarios (green integrity flag)

In this case the cumulative probability for horizontal safety index of 1 is much higher in the faulty cases, indicating that the fault detection has worked to remove the worst errors. Also,

although there are still larger errors at the tails for DFMC case, the % of solutions with safety index less than 1 is greater for the DFMC case.

The purpose of these simulations was to provide some extra validation of the MGRAIM functionality and to gain a better understanding of the performance difference when using DFMC rather than GPS L1.

In terms of performance:

- We did not study the ocean case as GPS L1 could cover the requirements for that (100m accuracy). Therefore, the results are just for the coastal case (10m horizontal accuracy 95%).
- The DFMC solutions include GPS L1/L5 + Galileo E1/E5a. As the current GPS constellation does not include L5 signals on all GPS satellites, we considered both the current case and the future case (where all GPS satellites have L5 measurements).
- In the fault-free case with DFMC, the smaller errors and improved geometry compared to GPS L1 mean that the reported 95% accuracy and actual position errors are smaller and there are more sample epochs with green integrity flag.
  - For current DFMC case, the difference is marginal but for future DFMC case there is a significant improvement with 100% of sample epochs with green status flag and a maximum horizontal position error of just 10.4m.
- The errors in the solution (and also the error model used in the checks) can be further reduced through using EGNOS, which reduces the magnitude of the horizontal position errors and the reported 95% horizontal accuracy. In this case, the maximum error is reduced to just 6.88m for current DFMC and 4.91m for future DFMC.
- For both the DFMC and DFMC+EGNOS cases it is noted when using the full GPS constellation (which would be the future DFMC case) that there are no amber flags raised, i.e. the improved geometry and lower errors mean that the computed 95% horizontal accuracy is less than 10m for the all-in-view solution and the different subsets.
- When a single satellite fault of up to 50m is added to the data, then we see different performance to the GPS L1 case, and also quite difference performance between the current and future DFMC cases:
  - In the current DFMC case we see that the maximum errors without checks (59.82m) and after checks (33.19m) are larger than in the GPS L1 case, although the % of valid sample epochs with horizontal error > the 10m limit is reduced to 6.07%. This suggests that the general level of performance is improved but there are some significant outliers caused by the range errors – perhaps in cases where there are few GPS satellites in the solution and one has a large error.
  - In the future DFMC case, the maximum horizontal error and maximum valid horizontal position error are now much smaller than in the GPS L1 (and current DFMC) cases, and the % of 'valid' samples epochs with position error greater than the 10m threshold is now only 0.1%, which is a significant improvement.
- If DFMC EGNOS is used, then we see the best results as the smaller actual (and expected) errors means that faults can be detected earlier, and so those epoch samples where a fault is not detected have much smaller errors. In the future DFMC+EGNOS case this means that the maximum remaining horizontal position error after fault

detection is only 7.34m, although this is at the expense of availability as over 71% of epochs are marked as faulty (red flag) and so are unavailable.

- At first this may seem strange as it could be interpreted that the application of EGNOS leads to worse availability. However, it does make sense if we consider the actual meaning of the red flag for integrity. For the MGRAIM algorithm, if a fault is detected this indicates that the errors in the solution are larger than would normally be expected. It is not therefore indicating that the solution may be worse than some defined threshold – simply that there is some inconsistency compared to the normal level of error that would be expected. As the residual range errors are smaller (and expected to be smaller) after the application of EGNOS corrections, this means that it is easier to spot smaller range errors and flag them as unusual, compared to the GPS case where the usual level of range residual is higher. This mean that smaller faults can be detected, and so we may expect that possible faults are flagged more often than in the GPS only case.

5.2.3 MRAIM Results

5.2.3.1 General Parameters

Secondly, the baseline MRAIM algorithm described in [RD.50] is assessed for DFMC and DFMC+EGNOS combinations. The results of this alternative integrity approach are compared to those from the MGRAIM algorithm.

The general scenario parameters (e.g., start and end time, number of samples, latitude and Longitude limits, etc.) are kept the same as for the MGRAIM simulations. In addition, the error models (covering orbit/clock, ionosphere, troposphere and noise/multipath) are also kept the same. Some additional MRAIM specific configuration parameters are detailed in the table below. Note that these follow the values defined in [RD.50].

Table 5-66: MRAIM Configuration Settings for Monte Carlo Simulations

Configuration parameter	MRAIM No SBAS	MRAIM with SBAS
Constellation	GPS + Galileo	GPS + Galileo
Augmentation	None	EGNOS DFMC
False Alarm rate	10^{-5}	10^{-5}
Accuracy threshold 95%	10m	10m
ISD parameters		
GPS Rsat	10^{-5}/h	10^{-7}/h
Galileo Rsat	$3{\cdot}10^{-5}$/h	10^{-7}/h
GPS Rconst	10^{-8}/h	10^{-8}/h
Galileo Rconst	$2{\cdot}10^{-4}$/h	10^{-7}/h
GPS MTTNsat	3600s	3600s
Galileo MTTNsat	3600s	3600s
GPS MTTNconst	3600s	3600s
Galileo MTTNconst	3600s	3600s
Bnom	0.75m	0.1m
GPS URA	2 m	0.92 m
Galileo URA	6 m	0.92 m
GPS URE	1.33 m	1.37 m
Galileo SISE	4 m	1.37 m
Integrity Requirements and Design Parameters		
PHMI	$1/3 \cdot 10^{-5}$/h	$1/3 \cdot 10^{-5}$/h
Pfa	$5{\cdot}10^{-7}$	$5{\cdot}10^{-7}$
AL	25m	25m
P_{THRES}	$1 \cdot 10^{-6}$	$1 \cdot 10^{-6}$
F_C	0.01	0.01
N_{ITER_MAX}	10	10

TOL_{PL}	$5 \cdot 10^{-2}$ m	$5 \cdot 10^{-2}$ m
$N_{ES,INT}$	450	450
$N_{ES,CONT}$	450	450

It is also noted that the optional FDE is not configured during these tests for the MRAIM algorithm, i.e. there is fault detection only. This is so that we are consistent with the same assumptions as for the MGRAIM algorithm in order to provide a far comparison of performance.

In terms of the constellation, two options are considered. In both cases, the actual nav messages reflecting the operational GPS and Galileo constellation on 28th Sep 2022 are used. However, in one case only those GPS satellites that have L5 measurements are used (which is only a subset of the full constellation) to reflect the current situation, whereas in the second option all GPS satellites are used (representing the future case when all GPS satellites will have L5 measurements).

5.2.3.2 Coastal Scenarios

Only the coastal scenario is shown because, according to the WP2 results, GPS L1 was sufficient for the ocean case. Therefore, using DFMC to potentially improve performance in the coastal scenario is more interesting.

In coastal mode, the 95% horizontal accuracy threshold is 10m and the HAL is 25m.

Fault-Free

First, the fault free case is run. The intention is to check the performance in terms of false alarms and nominal accuracy and availability.

For the current DFMC case (with not all GPS satellites having L5), the level of accuracy is the same as in the MGRAIM case, but we find that the HPL values that are computed are always greater than 25m, and therefore the red status flag is always set, i.e., we have 0% availability of a valid solution.

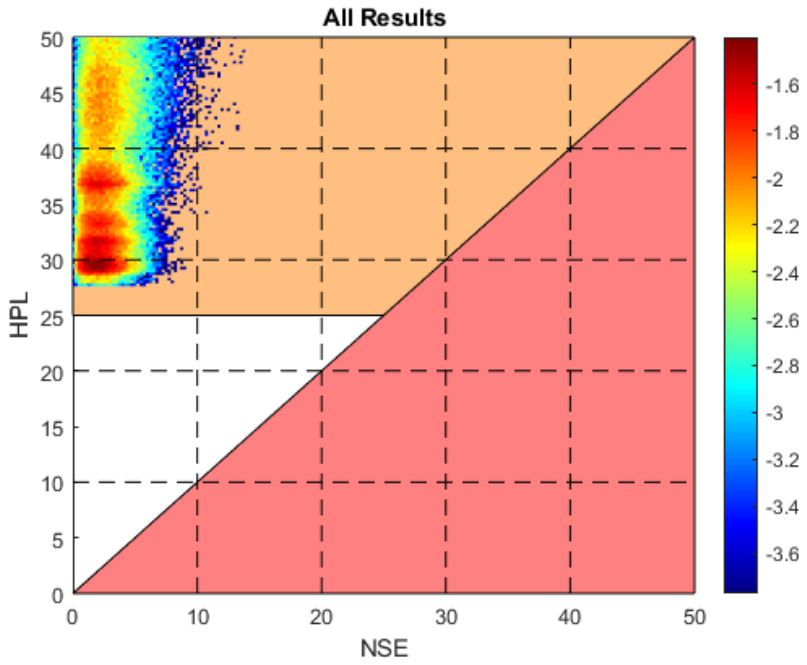

Figure 5-136: Plot of Computed Horizontal Position Error vs MRAIM HPL in Coastal Scenario current DFMC Fault-Free Case – all samples

If we consider the future DFMC case (with full set if GPS satellites) then this improvement in geometry means the computed HPL values are smaller and so we do get a lot of cases (around

98.8%) where the sample epochs have a green status flag because the HPL is less than the HAL of 25m. Overall we see a maximum horizontal position error (on any epoch) of 8.3m, and also on those epochs on which the HPL is less than 25m and a green status flag is raised.

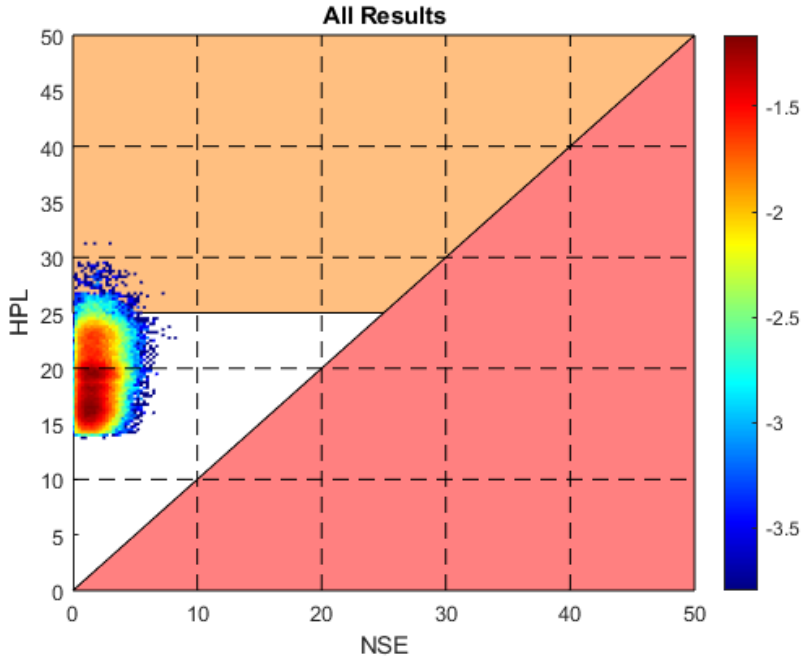

Figure 5-137: Plot of Computed Horizontal Position Error vs MRAIM HPL in Coastal Scenario future DFMC Fault-Free Case – all samples

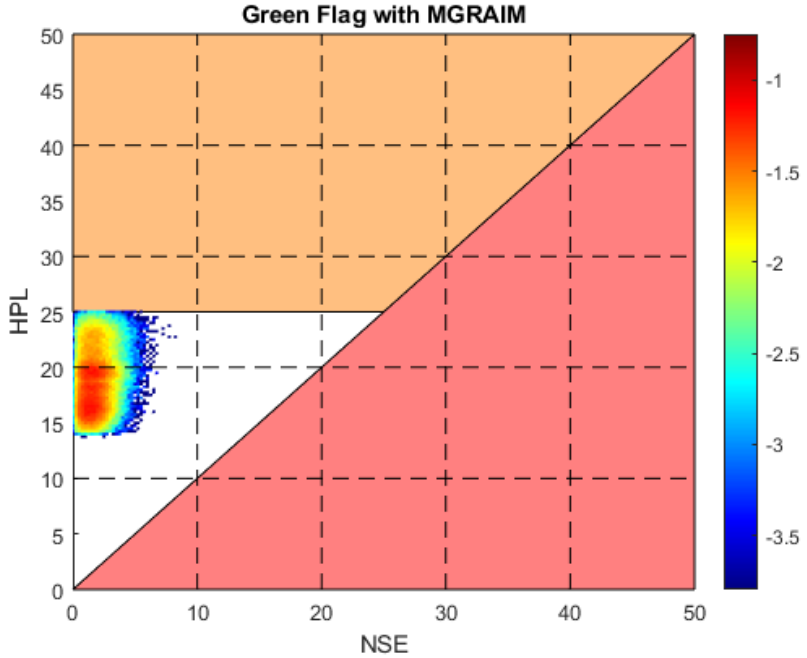

Figure 5-138: Plot of Computed Horizontal Position Error vs MRAIM HPL in Coastal Scenario future DFMC Fault-Free Case – only valid (green) sample epochs

As we see such poor performance for the current GPS constellation (very low availability) we discount that from further analysis and consider the MRAIM approach only for the case where all GPS satellites have L5 measurements (future DFMC).

The next analysis shows the MRAIM results in the fault-free case for future DFMC + EGNOS. Here the orbit and clock errors are smaller, and the failure rates for the satellites are significantly reduced because the SBAS itself should be able to identify and warn of such faults.

For the future DFMC + EGNOS case, the position error is much smaller than in the DFMC only case, with maximum position error of just 5.18m, and also the HPL values are much smaller. In fact, they are always below the HAL of 25m and so the availability of a valid solution with green status flag is 100%. The position errors and HPL values are shown in the plot below.

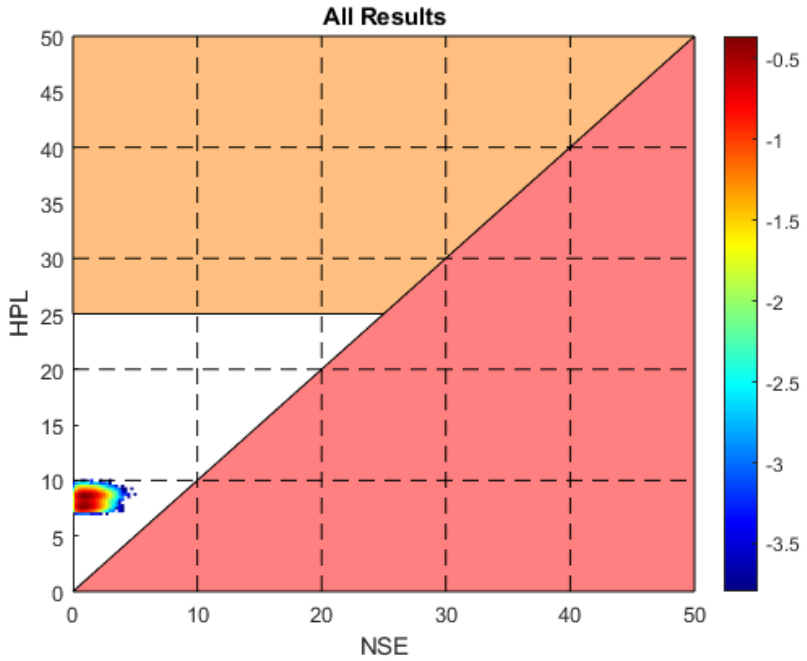

Figure 5-139: Plot of Computed Horizontal Position Error vs MRAIM HPL in Coastal Scenario future DFMC+EGNOS Fault-Free Case – all samples

Faulty Case

To investigate the fault detection capability and impact of faults, we run the MRAIM cases with a single fault added. Like in the MGRAIM analysis, on each sample epoch a random fault of between 0 and 50m is added to a random satellite (in view) on each sample epoch.

Firstly, we consider the future DFMC case with GPS L1/L5 and Galileo E1/E5a. For this case we see that with the addition of the range errors, the maximum horizontal position error we then see on any epoch is 27.3m, which is consistent with what we saw for the MGRAIM case (which is not surprising as the positioning algorithm and the error models are the same). We also see that after applying fault detection, there are 64.3% of epochs that have valid (green) status and the maximum remaining error for any sample epoch with green status flag is 16.5m. At first glance this does not seem to be a good result because the position error is greater than the required accuracy of 10m, even though the status is green. However, what is important is that in this case the HPL that is output is always larger than the actual horizontal position error and so can be used as an indicator of the performance – even in faulty cases.

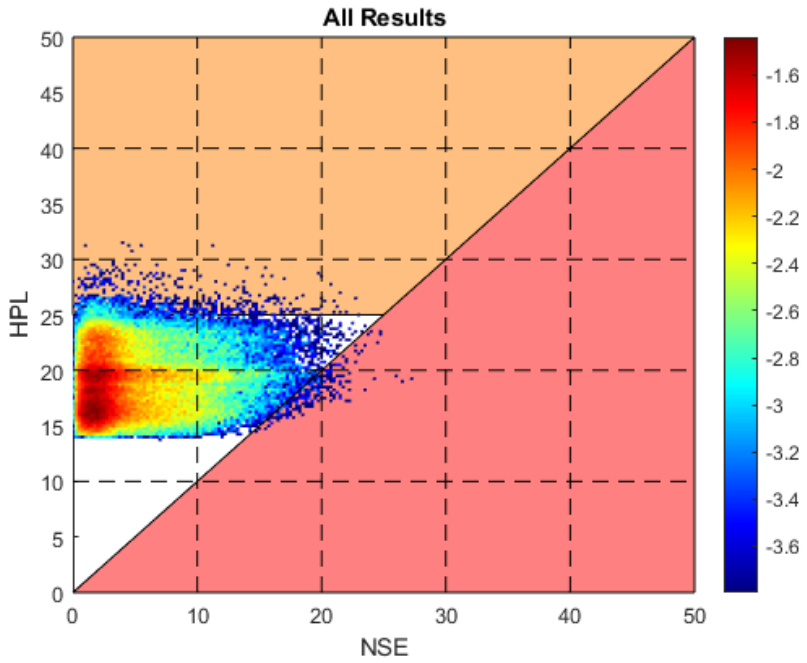

Figure 5-140: Plot of Computed Horizontal Position Error vs MRAIM HPL in Coastal Scenario future DFMC in single fault Case (up to 50m) – all samples

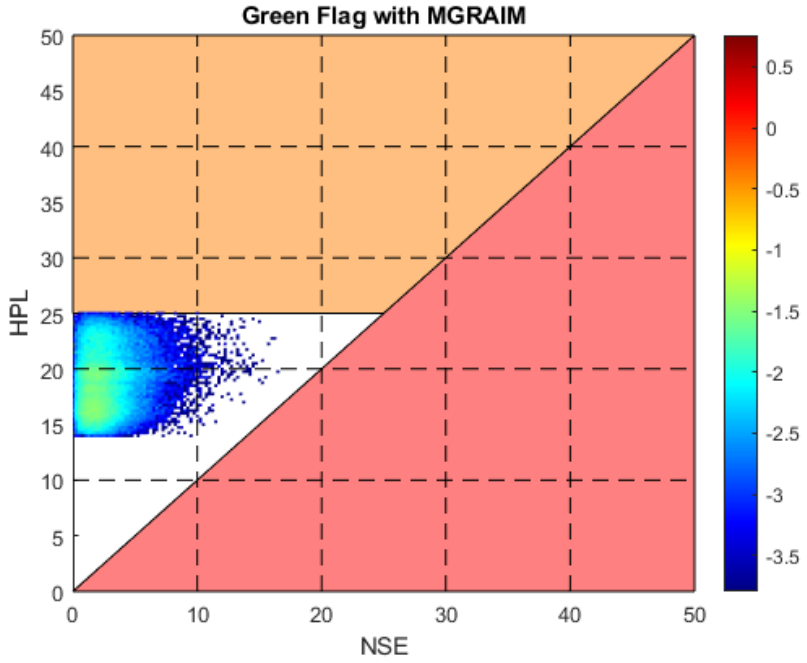

Figure 5-141: Plot of Computed Horizontal Position Error vs MRAIM HPL in Coastal Scenario future DFMC in single fault Case (up to 50m) – only valid (green) sample epochs

Finally, we perform the same fault in the future DFMC + EGNOS case. In this case the correction messages from SBAS would lead to smaller orbit and clock errors (and uncertainties) and lower failure rates for the satellite errors, and so we should expect better fault detection capability.

For this case we see that with the addition of the range errors, the maximum horizontal position error we then see on any epoch is 18.7m, which is similar to what we saw for the MGRAIM case (which is not surprising as the positioning algorithm and the error models are the same).

We also see that after applying fault detection, there are 48.6% of epochs that have valid (green) status and the maximum remaining error for any sample epoch with green status flag is 15.3m. At first glance this does not seem to be a good result because the position error is greater than the required accuracy of 10m, even though the status is green. However, it is a smaller error than what is achieved in the DFMC only case (no EGNOS) and what is important is that in this case the HPL that is output is almost always larger than the actual horizontal position error and so can be used as an indicator of the performance – even in faulty cases.

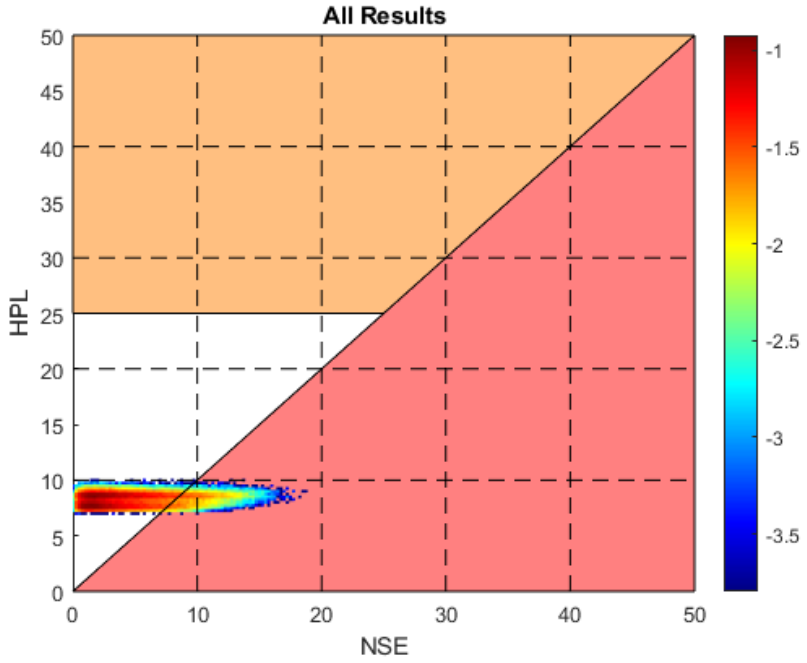

Figure 5-142: Plot of Computed Horizontal Position Error vs MRAIM HPL in Coastal Scenario future DFMC+EGNOS in single fault Case (up to 50m) – all samples

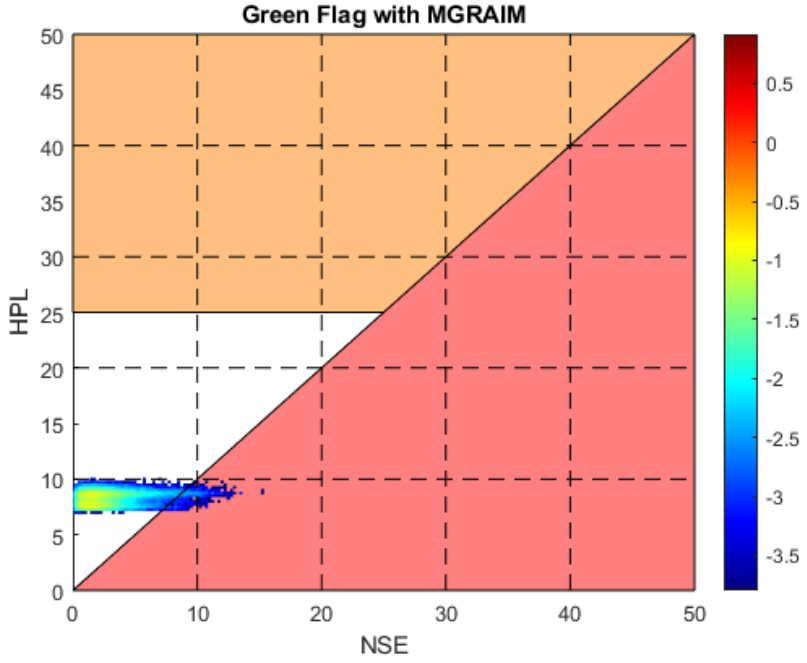

Figure 5-143: Plot of Computed Horizontal Position Error vs MRAIM HPL in Coastal Scenario future DFMC+EGNOS in single fault Case (up to 50m) – only valid (green) sample epochs

5.2.3.3 Summary

The key results from the different MRAIM scenarios (all for Coastal requirements) are summarised in the following table.

Table 5-67: Summary of Key Results from Different Monte Carlo Simulation Scenarios for DFMC MRAIM

Constellations	GPS	Faults	Max Hz Err	Mx valid Hz Err	Red flag %	Amber flag %	Green flag %	% Valid Hz Err > HPL	% Valid Hz Err > HAL
GPS+GAL DF	Current	Fault Free	14.5m	NA	100.0	0.0	0.0	NA	NA
GPS+GAL DF	Future	Fault Free	8.3m	8.3m	1.1	0.0	98.9	0.0	0.0
GPS+GAL DF	Future	Single fault – up to 50m	27.3m	16.6m	35.7	0.0	64.3	0.0	0.0
GPS+GAL + DFMC EGNOS	Future	Fault Free	4.9m	4.9m	0.0	0.0	100.0	0.0	0.0
GPS+GAL + DFMC EGNOS	Future	Single fault – up to 50m	18.7m	15.3m	51.4	0.0	48.6	1.3	0.0

These can be compared with the earlier MGRAIM results.

In addition, the cumulative distributions of the horizontal safety index for each scenario are shown. In this case (for the MRAIM algorithm) the horizontal safety index is defined as the ratio between the actual horizontal error and the HPL value. In the first plot the values are generated considering all solutions, no matter what the value of the integrity flag. The scale of the plot is kept the same as for MGRAIM results in order to make the comparison easier.

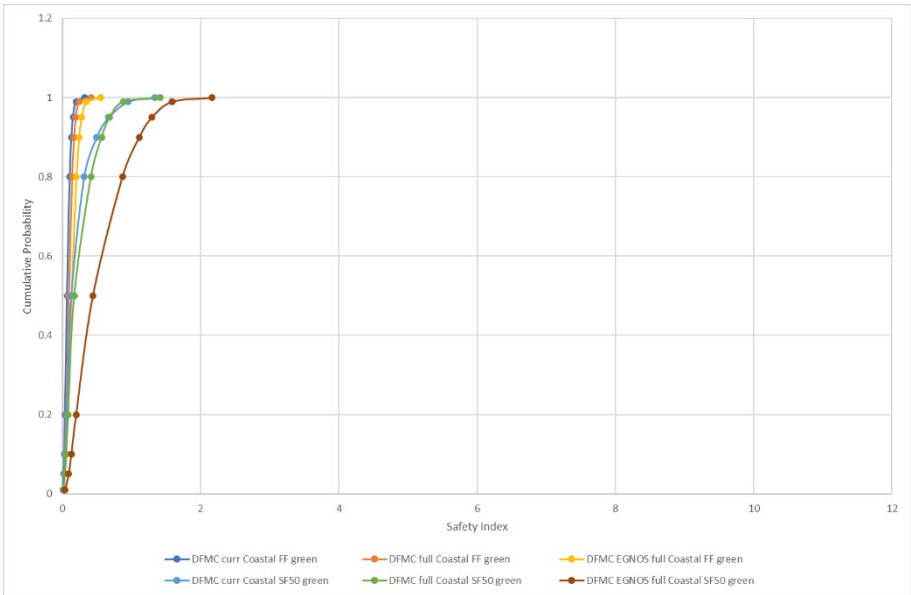

Figure 5-144: Cumulative Distribution of Horizontal Safety Index for DFMC MRAIM Scenarios (all results)

It can be seen from the plot that the cumulative distributions show much smaller safety index values that for the MGRAIM algorithms, i.e. there is far more margin in the HPL values from MRAIM to bound the actual errors. This is particularly the case in the fault-free cases, but even in the faulty cases there is a very high % of solutions where the safety index is below 1 (i.e. HPL > horizontal error) even when there are faults in the measurements.

If we look at the results considering only those with green integrity flag status then we see the following results.

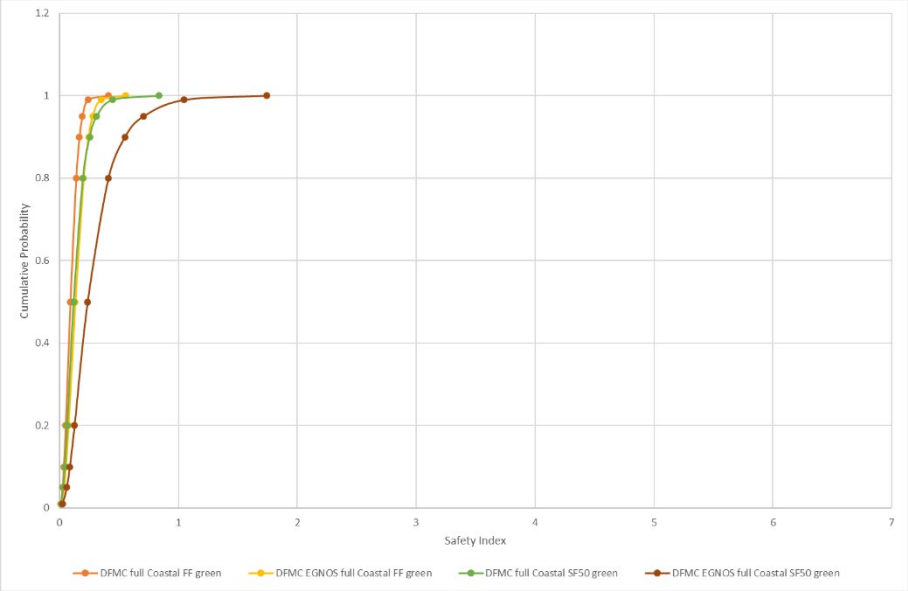

Figure 5-145: Cumulative Distribution of Horizontal Safety Index for DFMC MRAIM Scenarios (green integrity flag)

In this case the cumulative probability for horizontal safety index of 1 is quite similar to in the fault free case, although with some small change for the faulty cases.

The purpose of these simulations was to provide some extra validation of the MRAIM functionality.

In terms of performance:

- We did not study the ocean case as GPS L1 can cover the requirements for that (100m accuracy). Therefore, the results are just for the coastal case (10m horizontal accuracy 95%, 25m horizontal alarm limit).
- The DFMC solutions include GPS L1/L5 + Galileo E1/E5a. As the current GPS constellation does not include L5 signals on all GPS satellites, we considered both the current case and the future case (where all GPS satellites have L5 measurements).
- In the fault-free case with DFMC, we could see for the current DFMC case that the HPL values were never below the HAL of 25m, and so there was 0% availability of valid status. Therefore, we only considered the future DFMC case (with all GPS satellites) for the rest of the analysis.
- In the fault-free case with future DFMC, we see that position errors are similar to the DFMC case with MGRAIM, with maximum horizontal position error 8.3m. However, there are 1.1% of sample epochs where the computed HPL is greater than the HAL (of 25m) and so those samples are marked as faulty (red flag). This means there is a lower solution availability than in the MGRAIM case, although the output HPL values do bound the horizontal errors and so can be used to indicate horizontal error performance to the user.

- The errors in the solution (and also the error model used in the checks) can be further reduced through using EGNOS, which reduces the magnitude of the horizontal position errors and the reported HPL values. In this case, the maximum error is reduced to just 4.9m for future DFMC + EGNOS and there are 100% of sample epochs with HPL less than the HAL of 25m.
- When a single satellite fault of up to 50m is added to the data, then we see different performance to the MGRAIM case:
  - In the future DFMC case we see that the maximum errors after checks (16.6m) are similar to the MGRAIM case, but fewer epochs are identified as faulty (35.7%). However, the HPL values do bound the actual position errors on all the valid epochs, which is potentially advantageous compared to the MGRAIM case where the position errors exceed the reported 95% horizontal accuracy values on many epochs (~20% of the time in the single fault scenarios).
  - In the future DFMC+EGNOS case, the errors are reduced compared to the DFMC only case. We see that the maximum errors after checks (15.3m) are larger than in the MGRAIM case, and fewer epochs are identified as faulty. However, the HPL values do bound the actual position errors on almost all the valid epochs, which is potentially advantageous compared to the MGRAIM case where the position errors exceed the reported 95% horizontal accuracy values on many epochs (~20% of the time in the single fault scenarios).

5.2.4 Modified MRAIM Results

5.2.4.1 General Parameters

Finally, the modified MRAIM algorithm described in [RD.50] is assessed for DFMC and DFMC+EGNOS combinations. This algorithm has a simplification (using the Rayleigh distribution) to directly compute horizontal protection level, rather than computing East and North components separately and then combining. The results of this alternative integrity approach are compared to those from the baseline MRAIM algorithm.

Apart from the HPL computation, all other scenario and algorithm parameters are kept the same as for the baseline MRAIM algorithm, as detailed in section 5.2.3.1. We consider only the future GPS constellation as it has previously been shown that the performance cannot be achieved with the current GPS constellation (with only a subset of satellites having L5 measurements).

5.2.4.2 Coastal Scenarios

Only the coastal scenario is shown because, according to the WP2 results, GPS L1 was sufficient for the ocean case. Therefore, using DFMC to potentially improve performance in the coastal scenario is more interesting.

In coastal mode, the 95% horizontal accuracy threshold is 10m and the HAL is 25m.

Fault-Free

First, the fault free case is run. The intention is to check the performance in terms of false alarms and nominal accuracy and availability.

If we consider the future DFMC case (with full set if GPS satellites) then we get overall lower HPL values than for the baseline MRAIM algorithm and so we have 100% of cases the sample epochs have a green status flag because the HPL is less than the HAL of 25m. Overall we see a maximum horizontal position error (on any epoch) of 7.6m.

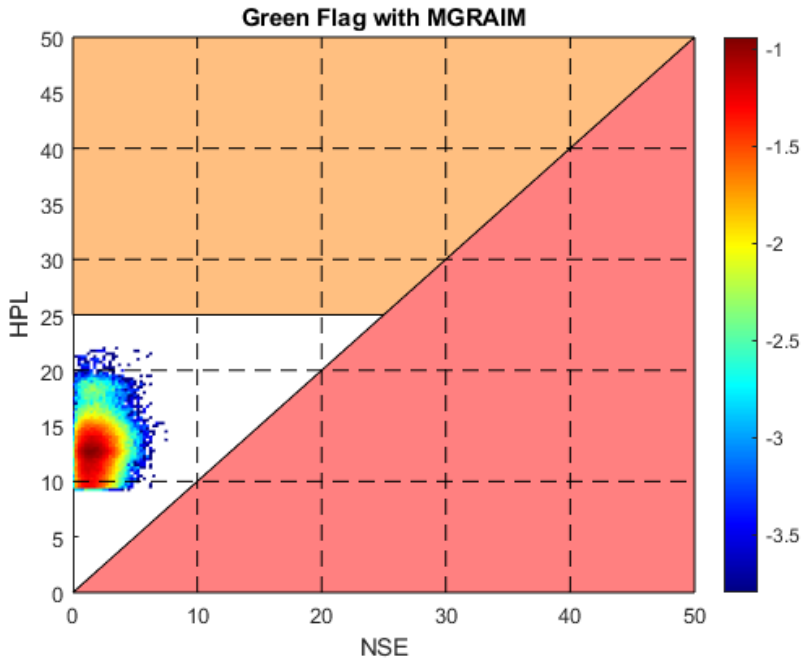

Figure 5-146: Plot of Computed Horizontal Position Error vs modified MRAIM HPL in Coastal Scenario future DFMC Fault-Free Case – only valid (green) sample epochs

The next analysis shows the MRAIM results in the fault-free case for future DFMC + EGNOS. Here the orbit and clock errors are smaller, and the failure rates for the satellites are significantly reduced because the SBAS itself should be able to identify and warn of such faults.

For the future DFMC + EGNOS case, the position error is much smaller than in the DFMC only case, with maximum position error of just 4.79m, and also the HPL values are much smaller. In fact, they are noticeably smaller than for the baseline MRAIM algorithm and are always well below the HAL of 25m and so the availability of a valid solution with green status flag is 100%. The position errors and HPL values are shown in the plot below.

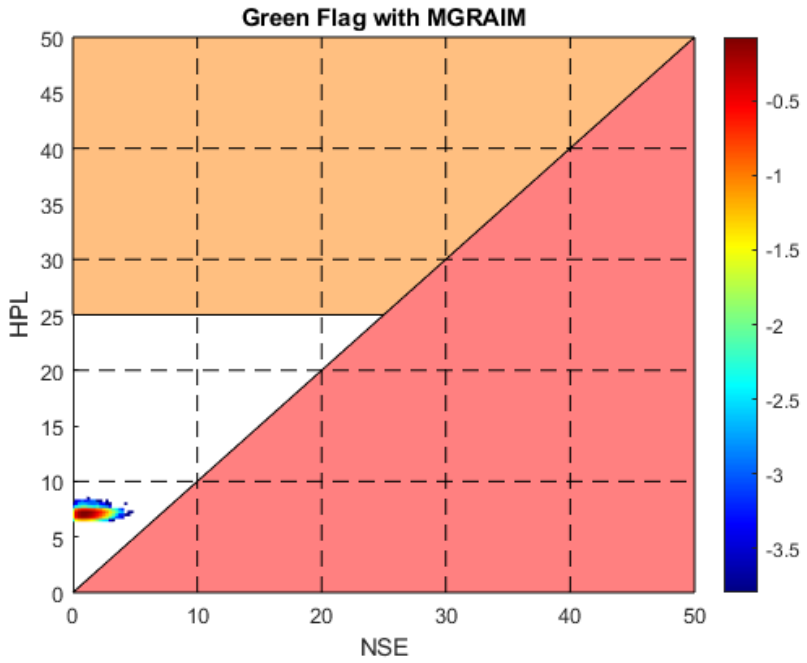

Figure 5-147: Plot of Computed Horizontal Position Error vs modified MRAIM HPL in Coastal Scenario future DFMC+EGNOS Fault-Free Case – all samples

Faulty Case

To investigate the fault detection capability and impact of faults, we run the MRAIM cases with a single fault added. Like in the earlier analysis, on each sample epoch a random fault of between 0 and 50m is added to a random satellite (in view) on each sample epoch.

Firstly, we consider the future DFMC case with GPS L1/L5 and Galileo E1/E5a. For this case we see that with the addition of the range errors, the maximum horizontal position error we then see on any epoch is 25m, which is consistent with what we saw for the baseline MRAIM case (which is not surprising as the positioning algorithm and the error models are the same). We also see that after applying fault detection, there are 62.9% of epochs that have valid (green) status and the maximum remaining error for any sample epoch with green status flag is 17.9m. At first glance this does not seem to be a good result because the position error is greater than the required accuracy of 10m, even though the status is green. However, what was important with the baseline MRAIM algorithm was that the HPL still bounded the actual position error in the green cases and so could be used as an indicator of the performance – even in faulty cases. This time we see there are a few cases (0.05%) where the HPL does not bound the actual error, but it is still the vast majority.

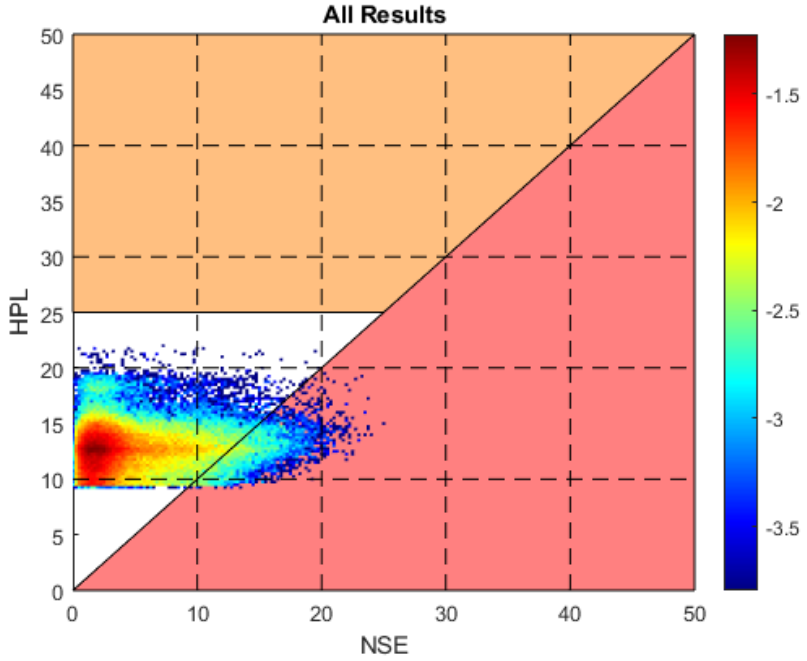

Figure 5-148: Plot of Computed Horizontal Position Error vs modified MRAIM HPL in Coastal Scenario future DFMC in single fault Case (up to 50m) – all samples

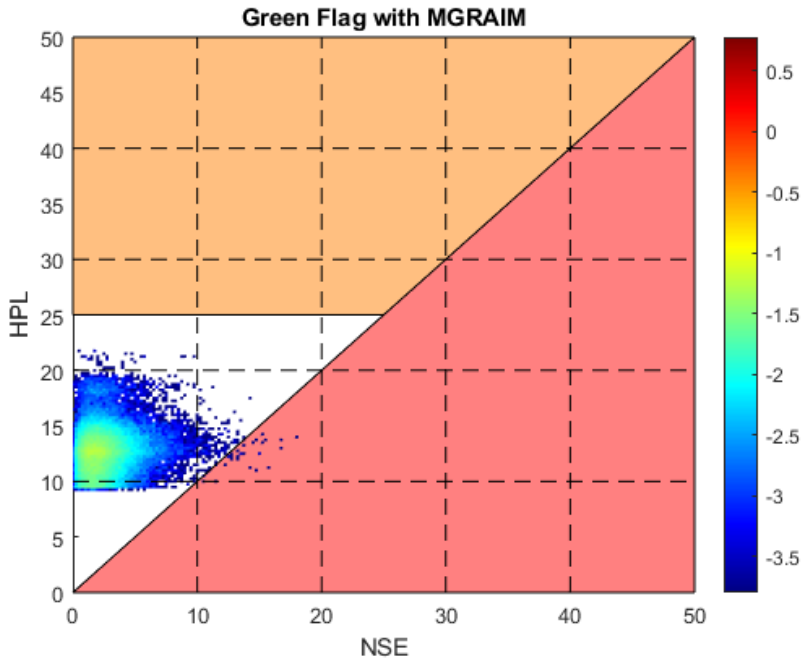

Figure 5-149: Plot of Computed Horizontal Position Error vs modified MRAIM HPL in Coastal Scenario future DFMC in single fault Case (up to 50m) – only valid (green) sample epochs

Finally, we perform the same fault in the future DFMC + EGNOS case. In this case the correction messages from SBAS would lead to smaller orbit and clock errors (and uncertainties) and lower failure rates for the satellite errors, and so we should expect better fault detection capability.

For this case we see that with the addition of the range errors, the maximum horizontal position error we then see on any epoch is 18.4m, which is similar to what we saw for the baseline MRAIM case (which is not surprising as the positioning algorithm and the error models are the same). We also see that after applying fault detection, there are 48.4% of epochs that have valid (green) status and the maximum remaining error for any sample epoch with green status flag is 14.95m. In terms of bounding the position error, we now see 2.8% of epochs of epochs with green status where the position error is larger than the reported HPL, which is an increase over the baseline MRAIM case. This is still better than in the MGRAIM algorithm but is starting to get higher than we would like. Whether that is a limitation of the modified algorithm and the assumptions within it do not fully bound the errors, or a limitation of the Monte Carlo simulations themselves introducing some unrealistic error behaviour is something that would need investigating further in a future study if this was to be taken forward.

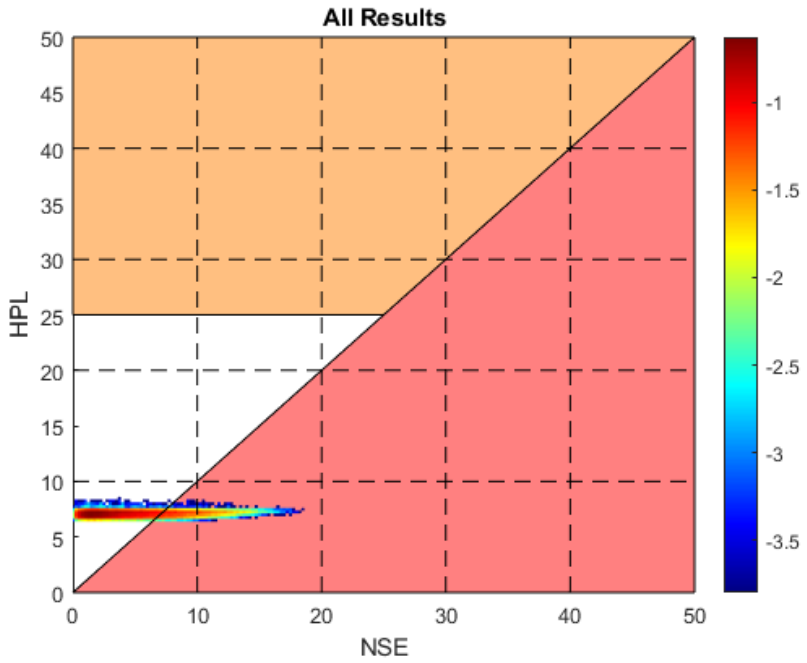

Figure 5-150: Plot of Computed Horizontal Position Error vs modified MRAIM HPL in Coastal Scenario future DFMC+EGNOS in single fault Case (up to 50m) – all samples

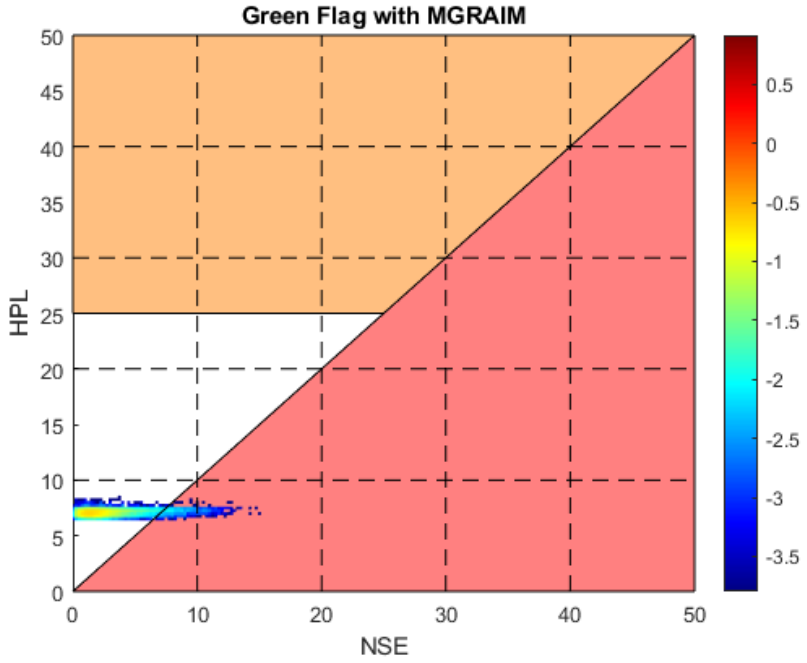

Figure 5-151: Plot of Computed Horizontal Position Error vs modified MRAIM HPL in Coastal Scenario future DFMC+EGNOS in single fault Case (up to 50m) – only valid (green) sample epochs

5.2.4.3 Summary

The key results from the different modified MRAIM scenarios (all for Coastal requirements) are summarised in the following table.

Table 5-68: Summary of Key Results from Different Monte Carlo Simulation Scenarios for DFMC modified MRAIM

Constellations	GPS	Faults	Max Hz Err	Mx valid Hz Err	Red flag %	Amber flag %	Green flag %	% Valid Hz Err > HPL	% Valid Hz Err > HAL
GPS+GAL DF	Future	Fault Free	7.6m	7.6m	0.0	0.0	100.0	0.0	0.0
GPS+GAL DF	Future	Single fault – up to 50m	25.0m	17.9m	37.1	0.0	62.9	0.05	0.0
GPS+GAL + DFMC EGNOS	Future	Fault Free	4.8m	4.8m	0.0	0.0	100.0	0.0	0.0
GPS+GAL + DFMC EGNOS	Future	Single fault – up to 50m	18.4m	15.0m	51.6	0.0	48.4	2.8	0.0

These can be compared with the earlier baseline MRAIM results.

In addition, the cumulative distributions of the horizontal safety index for each scenario are shown. In this case (for the modified MRAIM algorithm) the horizontal safety index is defined as the ratio between the actual horizontal error and the HPL value. In the first plot the values are generated considering all solutions, no matter what the value of the integrity flag. The scale of the plot is kept the same as for earlier results in order to make the comparison easier.

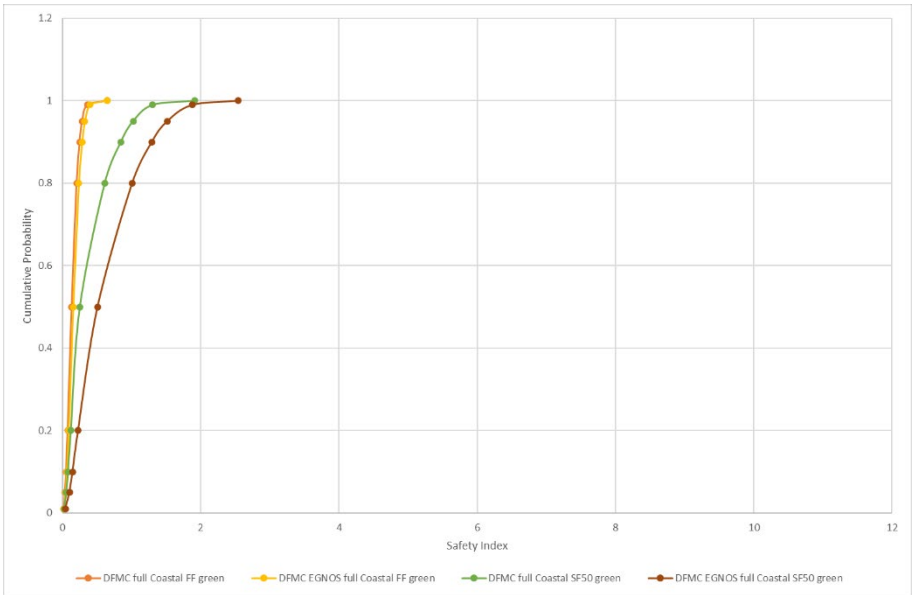

Figure 5-152: Cumulative Distribution of Horizontal Safety Index for DFMC modified MRAIM Scenarios (all results)

It can be seen from the plot that the cumulative distributions show slightly bigger safety index values that for the baseline MRAIM algorithms, i.e. there is a bit less margin in the HPL values from modified MRAIM to bound the actual errors.

If we look at the results considering only those with green integrity flag status then we see the following results.

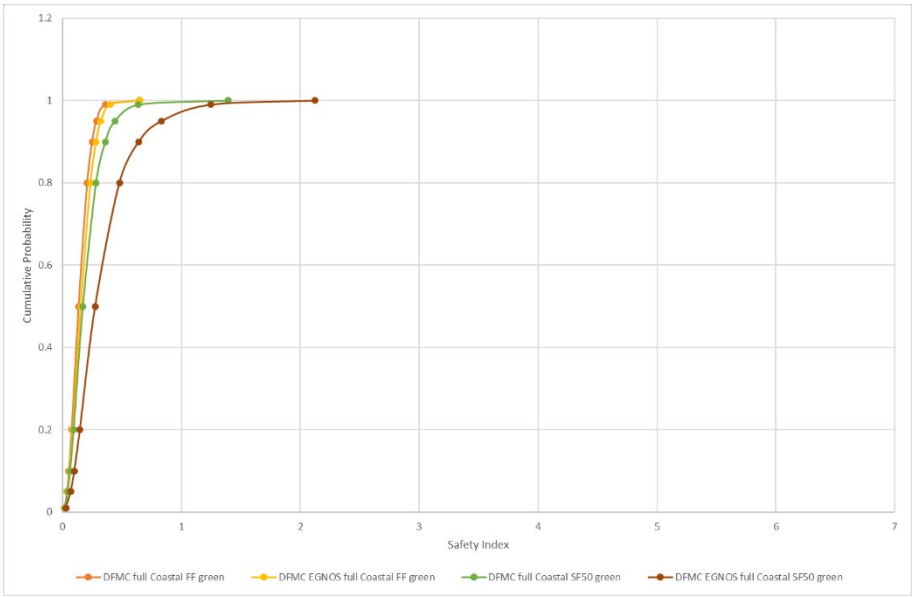

Figure 5-153: Cumulative Distribution of Horizontal Safety Index for DFMC modified MRAIM Scenarios (green integrity flag)

In this case the cumulative probability for horizontal safety index of 1 is quite similar to in the fault free case, although with some small change for the faulty cases.

The purpose of these simulations was to provide some extra validation of the modified MRAIM functionality.

In terms of performance:

- We did not study the ocean case as GPS L1 can cover the requirements for that (100m accuracy). Therefore, the results are just for the coastal case (10m horizontal accuracy 95%, 25m horizontal alarm limit).
- The DFMC solutions include GPS L1/L5 + Galileo E1/E5a. As the current GPS constellation does not include L5 signals on all GPS satellites, previous results showed the performance was poor, and so only the future case (where all GPS satellites have L5 measurements) is considered.
- In the fault-free case with future DFMC, we see that position errors are similar to the DFMC case with baseline MRAIM, with maximum horizontal position error 7.6m. There are no sample epochs where the computed HPL is greater than the HAL (of 25m), which gives 100% green integrity flag. This is an improved availability compared to baseline MRAIM. Also, the output HPL values bound the horizontal errors and so can be used to indicate horizontal error performance to the user.
- The errors in the solution (and the error model used in the checks) can be further reduced through using EGNOS, which reduces the magnitude of the horizontal position errors and the reported HPL values. In this case, the maximum error is reduced to just 4.8m for future DFMC + EGNOS and there are 100% of sample epochs with HPL less than the HAL of 25m.
- When a single satellite fault of up to 50m is added to the data, then we see some different performance to the baseline MRAIM case:
  - In the future DFMC case we see that the maximum errors after checks (16.6m) are similar to the baseline MRAIM case, and slightly more epochs are identified as faulty (37.1%). The HPL values almost always bound the actual position errors on

all the valid epochs, although there is a small % (0.05%) not bounded, which is larger than the baseline MRAIM case.

- In the future DFMC+EGNOS case, the errors are reduced compared to the DFMC only case. We see that the maximum errors after checks (15m) are similar to the baseline MRAIM case. However, the % of epochs where the HPL does not bound actual position error for green integrity flag cases is increased to 2.8%, which is becoming larger than we would like. Whether that is a limitation with the algorithm or something in the Monte Carlo simulations would need further investigation in the future.

5.2.5 Conclusions

The MGRAIM, baseline MRAIM and modified MRAIM algorithms have been analysed for fault-free and faulted cases using Monte-Carlo simulations for DFMC and DFMC+EGNOS cases. The detailed results for each are shown in the previous sections. From the results we can make the following conclusions:

- For MGRAIM in the fault-free case, current DFMC (with only a subset of GPS satellites having L5) cannot meet the Coastal horizontal accuracy requirement of 10m (95%), because there are 3.1% of epochs with red or amber status flag.
- However, if we consider future DFMC (where all GPS satellites have L5) for MGRAIM then the improved geometry means that 99.999% of sample epochs have valid (green) status, and all horizontal position errors are less than 10m.
- The addition of EGNOS DFMC (to reduce errors and uncertainty for the orbit and clock errors) has a significant impact on the performance – for both the current and future DFMC cases. With EGNOS, the MGRAIM algorithm provides 100% solution availability in the coastal scenario, and the maximum position errors are well within 10m.
- With the addition of a single satellite fault, we see that without fault detection this can lead to horizontal position errors of tens of metres. However, the fault detection within the MGRAIM algorithm can help detect and indicate faulty sample epochs.
- For the DFMC only cases, we see that for current DFMC the MGRAIM algorithm detects faults on 38% of epochs and those epochs that are flagged as valid (green) have a maximum error of 33m. For future DFMC, with improved geometry, the fault detection is more successful (detecting a fault on 45% of epochs) and the maximum error in those epochs marked valid (green) is 15m.
- For the DFMC+EGNOS cases in MGRAIM, the smaller errors and uncertainty values mean that faults can be detected earlier (and so over 70% of epochs are flagged as faulty) and the maximum remaining error for sample epochs marked as valid (green) is reduced to 18m in the current DFMC+EGNOS case and 7.3m in the future DFMC+EGNOS case.
- Although the fault detection is quite successful in MGRAIM, it is also true that the reported 95% horizontal accuracy values do not adequately represent the true error in faulted cases, with more than 20% of actual horizontal position errors for 'valid' sample epochs being larger than the reported 95% horizontal accuracy values.
- For baseline MRAIM, the algorithm provides an additional metric (the HPL) for checking if the solution is 'valid'. Overall, this has the effect (compared to MGRAIM) of reducing the solution availability (as more sample epochs are marked invalid) but providing a

metric that is more representative estimate of the true position error that can be achieved.

- For the current DFMC case, the situation is such that the coastal requirements cannot be met as no sample epochs have computed HPL less than the assumed requirement of 25m. It is only with future DFMC (and improved geometry) that we get HPL values less than 25m – in fact we have 98.9% availability of valid solutions in this case. This is less than for MGRAIM.
- If we add EGNOS to the future DFMC, then the reduced orbit and clock errors and uncertainty values – and assumptions that many faults will be detected by EGNOS – mean that HPL values are much smaller, and we achieve 100% valid solution availability.
- For the single fault scenarios, it is interesting to note that for baseline MRAIM there are fewer epochs on which faults are detected than for the equivalent MGRAIM scenarios, and this means that the remaining errors in solutions marked as valid are larger. However, even in those faulty cases we see virtually all 'valid' sample epochs with reported HPL value larger than the actual position error, and so the user can be more certain of the position error in this case – unlike in the MGRAIM algorithm where the reported 95% horizontal accuracy does not always reflect the remaining errors very well.
- For the modified MRAIM algorithm, we typically see that HPL values are smaller and so availability of green integrity flag in the fault free cases is increased. However, in the faulty cases there is a higher % of epochs with green integrity flag but where the position error is not bounded by the HPL. The values are still small (and much smaller than the MGRAIM case) but is something that would be interesting to investigate further in the future to determine if the simplification in HPL computation increases this risk, or if there is some simplification in the Monte Carlo simulations, or in the configuration and assumptions, that would need to be modified.

As with the GPS L1 results from WP2 results, it should be remembered that these results and conclusions are very dependent on the assumptions used in the generating the data. In particular:

- The fault free performance against requirements is completely dependent on the assumed values for the error models. If it is found that the error models need to be larger or smaller to represent the true errors then this will have a direct impact on the computed values,
- The integrity related parameters (e.g., satellite failure rates) and performance metrics (e.g., HAL) for MRAIM are still somewhat open for the maritime domain. Therefore, the results here – particularly for the solution availability (green status flag) – are very dependent on the chosen parameters and would be different if it is decided in the future that a different HAL, integrity risk, etc. is appropriate,
- The representativeness of the reported metrics, and the fault detection performance, is very dependent on how accurately the error models represent the actual errors. This can be clearly seen in the MGRAIM faulty cases where the reported 95% accuracy is no longer a good estimate of the actual error in the position solution. This means that it is critical that validated error models are defined for use in the actual algorithms on receivers – and for further validation activities.

6 REQUIREMENTS DEFINITION FOR MARITIME-SPECIFIC INTEGRITY DATA

Integrity concept is understood as the ability of the system to provide timely warnings to users when the system should not be used for navigation.

In general, there are two different integrity concept levels: system level integrity, where some fixed infrastructure monitors the GNSS satellites to identify potential faults and disseminates alerts to user receivers, and user level integrity, where the user receiver itself checks the GNSS signals to detect faults considering the surrounding environment.

This section aims to explain the SBAS maritime system integrity provision, focusing on the expected development and detailing current SBAS status to analyse the need for a maritime specific EGNOS message.

The analysis of the SBAS adoption in maritime domain, together with the development plan of EGNOS Maritime Safety Service and the message architecture was performed in INSPIRe D2.1 Technical Report of Developments and Test of GPS M(G)RAIM [RD.49] and information is not repeated in this document to avoid repetition.

6.1 Benefits of system-level Integrity

SBAS is a wide coverage augmentation system in which the user receives augmentation information from a satellite-based transmitter. It is composed of a network of monitoring stations which collect GNSS data from constellations, the data is analysed at a processing facility analyses to generate the corrections to the SiS data. This information is sent by a set of uplink stations to geostationary satellites which broadcast the corrections to the user.

Therefore, the SBAS integrity service should protect the user that implements MRAIM algorithm from both:

- Failures of GNSS/GEO satellites (drifting or biased pseudo ranges) by detecting and excluding faulty satellites through the measurement of GPS signals with the network of reference ground stations
- Transmission of erroneous or inaccurate differential corrections. These erroneous corrections may in turn be induced from either:
  - Undetected failures in the ground segment
  - Processing of reference data corrupted by the noise induced by the measurement and algorithmic process.

Finally, the last type of failure that a system-level integrity concept is not able to detect is the one that may occur when the system is in a nominal state (no GNSS/GEO satellite failure, no ground segment/user equipment failure) and it is usually known as “fault free case”. This is the kind of error that is addressed by the User level integrity concepts detailed in section 3.

Focusing on the DFMC EGNOS system, the future EGNOS V3 Maritime Safety Service detailed in section 7.1.4 of [RD.49], system is designed to provide what in aviation is called ground system integrity. It is an equivalent concept to system level integrity and its risk allocation (10^{-7}/ per approach in case of APV and Cat I aviation operations) should cover:

- Failures on navigation code and data transmitted by GNSS satellites (including evil waveforms).
- Corruption of data to be transmitted to the user, through the geo satellites.
- Failures issued from the ground system hardware, software design or corruption of data through the Wide Area Network connecting the ground elements.
- Errors bounding in the calculated model for ionospheric of the iono-free combination used induced delay over the EGNOS service area.

This protection guarantees the SiS performance in terms of safety and would limit the integrity risk for maritime user only to those events that could corrupt the signal in the vessel's surroundings.

However, the MRAIM algorithm detailed in section 3.2. already provides the required level of integrity for maritime when error models and ISM parameter are well characterised. Then, the added value of SBAS system is double:

- SBAS mitigates system level events excluding the detected errors.
- SBAS commitments in terms of error bounding models and system integrity risk allows the fine tuning of the ISM parameters, which are provided in real time to the user, and therefore much less conservative assumption would be taken. This significantly improves the performances of the MRAIM algorithm in terms of computational load and also the size of the Protection Level enabling some navigation phases.

The proposed solution combining SBAS and MRAIM uses two consolidated technologies which are already standardised/qualified/certified for Aviation, implying a lower level of effort, complexity and risks of standardisation/qualification/certification process for Maritime.

6.2 Assessment of dedicated maritime EGNOS V3 message

The analysis of the SBAS DFMC message structure is fully detailed in section 7.4.2 in INSPIRe D2.1 Technical Report of Developments and Test of GPS M(G)RAIM [RD.49] and they are aligned with aviation standards [RD.47].

The SBAS L5 messages and their parameters are fully independent from the SBAS L1 messages and parameters and L1 messages will still be broadcasted by retro compatibility purposes.

L1 messages are intended for use with L1 SBAS service and L5 messages are intended for use with DFMC SBAS service. The messages on each frequency will be treated independently. Type 0, 62, and 63 messages act respectively for the frequency band on which they are broadcast.

In case system level integrity provision would be required, equivalent messages to MT#0 and MT#2 to 5, #24, and #6 are now MT#0, MT#34 to 36 and 37 respectively. In addition, any further information would be required to guarantee the SiS safety. Ionospheric information is not required in this case due to the use of double frequency processing that get rid of almost totally the error. Latest version of the SBAS DFMC standard provides an overbounding error model for the residual error not corrected by the iono-free combination.

However, the intended EGNOS V3 Maritime Safety Service aims to provide user level integrity and thus provide protection against "processing of reference data corrupted by the noise induced by the measurement and algorithmic process". To do so, SBAS messages L1 legacy or L5, needs to be decoded and processed, depending on the receiver configuration, to provide at least integrity at system level.

Then, how to provide integrity at user level depends on the implementation at user receiver. SBAS MOPS [RD.4] and [RD.47] provide in their annexes the process to be followed in order to compute a safe Protection Level. However, these procedures are tailored for aviation domain and, in case a PL concept is adopted by maritime and same rationale is selected, a deep adaptation would be required. The need of specific SBAS message is discussed in the following section.

Considering the MRAIM algorithm explained in section 3.2 and described in detailed in [RD.50], which is based on the ARAIM concept, some external information may be needed. Following input ISD parameters [RD.51] may be modified or superseded by the combination of MRAIM with SBAS, these parameters include:

- Rconst: Probability of satellite failure is affected by system and user level error contributions. By the usage of SBAS and its commitments this value could be significantly reduced in the maritime domain until the main contribution would be the probability the local error is higher than the configured models. Therefore, if this assumption is made there is no need to broadcast this parameter. In addition, not only maritime but also other transportation domain may tune this parameter depending on their environment.
- Rsat: Probability of constellation failure should be significantly reduced, taking into account SBAS commitments at system level, since local errors are very unlikely causing and error of the full constellation. Only security threads like spoofing could cause a whole constellation error. Therefore, if this assumption is made there is no need to broadcast this parameter.
- Bnom: The remaining nominal bias could be significantly reduced by the usage of SBAS corrections, since they guarantee the error is bounded by a non-biased Gaussian distribution. Taking into account safety checks of SBAS, this value could be set to few tens of centimetres. Since this value depends on design considerations, it very unlikely this value change and therefore there is no need to broadcast this parameter.
- Error models: Models used by MRAIM to compute the Protection Level should be provided, in particular Orbit, Clock, Tropospheric and Ionospheric error models. SBAS is able to provide on real time error bounding models for Orbit, Clock (UDRE information) and Ionospheric errors. Tropospheric error model is hardcoded in the receiver. Therefore, as the error models are already provided up to an integrity risk of 10^{-7} there is not a strong need to modify the SBAS message for applications with an equal or lower integrity requirement.
- Validity Time: The validity time should be modified to align the MRAIM ISM and error models information with the one provided by SBAS. Again, this is a design consideration and therefore is not expected to change frequently, therefore there is no need to broadcast this parameter.

There could be some potential improvements made in the MRAIM+SBAS integrity concept, such as the broadcast of specific Rsat probability and error models for each transportation domain in a new SBAS message. However, the proposed approach proposes the less changes possible to exploit synergies and reduce deployment costs, trying to perform any adaptation required for maritime at user level.

For example, in case that SBAS error model would need to be refined to provide a smaller PL, a different overbounding sigma may be broadcasted considering the integrity risk required in maritime domain. This adaptation would allow, in this case, the maritime users to compute smaller PL since the integrity risk required for maritime general navigation is less demanding than aviation one [RD.24]. A new maritime tailored SBAS message could consider that requirement reduction to provide new UDREs. It will also allow maritime users to equip vessels with aviation-like certified receivers, since with the new messages the processing will be equivalent.

In addition, local error models should be adapted as well, and despite they use to be hardcoded in the receiver, there could be some applications where local error models could be broadcasted. For example, port authority may broadcast a validated multipath model for an specific port approach. However, it is recognised the dissemination mean not likely to be through SBAS SiS and is more likely through internet or direct RF connection between the authority and the vessel.

6.3 System-level integrity data requirements

As outlined in previous sections, the proposed integrity algorithm does not necessitate the introduction of any new SBAS messages or modifications to existing ones. However, this section details which would be the foreseen high-level requirements for a maritime specific SBAS message. Current SBAS messages could be used directly with a different receiver implementation specific for maritime, where some messages could be optionally used. In

addition, to take into account a different integrity requirement at user level, different scale factor could be used to compute Protection Level.

However, there are potential optimisation of SBAS services for maritime. Service monitoring system is based on aviation and its requirements for integrity and accuracy, therefore overbounding sigma errors could be inflated with respect to the requirements for maritime. In addition, healthy checks are also driven by aviation requirements and satellite healthy flags may be different for each transportation domain. Nevertheless, this optimisation may imply to duplicate the ground segment processing chain and the performance improvements may be small. Because of that, this trade-off should be carefully assessed due to its technical and economic implications.

In case this trade off concludes that a new maritime SBAS message is required, it is expected that any potential new SBAS message would be designed according to the following requirements, whose specific values must be defined case by case.

- **Minimum affordable update rate**: Set a maximum time for message update. Some information might be refreshed often, like SBAS Fast Corrections, and some others could be updated in a much longer term.
- **Message Time Out:** Set a maximum time for the message validity from its application time. Again, depending on the type of information the expiration time could be from few tens of seconds to several hours.
- **Bandwidth**: This requirement refers to the percentage of the new message bits in each period of time. It is a combined requirement since it depend on the refreshment rate needed and the length of the message. Please consider that SBAS messages are limited to 250 bits including message header and tails, therefore if more information is needed more messages need to be sent.
- **Integrity associated to broadcasted errors**: This requirement refers to the integrity risk associated with the error models broadcasted by the potential new SBAS messages. Aviation broadcast UDRE information associated with a level of integrity, which could be reduced for less demanding application, and therefore other UDRE could be broadcasted for a different integrity level requirement.